The identification and characterisation of Arfophilin-2

A thesis submitted to the

FACULTY OF BIOMEDICAL AND LIFE SCIENCES

For the degree of

DOCTOR OF PHILOSOPHY

By

Gilles Reisan Xavier Hickson

Division of Biochemistry and Molecular Biology
Institute of Biomedical and Life Sciences
University of Glasgow

November 2001

Declaration

I declare that the work described in this thesis has been carried out by myself unless otherwise cited or acknowledged. It is entirely of my own composition and has not, in whole or in part, been submitted for any other degree.

Gilles R. X. Hickson

November 2001.

Abstract

ADP-ribosylation factors (Arfs) are ubiquitously expressed small molecular weight GTPases whose known functions in mammalian cells are as key regulators of vesicle biogenesis and modulators of the actin cytoskeleton in the Golgi and plasma membrane systems. Previous studies have paid particular attention to the class I Arf1 and the class III Arf6, while there is virtually no information on the cellular functions of the class II Arf isoforms, Arf4 and Arf5. While the different Arf isoforms have the same activities in a number of *in vitro* and *in vivo* assays, several observations point to specific functions for the class II members. These include the identification of an Arf5-specific guanine nucleotide exchange factor, GBF1, and the identification of Arfophilin, a putative effector protein of unknown function that shows specificity for class II and III isoforms.

Here a yeast two-hybrid screen has been performed to identify novel GTP-dependent Arf5 binding proteins. This yielded two previously identified Arf-interacting proteins, Arfaptin 2/POR1 and Arfophilin, but also two novel ones, HCR and an Arfophilin homologue that we have named Arfophilin-2. In the yeast two-hybrid system, Arfophilin-2, like Arfophilin-1, appeared to specifically interact with the GTP-bound conformations of class II and III Arfs and did not interact with class I isoforms. HCR displayed unique specificity for Arf5, but was not analysed further.

A full-length Arfophilin-2 open reading frame (ORF) was cloned from testis cDNAs, although there is evidence of 5' alternative splicing. Northern blotting revealed that Arfophilin-2 mRNA is highly expressed in testis but also at low levels in many other tissues, while Arfophilin-1 is predominantly expressed in testis, kidney and skeletal muscle. Arfophilin-2-specific polyclonal antibodies were raised against the C-terminal domain and used to analyse the native protein. They recognised a single band with an apparent molecular weight of 83 kDa in HeLa and HEK 293 cells, as well as in a human testis homogenate. Moreover, these bands had the same electrophoretic mobility as the protein product produced from the cloned ORF. Using immunofluorescence microscopy, endogenous Arfophilin-2 was found to reside primarily in a brefeldin A-sensitive, cation-independent mannose-6-phosphate receptor-positive, *trans*-Golgi network (TGN) compartment. Some staining was also observed at the centrosome, where it partially colocalised with γ-tubulin, and at the plasma membrane in structures resembling focal contacts or actin-rich protrusions. Overexpression of green fluorescent protein (GFP) fused to the C-terminal Arf-binding domain of Arfophilin 2, or indeed to full-length Arfophilin

2, resulted in a tight pericentrosomal localisation in HeLa, HEK 293 and CHO cells. Strikingly, transferrin receptors (TfRs) and Rab11, a marker for the perinuclear recycling endosomes, were also redistributed to the same location while early endosomal and Golgi/TGN markers were unaffected. Trafficking of TfRs through the compartment did not seem to be compromised, as evidenced by pulse-chase experiments using fluorescent transferrin in transiently transfected HeLa cells. The pericentrosomal localisation of the GFP-Arfophilin 2/TfR/Rab11 compartment was sensitive to microtubule disruption using nocodazole, which caused the compartment to disperse into punctate structures throughout the cytoplasm. Conversely, Brefeldin A treatment was without discernible effect.

Amino acid sequence analysis revealed that the Arfophilins are homologous to Nuclear Fallout (Nuf) in their C-termini. Nuf is a cell-cycle regulated protein that plays a critical role in *Drosophila melanogaster* cellularisation where it is believed to facilitate the loading of vesicles onto microtubules at the centrosome for subsequent transport to the periphery. GFP-Nuf constructs were engineered and expressed in HeLa cells to see whether a similar phenotype would arise. Strikingly, the same clustering of TfRs and Rab11 was observed, again without noticeably compromising the ability of fluorescent transferrin to traffic through the compartment. These data suggest that Nuf and Arfophilins are functionally homologous.

In summary, this work has uncovered a novel putative Arf effector protein and has provided the first functional analysis of the mammalian Arfophilins. The results suggest they may be important in regulating the spatial distribution of the endosomal recycling compartment, and by analogy with the Nuf protein, they may be involved in regulating membrane trafficking during cytokinesis.

Acknowledgements

First and foremost I would like to thank my supervisor Prof. Gwyn Gould for giving me the opportunity to work in his lab., for always being enthusiastic, helpful, and encouraging and for proof-reading this thesis at lightning speed. Thanks also go to Diabetes UK for funding my studentship.

I would like to thank all the past and present Gould lab members (C36, C6 and lab 241!) for a great three years. Thanks for the good discussions, helpful suggestions and inpromptu pub lunches! I would especially like to thank Luke Chamberlain, Ian Salt, Valerie Maier and Sam Yarwood for their help and advice with various aspects of the work presented in this thesis.

I am also greatly endebted to Francis Barr for giving me precious bench space and lots of invaluable advice with yeast-two hybrid screening and molecular biology particularly in the early stages. This project would not have got off the ground without him. Thanks also go to Chris McInnerny for his help with northern blotting, and to Giorgia Riboldi-Tunnicliffe for a great sequencing service.

A very big thank you to Catherine Sheppard for her constant support, encouragement and advice over the past three years. Looking forward to our adventures across the water!

Last, but not least, I would like to thank my parents, my gran and my sister, Nathalie for all their support and encouragement over the years.

Table of contents

List of Figures

List of Tables

Abbreviations

AP	adaptor protein
ARD1	Arf domain protein 1
Arf	ADP-ribosylation factor
Arl	Arf-like protein
Arno	Arf Nucleotide binding site opener
ARP	Actin-related protein
ATP	Adenosine 5'-triphosphate
BAC	bacterial artificial chromosome
BFA	Brefeldin A
BHK	baby hamster kidney
BLAST	basic local alignment search tool
bp	base pairs
BSA	bovine serum albumin
CCV	clathrin-coated vesicle
CD-MPR	cation-dependent mannose-6-phosphate receptor
cDNA	complementary DNA
Ce	*Caenorhabditis elegans*
CGN	*cis*-Golgi network
CHO	Chinese hamster ovary
CIP	calf intestinal alkaline phosphatase
CI-MPR	cation-independent mannose-6-phosphate receptor
CLIP	cytoplasmic linker protein
COP	coatomer proteins
Dah	discontinuous actin hexagon
Dm	*Drosophila melanogaster*
DMEM	Dulbecco's modified Eagle's medium
DMSO	dimethyl sulphoxide
DNA	deoxyribonucleic acid
dNTPs	deoxyribonucleic nucleoside 5'-triphosphates
DTT	dithiothreitol
ECL	enhanced chemiluminescence
EDTA	diaminoethanetetra-acetic acid, disodium salt
EE	early endosome
EEA1	Early endosomal auto-antigen 1

EFA6	exchange factor for Arf6
EGF	epidermal growth factor
eGFP	enhanced green fluorescent protein
ER	endoplasmic reticulum
EST	expressed sequence tag
FAK	focal adhesion kinase
FCS	foetal calf serum
FITC	fluorescein isothiocyanate
GAL4-AD	GAL4 transcriptional activation domain
GAL4-BD	GAL4 DNA binding domain
GAP	GTPase activating protein
GBF1	Golgi brefeldin A resistance factor
GDI	guanine nucleotide displacement inhibitor
GDPβS	Guanosine 5'-[β-thio]diphosphate
GEF	guanine nucleotide exchange factor
GGA	Golgi localised, gamma adaptin ear homology domain containing Arf binding protein
GFP	green fluorescent protein
GLUT4	glucose transporter 4
GLUT1	glucose transporter 1
GPI	glycosylphosphatidylinositol
GRP1	general receptor for phosphoinositides 1
GSP	gene-specific primer
GST	glutathione *S*-transferase
GTPγS	Guanosine 5'-[γ-thio]diphosphate
GTP	Guanosine 5'-triphosphate
h	hour
IgG	immunoglobulin gamma
HCR	α-helix coiled-coil rod homologue
HEK	human embryonic kidney
HEPES	*N*-2-hydroxyethylpiperazine *N'*-2-ethane sulphonic acid
HRP	horseradish peroxidase
Hs	*Homo sapiens*
kDa	kilo Dalton
LatA	Latrunculin A
LB	Luria-Bertani broth

LDL	low density lipoprotein
LE	late endosome
MAP	microtubule associated protein
MMAP	microtubule and microfilament associated protein
MDCK	Madine Darby canine kidney
min	minutes
MKLP1	mitotic kinesin-like protein 1
MOPS	3'-(*N*-morpholino)propanesulphonic acid
MPR	mannose-6-phosphate receptor
mRNA	messenger RNA
MTOC	microtubule organising centre
MTs	microtubules
NF1	neurofibromatosis type 1
NIDDM	non-insulin-dependent Diabetes mellitus
noco	nocodazole
NSF	N-ethyl-maleimide sensitive fusion protein
Nuf	nuclear fallout
ORF	open reading frame
PBS	phosphate buffered saline
PCR	polymerase chain reaction
PH	pleckstrin homology
PICK1	protein interacting with C kinase 1
PI(3) kinase	phosphatidylinositol 3' kinase
PI(3)P	phosphatidylinositol (3) phosphate
PI(3,4,5)P3	phosphatidylinositol (3,4,5) triphosphate
PI(4,5)P2	phosphatidylinositol (4,5) bisphosphate
PLD	phospholipase D
PMSF	phenylmethanesulphonyl fluoride
POR1	partner of Rac1
QDO	quadruple drop-out
RACE	rapid amplification of cDNA ends
RE	recycling endosome
RNA	ribonucleic acid
RNase A	ribonuclease A
rpm	revolutions per minute
SAT	suppressor of Arf-ts

SDS	sodium dodecyl sulphate
SDS-PAGE	sodium dodecyl sulphate polyacrylamide gel electrophoresis
SNARE	soluble NSF attachment protein receptor
SNX	sorting nexin
TDO	triple dropout
TEMED	*N,N,N',N'*-tetramethylenediamine
TfR	transferrin receptor
TGN	*trans*-Golgi network
ts	temperature senstive
UAS	upstream activating sequence
UTR	untranslated region
VTC	vesicular tubular cluster
v/v	volume/volume ratio
WASP	Wiscott-Aldrich syndrome protein
w/v	weight/volume ratio

Chapter 1

General Introduction

1.1 An overview of membrane trafficking

Membrane trafficking is a major field of study in cell biology. Eukaryotic cells have developed highly sophisticated mechanisms for the internalisation and uptake of various nutrients and substances as well as for both constitutive and regulated modes of secretion. These mechanisms have fascinated cell biologists for the last quarter of a century and will undoubtedly continue to do so for many years to come. The endocytic system allows for the uptake of material from the extracellular milieu, while the secretory membrane system allows cells to direct newly synthesised proteins, carbohydrates and lipids to the cell surface, all of which are necessary for cell homeostasis and growth. The two systems are intricately linked and use similar mechanisms and logic. They consist of distinct membrane-bound organelles, including the endoplasmic reticulum (ER), the Golgi complex and the plasma membrane as well as intermediate tubulo-vesicular compartments such as the *trans*-Golgi network (TGN) and the endosomal system (Fig. 1.1.1). These all have different biochemical compositions and serve different functions. Membrane traffic occurs dynamically within these systems in a highly controlled manner along organised, directional routes and mechanisms exist to ensure that the biochemical heterogeneity between subcompartments is maintained. Much of our understanding of general membrane trafficking events have come from powerful genetic studies, particularly in the budding yeast *Saccharomyces cerevisiae* and also from ingenious "cell free" systems where individual trafficking events can be monitored in isolation. In general, membrane trafficking occurs via vesicular transport whereby proteins and lipids are sorted and packaged into membranous vesicles that bud from donor membranes. These are then carried along cytoskeletal tracks to an appropriate acceptor compartment to which they dock and then subsequently fuse (Fig. 1.1.2). As well as being an interesting subject of research, the importance of studying these aspects of cell biology is highlighted by the fact that defects in membrane trafficking pathways give rise to many pathological disorders in humans (reviewed in Olkkonen and Ikonen, 2000; Aridor and Hannan, 2000).

1.1.1 The secretory pathway

Classical morphological analysis of fixed cells has provided the basis for our knowledge of the architecture of the secretory pathway (Palade, 1975), and much has since been learned through the use of powerful genetic and biochemical approaches (Rothman and Wieland, 1996; Schekman and Orci, 1996). The ER represents the start of the secretory pathway (Fig. 1.1.3), and it is the largest intracellular compartment consisting of many

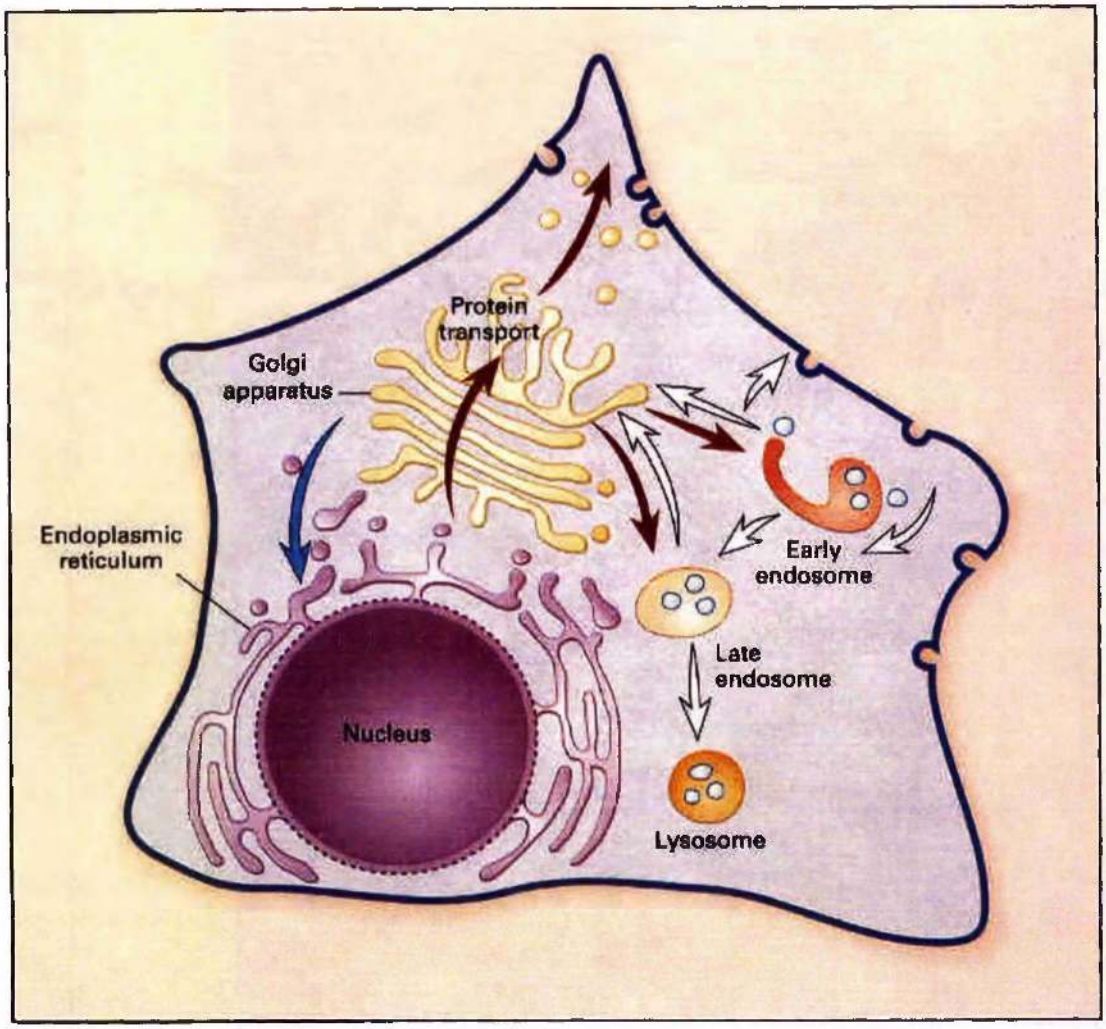

Fig. 1.1.1 **Intracellular membrane trafficking.**

A diagrammatic overview of membrane trafficking pathways in a typical eukaryotic cell. The biosynthetic/secretory pathway (indicated by red arrows) transports newly synthesised proteins from the endoplasmic reticulum, through the Golgi apparatus and to the cell surface. Internalised molecules enter the endocytic pathway (indicated by white arrows) and are sorted in the early endosomes from where they may be recycled back to the cell surface or transported to the late endosomes and lysosomes for degradation. The secretory and endocytic systems exchange material at the level of the Golgi apparatus and endosomes. *Reproduced from Olkkonen & Ikonen, 2000.*

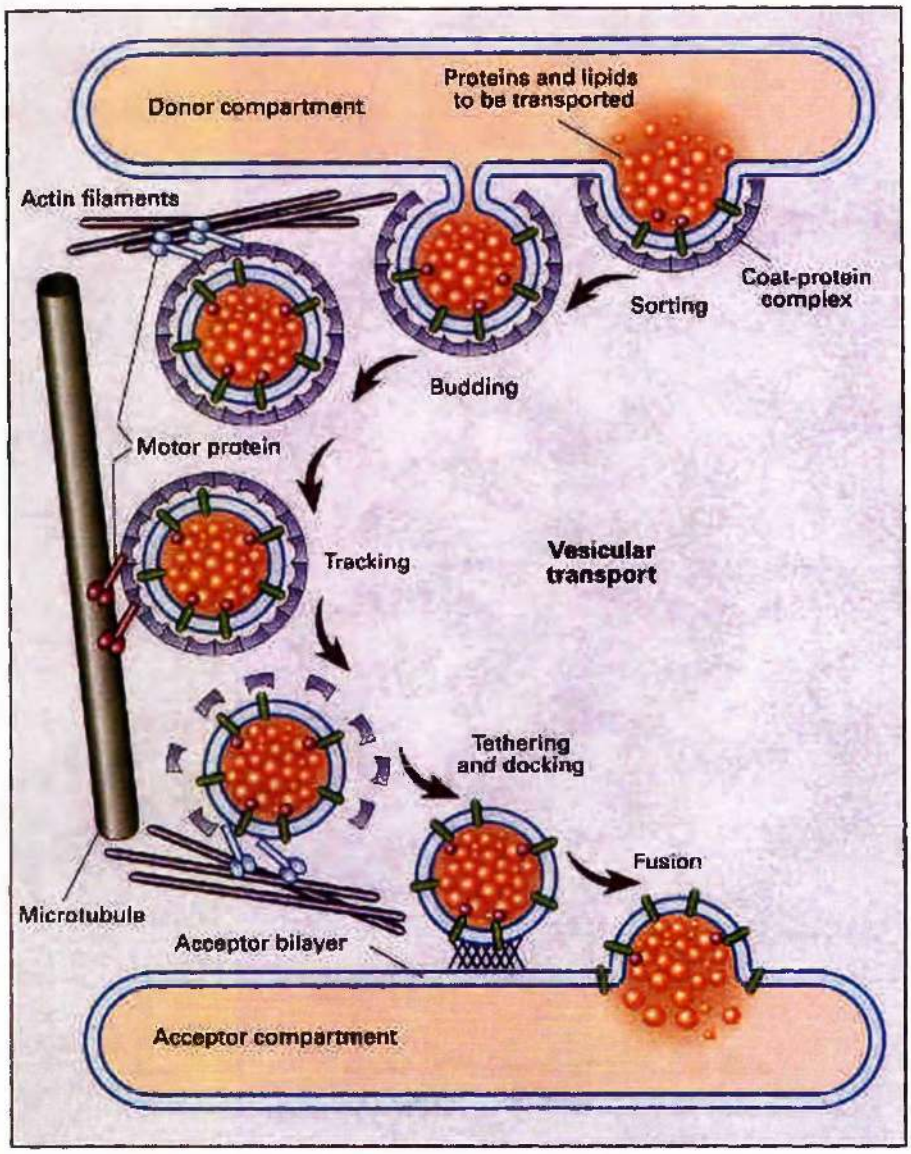

Fig. 1.1.2 **Principles of vesicular transport.**

In general terms, vesicular transport involves a number of steps including the formation of vesicles at a donor membrane. This is facilitated by cytosolic coat-protein complexes and is coupled to cargo-selection/sorting. The newly formed vesicles move along cytoskeletal tracks consisting of microtubules or actin filaments, attached to motor proteins. They are then tethered to an appropriate acceptor compartment, where they subsequently fuse with the membrane bilayer thus delivering their contents. *Reproduced from Olkkonen & Ikonen, 2000.*

interconnecting membrane tubules and cisternae. Nascent polypeptides destined for the secretory pathway are recognised by the signal recognition particle and co-translationally translocated via the Sec61 translocon into the ER lumen (High, 1995). The correct folding of the newly synthesised protein is facilitated by the actions of lumenal chaperones such as BiP, calnexin and calreticulin (Ellgaard and Helenius, 2001). In this respect, the ER plays an important role as a quality control centre as only correctly folded proteins are able to progress into the secretory pathway (Ellgaard and Helenius, 2001). Proteins destined for this route are then sorted away from ER resident proteins at discrete ER exit sites: highly organised membrane domains that direct membrane flow out of the ER into an ER-Golgi-intermediate compartment. This transport step is under the control of the small GTPase Sar1, which recruits and assembles cytosolic COPII coat protein complexes (Barlowe et al., 1994, see below). This then leads either to the continual budding of vesicles that can then proceed to and fuse with pre-Golgi intermediates (Bannykh et al., 1996), or the tubulation of the ER that then becomes a pre-Golgi intermediate (Clermont et al., 1994; Krijnse-Locker et al., 1994). It has generally been assumed that all secretory proteins leave the ER together and that sorting only occurs at later stages. Recent evidence, however, shows that this is not strictly the case since glycosylphosphatidylinositol (GPI)-linked proteins leave the ER in separate vesicles from non-GPI-liked proteins suggesting that there is some sorting at the level of the ER (Muniz et al., 2001). Nevertheless, pre-Golgi intermediates, also known as vesicular tubular clusters (VTCs), deliver secretory and membrane proteins to the *cis* face of the Golgi complex, the next major station along the secretory pathway.

The Golgi apparatus is where proteins and lipids are modified and sorted and where many decisions are made for onward travel to the plasma membrane or retention in the ER/Golgi system. Transport occurs sequentially through a characteristic stack of 3-5 Golgi cisternae, from *cis*, through medial, to *trans*, during which time secretory cargo undergoes a maturation process. For example, glycoproteins have their oligosaccharides trimmed and rebuilt, proteins may become sulphated or phosphorylated and appropriate proteolytic cleavages may be performed (Helenius and Aebi, 2001; Varki, 1998; Steiner et al., 1984). There has been some debate as to whether transport through the Golgi involves static cisternae between which vesicles shuttle in both directions, or whether it entails the movement and maturation of the cisternae themselves as they progress from the *cis* to the *trans* Golgi, or indeed a combination of both (reviewed in Pelham and Rothman, 2000). In any case, cargo proceeds to the TGN where it is sorted and packaged into distinct vesicles for delivery to the endosomal system, the plasma membrane or for the formation of

secretory granules in cells that undergo regulated secretion. A diagrammatic overview of the secretory pathway is given in Figure 1.1.3.

Fig. 1.1.3 **The secretory pathway.**

A diagrammatic overview of the secretory pathway is shown. It begins at the endoplasmic reticulum (ER), progresses through a pre-Golgi intermediate compartment consisting of vesicular tubular structures (VTCs) before entering the *cis*-Golgi network (CGN). From here proteins are directed through the Golgi stack from the *cis* to the *trans* face, either by cisternal maturation or by vesicular transport, and are delivered to the *trans*-Golgi network (TGN). Cargo can then be routed directly to plasma membrane (PM) in constitutive secretion pathways (A), or be directed into a specialised compartment in cells that undergo regulated exocytosis (B), or traffic into the endosomal system (C). In the early secretory pathway, anterograde transport from the ER is mediated by COPII coated vesicles (black circles) whereas retrograde Golgi-ER vesicles are COPI coated (blue circles).

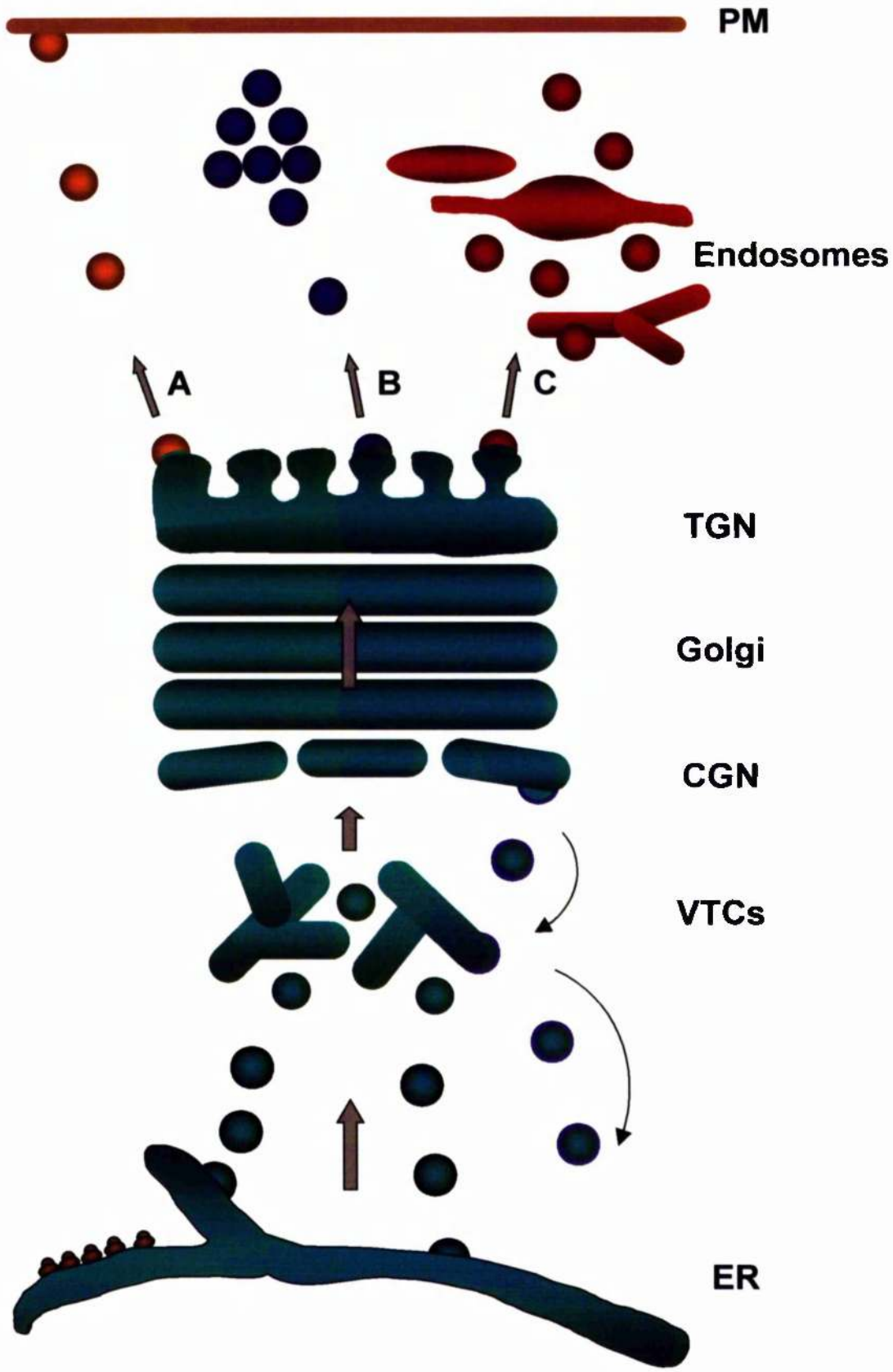
PM
Endosomes
A
B
C
TGN
Golgi
CGN
VTCs
ER

1.1.2 The endosomal pathway

While the secretory pathway directs newly synthesised proteins and lipids out towards the cell surface, nutrients, membrane and other components are continually being internalised in the opposite direction. This occurs primarily by the process of endocytosis, but also by other mechanisms such as pinocytosis. Endocytosis can itself be divided into clathrin-dependent and clathrin-independent mechanisms, such as that occurring via caveolae (Mellman, 1996). The former is by far the best understood at the molecular level and it is the route taken by recycling receptors such as the transferrin receptor. Ligand-bound signalling receptors are also rapidly internalised by clathrin-mediated endocytosis to prevent the prolonged stimulation of signal transduction cascades.

The endosomal system coordinates protein transport from both the biosynthetic secretory pathway and the endocytic pathway (Gruenberg and Maxfield, 1995; Mellman, 1996). It encompasses multiple sub-compartments including early or sorting endosomes, recycling endosomes, and late endosomes (see Fig. 1.1.4). All of these compartments have distinct biochemical compositions (Sheff et al., 1999), can sometimes be distinguished morphologically (Sönnichsen et al., 2000) and serve different functions (Mellman, 1996). On the other hand, the precise boundaries are still somewhat unclear and are variable between cell types. Within the endosomal system, many decisions are made in the sorting of proteins, such as the internalised receptors and their ligands, to determine whether they are to be delivered to the lysosomes, the Golgi complex or recycled back to the plasma membrane. The situation is further complicated in polarised cells where there is both an apical and a basolateral plasma membrane domain, each having separate recycling systems that, for example, need to differentiate between recycling and transcytosing molecules (Mellman, 1996).

1.1.2.1 The transferrin receptor

The archetypal marker protein of the endosomal system is the transferrin receptor (TfR). This has been an excellent tool for studying the endocytic pathway because its ligand, holotransferrin, can be easily labelled and monitored. The TfR is an 80 kDa integral membrane protein involved in cellular uptake of iron required for the maintenance of cell homeostasis (see Ponka and Lok, 1999). TfRs are internalised via clathrin-coated pits before entering the sorting endosomes that are located in the peripheral regions of the cell. Here the acidic environment (pH ~6.0) causes them to release their iron cargo and many of the receptors are then rapidly recycled back to the cell surface for another round of

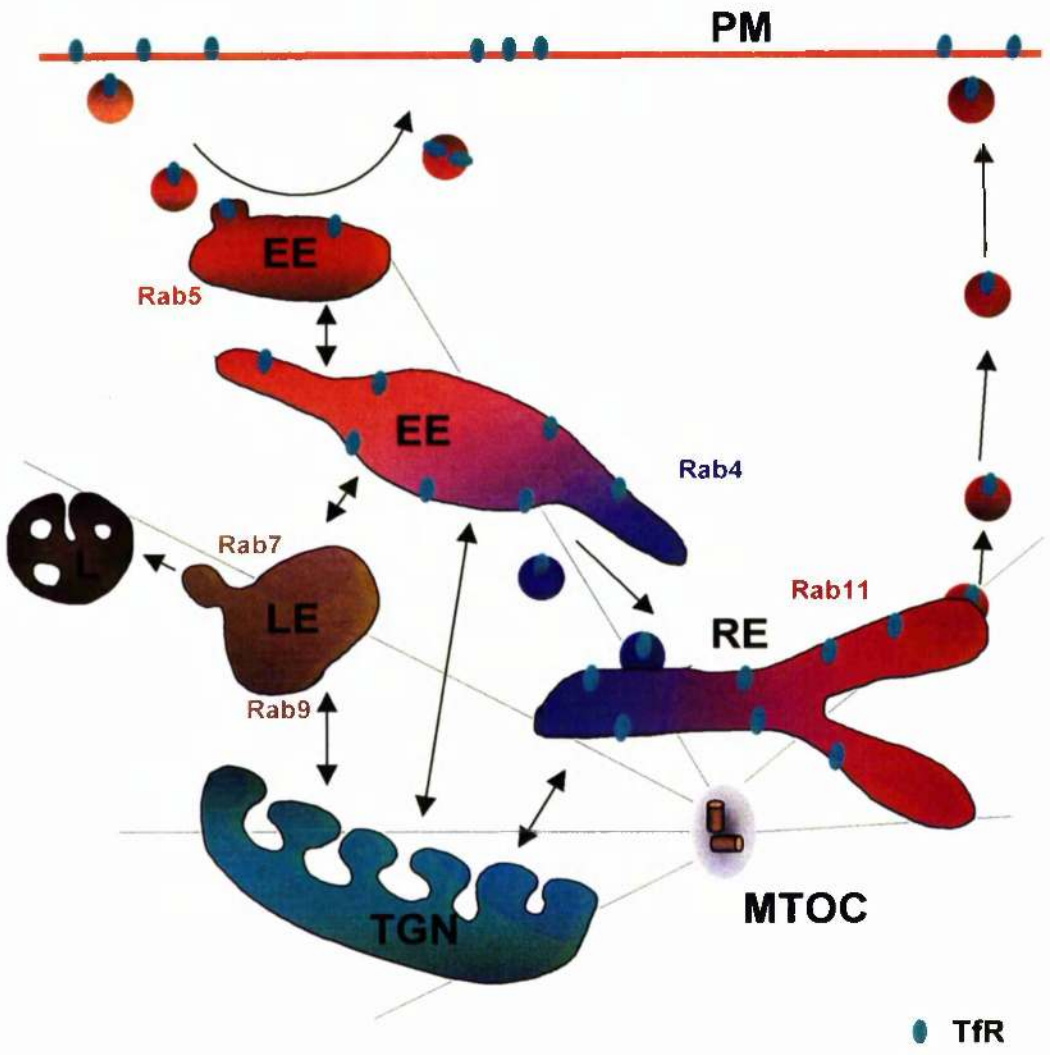

Fig. 1.1.4 **The endosomal system.**

The different subcompartments of the endosomal system are shown, including the early/sorting endosomes (EE), recycling endosomes (RE) and late endosomes (LE). The *trans*-Golgi network (TGN), plasma membrane (PM) and lysosomes (L) are also shown. Recycling receptors such as the transferrin receptor (TfR, in green) are internalised via clathrin coated vesicles and enter the EE. The acidic environment causes ligand dissociation and many receptors are then rapidly recycled back to the PM. Some, however, progress into a separate peri-centriolar compartment (RE) before being returned to the PM. Proteins to be degraded are delivered from the EE to the LE and then to the lysosomes. Different subdomains of the TfR-positive endosomal system contain specific Rab family GTPases that do not significantly overlap, as shown. Well-characterised transport routes are denoted by arrows. Microtubules, which form the cytoskeletal network to which many of the organelles are anchored, are shown with their minus ends emanating from the microtubule-organising centre (MTOC).

internalisation (Dautry-Varsat, 1986). This occurs with a half-time of two to three minutes (Schmid et al., 1988; Mayor et al., 1993). In addition to the rapidly recycling pool, a substantial number of TfRs traffic further into the cell to a distinct compartment, the peri-centriolar recycling endosomes (see below). From here, TfRs recycle back to the plasma membrane but this is markedly slower than the recycling from the sorting endosomes with a half-time of five to ten minutes (Schmid et al., 1988; Hopkins, 1983; Daro et al., 1996). In migrating fibroblasts, this slower transport route through the recycling endosomes has been shown to direct TfRs to the leading lamellae at the plasma membrane, suggesting that exit from the compartment is directed to discrete sites at the cell surface (Hopkins et al., 1994). Up to 75% of the total TfR population is found intracellularly and a large proportion of this is in these peri-centriolar recycling endosomes (van der Sluijs et al., 1992b). Other internalised molecules such as the epidermal growth factor (EGF) receptor or low density lipoprotein (LDL) do not follow the same route and are retained in the sorting endosomes before being delivered to late endosomes and lysosomes via endosomal carrier vesicles (reviewed in Luzio et al., 2000). Lysosomes are even more acidic than the early endosomes (pH ~5.0) and contain hydrolytic enzymes for the degradation of unwanted macromolecules (Rouille et al., 2000).

1.1.2.2 The peri-centriolar recycling endosomes

These are tubulo-vesicular structures adjacent to the microtubule organising centre that are tethered to the microtubule cytoskeleton (Cole and Lippincott-Schwartz, 1995). The microtubule cytoskeleton is not, however, required for their recycling function, at least in terms of the TfR, since it persists in the absence of microtubules (Daro et al., 1996; Jin and Snider, 1993; Sakai et al., 1991). They are biochemically and functionally distinct from the early sorting endosomes in a number of ways. Firstly, they lack proteins that are destined for the late endosomes and lysosomes, such as the EGF receptor and LDL mentioned above. Early studies revealed that they are also slightly less acidic than the early endosomes with a pH of ~6.5-6.8 (Yamashiro et al., 1984; Yamashiro and Maxfield, 1984). It was also noted that while the VAMP-related v-SNARE involved in TfR recycling, cellubrevin, was found in both compartments, the early endosomes alone contained Rab4 (Daro et al., 1996). At the same time, it was reported that the expression of Rab11 mutants selectively perturbed the trafficking of the TfR through the peri-centriolar endosomes (Ullrich et al., 1996), where Rab11 had previously been shown to reside in addition to the TGN and secretory vesicles (Urbe et al., 1993). More recent studies have shown that the two distinct populations can be partially resolved by density gradient centrifugation of polarised MDCK cells (Sheff et al., 1999), and different pharmacological

sensitivities have been observed for the two compartments. Only the Rab4-positive structures become tubulated upon brefeldin A treatment (Daro et al., 1996), and only the Rab11-positive, peri-centriolar recycling compartment selectively retains fluorescent transferrin following treatment with the G protein activator AlF_4 (Sheff et al., 1999). The latter recycling compartment is also unique in that it selectively retains TfRs that have been artificially oligomerised by using multivalent, chemically cross-linked transferrin as a ligand (Marsh et al., 1995). A TGN marker protein, TGN38, has been shown to traffic through the recycling compartment on its journey from the plasma membrane to the TGN (Ghosh et al., 1998) and this is a route distinct from that followed by other proteins such as the cation-independent mannose-6-phosphate receptor (CI-MPR) and furin that traffic via the late endosomes (Mallet and Maxfield, 1999). Similarly, the insulin-regulated amino-peptidase (IRAP) cytoplasmic tail fused to the lumenal domain of the TfR passes through the compartment in CHO cells and in 3T3-L1 adipocytes (Johnson et al., 1998; Subtil et al., 2000). While the TfR has been well established as a marker protein for the recycling endosomal compartment, it was recently demonstrated that there is a subpopulation of peri-centriolar endosomes that is cellubrevin-positive but TfR-negative, indicating that heterogeneity exists (Teter et al., 1998). These two subpopulations have different pH values, different sensitivities to ion transport inhibitors and undoubtedly have different functions (Teter et al., 1998), although these have not yet been elucidated.

Information as to the identities and/or functions of specific regulators of the peri-centriolar recycling endosomes is sparse. Rab11 is a clear candidate that has been implicated in regulating exit from the compartment (see below), but its precise role is unknown. Similarly, Rab17 appears to be a polarised cell-specific regulator since it localises to the compartment in mammary epithelial cells, and the expression of a dominant negative mutant inhibits transcytosis but not basolateral recycling (Hunziker and Peters, 1998; Lutcke et al., 1993; Zacchi et al., 1998). The t-SNARE syntaxin 13 is another protein that localises to the peri-centriolar recycling endosomes in neurons (Prekeris et al., 1999) and in non-polarised cells (Prekeris et al., 1998), where it is enriched on Rab11 immunoadsorbed endosomes (Trischler et al., 1999).

Recent studies, however, have implicated two additional proteins involved in regulating the distribution and function of the recycling compartment: RME-1 (Grant et al., 2001; Lin et al., 2001) and myosin Vb (Lapierre et al., 2001). RME-1 was identified in a *C. elegans* screen for mutants defective in receptor mediated endocytosis, hence the name. It belongs to a family of Eps15-homology (EH)-domain containing proteins, and these generally have a role in endocytosis often via interactions with clathrin accessory proteins (Santolini et al.,

1999). RME-1 also has coiled-coil domains and a P-loop that is predicted to bind nucleotides. In *C. elegans*, RME-1 is found associated with intracellular membranes and these become enlarged and filled with endocytosed markers in worms harbouring mutations in the P-loop or near the EH domain, suggesting a block in recycling (Grant et al., 2001). In mammalian CHO cells, where the recycling compartment is better characterised, expression of analogous dominant-negative mutants of murine RME-1 (mRme1) altered the morphology of the TfR-positive pericentriolar endosomes and slowed Tf transferrin recycling, again suggestive of a role in regulating exit from the compartment (Lin et al., 2001). Myosin Vb has been implicated in recycling endosomal function based on studies using a GFP construct fused to the tail domain of the protein, which acts as a dominant-negative mutant since it lacks the motor/actin-binding domain. Expression of this construct in mammalian cells caused TfR- and Rab11-positive endosomes to accumulate around the centrosome in a microtubule-dependent manner (Lapierre et al., 2001). Moreover, internalised fluorescent transferrin could readily access this compartment but could not be chased out by unlabelled transferrin, indicating a block in recycling (Lapierre et al., 2001). The proposed regulators of the endosomal recycling compartment are depicted in Fig. 1.1.5.

1.1.2.3 Rab proteins as markers for endosomal subcompartments

The idea of distinct subdomains of the TfR pathway being delineated by distinct Rab GTPases has recently been substantiated in an elegant study by Sönnischen *et al.*, (2000). They co-expressed Rab 4, Rab5 and Rab11 fused to different fluorescent proteins and monitored their distributions relative to each other and to the TfR using confocal microscopy. Using this approach they found that each of these GTPases do indeed mark distinct, although partially overlapping, subdomains of the pathway. Rab5 marks the very early endosomes and partially overlaps with Rab4 that is found on slightly later structures. Rab4 in turn partially overlaps with Rab11 in the perinuclear region but no overlap at all exists between Rab5 and Rab11 (Sönnichsen et al., 2000; see Fig. 1.1.4). Interestingly, in this study the different proteins were sometimes seen on the same continuous membrane without significant mixing, indicating a high degree of spatial organisation at the membrane. Immunoadsorption of endosomes using antibodies to Rab5 and Rab11 has also demonstrated that these two GTPases are segregated (Trischler et al., 1999). Other studies have shown Rab7 (Bucci et al., 2000) and Rab9 (Lombardi et al., 1993; Riederer et al., 1994) to be specific markers for late endosomes and lysosomes, which are devoid of TfRs.

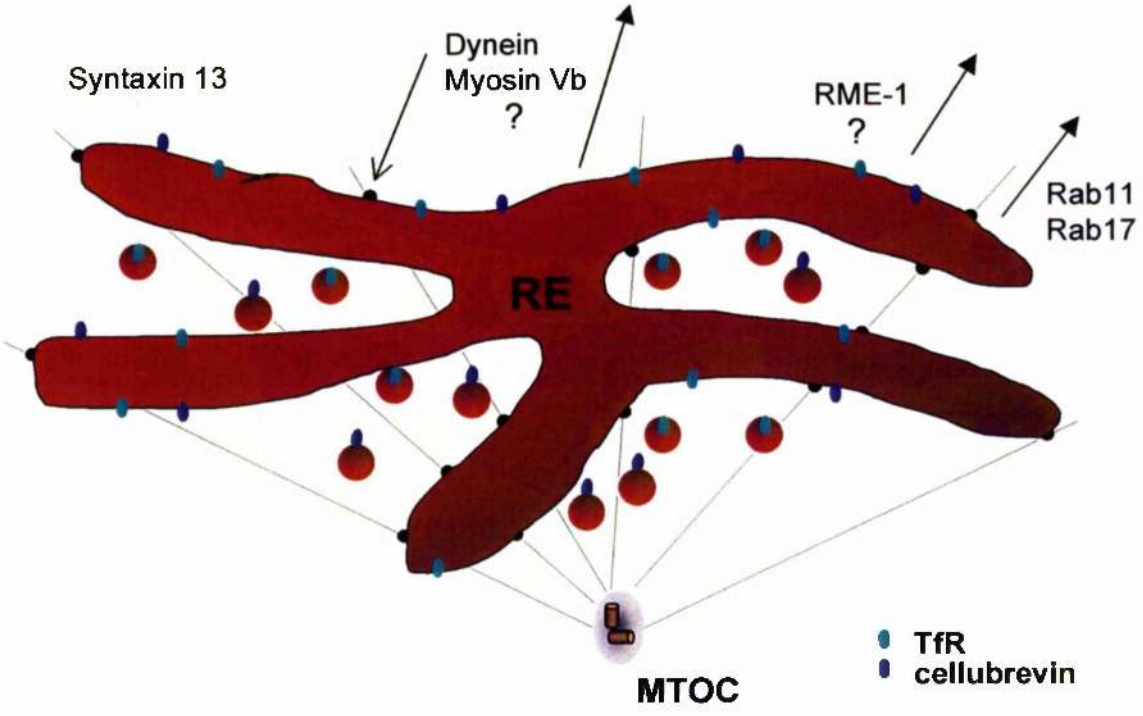

Fig. 1.1.5 **Regulators of the recycling endosomal compartment.**

The pericentriolar recycling endosomes (RE) are tethererd to the microtubule cytoskeleton by cytoplasmic dynein, in the vicinity of the microtubule organising centre (MTOC). Recycling markers of the compartment include the v-SNARE cellubrevin and the transferrin receptor (TfR), although these two molecules are segregated to some extent, suggesting heterogeneity within the compartment. The small GTPase Rab11 is a good specific marker and it appears to regulate the exit of cargo from the compartment. Rab17 is a polarised cell-specific marker that may also regulate membrane traffic out of the recycling endosomes. The t-SNARE syntaxin 13 has also been localised to the compartment. Myosin Vb and RME-1 have recently been implicated in regulating the distribution and function of the RE. See text for more detail.

Rab5 is the best studied mammalian Rab protein and it is well known for its role in controlling homotypic early endosome fusion (Gorvel et al., 1991; reviewed in Woodman, 2000), but it also has additional functions in endocytosis (Bucci et al., 1992; McLauchlan et al., 1998) and in the regulation of early endosome motility (Nielsen et al., 1999). It has a large set of effectors including Rabaptin5, phosphatidyinositol 3-kinase and early endosomal autoantigen 1 (EEA1), and its activation gives rise to a positive feed-forward loop recruiting many components, both directly and indirectly, to discrete membrane sites (reviewed in Zerial and McBride, 2001). Rab4 has been less well studied but it also seems to regulate aspects of early endosomal traffic, particularly in recycling receptors to the cell surface (van der Sluijs et al., 1992b), possibly via its novel downstream effector Rabip4 (Cormont et al., 2001).

Conversely, Rab11 has been localised to the TGN, secretory vesicles and the peri-centriolar recycling endosomes in some cell types (Urbe et al., 1993). Confocal and electron microscopic analyses also found Rab11 colocalised with the TfR in the peri-centriolar recycling compartment of Chinese hamster ovary (CHO) and baby hamster kidney (BHK) cells (Ullrich et al., 1996). Furthermore, expression of constitutively active mutants of Rab11 resulted in an accumulation of internalised transferrin in the recycling compartment while a dominant negative mutant dispersed the compartment (Ullrich et al., 1996). Two downstream Rab11 effectors have since been purified: Rab11BP/Rabphilin-11 (Mammoto et al., 1999; Zeng et al., 1999) and Rip11 (Prekeris et al., 2000). In cells cultured on fibronectin, Rab11BP/Rabphilin-11 colocalised with Rab11 on microtubules oriented towards lamellipodia, and expression of a dominant negative Rabphilin-11 mutant lacking the Rab11 binding domain decreased the accumulation of fluorescent transferrin in the recycling endosomes and also inhibited cell motility (Mammoto et al., 1999). More recently, Rabphilin-11 has been shown to directly bind to the mammalian counterpart of Sec13p, a constituent of COPII vesicles, and in a manner that is enhanced by Rab11-GTP (Mammoto et al., 2000). Rabphilin-11 might, therefore, serve to link newly formed vesicles with the Rab11 machinery, although COPII vesicles are generally believed to form only on the ER. Rip11 was found to be enriched in polarised epithelial cells where it localised to apical recycling endosomes and from where it appeared to regulate trafficking to the apical plasma membrane (Prekeris et al., 2000).

1.1.3 The trans-Golgi network

The *trans*-Golgi network (TGN) is the final station of the Golgi complex and it plays a very important role in determining the fate of the newly synthesised proteins that reach it. Despite its close proximity to the rest of the Golgi complex, the TGN can be separated both structurally and functionally by treatment with brefeldin A, suggesting that it is a distinct organelle (Ladinsky and Howell, 1992). From the TGN, proteins may be constitutively directed to the plasma membrane, or be directed to the endosomal/lysosomal system or, in cells that undergo regulated secretion, they may be packaged into immature secretory granules which then mature as they progress towards the plasma membrane (Griffiths and Simons, 1986). Many TGN residents such as TGN38 also recycle to and from the plasma membrane (Luzio et al., 1990; Ladinsky and Howell, 1992).

1.1.4 Vesicle biogenesis

Membrane transport between subcellular compartments relies on a series of vesicle budding, translocation and fusion events. Furthermore, sorting mechanisms are required to ensure that only the appropriate cargo molecules are packaged into vesicles for transport. In general, vesicle biogenesis involves the recruitment of proteinaceous coat complexes, membrane invagination to produce a bud and finally the pinching off or scission of the newly formed coated vesicle. There are two main types of coats that are known: COPs and clathrin coats and both types actively participate in the membrane deformation required to produce the vesicle.

1.1.4.1 COP-coated vesicles

COPs are subdivided into multi-subunit COPI (coatomer) and COPII coats which are recruited to Golgi and ER membranes, respectively (reviewed in Barlowe, 2000). They are unrelated in terms of their protein composition but there are mechanistic parallels. The key trigger for the assembly of the coat complexes comes from GTPases of the Arf family (refer to section 1.3). GTP loading of Arf, in the case of COPI, or Sar1 in the case of COPII, initiates the recruitment of the pre-assembled cytosolic coat complexes to the membrane (Palmer et al., 1993; Barlowe et al., 1994; reviewed in Springer et al., 1999). This is sufficient to drive polymerisation of the coats *in vitro* and the subsequent formation of vesicles, provided that the membranes are of the correct phospholipid compostion (Matsuoka et al., 1998b). This process plays an active role in cargo selection since the coats directly interact with cargo molecules such as transmembrane proteins with

cytoplasmic KKXX motifs or p24 proteins (Cosson and Letourneur, 1994; Kuehn et al., 1998; Springer and Schekman, 1998). Moreover, COPs are sufficient to ensure the inclusion of important components such as v-SNAREs which are later required for fusion of the vesicle with acceptor membranes (Matsuoka et al., 1998a). The non-hydrolysable GTP analogue, GTPγS, allows vesiculation to occur in reconstituted *in vitro* systems indicating that the energy of coat polymerisation drives budding rather than GTP hydrolysis, and the GTPases appear to act as catalysts to the process (Rothman and Wieland, 1996). GTP hydrolysis catalysed by GTPase activating proteins is, however, required for disassembly of the coat and to allow for further rounds of budding (Tanigawa et al., 1993; Rothman and Wieland, 1996). On the other hand, while GTPγS and GTPase-defective Arf1 allow for the formation of COPI-coated vesicles, specific enrichment of such vesicles with the *medial/trans* Golgi marker α1,2-mannosidase II in an *in vitro* system is only observed when GTP hydrolysis occurs, suggesting that this plays an active part in sorting (Lanoix et al., 1999).

Although COPI is best characterised at the Golgi complex, it has been found to localise to endosomal compartments using immunoblotting of purified fractions (Whitney et al., 1995; Aniento et al., 1996). In support of this, a mutant CHO cell line with a temperature sensitive defect in ε-COP has an endosomal defect, where LDL receptors are rapidly degraded, in addition to defects in the ER/Golgi system (Guo et al., 1994). Further studies using the same cell line demonstrated that, at the restrictive temperature, transferrin recycling and bulk-phase uptake are markedly diminished (Daro et al., 1997). In addition, these cells can no longer be infected with viruses such as the vesicular stomatitis virus that require delivery to acidic endosomes before they can enter the cytosol (Daro et al., 1997). COPI association with endosomal membranes has been shown to be dependent on the acidic pH of the endosomal lumen and both membrane association and pH-sensing depends on Arf1-GTP (Gu and Gruenberg, 2000). The role(s) of the endosomal COPs is not clear although they may be involved in the biogenesis of multi-vesicular bodies that mediate transport from early to late endosomes (Gu and Gruenberg, 1999; Gu and Gruenberg, 2000).

1.1.4.2 Clathrin-coated vesicles and clathrin adaptors

Clathrin plays a major role in vesicle biogenesis at the *trans*-Golgi network and plasma membrane. It is a hexameric complex consisting of heavy and light chains arranged to form three appendages emanating from a central hub to produce a triskelion (for a comprehensive review on clathrin see Kirchhausen, 2000). Clathrin triskelia assemble into

polyhedral cages and these constitute the clathrin coats on vesicles. Clathrin does not directly contact membrane components but interacts indirectly via clathrin adaptor complexes (APs). Four such AP complexes have been identified in mammalian cells: AP-1, AP-2, AP-3 and AP-4 (see Fig. 1.1.6; Robinson & Bonifacino, 2001). GGA proteins can also act as clathrin adaptors but these will be considered in the next section. The APs are heterotetrameric complexes comprising two large subunits (γ/α/δ/ε, β) and two small subunits (μ, σ). The first identified and best characterised are AP-1 and AP-2 which mediate clathrin-coated vesicle (CCV) biogenesis at the TGN and plasma membrane, respectively (Robinson and Pearse, 1986; Ahle et al., 1988). The μ subunits are important in recognising sorting motifs in the cytoplasmic tails of receptors that are to be included into CCVs (Ohno et al., 1995). Following adaptor binding, clathrin is recruited from the cytosol and assembly of the clathrin lattice ensues (Kirchhausen, 2000). In the case of AP-1 (Stamnes and Rothman, 1993; Traub et al., 1993; Austin et al., 2000) and AP-3 (Ooi et al., 1998), recruitment of the adaptor is dependent on a direct interaction with Arf, again underlining the central importance of this family of GTPases in vesicle formation. No such Arf involvement has been documented for the formation of AP-2 dependent endocytic CCVs but there is a wide array of known accessory proteins, both primary and secondary, including amphiphysins, Eps15, AP180/CALM, synaptojanin, synaptotagmins, stonins, intersectins, endophilins. It is beyond the scope of this introduction to describe these here, but they have been adequately reviewed elsewhere (Jarousse and Kelly, 2001; Brodsky et al., 2001). Despite the complex picture obtained for AP-2 mediated CCV formation, it is not known whether similar regulatory mechanisms are at work with the other APs.

AP-3 localises around the TGN and peripheral endosomes in mammalian cells (Simpson et al., 1996; Dell'Angelica et al., 1997; Simpson et al., 1997) and mutations in AP-3 subunits give rise to Hermansky-Pudlak syndrome (Dell'Angelica et al., 1999b). This is characterised by defects in lysosomes and related organelles implicating AP-3 in trafficking to these compartments. However, there appears to be conflicting data as to whether AP-3 vesicles are actually clathrin-coated. On the one hand, a direct *in vitro* interaction with clathrin has been reported (Dell'Angelica et al., 1998) as has co-immunoprecipitation (Liu et al., 2001), and AP-3 can instigate clathrin assembly onto synthetic liposomes in a reaction that only requires AP-3, clathrin and Arf-GTP (Drake et al., 2000). Conversely, AP-3 does not co-purify with clathrin-coated vesicles (Simpson et al., 1996), and AP-3-dependent transport of yeast alkaline phosphatase to the vacuole occurs in cells lacking clathrin function (Vowels and Payne, 1998).

The fourth adaptor complex AP-4 is absent from yeast, worm and fly genomes, but the protein appears to reside around the TGN in mammalian cells where it colocalises with TGN38 and furin (Dell'Angelica et al., 1999a; Hirst et al., 1999). Membrane association appears to be Arf-regulated since brefeldin A treatment causes its dissociation, but it seems to function independently of clathrin (Hirst et al., 1999) and its cellular role is unknown.

Once endocytic CCVs have been formed, members of the dynamin family of enzymes play an important role in directing their scission from the membrane. Dynamins are large (100 kDa) GTPases that were originally implicated in endocytosis by studies of the *Drosophila shibire* temperature-sensitive mutant (Kosaka and Ikeda, 1983a; Kosaka and Ikeda, 1983b). Dynamin can self-assemble into rings and tubules *in vitro* (Carr and Hinshaw, 1997; Hinshaw and Schmid, 1995) and its GTPase activity is associated with a conformational change (Marks et al., 2001). The mode of action of dynamin has been highly contentious, particularly with respect to the role of the GTPase activity, and several models have been proposed (reviewed in Sever et al., 2000). Although best known for its role at the plasma membrane, it is becoming clear that dynamins also function in vesicle scission at other intracellular locations (see McNiven et al., 2000). For example, dynamin is implicated in vesicle scission from the TGN (Jones et al., 1998 and references therein) and from late endosomes (Nicoziani et al., 2000).

Once the vesicles have been formed, the clathrin coats are shed to allow the vesicle to dock and fuse with the acceptor compartment, and also to allow the recycling of the coat components for the formation of additional vesicles. This uncoating step appears to require the ATP-dependent chaperone hsc70 and auxilin (reviewed in Lemmon, 2001), and the inositol-5- phosphatase synaptojanin (Cremona et al., 1999).

Although primarily characterised at the plasma membrane and TGN, clathrin-coated vesicles have been localised to endosomal membranes by electron microscopy (Stoorvogel et al., 1996). With diameters of 60 nm as opposed to 100 nm, these were found to be smaller than known CCVs and they lacked α- and γ-adaptin characteristic of AP-1 and AP-2, but their functions are currently unknown (Stoorvogel et al., 1996). A recent study has also implicated clathrin function in the regulation of early endosome distribution. Bennett et al., (2001) found that the induced expression of clathrin hub, which acts as a dominant-negative mutant, in stably transfected HeLa cells resulted in a clustering of the EEA1-positive early endosomes around the centrosome. However, this did not seem to affect the kinetics of TfR trafficking suggesting that clathrin's role in the endosomal compartment is distinct from that at the plasma membrane or TGN.

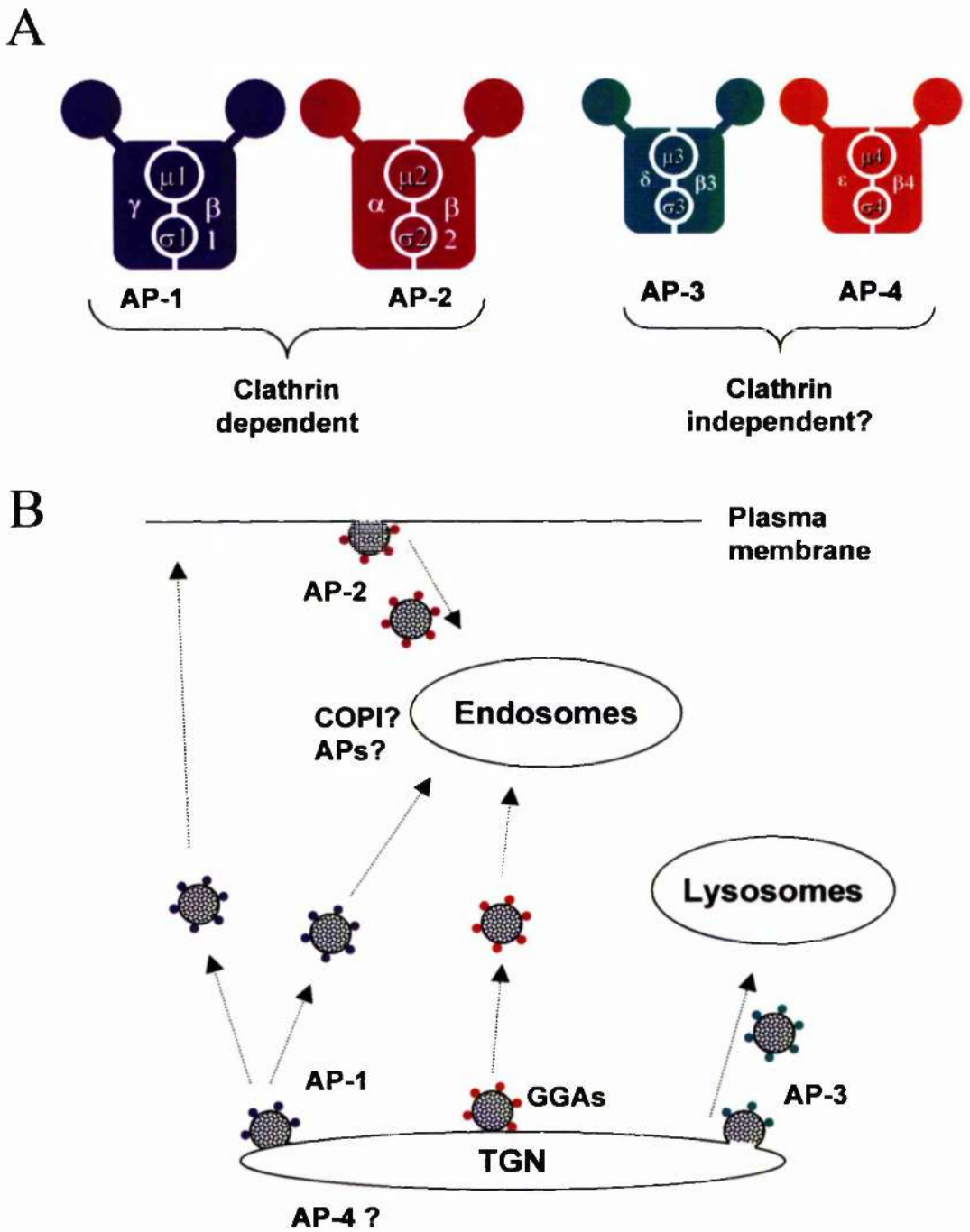

Fig. 1.1.6 **Adaptor Proteins.**

A) Diagrammatic representations of the four heterotetrameric adaptor complexes AP-1, AP-2, AP-3 and AP-4 are shown. They each have two large subunits (γ,α, δ,ε and β) and two small μ and σ subunits. The large subunits have appendages or 'ear' domains. While AP-1 and AP-2 are well established clathrin adaptors, it is not clear whether AP-3 and AP-4 function with clathrin.

B) Intracellular trafficking steps mediated by the adaptors. AP-1 mediates the formation of clathrin-coated vesicles destined for the endosomes and plasma membrane at the *trans*-Golgi network (TGN). AP-2 mediates endocytic clathrin-coated vesicle formation at the plasma membrane. AP-3 regulates vesicular traffic from the TGN to the lysosomes. AP-4 localises to the TGN region but its function is unclear. GGAs are also clathrin adaptors involved in TGN to endosome traffic. See text for details.

1.1.5 Mannose-6-phosphate receptors and GGAs at the TGN.

Mannose 6-phosphate receptors (MPRs) are transmembrane proteins that are essential for the targeting and delivery of soluble lysosomal hydrolases from the TGN to lysosomes. These enzymes are required for the degradation of internalised and endogenous macromolecules. There are two distinct MPRs with overlapping functions: a large 300 kDa cation-independent MPR (CI-MPR) and a smaller 46 kDa cation-dependent MPR (CD-MPR) (reviewed in Le Borgne and Hoflack, 1998). They are actively sorted away from secretory proteins in the TGN, by a mechanism that depends on the MPR cytoplasmic tails (Le Borgne and Hoflack, 1997; Dell'Angelica and Payne, 2001). Cargo-bound MPRs bud from the TGN in clathrin-coated vesicles and deliver the hydrolases to endosomes, where the acidic pH causes dissociation of their ligands. The enzymes then progress into mature lysosomes while the receptors are retrieved back to the TGN.

Until recently, the prevailing view was that MPR trafficking out of the TGN was mediated by the AP-1 clathrin adaptor complex (Le Borgne and Hoflack, 1998). This was based largely on the fact that AP-1 is concentrated at this organelle, binds MPR tails *in vitro* and because overexpressed MPRs assemble into AP-1 positive clathrin-coated buds and vesicles in the TGN region (Le Borgne and Hoflack, 1998). However, the recent discovery (Hirst et al., 2000; Dell'Angelica et al., 2000; Boman et al., 2000; Takatsu et al., 2001) and fervent study of GGA proteins (Golgi localised, gamma-adaptin ear homology domain containing, Arf binding proteins) have challenged this (reviewed in Black and Pelham, 2001).

GGAs are evolutionarily conserved, multi-domain proteins encoded by two yeast genes and three human genes. They are characterised by a GAT domain (GGA and TOM1 [target of myb 1]), a VHS domain (Vps27p/Hrs/STAM domain), a hinge region, and a GAE domain (gamma-adaptin ear domain). The GAT domains have been shown to confer Arf binding and Golgi localisation (Boman et al., 2000), the GAE and hinge domains bind γ-synergin and clathrin, respectively (Takatsu et al., 2001; Puertollano et al., 2001b), while the VHS domains directly interact with the acidic-cluster-dileucine motifs of the MPRs (Zhu et al., 2001; Puertollano et al., 2001a; Takatsu et al., 2001). These latter findings are particularly important since the acidic dileucine motif was known to be important in TGN to endosome MPR trafficking (Chen et al., 1997), and yet it did not interact with AP-1 suggesting that an alternative mechanism was involved. It now seems highly likely that the GGAs, and not AP-1, are responsible for this trafficking step, and this is substantiated by the fact that dominant negative GGA mutants block MPR exit from the TGN (Puertollano

et al., 2001a). GGAs have also been shown to interact with the cytoplasmic tail of sortilin (Nielsen et al., 2001), a protein that follows a similar trafficking itinerary to the MPRs, and in yeast double GGA knockouts have defects in the trafficking of carboxypeptidase Y and the sortilin homologue Vps10p to the vacuole, the equivalent to the mammalian lysosome (Dell'Angelica et al., 2000; Hirst et al., 2000). Furthermore, such yeast strains are also defective in the signal-dependent trafficking of the syntaxin Pep12p, which is normally sorted from the Golgi to the late endosomes (Black and Pelham, 2000). Elegant studies by Juan Bonifacino and colleagues have further established direct binding of the GGAs to clathrin, and provided further insight into the role of Arf GTPases in these events (Puertollano et al., 2001b). In an incredibly short time, the GGAs have thus emerged as major players in clathrin-mediated TGN to endosomal membrane transport and a current working model for their action at the TGN is shown in Fig. 1.1.7.

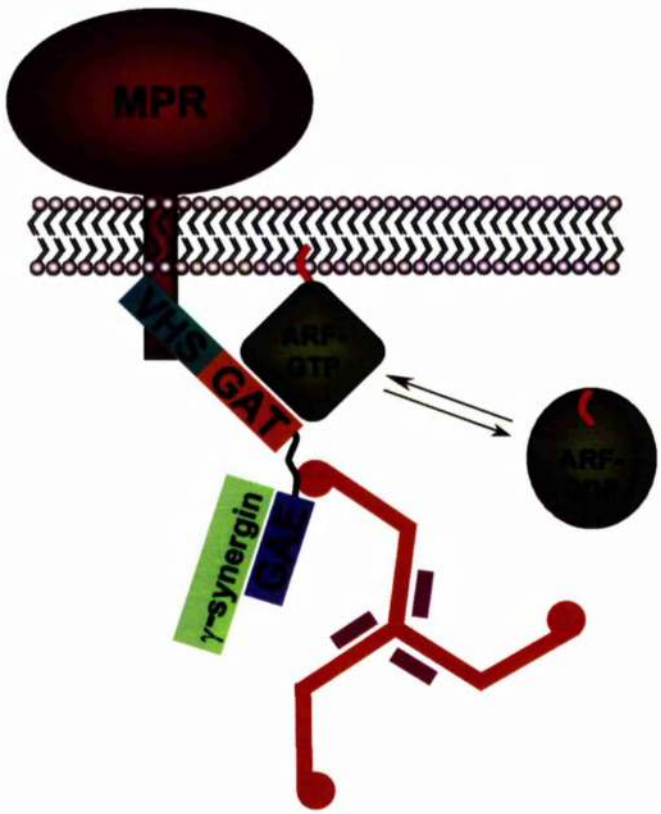

Fig. 1.1.7 **The proposed function of GGA proteins as clathrin adaptors.**

GGA GAT domains interact with GTP-bound ARF GTPases that become membrane-associated upon activation. GGA VHS (Vps27/Hrs/STAM homology) domains can then interact with acidic clusters of the cytosolic tails of transmembrane proteins such as the cation-independent mannose-6-phosphate receptor (MPR) or sortilin. The hinge region of the GGAs can directly associate with clathrin (red triskelion) thereby recruiting it for the formation of clathrin coated vesicles. The GAE (gamma adaptin ear homology) domain is also known to bind γ-synergin.

1.1.6 Intracellular protein sorting mechanisms

Sorting signals are important mechanisms in determining the localisation and fate of proteins, and are important in the maintenance of heterogeneity between different organelles. A number of signals have been described and they are often intrinsic signals conferred by specific amino acid residues but can also be moieties appended post-translationally.

One of the best characterised sorting mechanisms concerns the specific retrieval of lumenal ER resident proteins that have 'escaped' into later compartments such as the VTCs or *cis*-Golgi. Such proteins terminate in the KDEL (HDEL in yeast) amino acid sequence and this binds to the KDEL receptor, ERD2, allowing efficient retrieval to the ER (Munro and Pelham, 1987; Lewis and Pelham, 1992; Semenza et al., 1990). Similarly, ER resident transmembrane proteins typically have KKXX/ RRXX motifs (where X is any amino acid) and these interact with COPI coats allowing for their specific retrieval (Cosson and Letourneur, 1994).

Sorting signals are also present in the cytoplasmic tails of cargo molecules in the TGN/endosomal systems. These are involved in binding to the adaptor proteins mentioned earlier, thus enabling cargo receptors to be concentrated into clathrin-coated pits. They fall into two main classes: tyrosine-based and dileucine-based sorting motifs. The tyrosine-based motifs, which mostly conform to the amino acid sequence YXXØ (where X is any amino acid and Ø is is an amino acid with a bulky hydrophobic side chain), are the best characterised (reviewed in Kirchhausen et al., 1997; Bonifacino and Dell'Angelica, 1999) and are present in proteins such as TGN38 (a YQRL motif) and the transferrin receptor (a YTRF motif). They can direct endosomal and lysosomal targeting, internalisation from the plasma membrane, and sorting at the TGN (Kirchhausen et al., 1997). YXXØ motifs have been shown to bind conserved regions of the μ subunits of adaptor complexes using yeast two-hybrid and biochemical approaches (Ohno et al., 1995; Ohno et al., 1996; Boll et al., 1996; Ohno et al., 1998). However, the motifs often show preferences for particular μ chains. For example, the signal in the TGN38 tail is better recognised by μ1 than μ3, whereas the opposite is true for the signal in the lysosomal glycoprotein, LAMP-1 (Ohno et al., 1996; Ohno et al., 1998). It also seems likely that the affinity of the interactions with the adaptors is modulated by other factors since AP-2 binds more strongly to tyrosine-based motifs when present in clathrin coated pits and also in the presence of phosphatidylinositol-3 phosphates (Rapoport et al., 1997). Similarly, phosphorylation of

AP-2 may directly regulate the interaction with sorting signals (Fingerhut et al., 2001; Olusanya et al., 2001).

Dileucine-based motifs are also found in the cytoplasmic tails of membrane proteins such as the MPRs (Chen et al., 1993) and the melanosomal protein tyrosinase (Calvo et al., 1999; Honing et al., 1998). However, it is less clear which adaptor subunits are required for the interactions. The dileucine motif of the CD3γ chain can bind to β-adaptin subunit of AP-1 (Rapoport et al., 1998), while the μ1 and μ2 chains can interact with the MHC invariant chain (Rodionov and Bakke, 1998; Hofmann et al., 1999).

It has recently become apparent that ubiquitination can act as a sorting signal. Ubiquitin is a 76 amino acid polypeptide that becomes conjugated to lysine residues in target proteins via the concerted action of three enzymes: a ubiquitin-activating enzyme (E1), a ubiquitin-conjugating-enzyme (E2), and a ubiquitin ligase (E3). While polyubiquitination is well known to target proteins for degradation via the 26S proteasome, a role for monoubiquitination has recently been uncovered in endocytosis (see Hicke, 2001). It also seems to positively regulate traffic from the late endosome to the yeast vacuole via the ESCRT-1 complex which acts in sensing the ubiquitin moiety (Katzmann et al., 2001).

In addition to protein sorting, lipid based sorting also occurs. This was elegantly demonstrated in a recent study using lipid analogues differing only in the length and saturation of their hydrophobic tails (Mukherjee et al., 1999). These analogues were shown to partition into different endocytic compartments indicating that sorting can occur in a manner dependent on the membrane composition. The fact that Shiga toxin B fragment follows a specific trafficking itinerary (Mallard et al., 1998) and is a cytosolic protein that binds to the glycolipid globotriaosylceramide (Lingwood, 1993), is again suggestive of lipid-based sorting.

1.1.7 Membrane fusion

Once vesicles have budded from donor organelles, they need to travel to, and subsequently fuse with, the correct acceptor membranes. Membrane fusion is an energetically unfavourable event that requires energy in the form of ATP. Our knowledge of the molecular basis for membrane fusion has increased massively over the last decade or so due to intensive research from many laboratories. Much of the work has come from studying neuronal synaptic vesicle exocytosis but the processes are so highly conserved that the principles are applicable to most, if not all, eukaryotic membrane fusion events. They occur via a highly ordered mechanism that has multiple co-ordinated steps including vesicle docking/tethering, priming and finally fusion. Fusion is mediated by soluble NSF attachment protein receptors (SNAREs, where NSF stands for *N*-ethyl-maleimide-sensitive fusion protein). There are over 30 members of the mammalian SNARE family found in different subcellular compartments. The SNARE hypothesis, proposed in 1993 by Rothman and co-workers, postulated that for each membrane transport pathway there exists a distinct pair of SNARE proteins, one on the vesicle, termed a v-SNARE, and the other on the target membrane termed a t-SNARE (Sollner et al., 1993). It was originally proposed that specific v-SNARE/t-SNARE pairing conferred the specificity of membrane fusion. While it no longer seems quite so simple, since many SNARE interactions are promiscuous (Yang et al., 1999) and Rab GTPases may be more important in determining vesicular transport specificity (reviewed in Zerial and McBride, 2001; see below), SNAREs are unquestionably central to the fusion process.

SNARE proteins all contain conserved heptad repeats that form coiled-coil structures. They have been grouped into members of the VAMP (vesicle-associated membrane protein), syntaxin and SNAP-25 (synaptosome-associated protein of 25 kDa) families based on the neuronal isoforms first identified. One member from each of these families assembles into a ternary SNARE 'core complex' that is extremely stable being resistant to SDS and temperatures up to 90 °C. The crystal structure of the neuronal SNARE core complex has been solved revealing a four-helical bundle comprising one syntaxin, one VAMP and two SNAP-25 coils (Sutton et al., 1998), as depicted in Fig. 1.1.8. These are arranged in a parallel fashion, such that the formation of the complex brings the two membranes into close apposition and this is believed by many to provide the force required to drive membrane fusion. A number of other regulatory molecules are known. For example Sec1 proteins such as n-Sec1/Munc18 are peripheral chaperone proteins that bind tightly to syntaxin family members and are important regulators of SNARE complex

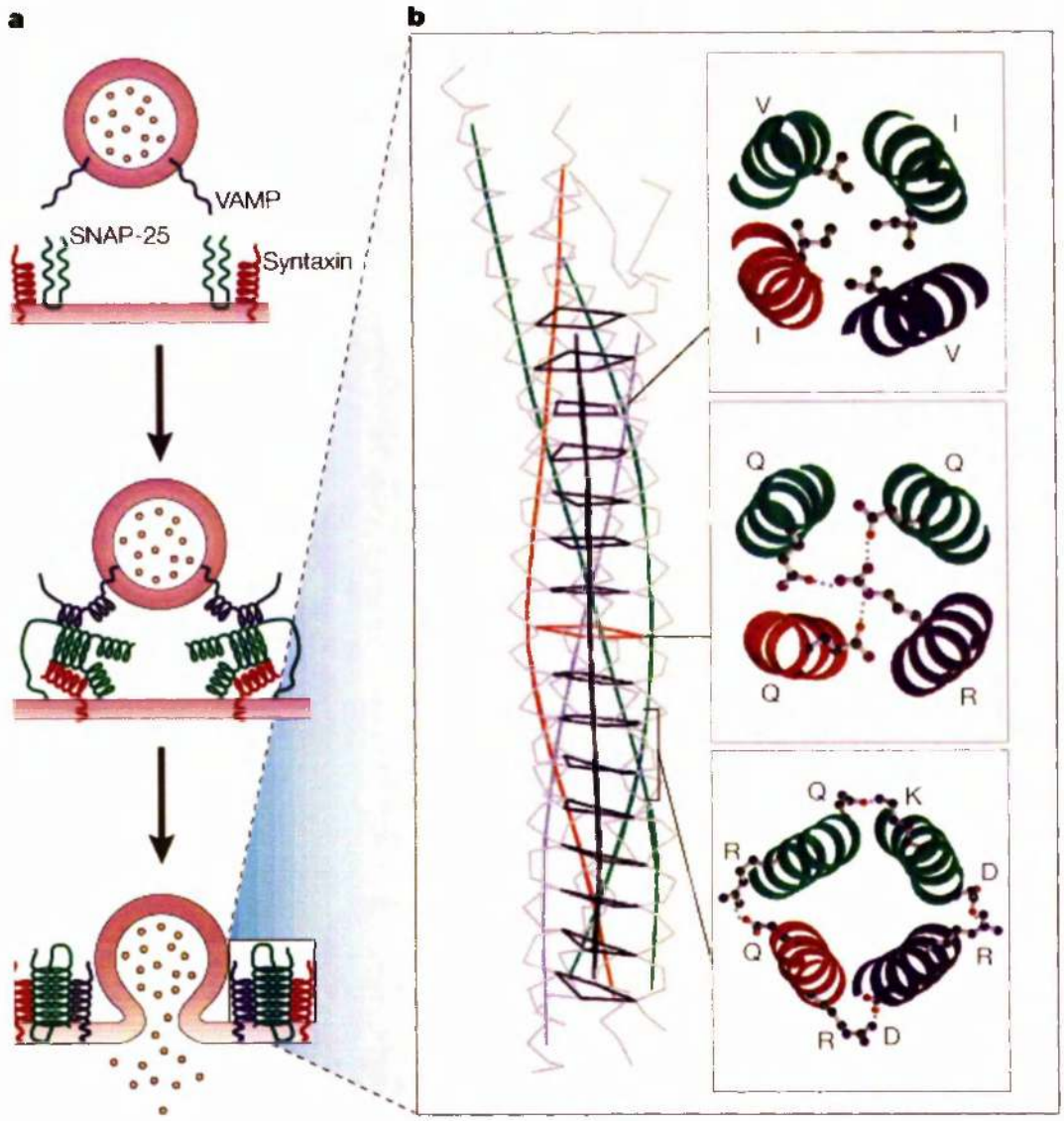

Fig. 1.1.8 **Model for SNARE complex formation.**

Schematic showing the assembly of the archetypal neuronal SNARE complex during vesicle/plasma membrane fusion (**a**). VAMP (blue) on the incoming vesicle interacts with syntaxin (red) and SNAP-25 (green) at the plasma membrane to form a four-helical bundle that then 'zips' together pulling the two membranes together thus allowing membrane fusion to occur. (**b**) The left hand panel shows the arrangement of the four helices in the core complex, with with cross-sectional views of the indicated positions given on the right. Q-SNAREs have glutamine residues in the central layer of the complex, while R-SNAREs have arginine residues. *Reproduced from Chen & Scheller, 2001.*

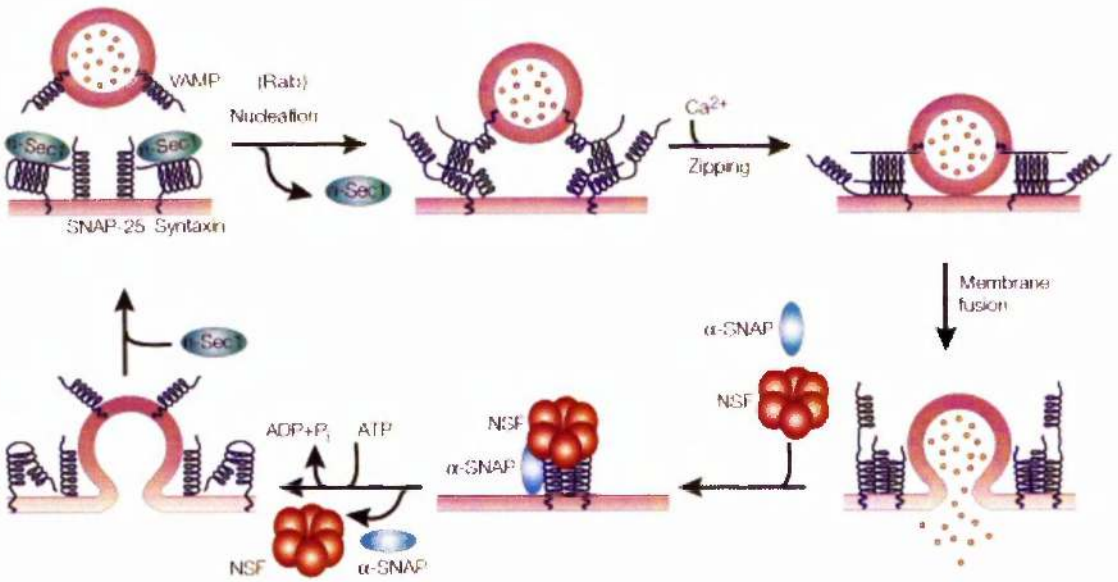

Fig. 1.1.9 **Model of membrane fusion**

Syntaxin in the plasma membrane is bound to n-Sec1/Munc18. Upon n-Sec1 dissociation, possibly under the control of a Rab GTPase, syntaxin changes from a closed to an open conformation allowing assembly of the ternary syntaxin/VAMP/SNAP-25 SNARE complex (for simplicity,only one coil is shown for SNAP-25). The coiled coil structures 'zip' together in a parallel fashion that is triggered by Ca2+, resulting in membrane fusion. NSF and α-SNAP are then recruited from the cytosol and cause the complex to dissociate upon ATP hydrolysis. The components are then free to be recycled and used in a further round of membrane fusion. *Reproduced from Chen & Scheller, 2001.*

assembly (Hata et al., 1993; Pevsner et al., 1994). There has been genetic and biochemical evidence in support of both positive and negative roles for Sec1 proteins in membrane fusion and their precise roles have not yet been fully elucidated. One attractive model is that they act as regulated inhibitors of SNARE complex assembly by binding to and sequestering syntaxins in a closed, fusion-incompetent conformation until an appropriate signal is received, upon which they dissociate leaving the syntaxins in an open, fusion-competent conformation (Yang et al., 2000; Dulubova et al., 1999).

A few refinements to the SNARE hypothesis have been made in recent years. Firstly, the ATPase NSF (*N*-ethyl-maleimide-sensitive fusion protein) was originally thought to act early on in the fusion process, but it now seems that it is required at a later stage when the SNARE complex is dissassembled (Mayer et al., 1996). In a further refinement to avoid ambiguity arising from homotypic fusion events, SNAREs have been reclassified as R-SNAREs (arginine-containing SNAREs) and Q-SNAREs (glutamine-containing SNAREs) based on the identity of highly conserved residues present in the central ionic interaction layer (Fasshauer et al., 1998). A schematic of the current model for membrane fusion is given in Fig. 1.1.9.

1.1.8 Rab proteins as regulators of membrane traffic

Rab proteins make up the largest subfamily of the Ras superfamily of small molecular weight GTPases, with over 40 human members identified to date. They are key regulators of vesicular membrane traffic, with individual Rabs localised to specific subcellular compartments (see Fig 1.1.10) and governing discrete endocytic and exocytic transport steps (reviewed in Zerial and McBride, 2001). Rabs are doubly geranylgeranylated at their C-termini and this is necessary for membrane association and function (Newman et al., 1992; Farnsworth et al., 1994). While the majority of Rabs are membrane associated, they are also found in the cytosol bound to Rab GDIs (GDP dissociation inhibitors) that sequester them in the GDP-bound inactive state (Sasaki et al., 1990; Ullrich et al., 1993). Rab GDI is then displaced by a GDI-displacement factor (GDF) (Dirac-Svejstrup et al., 1997), allowing membrane association and nucleotide exchange to ensue. It was originally believed that Rab association with transport vesicles and recycling via GDI extraction were of fundamental importance. However, this was brought into question by the finding that the yeast Rab Ypt1 constitutively anchored to the target membrane with transmembrane anchor is still fully functional and cannot be extracted from the membrane by GDI (Ossig et al., 1995).

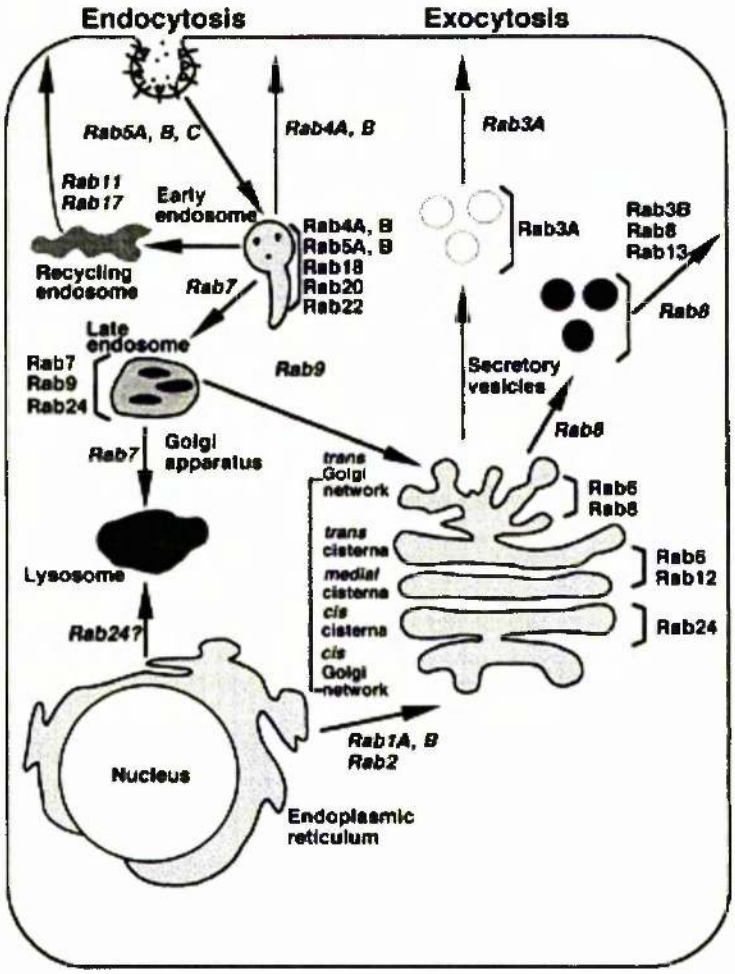

Fig. 1.1.10 **Subcellular distributions of Rab proteins.**

Rab proteins are localised in discrete subcelluar localisations as indicated. Reproduced from Takai et al., 2001

Rabs appear to function in a number of different ways. Firstly, they are believed to contribute substantially to the specificity and fidelity of membrane fusion events. As discussed in the previous section, SNARE interactions can occur promiscuously and at multiple transport steps and are therefore unlikely to confer the specificity of vesicle targeting. The loss of the *Saccharomyces cerevisiae* Rab, Ypt1p, can be suppressed by the overexpression of SNAREs involved in ER to Golgi transport indicating genetic interactions (Lian et al., 1994). Ypt1p has also been shown to activate the t-SNARE Sed5p by promoting the dissociation of the regulatory Sly1p, thus allowing v-/t-SNARE pairing (Lupashin and Waters, 1997). They are believed to recruit factors required for the tethering or docking of vesicles at the target membrane prior to fusion (see Waters and Hughson, 2000). For example, the yeast Rab Sec4p tethers exocytic vesicles to the plasma membrane via a direct interaction with the sec6/sec8 exocyst complex (Guo et al., 1999b). This is an octameric complex present in both yeast (Terbush et al., 1996; Guo et al., 1999a) and mammals (Hsu et al., 1996). It is believed to function in the targeting of vesicles to the plasma membrane in yeast (Terbush et al., 1996) where it is positioned at secretion 'hot-spots' (Finger and Novick, 1998).

In addition, Rab5 regulates the tethering of early endosomes prior to their homotypic fusion through interactions with the early endosomal auto antigen (EEA1) (Christoforidis et al., 1999a; Callaghan et al., 1999). Rab5 is the best studied family member and it interacts with a very large set of effector molecules including Rabaptin 5 (Stenmark et al., 1995), EEA1 (Simonsen et al., 1998) and PI 3-kinases (Christoforidis et al., 1999b). These appear to cluster and function in a feed-forward mechanism whereby Rab5 is sustained in its active conformation. For example, Rabaptin 5 is complexed with Rabex5 which is itself a GEF for Rab5 (Horiuchi et al., 1997). The Rab5-induced activation of PI 3-kinase also increases EEA1 recruitment via PI(3)P/ FYVE domain interactions. This has given rise to the notion of complex "Rab domains" involving multiple effectors and signalling molecules that could be general features in Rab signalling (Zerial and McBride, 2001).

In addition to these vesicle-tethering roles, Rabs are involved in vesicle motility. Rab5 again has been shown to affect the association and motility of endosomes on microtubules (Nielsen et al., 1999) and a direct interaction of Rab6 with a kinesin family member has also been reported (Echard et al., 1998). Furthermore, associations with actin based motor proteins as evidenced by interactions between Rab27a and myosin Va in melanosome motility (Wu et al., 2001), point to regulation of traffic on both microtubule and microfilament tracks.

Yet a third potential role for Rabs in membrane transport is in the budding of vesicles. For example, Rab1 has been implicated in vesicle budding from the ER (Nuoffer et al., 1994), and Rab9 appears to regulate lysosome biogenesis (Riederer et al., 1994). Rab9 has also been shown to positively regulate the association of the TIP47 adaptor with mannose-6-phosphate receptors, thereby facilitating their retrieval from the endosomes to the TGN (Carroll et al., 2001). A role for Rab5 in vesicle formation is also apparent since its overexpression has been shown to increase the rate of endocytosis (Bucci et al., 1992), and Rab5 complexed with GDI is required for ligand sequestration into deeply invaginated clathrin-coated pits in an *in vitro* assay system (McLauchlan et al., 1998).

1.1.9 Lipid metabolism in membrane trafficking

So far I have concentrated on the role of proteins in membrane trafficking events. However, regulation by lipid-based molecules is of equal importance. Phosphoinositides in particular have emerged as central players in membrane traffic (reviewed in Simonsen et al., 2001). The membrane phospholipid phosphatidylinositol (PI) can be phosphorylated by a number of lipid kinases on the 3-, 4- and 5- positions of the inositol ring, giving rise to numerous different phosphoinositides. These have emerged as major second messengers in signal transduction and membrane trafficking pathways and their synthesis and turnover within cells is tightly regulated both temporally and spatially. One pivotal class of enzymes are the PI 3-kinases that produce PI(3)P and PI(3,4,5)P_3. Their importance in membrane trafficking is exemplified by the ability of the PI 3-kinase inhibitor wortmannin to inhibit a number of events such as TfR recycling (Spiro et al., 1996; Martys et al., 1996), fluid-phase endocytosis (Li et al., 1995; Clague et al., 1995) and insulin-stimulated GLUT4 translocation (Cheatham et al., 1994; Haruta et al., 1995). Direct evidence for a role for this class of enzyme in membrane trafficking also came from the discovery that Vps34p, a yeast PI 3-kinase, regulated the transport of carboxypeptidase Y from the Golgi to the vacuole (Schu et al., 1993).

PI (3) P binds directly to FYVE-domain containing proteins and participates in their membrane recruitment (Kutateladze et al., 1999 and references therein). FVYE domains are conserved modules found in numerous trafficking proteins including EEA1, the Rab5 effector involved in early endosome fusion (Stenmark et al., 1996); Hrs, another endosomal protein that plays a role in clathrin recruitment (Raiborg et al., 2001); and Rabip4, a Rab4 effector also implicated in endosomal function (Cormont et al., 2001).

The pleckstrin homology (PH) domain is another protein module regulated by phosphoinositides. It is an important feature common to many proteins including the cytohesin and centaurin families of Arf GTPase guanine nucleotide exchange factors (GEFs) and GTPase activating proteins (GAPs), respectively (see sections 1.3.2 and 1.3.3). The Arf GEFs ARNO cytohesin-1 and GRP1, translocate to the plasma membrane via PH domain interactions with $PI(3,4,5)P_3$ produced by PI 3-kinase (Venkateswarlu et al., 1998a; Venkateswarlu et al., 1998b; Venkateswarlu et al., 1999). Furthermore, $PI(3,4,5)P_3$ or $PI(4,5)P_2$ is required for the nucleotide exchange activity of ARNO and GRP1 on Arf (Santy et al., 1999; Klarlund et al., 1998). This gives rise to multiple feedback loops since, for example, PI(4)P 5-kinases are Arf effectors (Honda et al., 1999; and see section 1.3.4 for more details). Dynamin also has a PH domain that binds $PI(4,5)P_2$ (Zheng et al., 1996) and this is required for its role in endocytosis (Lee et al., 1999; Vallis et al., 1999).

A further recently described PI(3) P-interacting protein domain is the Phox homology or PX-domain (Cheever et al., 2001; Xu et al., 2001; Kanai et al., 2001; Ellson et al., 2001). This was first identified in the $p40^{Phox}$ and $p47^{Phox}$ subunits of NADPH oxidase (Ponting, 1996), but is found in numerous proteins involved in vesicle trafficking such as phospholipase D and sorting nexins. The yeast t-SNARE Vam7 has a PX-domain that is required for trafficking to the yeast vacuole (Cheever et al., 2001). Mammalian sorting nexins (SNXs) are a large family of proteins that are believed to be regulators of early endosomes. For example, overexpression of SNX15 in COS7 cells affects membrane trafficking in the entire endosomal system leading to defects in transferrin endocytosis and TGN38 and furin recycling (Barr et al., 2000).

In addition to regulating specific proteins, lipid-modifying enzymes can affect the properties of membrane bilayers themselves by generating phospholipid asymmetries that may promote membrane curvature in favour of vesicle budding and fusion events. For example, acidic phospholipids, such as phosphatidic acid (PA), may be important during vesicle formation as they promote membrane curvature. Phospholipase D generates PA from phosphatidylcholine (reviewed in Liscovitch et al., 2000). Since it is activated by Arf GTPases, it may couple membrane invagination with Arf-mediated vesicle coat recruitment although this is controversial (see section 1.3.4). Similarly, endophilin I, which localises to the neck of nascent clathrin-coated synaptic vesicles via interactions with dynamin, transfers arachidonic acid to lysophosphatidic acid in a step that is required for scission (Schmidt et al., 1999; see also Barr and Shorter, 2000).

Many proteins involved in clathrin-coated pit formation, such as AP-2, AP180 and synaptotagmins, have been found to interact with phosphoinositides, and in particular $PI(4,5)P_2$, and this may aid their recruitment to the bilayer (reviewed in Cremona and De Camilli, 2001). The inositol-5-phosphatase synaptojanin also plays a critical role in endocytosis. Analysis of neurons from synaptojanin knockout mice revealed an increased number of clathrin-coated vesicles and increased $PI(4,5)P_2$ (Cremona et al., 1999). Since AP-2 binding to CCVs requires $PI(4,5)P_2$ (Beck and Keen, 1991), synaptojanin may participate in the uncoating of CCVs by decreasing the affinity of the adaptor for the membrane.

A genetic screen designed to identify components that interface with Arf function in yeast discovered a role for a protein called Drs2p in regulating membrane traffic out of the Golgi complex (Chen et al., 1999). It seems to be involved in CCV formation at the TGN potentially through aminophospholipid translocase activity that would give rise to membrane lipid asymmetry (Chen et al., 1999).

1.1.10 Green fluorescent protein as a tool for the study of membrane trafficking

The use of green fluorescent protein (GFP), originally cloned from the jellyfish *Aequorea victoria*, and its derivatives represents a major technical advance in cell biology, and one that deserves mentioning here (reviewed in Lippincott-Schwartz et al., 2000; Lippincott-Schwartz et al., 2001). It is an auto-fluorescent molecule that can be fused to other proteins through the use of molecular biological techniques, and has therefore enabled researchers to analyse specific proteins in live cells in real time by fluorescence microscopy. Its use has enlightened us to many aspects of membrane trafficking. For example, the analysis of the COPII component Sec13-GFP has revealed that ER exit sites are extremely long-lived and static structures (Stephens et al., 2000). Similarly, by fusing domains such as pleckstrin homology domains to GFP, transient changes in phosphoinositide generation can be visually monitored.

1.1.11 Defects in membrane trafficking pathways and human disorders

There are many human disorders that result from defects in membrane trafficking pathways. For example, non-insulin dependent Diabetes mellitus (NIDDM), which has

officially been declared an epidemic by the World Health Organisation, is characterised by defects in the trafficking of the insulin regulated glucose transporter GLUT4. In healthy muscle and adipose tissues, insulin induces a rapid translocation of GLUT4 containing vesicles from intracellular sites to the plasma membrane with a concomitant increase in glucose transport (Rea and James, 1997). However, in NIDDM patients GLUT4 translocation is defective resulting in elevated blood glucose levels. The precise molecular basis for this dysfunction is not known but it is likely to involve both insulin signalling and membrane trafficking defects. In addition there are many rare single gene defects that give rise to syndromes such as Hermansky-Pudlak syndrome (mutation of β3A subunit of the AP-3 adaptor) or Griscelli disease (mutation of Rab27) in which membrane trafficking is affected (see Aridor and Hannan, 2000 for a full list).

1.2 The role of the cytoskeleton in membrane trafficking

The architecture and structure of the cell is maintained by a complex and dynamic cytoskeleton that serves as a scaffold for the spatial distribution of organelles and signalling complexes, as well as providing the mechanical force required for cell locomotion and cell division. Major elements of the cytoskeleton can be divided into microtubules, microfilaments (actin filaments) and intermediate filaments and these are continually being nucleated and disassembled in a highly orchestrated manner. Membrane trafficking and the cytoskeleton have in the past been regarded as two quite separate fields of study. However, it is becoming increasingly clear that these two major branches of cell biology are intricately linked and such distinctions may no longer be feasible. In particular, many membrane trafficking events use the cytoskeletal networks as 'tracks' along which vesicles and organelles are carried by molecular motor proteins (Allan and Schroer, 1999). It is generally believed that long distance travel is mediated by microtubule based mechanisms while the actin cytoskeleton facilitates movement over short distances.

1.2.1 The actin cytoskeleton

The actin cytoskeleton consists of microfilaments that are produced by the polymerisation of actin monomers to form dynamic networks that are thought to drive the protrusion of the plasma membrane during such processes as cell spreading, locomotion and phagocytosis. Furthermore, microfilaments are attached to focal adhesion complexes that mediate cellular interactions with the extracellular matrix, thus providing a structural framework for anchored cells. Studies using actin depolymerising drugs, such as cytochalasin D, have revealed defects in numerous trafficking steps although complete inhibition is rarely seen (see Apodaca, 2001). The actin cytoskeleton appears to facititate membrane trafficking through two mechanisms: one by the use of myosin motor proteins tethered to membrane structures, and the other using the *de novo* nucleation of actin filaments as a propulsive force.

Myosins are motor proteins that directly interact with actin filaments and use ATP to move along them in a unidirectional manner. There are 18 different classes of myosin identified to date (Berg et al., 2001) and they regulate many important processes such as muscle contraction, cell motility, cytokinesis and three classes of unconventional mysosins, namely myosins I, V and VI, have been implicated in membrane traffic (reviewed in Tuxworth and Titus, 2000). They all have a highly conserved motor or head domain that

confers the catalytic ATPase activity and actin binding properties, followed by a neck region of variable length. Then there are C-terminal tail regions that are highly divergent between classes and that are believed to influence aspects such as subcellular localisation and cargo binding. Several lines of evidence directly implicate myosins in trafficking events. Firstly, the yeast class I myosin Myo5p is required for endocytosis (Geli and Riezman, 1996). Recent work has also uncovered a role for the mammalian myosin VI in endocytosis since it associates with AP-2 positive clathrin-coated vesicles and inhibits TfR internalisation when its tail is overexpressed in polarised cells (Buss et al., 2001). This is the only known myosin that moves towards the minus ends of actin filaments thus allowing it to travel into the cell from the cell periphery (Wells et al., 1999). In addition, myosin I localises to endosomes and lysosomes, and its overexpression inhibits the transfer of fluid-phase markers between these two organelles (Raposo et al., 1999). The mouse coat colour mutation *dilute* encodes myosin Va, indicating its requirement in melanosome transport (Marks and Seabra, 2001 and references therein). Myosin Vb appears to regulate both the distribution and the function of recycling endosomes, since overexpression of its tail region as a green fluorescent protein chimera causes them to cluster around the centrosome and retain cycling transferrin receptors (Lapierre et al., 2001). Myosin II, the conventional myosin normally associated with muscle contraction and cytokinesis, also appears to have a role in membrane trafficking since it transiently associates with the TGN where it may regulate the budding of a subpopulation of vesicles (reviewed in Stow et al., 1998).

The major factor involved in the nucleation of actin filament assembly is believed to be the Arp2/3 complex: a highly conserved seven-subunit complex at the heart of which are two actin-related proteins Arp2 and Arp3 (Welch, 1999). While the complex appears to be essential for actin assembly, it exhibits only weak activity alone but is potently stimulated by members of the Wiskott-Aldrich syndrome protein (WASP) family (Welch, 1999). WASP is found in an autoinhibited conformation (Kim et al., 2000), and becomes activated by phosphatidylinositol (4,5) bisphosphate and GTP-bound Cdc42 (Rohatgi et al., 1999), a Rho family GTPase that has long been associated with actin remodelling and filopodia formation (Hall, 1998). Some pathogenic microorganisms exploit these mechanisms to invade and move inside host cells. For example, *Listeria monocytogenes* has an ActA protein on its outer membrane that potently stimulates Arp2/3-mediated actin polymerisation, resulting in actin 'comet tails' that physically propel it through the host cytoplasm (Welch et al., 1997). It is now becoming clear that similar mechanisms exist for propelling membrane-bound vesicles (reviewed in Taunton, 2001). For example, actin comet tails have been observed on endosomes and lysosomes following protein kinase C activation in an *in vitro Xenopus* egg extract system (Taunton et al., 2000). Newly formed

pinosomes are also propelled away from their sites of formation by actin polymerisation in mast cells (Merrifield et al., 1999) and in fibroblasts expressing constitutively active Arf6 (Schafer et al., 2000). They have also been implicated in the movement of TGN-derived vesicles containing haemagglutinin protein in cells infected with influenza virus (Rozelle et al., 2000). Given that this protein is exclusively sorted into lipid raft-enriched vesicles and the fact that cholesterol depletion with methyl β-cyclodextrin abrogated actin polymerisation, it seems likely that lipid rafts are important in these events (Rozelle et al., 2000).

1.2.2 The microtubule cytoskeleton

Unlike actin filaments, microtubules seem to be nucleated primarily from one central location in the cell: the microtubule organising centre (MTOC), which corresponds to the spindle pole body in yeast or the centrosome in metazoans. Here α and β tubulin heterodimers are assembled in a process that requires γ tubulin (Jeng and Stearns, 1999). Studies with microtubule-disrupting drugs such as nocodazole have revealed an important role for this cytoskeletal network in the positioning and movement of cellular organelles (for example, see Thyberg and Moskalewski, 1985). Microtubule-based motors provide the mechanism for this important mode of membrane transport. These motors also move in a unidirectional manner and either belong to the kinesin family which move towards the plus ends of microtubules (i.e. away from the MTOC), or the dynein family that move in the opposite direction (see Fig. 1.2.1; reviewed in Hirokawa, 1998). There are potentially hundreds of different variants in eukaryotic cells and each consists of two heavy chains and two light chains, giving rise to rod-like structures with two globular heads that bind microtubules, a stalk, and a more divergent tail made up from the light chains (Hirokawa, 1998). These tails are likely to be involved in cargo recognition and binding, although information as to the identity of motor receptors is sparse. A recent study has, however, identified a direct interaction between the kinesin KIF13A and the β-adaptin subunit of the AP-1 adaptor complex providing the first real evidence linking vesicle formation to vesicle transport machinery (Nakagawa et al., 2000). Studies into the regulation of kinesin activity have uncovered an autoinhibitory regulatory mechanism, whereby the C-terminal domain interacts with the motor domain sequestering it in an inactive conformation (Stock et al., 1999; Coy et al., 1999). Upon cargo binding to the C-terminal tail, this autoinhibition is relieved, a conformational change occurs and the motor domain becomes active (reviewed in Wochlke and Schliwa, 2000). Dynein function in membrane traffic appears to be different; since it relies on an auxilliary complex called the dynactin complex to link it to

its cargo (reviewed in Karki and Holzbaur, 1999). The dynactin complex consists of ten subunits including dynamitin, actin-related protein 1 (Arp1) and $p150^{Glued}$, which binds the dynein intermediate chain (Karki and Holzbaur, 1995). Disruption of the dynactin complex by overexpression of dynamitin causes endosomes and lysosomes to redistribute to the cell periphery (Burkhardt et al., 1997), or to stop moving completely (Valetti et al., 1999). The Arp1 filament of dynactin resembles the short actin filaments associated with spectrin in erythrocytes (Schafer et al., 1994). Spectrin is also found as a meshwork around many intracellular membranes, and it is recruited to membranes by Arf and PH-domain dependent interactions with phospholipids (Godi et al., 1998; reviewed in De Matteis and Morrow, 2000). It has now been directly shown that dynein/dynactin can indeed associate with and move liposomes containing acidic phospholipids via interactions with spectrin (Muresan et al., 2001). Since Arf is well-known to activate lipid kinases and phopholipase D, giving rise to acid phospholipid generation, (see section 1.3.4) and the fact that it recruits spectrin (Godi et al., 1998), could present an appealing model linking vesicle biogenesis to motor recruitment.

In addition to the motor protein complexes themselves, other microtubule-associated proteins (MAPs) may influence membrane transport, by interfering with motor binding or movement along the microtubule. For example, overexpression of the neuronal MAP Tau causes a redistribution of organelles towards the cell centre, suggesting that it blocks plus-end directed travel (Ebneth et al., 1998). These MAPs are themselves regulated by other proteins, such as mapmodulin which competes for microtubule binding thus promoting motor recruitment/motility (Itin et al., 1999). A recent study provided evidence that the γ-adaptin subunit of AP-1 directly interacts with MAPs, since the two could be co-immunoprecipitated from rat brain cytosol and AP-1 could associate with microtubules *in vitro* in the presence of purified MAPs (Orzech et al., 2001). This may be another mechanism whereby nascent vesicles contact the cytoskeleton.

Functional interactions between the actin and microtubule cytoskeletons are apparent. For example, it has been demonstrated that myosin V can directly interact with kinesin in yeast two-hybrid and co-immunoprecipitation experiments (Huang et al., 1999). This provides a potential mechanism for vesicles to switch between actin and microtubule tracks. Also intriguing is the finding that myosin V and dynein share a light chain subunit that allows them to dimerise and may enable them to bind the same cargo receptor (Benashski et al., 1997). In addition, a number of dual microtubule and microfilament associated proteins (MMAPs) have been identified providing evidence that the two networks are physically

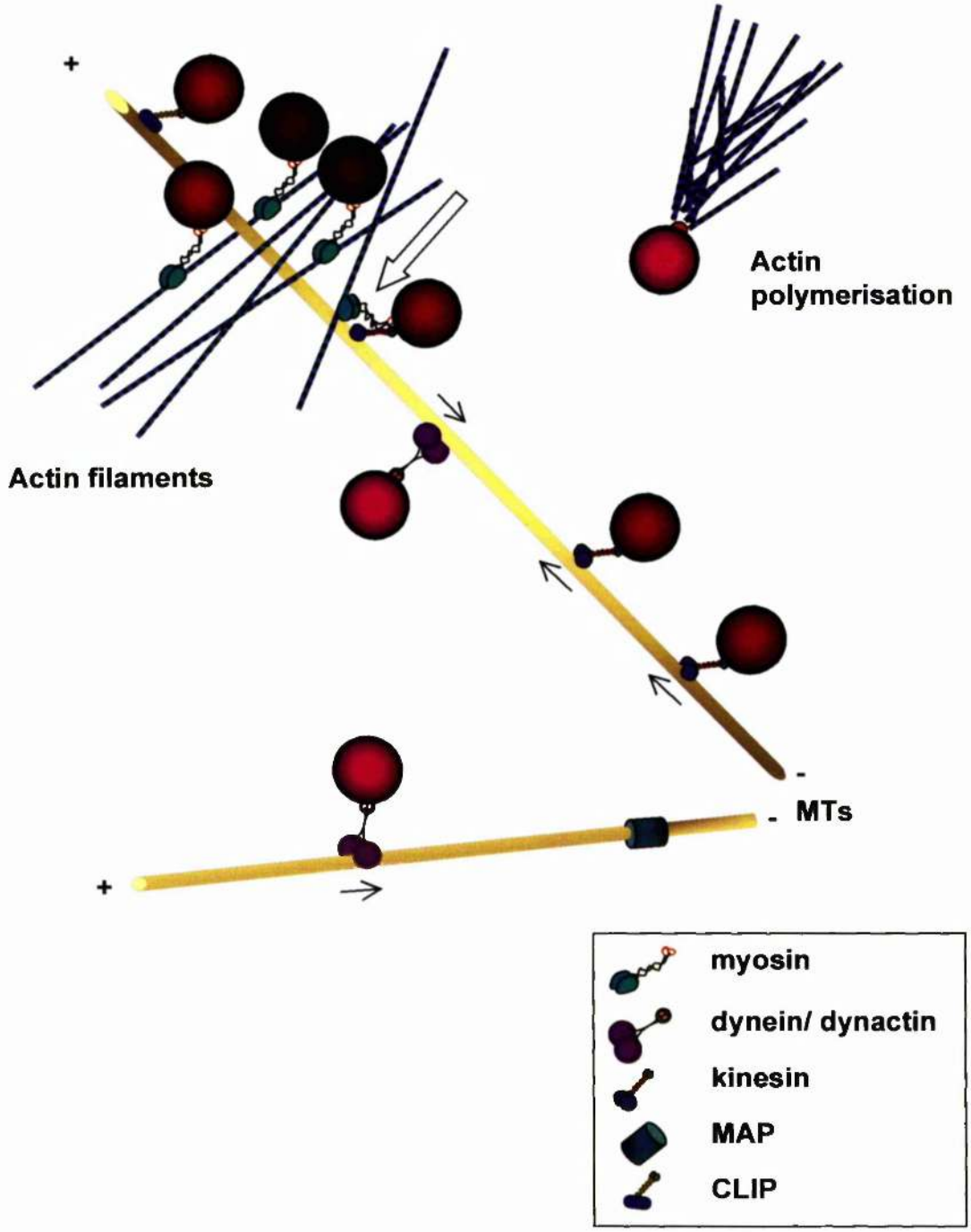

Fig. 1.2.1 **The cytoskeleton and membrane traffic.**

A diagrammatic overview of how the cytoskeleton participates in the movement of vesicles. Membrane-bound vesicles/organelles may be transported along microtubules (MTs) by dynein/dynactin (towards the minus ends) or kinesin (towards the plus ends). Cytoplasmic linker proteins (CLIPs) such as CLIP-170 tether vesicles near the plus ends of MTs, and microtubule associated proteins (MAPs) can block motor protein motility. Movement along actin filaments also occurs, by virtue of myosin motor proteins. *De novo* actin polymerisation (actin 'comet tails') at the surface of vesicles can also provide a propulsive force. Myosins and kinesins have been shown to directly interact (white arrow) potentially allowing vesicles to switch between MT and actin tracks.

linked (Sisson et al., 2000). Similarly, a homologue of CLIP-170, which is believed to link endocytic vesicles to microtubules (Pierre et al., 1992), interacts with an unconventional myosin in *Drosophila* (Lantz and Miller, 1998).

1.2.3 Membrane traffic during mitosis

Mitosis, or M phase of the cell cycle, is the process by which a cell divides to produce two daughter cells each containing exact copies of the parental chromosomal DNA. In addition to nuclear components, other organelles need to be partitioned and packaged into each daughter cell to ensure that the full complement of cellular processes can be carried out. Mitosis can be subdivided into a number of well characterised stages including prophase, metaphase, anaphase, telophase and finally cytokinesis. These pass through a number of checkpoint mechanisms and coincide with dramatic morphological changes that are well described in any textbook. The cytoskeleton plays a very important role during mitosis, not least in the formation of the microtubule based spindle, but also in the acto-myosin contractile mechanism that is required for cytokinesis (see Glotzer, 2001).

However, numerous changes in membrane dynamics are apparent during mitosis. Much work has been performed investigating the Golgi complex in this respect (reviewed in Lowe et al., 1998a; Roth, 1999; Rossanese and Glick, 2001). During the transition from interphase to mitosis, the Golgi apparatus fragments and vesiculates to become scattered throughout the cell (Lucocq and Warren, 1987). This disassembly is believed to involve the continued budding of vesicles that have lost the ability to fuse (see Lowe et al., 1998a and references therein). Endocytosis is also shut down (Warren et al., 1984; Pypaert et al., 1991), and endosome-endosome fusion stops (Tuomikoski et al., 1989; Thomas et al., 1992). Endosomes and lysosomes have been less well studied during the cell cycle but they have been reported to cluster around the microtubule organising centre either during mitosis (Zeligs and Wollman, 1979; Tamaki and Yamashina, 1991; Kaplan et al., 1992; Tooze and Hollinshead, 1992), or 30 minutes after cytokinesis (Bergeland et al., 2001). Many of these events seem to be initiated by mitotic phosphorylation events. For example, Rab4 and Rab5 are phosphorylated *in vitro* by cdc2 (Bailly et al., 1991), a kinase which has been shown to inhibit endosome fusion (Tuomikoski et al., 1989). Indeed Rab4 phosphorylation during mitosis prevents its association with endosomal membranes (Ayad et al., 1997; van der Sluijs et al., 1992a). Golgi fragmentation and reassembly is also regulated by cdc2 kinase phosphorylation of the Golgi matrix protein GM130 (Lowe et al., 1998b). Similarly there are cell cycle-regulated motor proteins implicated in membrane traffic. For example, two have been identified that mediate brefeldin A-induced membrane

tubulation (see section 1.3.2.3) (Robertson and Allan, 2000), and their motor activities and/or microtubule binding is inhibited in metaphase, a stage of the cell cycle when BFA no longer induces tubulation (Robertson and Allan, 2000). Cdc2 kinase has also been shown to phosphorylate the light intermediate chain of cytoplasmic dynein during mitosis, a modification that inhibits dyncin-mediated membrane transport (Dell et al., 2000).

There is now a good body of evidence indicating that cytokinesis requires the delivery and insertion of intracellular membrane to the site of abscission (O'Halloran, 2000; Glotzer, 2001). For example, t-SNAREs of the syntaxin family are required for cytokinesis in diverse organisms including *Arabidopsis thaliana, Caenorhabditis elegans* and *Drosophila melanogaster* (Burgess et al., 1997; Lauber et al., 1997; Jantsch-Plunger and Glotzer, 1999; Conner and Wessel, 1999). Similarly, the Golgi-associated coiled-coil protein Lava Lamp is required for furrow ingression during cellularisaion of the *Drosophila* embryo, a process mechanistically akin to cytokinesis (Sisson et al., 2000). Consistent with a role for Golgi-derived membrane in these processes, BFA treatment also inhibits cellularisation (Sisson et al., 2000)and cytokinesis in the early *C.elegans* embryo (Skop et al., 2001). Clathrin is another membrane trafficking protein implicated in cytokinesis since clathrin-null *Dictyostelium* fail to divide due to problems associated with furrow ingression (Niswonger and O'Halloran, 1997; Gerald et al., 2001).

1.3 The ADP-ribosylation factor family of GTPases

The Ras superfamily of small molecular weight GTPases is subdivided into the Arf, Ras, Rab, Rho and Ran sub-families. These are all GTP-binding proteins of approximately 21 kDa that regulate many diverse cellular processes affecting cell morphology, intracellular trafficking, proliferation, differentiation and apoptosis. One of their hallmarks is that they act as binary switches cycling between inactive GDP-bound and active GTP-bound forms, the latter having a different structure allowing interactions with downstream effector molecules. The mammalian ADP-ribosylation factor (Arf) family consists of six Arf isoforms, more than ten Arf-like (Arl) isoforms (Clark et al., 1993a), Arf domain protein (ARD1) and Sar1 is also a more distantly related member. In yeast there are three Arfs, three Arls, SAR1 and CIN4.

1.3.1 ADP-ribosylation factors

ADP-ribosylation factors (Arf) were originally purified and identified as cofactors for cholera toxin-catalysed ADP-ribosylation of G_s, the heterotrimeric G protein that stimulates adenylyl cyclase (Kahn and Gilman, 1984; Kahn and Gilman, 1986). There are six mammalian isoforms that share >60% sequence identity and these have been sub-divided into three classes based on primary amino acid sequence, size, gene structure and phylogenetic analysis. The main differences between the classes are evident in the extreme N- and C-termini (see Fig. 1.3.1 for an amino acid sequence alignment). Arfs 1-3 constitute the class I enzymes, Arfs 4 and 5 make up class II while Arf6 is the most divergent and hence the sole member of class III (see Fig. 1.3.1). There are three Arf proteins in the yeast *Saccharomyces cerevisiae*. Yeast Arf1 and Arf2 share 96% identity, are most similar to the mammalian class I isoforms and are functionally redundant. They are required for protein secretion (Stearns et al., 1990b), sporulation (Rudge et al., 1998), respiration and mitotic growth (Zhang et al., 1998a). Double knockout of these is lethal, while the deletion of either gene alone has no severe phenotype (Stearns et al., 1990b). Arf2 deletion exhibits a wild-type phenotype, while the removal of the Arf1 gene has been reported to confer slower growth and increased sensitivity to fluoride (Stearns et al., 1990c; Kahn et al., 1995), but this is probably attributable to the fact that Arf1 is expressed at 10 fold higher levels than Arf2 (Stearns et al., 1990b). Yeast Arf3, which exhibits 54% identity with yeast Arf1 and about 60% with mammalian Arf6, is not required for viability and most likely corresponds to a class III isoform (Lee et al., 1994b). Yeast cells do not possess a class II-like isoform, whereas metazoans such as *Caenorhabditis elegans* and *Drosophila*

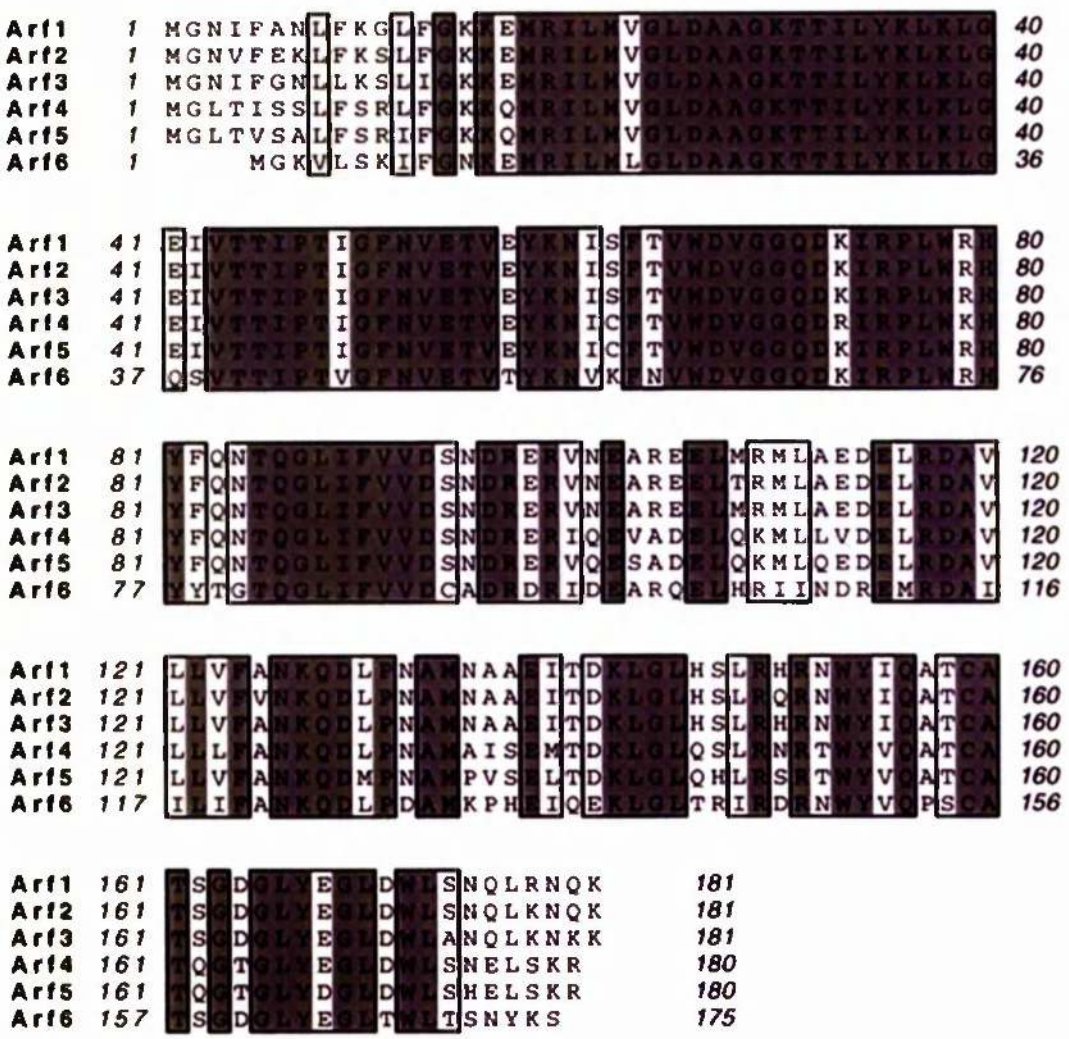

Fig. 1.3.1 **Sequence alignment of mammalian Arf proteins**

The amino acid sequences of human Arfs 1,3,4,5 & 6 are shown together with murine Arf2 (no human Arf2 has yet been discovered). Arfs 1, 2 & 3 are known as class I Arfs, Arfs 4 & 5 make up class II and Arf6, which is the smallest and most divergent, is the sole member of class III.

melanogaster have at least one orthologue from each class (Lee et al., 1994a). Arfs are well conserved between species and this is exemplified by the finding that isoforms from many species including *Drosophila* (Murtagh et al., 1993) and *Giardia* (Lee et al., 1992) can restore vegetative growth to *arf1⁻arf2⁻* mutants. There also appears to be a high degree of redundancy or overlapping function between classes since, for example, this rescue can be achieved by any of the 6 mammalian Arfs.

Arfs have an N-terminal extension of about 17 amino acids that is not found in Ras. This folds into an amphipathic helix and is buried in a hydrophobic pocket at the surface of the core domain of Arf1-GDP (Amor et al., 1994; Greasley et al., 1995). Also unlike Ras, Arfs are myristoylated at their N-termini on the position 2 glycine and this is essential for function since a mutation of the glycine to alanine behaves as a null allele in yeast (Kahn et al., 1995) and produces an inactive protein in mammalian cells (D'Souza-Schorey and Stahl, 1995). The myristoyl moiety contributes to membrane insertion (Amor et al., 1994), as do hydrophobic residues within the N-terminal alpha helix, which only become exposed in the GTP-bound state (Antonny et al., 1997). Arf1 has a greater affinity for GDP than for GTPγS in the absence of phospholipids, and this is reversed upon addition of phospholipids. Since this is the case for myristoylated but not non-myristoylated Arf1, it implies that the lipid modification acts as a phospholipid switch ensuring activation only when in the correct environment at the membrane (Randazzo et al., 1995).

The Arf switch regions are the major sites of interaction with regulators and effectors, but these have almost identical amino acid sequences between isoforms. The structures of both Arf1 (Amor et al., 1994; Greasley et al., 1995) and Arf6 (Menetrey et al., 2000; Pasqualato et al., 2001) bound to GTP and GDP (or their analogues) have recently been solved (see Fig. 1.3.2). Interestingly, this has revealed that the GTP-bound conformations are more similar than the GDP-bound conformations suggesting that the switch regions probably only confer specific interactions in the inactive state (Pasqualato et al., 2001). This suggests that active Arfs may elicit specific functions more on the basis of their cellular context than on unique structural determinants.

1.3.2 Arf guanine nucleotide exchange factors

As with all Ras-like proteins, the Arf GTPase cycle is regulated by other accessory proteins. Among these are guanine nucleotide exchange factors (GEFs) that serve to activate the Arfs by catalysing the exchange of GDP for GTP. These all contain a

characteristic 200 amino acid Sec7 domain first identified in yeast Sec7p (Achstetter et al., 1988) that acts as the minimum catalytic domain. A role for these Sec7-related proteins in

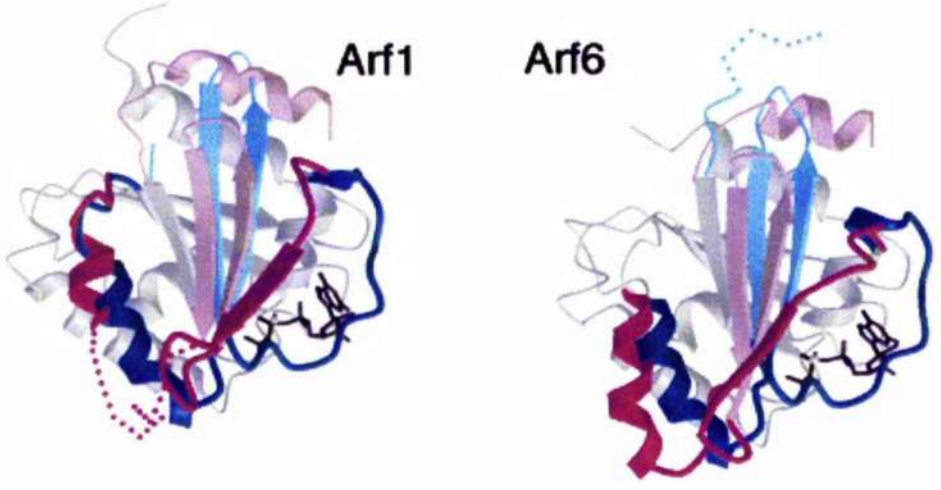

Fig. 1.3.2 **Structures of Arf1 and Arf6.**

Shown are the crystal structures of both Arf 1 and Ar6 in both the GDP-bound (in purple) and the GTP-bound (in dark blue) conformations. The switch I and II regions are in dark shades and other switch elements are in light shades. The dotted lines represent flexible regions. Note that the GTP-bound conformations appear more similar while the GDP-bound conformations appear most different. *Reproduced from Pasqualato et al., 2001.*

Arf function has been demonstrated genetically by the finding that human Arf4 expression rescues mutant Sec7 phenotype in *Saccharomyces cerevisiae* (Deitz et al., 1996). Biochemical analysis of the Sec7 domain itself has revealed that is has a groove containing mainly exposed hydrophobic residues that binds to the switch I and II regions of Arf1 (Beraud-Dufour et al., 1998; Betz et al., 1998; Cherfils et al., 1998; Goldberg, 1998; Mossessova et al., 1998). As this happens, a critical Sec7 domain glutamate residue probably destabilises GDP by displacing Mg^{2+} allowing rapid nucleotide exchange to ensue (Beraud-Dufour et al., 1998). The net result is a dramatic conformational change in which the myristoylated N-terminus of Arf1 becomes exposed as it binds to GTP.

1.3.2.1 High molecular weight GEFs

Arf GEFs can be broadly separated into two groups: high molecular weight GEFs and low molecular weight GEFs (see Fig. 1.3.3). The former includes yeast Gea1/2 (Peyroche et al., 1996; Peyroche et al., 2001), Sec7p (Achstetter et al., 1988) and mammalian GBF1 (Claude et al., 1999)and BIG1/2 (Yamaji et al., 2000). With the exception of GBF1, these are all sensitive to the fungal metabolite brefeldin A (BFA; see below) and function primarily in the ER/Golgi system. These large GEFs are cytosolic proteins that are able to associate with membranes. However, it is not presently known how they achieve this.

In yeast, Sec7p was first identified by Novick and Schekman in a screen for mutants defective in secretion (Novick et al., 1980). *GEA1* and *GEA2* are 50% homologous and exhibit functional redundancy since deletion of either gene alone has no detectable phenotype, while a double knockout strain is not viable (Peyroche et al., 1996). *SEC7* is also necessary for viability (Achstetter et al., 1988) indicating that Sec7p and Gea1p/Gea2p have distinct functions.

Mammalian BIG1 and BIG2 are two closely related Arf GEFs that colocalise in HeLa cells in punctate cytosolic and peri-nuclear/Golgi regions. Furthermore, they co-purify in a large ~700 kDa complex (Yamaji et al., 2000). *In vitro*, they exhibit GEF activity towards class I and II Arfs, but not Arf6 (Morinaga et al., 1999; Togawa et al., 1999).

Claude et al. (1999) used expression cloning to select cDNAs whose overexpressed products would allow Brefeldin A-sensitive 293 cells to grow in the presence of BFA. For this they used a cDNA library from a BFA-resistant CHO cell line and identified GBF1, which they discovered was a BFA-resistant Sec7-domain containing Arf GEF (Claude et al., 1999). It is a 205 kDa protein that is localised to the Golgi region where it colocalises

with the coatomer subunit β-COP. Intriguingly, GBF1 does not exhibit exchange activity towards the class I Arfs but is the only GEF to show specificity towards Arf5, suggestive of a specific Arf5 pathway (Claude et al., 1999).

1.3.2.2 Low molecular weight GEFs

In contrast to the larger GEFs, the low molecular weight GEFs are BFA-resistant, contain coiled coil and pleckstrin homology (PH) domains, and seem to function more in the endosomal/ plasma membrane systems. They are also absent from the *S. cerevisiae* genome suggesting that they perform functions unique to higher eukaryotes. They include cytohesins, ARNO (Arf nucleotide binding site opener), GRP1/ARNO3 and EFA6. While most of these appear to have *in vitro* GEF activity towards all Arf isoforms, EFA6 is unique in that it is specific for Arf6 (Franco et al., 1999). ARNO, cytohesin-1 and GRP1 seem to prefer the class I Arfs as *in vitro* substrates (Macia et al., 2001; Klarlund et al., 1998), but they may be important regulators of Arf6 *in vivo*. For example, transient expression of GFP-ARNO in HeLa cells augments the ability of epidermal growth factor (EGF) to induce Arf6 redistribution, while Arf1 and Arf5 are unaffected (Venkateswarlu and Cullen, 2000). Similarly, overexpression of GRP1 in mammalian cells resulted in a greater increase in Arf6-GTP than Arf1-GTP, as determined by direct analysis of nucleotides associated with Arfs immunoprecipitated from ^{32}P-orthophosphate-labelled cells (Langille et al., 1999). On the other hand others have reported that ARNO and ARNO3/GRP1 overexpression fragments the Golgi and inhibits secretion without affecting the endocytic pathway (Franco et al., 1998; Monier et al., 1998), suggesting effects on Arfs other than Arf6. Similarly, chimeric proteins consisting of the N-terminal coiled-coil domains of ARNO, ARNO3 and GRP1 fused to GFP are efficiently targeted to the Golgi apparatus (Lee and Pohajdak, 2000). Thus, the *in vivo* isoform specificity of these GEFs is questionable.

EFA6 localises to the plasma membrane and, when overexpressed, it induces actin-based membrane ruffles that can be inhibited by co-expression of dominant negative mutants of Arf6 and Rac1 (Franco et al., 1999). Overexpression also specifically induces a redistribution of transferrin receptors to the plasma membrane (Franco et al., 1999), in a manner reminiscent of expression of the Arf6Q67L mutant (D'Souza-Schorey et al., 1995). EFA6 also contains proline-rich domains that may mediate protein-protein interactions with as yet unidentified binding partners.

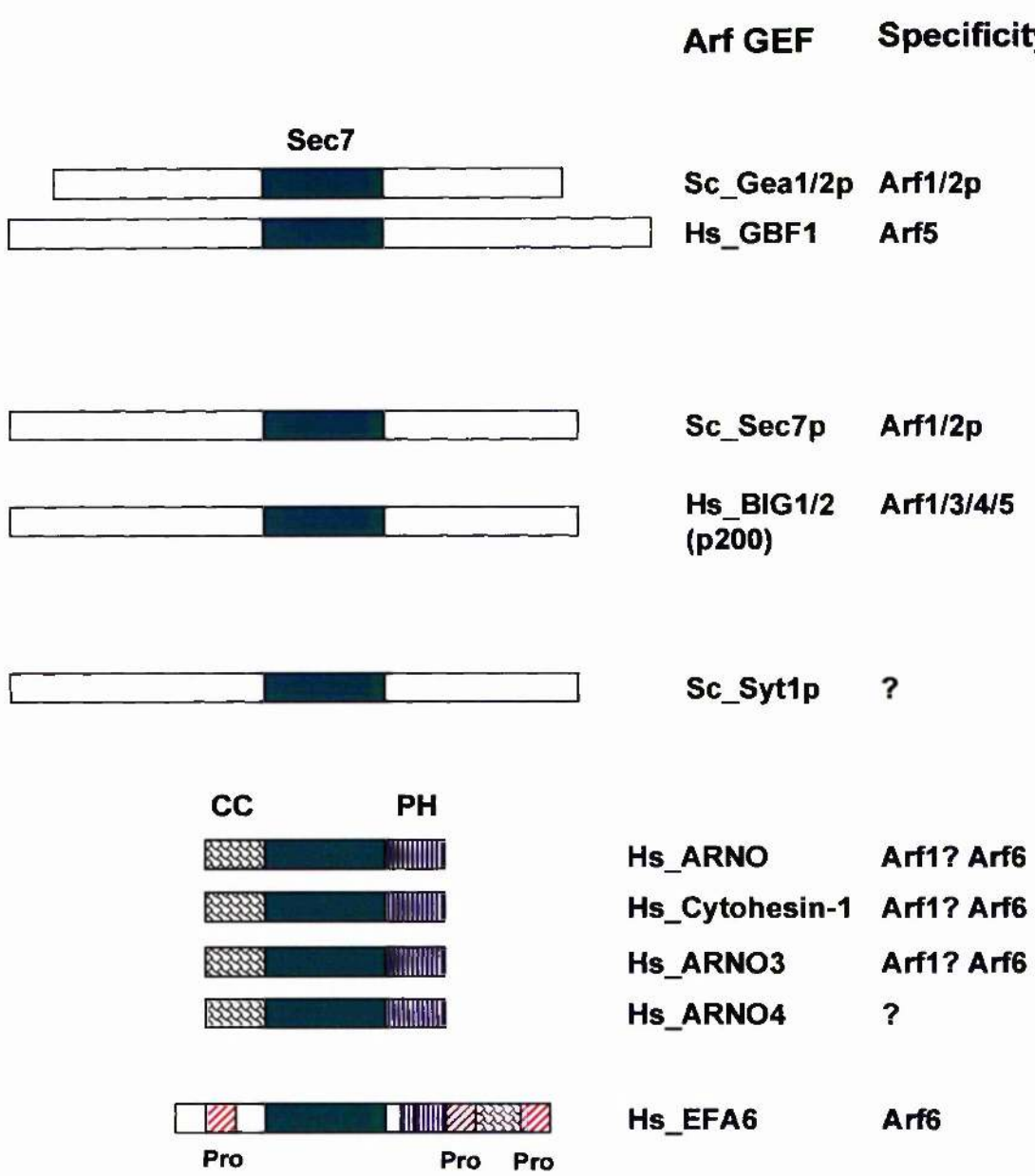

Fig. 1.3.3 **Arf Guanine nucleotide exchange factors (GEFs).**

Shown are the known human (Hs) and budding yeast (Sc) guanine nucleotide exchange factors for Arfs. They all contain a characteristic Sec7 domain that is necessary and sufficient for enzymatic activity. In addition, the small mammalian GEFs have pleckstrin homology (PH) domains and coiled-coil (CC) regions. EFA6 also has proline rich sequences. The Arf isoform specificities are shown where known. All of the large GEFs except GBF1 are brefeldin A-sensitive, while the exchange activities of the smaller GEFs and GBF1 are resistant to the drug. *Adapted from Donaldson & Jackson, 2000.*

The PH domains of the small Arf GEFs promote GEF activity and mediate associations with specific membrane sites in response to the generation of phosphoinositides (for reviews see Jackson and Casanova, 2000; Jackson et al., 2000). PH domain-dependent translocation to the plasma membrane, in response to elevated levels of $PI(3,4,5)P_3$, has been observed for ARNO (Venkateswarlu et al., 1998b) and cytohesin-1 (Venkateswarlu et al., 1999). Indeed in this respect, the GFP-ARNO-PH domain is a useful *in vivo* tool for monitoring $PI(3,4,5)P_3$ generation and hence PI3 kinase activation. The PH domain of EFA6 is slightly different in that it recognises $PI(4,5)P_2$ as well as $PI(3,4,5)P_3$ which may explain why it is more constitutively membrane associated (Jackson and Casanova, 2000).

1.3.2.3 Brefeldin A

Brefeldin A (BFA) is a small hydrophobic molecule produced by toxic fungi that is a potent inhibitor of protein secretion (Klausner et al., 1992). It does this by interfering with GDP/GTP exchange on Arf (Donaldson et al., 1992; Helms and Rothman, 1992). Recent structural studies have shown that BFA stabilises an abortive Sec7 domain/Arf-GDP complex by preventing the switch regions of Arf1-GDP from reorganising and contacting the Sec7 domain catalytic 'glutamic finger' (Peyroche et al., 1999; Robineau et al., 2000). BFA treatment causes Golgi resident proteins to redistribute into the ER (Lippincott-Schwartz et al., 1989). It can also induce membrane tubulation in endosomes, lysosomes and the TGN (Lippincott-Schwartz et al., 1991), and appears to affect vesicle budding in late secretory steps (Simon et al., 1996; Wood et al., 1991). Indeed many proteins peripherally associated with the Golgi disassociate upon BFA treatment (Kooy et al., 1992; Podos et al., 1994; Misumi et al., 1997) and it is not clear whether this is due to a direct requirement for Arf in Golgi localisation or whether it is an indirect consequence of alterations in Golgi structure and function. In addition, BFA probably has other non-Arf-mediated effects, such as via the 50 kDa protein Brefeldin A-ADP-ribosylated substrate (BARS50) (Silletta et al., 1997), or via Arl1 which also appears to be BFA-sensitive (Van Valkenburgh et al., 2001). Caution should therefore be used when ascribing an Arf function based on BFA inhibition. Similarly, since some Arf GEFs such as GBF1, EFA6 and ARNO are BFA-resistant, Arf functions cannot be ruled out based on the lack of BFA inhibition.

1.3.3 Arf GTPase activating proteins

In order for Arf signals to be switched off, the bound GTP nucleotide needs to be hydrolysed to GDP. In contrast to many other Ras superfamily GTPases, purified Arfs have virtually undetectable intrinsic GTPase activity so they rely exclusively on other proteins termed GTPase activating proteins (GAPs) to catalyse this reaction (reviewed in Donaldson & Jackson, 2000). The Arf GAP family is rapidly expanding with many new members having been identified in the last few years and this has become quite an intense area of research. The family includes the yeast proteins Gcs1 and Glo3 and mammalian ARFGAP1, centaurin α, ASAP1 and PAP, Git1 and Git2 (also known as Cat1 and Cat2) and Pkl (see Fig. 1.3.4). They all contain a characteristic GAP domain of about 70 amino acid residues that contains a zinc finger motif, CxxCx(16-17)CxxC (where C is cysteine and x represents any amino acid), that is critical for GAP activity (Cukierman et al., 1995). There is also a conserved arginine within the GAP domain, mutation of which results in a 100,000 fold decrease in activity (Mandiyan et al., 1999; Randazzo et al., 2000). Interestingly, many Arf GAPs also possess other features such as PH domains, src homology 3 (SH3) domains and ankyrin repeats (reviewed in Donaldson and Jackson, 2000). They have also been shown to interact with actin-regulating and integrin-binding proteins, suggesting that they may function at the interface of signalling, trafficking and cytoskeletal systems (Turner et al., 2001). Indeed, with the notable exception of ARFGAP1, which localises to the Golgi (Cukierman et al., 1995), many mammalian GAPs have been found at the plasma membrane, where they might be predicted to act on Arf6. In addition, many have been shown to bind paxillin, an adaptor protein in integrin signalling (reviewed in Turner et al., 2001). Indeed overexpression of the Arf GAPs PAPα and Git2-short, but not their respective GAP-inactive mutants, leads to a decrease in paxillin recruitment to peripheral focal adhesions (Kondo et al., 2000; Mazaki et al., 2001). This correlates nicely with the earlier finding that activated Arf1 recruits paxillin to focal adhesions (Norman et al., 1998). Similarly, the Arf GAP ASAP1 has been shown to alter the morphology of focal adhesions and to inhibit cell spreading when overexpressed, and this is reversed upon expression of a GAP domain mutant (Randazzo et al., 2000). Since this protein also binds Src, $PI(4,5)P_2$ and FAK, it is likely that ASAP1 co-ordinates multiple signalling pathways in the control of cortical actin rearrangements, with Arf protein signalling being central to this (Randazzo et al., 2000). Based on these findings, together with its localisation and observations regarding Arf6 (see below), it seems likely that Arf6 is the *in vivo* target for ASAP1, although *in vitro* it seems to prefer Arf1 and Arf5 as substrates (Brown et al., 1998). As with the GEFs, differences in phospholipid

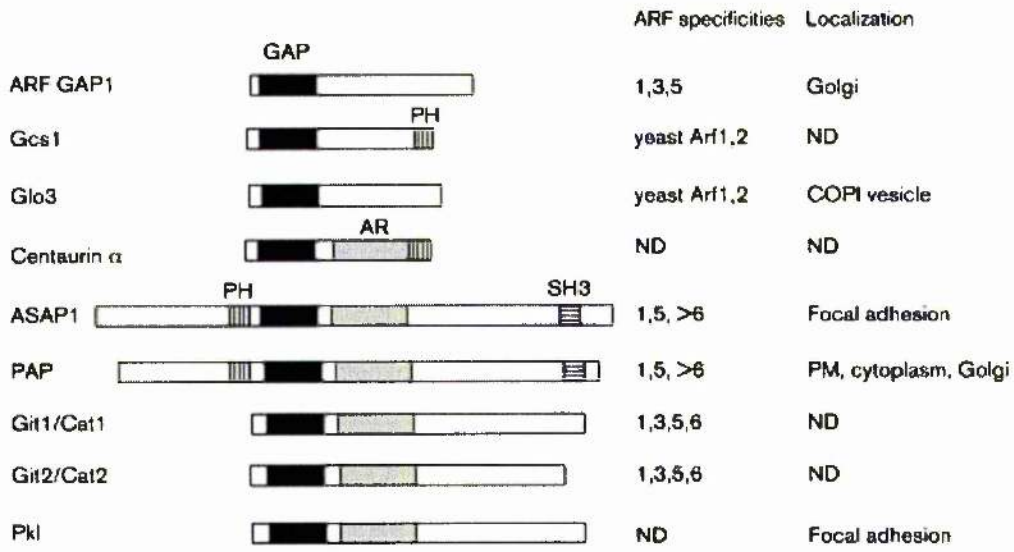

Fig. 1.3.4 **Arf GTPase activating proteins (GAPs).**

Shown are the known mammalian and budding yeast GTPase activating proteins for Arfs. They all contain a characteristic GAP domain (black) domain that contains a critical zinc finger motif. In addition, some have pleckstrin homology (PH) domains (vertical stripes), Src homology 3 (SH3) domains (horizontal stripes) and ankyrin repeats (AR; grey boxes). The Arf specificities and subcellular localisations are indicated. ND: not determined. *Reproduced from Donaldson & Jackson, 2000.*

dependencies exist between GAPs, implying that specific ones operate downstream of distinct signals. For example, ARFGAP1 and ARFGAP2 activities are stimulated by varying degrees by $PI(4,5)P_2$ (Randazzo, 1997b), while the GIT family GAPs are stimulated by $PI(3,4,5)P_3$ suggesting that they function downstream of PI3 kinase (Vitale et al., 2000b).

The crystal structure of the GAP domain of ARFGAP1 complexed with Arf1-GDP has been published (Goldberg, 1999). This revealed that the GAP domain made contacts with Arf1 at sites distant from the GTP binding pocket, implying that other molecules or effectors might participate in the GTP hydrolysis reaction. Indeed this does seem to be the case since coatomer greatly enhances the GAP activity of ARFGAP1 *in vitro* (Goldberg, 1999), while GGAs appear to delay the reaction *in vivo* (Puertollano et al., 2001b). It is likely that many Arf GAPs function as Arf effectors in addition to regulating the GTPase cycle. Consistent with this notion, it was found that the yeast homologue of ARFGAPs, Gcs1 was found to act as a suppressor of the loss of Arf function along with three other SAT proteins (Suppressors of Arf ts) (Zhang et al., 1998a).

1.3.4 Functions and effectors of Arf proteins

1.3.4.1 Vesicle coat proteins

Elucidating the functions of Arf proteins has been a remarkably intense area of research. Most attention has been on the class I isoforms, and Arf1 in particular, although the class III isoform Arf6 has also attracted much interest. By contrast, virtually nothing is known about the function of the class II Arfs, Arf4 and Arf5. As previously mentioned, Arf1 was found to be a component of the coatomer protein coat found on vesicles produced from isolated Golgi membranes and was subsequently found to be required for the formation of these vesicles, termed COPI vesicles (Palmer et al., 1993; Rothman and Wieland, 1996). *In vivo* evidence for a role for Arf1 in coatomer function came from yeast genetic studies whereby *arf1Δ* null mutations combined with mutations in coatomer subunits resulted in synthetic growth defects while the same *arf1Δ* null combined with other *sec* mutations did not (Stearns et al., 1990c; Gaynor et al., 1998). *In vitro* biochemical assays have also shown that Arf1 and coatomer subunits are the only cytosolic components required for the formation of COPI-coated vesicles from Golgi membranes (Orci et al., 1993). Similarly, Arf1 lacking the first 17 residues has been shown to directly bind the coatomer complex *in vitro* (Goldberg, 1999) and specifically β-COP and ε-COP in the yeast two-hybrid system (Eugster et al., 2000).

Since the initial studies on COPI, Arfs have been implicated in clathrin coated vesicle formation mediated by AP-1 (Stamnes and Rothman, 1993; Traub et al., 1993; West et al., 1997; Zhu et al., 1999), and AP-3 adaptor protein complexes (Ooi et al., 1998). The binding of AP-1 to Golgi membranes *in vitro* is dependent on Arf1 loaded with GTPγS (Stamnes and Rothman, 1993; Traub et al., 1993), and direct GTP-dependent interactions between Arf1 and AP-1 have been documented (Austin et al., 2000). Recent studies have also shown them to be important in the assembly of clathrin-coated vesicles mediated by GGA proteins, the novel class of clathrin adaptors (Boman et al., 2000; Puertollano et al., 2001b; reviewed in Robinson and Bonifacino, 2001). Furthermore, a screen in *Saccharomyces cerevisiae* for mutations exhibiting synthetic lethality with an *Arf1*Δ allele identified a mutation in the clathrin heavy chain gene, providing *in vivo* genetic evidence of Arf function in clathrin coat assembly (Chen and Graham, 1998).

1.3.4.2 Phospholipase D

In addition to the cofactor activity in the ADP-ribosylation of G_s, Arfs are all potent activators of phospholipase D (PLD) (Brown et al., 1993; Cockcroft et al., 1994). This finding raised the possibility of an alternative model for the role of Arf in membrane budding and fission. PLD catalyses the conversion of phosphatidylcholine to phosphatidic acid (reviewed in Liscovitch et al., 2000), the latter increasing membrane fluidity and having the propensity to promote membrane curvature. An *in vitro* assay whereby ethanol was used to competitively inhibit PLD activity revealed that COPI-coated vesicle formation on Golgi membranes could be inhibited in the presence of Arf, and that bacterial PLD could stimulate coatomer binding in the absence of Arf (Ktistakis et al., 1996). This led to the proposal that PLD activation mediated the action of Arfs on vesicle formation (Ktistakis et al., 1996). However, this now seems implausible for a number of reasons. Firstly, there is no Arf-regulated PLD activity in yeast (Rudge et al., 1998) and yet Arf mutants exhibit the same phenotypes in both yeast and mammalian cells. Secondly, Arf mutants defective in PLD activation can still recruit coatomer and produce profound morphological effects on the Golgi complex (Kuai et al., 2000). Thirdly, PLD inhibition using neomycin has no effect on Arf-dependent AP-1 recruitment to the TGN, although it does block AP-2 recruitment to the plasma membrane and endosomes (West et al., 1997). So, while PLD activation may explain some Arf effects, it certainly cannot account for all of them and the precise relationship between Arfs and PLD remains elusive.

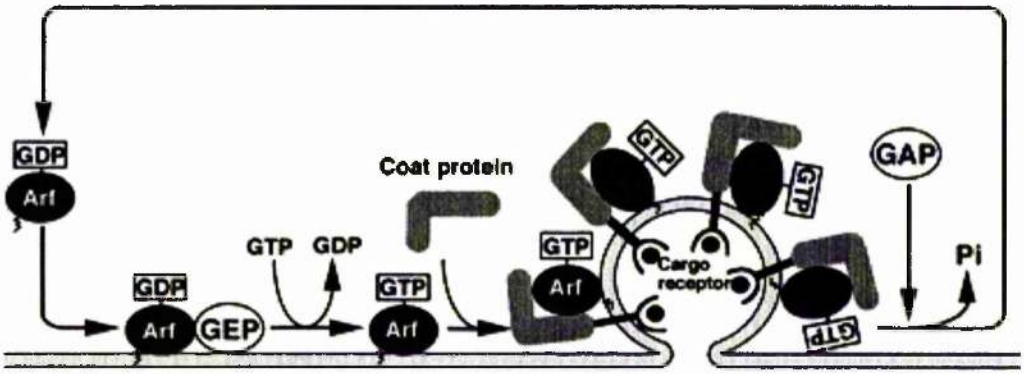

Fig. 1.3.5 **The Arf cycle during vesicle biogenesis.**

Cytosolic, inactive Arf-GDP is recruited to membrane sites during the nucleotide exchange catalysed by Sec7-domain containing guanine nucleotide exchange proteins (GEPs). Arf-GTP binds to cytosolic coat proteins that assemble and polymerise at the membrane where they also interact with specific cargo receptors. The energy of polymerisation is sufficient to deform the membrane and drive the budding process. GTPase activating proteins (GAPs) trigger the GTP hydrolysis on Arf, reverting it to the inactive GDP-bound conformation. GTP hydrolysis contributes to the uncoating of the newly formed vesicle. *Reproduced from Takai et al., 2001.*

1.3.4.3 Phosphatidylinositol 4-phosphate 5-kinases

Another class of recently identified Arf effectors are phosphatidylinositol 4-phosphate 5-kinases (PI(4)P 5-kinases). These enzymes produce the lipid second messenger $PI(4,5)P_2$ by phosphorylating the 5-position of PI(4)P and at least three isoforms are known; α, β and γ (Ishihara et al., 1996; Ishihara et al., 1998). $PI(4,5)P_2$ is crucial for many cellular processes (for reviews see Toker, 1998; Martin, 2001). These include the regulation of the actin cytoskeleton through interactions with actin-binding proteins (Janmey and Stossel, 1987; Fukami et al., 1992) and by stimulating actin polymerisation, for example via the activation of N-WASP (Ma et al., 1998; Miki et al., 1996). It is also a key modulator of endocytosis since it interacts with ENTH (epsin N-terminal homology) domains present in many proteins of the endocytic machinery, and the AP-2 adaptor requires $PI(4,5)P_2$ to bind to the plasma membrane (Beck and Keen, 1991). Importantly, $PI(4,5)P_2$ is also directly involved in Arf GTPase cycles since it stimulates some of the guanine nucleotide exchange factors (Terui et al., 1994) and GTPase-activating proteins (Kam et al., 2000; Randazzo, 1997b; Randazzo and Kahn, 1994), as well as directly interacting with Arf itself (Randazzo, 1997a). By assaying recombinant mouse PI(4)P 5-kinase α activity in the presence of bovine brain cytosol sequentially fractionated by column chromatography, Honda et al. (1999) purified Arf1 and Arf3 as the most abundant upstream activators of the enzyme. This is a particularly interesting finding because PI(4)P 5-kinase activity is also dependent on phosphatidic acid (see Honda et al., 1999 and references therein), the product of PLD enzymes, which are themselves activated by Arfs (Cockcroft et al., 1994; Brown et al., 1993). Subsequent experiments showed that in transfected HeLa cells, PI(4)P 5-kinase colocalised with HA-tagged Arf6 but not Arf1 or Arf5, and that Arf6 recruited the lipid kinase to plasma membrane suggesting that it is the *in vivo* activator. Another study using an *in vitro* system consisting of liposomes, PI(4)P 5-kinase, ARNO, Arf1 and guanine nucleotides showed that the stimulation by Arf is direct and not via PLD (Jones et al., 2000). However, epitope tagged PI(4)P 5-kinase and PLD isoforms can be co-immunoprecipitated from cells co-expressing them, and PLD2 activity is enhanced by the expression of PI(4)P 5-kinase (Divecha et al., 2000). So it seems likely that there is a complex relationship between Arfs, PLDs and PI(4)P 5-kinases involving multiple positive and negative feedback mechanisms.

1.3.4.4 Spectrin and actin assembly

Spectrin and ankyrin assembly onto Golgi membranes is stimulated by GTPγS in an Arf-dependent manner as evidenced by immunodepletion and add-back experiments using an

in vitro assay (Godi et al., 1998). Furthermore, this is dependent on Arf-stimulated $PI(4,5)P_2$ generation which interacts with spectrin PH domains (Godi et al., 1998). Spectrin is best known for its role in maintaining the structural integrity of the erythrocyte cortical cytoskeleton, and its role at the Golgi could be analogous. Arf-regulated Golgi spectrin might actively participate in vesicular transport. This is supported by the finding that disruption of the spectrin cytoskeleton by expression of the Golgi targeting domains of spectrin inhibits the transport of the Na/K-ATPase and vesicular stomatitis virus-G protein from the ER to the Golgi (Devarajan et al., 1997). Spectrin can also directly bind the ARP1 component of the dynactin complex and may therefore be a link between membranes and dyncin microtubule motor proteins (Holleran et al., 1996). Arf has also been shown to assemble at least two distinct pools of actin onto Golgi membranes in a GTP-dependent manner (Fucini et al., 2000). One pool was found to be sensitive to salt extraction and cytochalasin D treatment, while the other was insensitive to both (Fucini et al., 2000). Furthermore, the sensitive pool co-fractionated with COPI-coated vesicles and these were more readily removed from Golgi membranes by high salt following cytochalasin D treatment, suggesting that Arf-dependent actin plays a role in linking COPI-vesicles to the Golgi (Fucini et al., 2000).

1.3.4.5 Arfaptins

Among the first proteins found to be direct binding partners of activated Arfs were Arfaptins 1 and 2 (Kanoh et al., 1997). They were identified in a yeast two-hybrid screen using a "GTP-locked" Arf3Q71L mutant as bait and both interacted specifically with GTP-bound Arfs in *in vitro* assays. These share 60% identity and a truncated form of Arfaptin 2 lacking the first 38 amino acids had been previously identified as a Rac1-GTP interacting protein called POR1 (van Aelst et al., 1996). POR1 has been shown to coordinate rearrangements of the cortical actin cytoskeletal mediated by Arf6 and Rac1 (D'Souza-Schorey et al., 1997). However, it binds much more tightly to class I Arfs than to Arf6 and may, therefore, function downstream of these isoforms as well (Kanoh et al., 1997; Shin and Exton, 2001; Tarricone et al., 2001). Arfaptin 1 has been less well studied but appears to localise to the Golgi in immunofluorescence experiments and associates with intracellular membranes in the presence of Arf and GTPγS (Kanoh et al., 1997). Arfaptin 1 has also been reported to inhibit Arf-mediated PLD activity *in vitro* (Tsai et al., 1998) and in cells overexpressing the protein where a modest inhibition of ER/Golgi transport was also documented (Williger et al., 1999). However, its precise cellular function is yet to be determined.

1.3.4.6 Mitotic kinesin-like protein

Mitotic kinesin like protein (MKLP1) was also recently identified as a putative Arf effector (Boman et al., 1999). The C-terminal tail domain was recovered from a yeast two-hybrid screen using Arf3Q71L as bait, although it was later found that all six Arf isoforms interacted equally well. The mysristoylated N-terminal alpha-helix of Arf3 was not required for the interaction since a mutant lacking the first 13 amino acids still interacted in the two-hybid system (Boman et al., 1999). *In vitro* biochemical assays were also performed to confirm the validity and GTP-dependence of the interactions. MKLP1 is best known for its role during cytokinesis, where it appears to be a core component of the central spindle (reviewed in Glotzer, 2001). It has an amino terminal kinesin motor domain and exhibits plus-end directed motility (Nislow et al., 1992), and it can cross-link microtubules in anti-parallel bundles via two microtubule binding sites (Nislow et al., 1992). Mutants of the *Drosophila* and *C. elegans* homologues, *pavarotti* and ZEN-4, respectively, show spindle and cytokinetic defects (Adams et al., 1998; Powers et al., 1998; Raich et al., 1998). The protein is found in the nucleus in interphase cells, at the spindle poles during metaphase, and concentrates at the midbody and on the midzone microtubules during anaphase (Nislow et al., 1992; Sellitto and Kuriyama, 1988). Moreover, MKLP1 has also been shown to co-immunoprecipitate with Polo kinase (Lee et al., 1995), a cell-cycle regulated kinase required for cytokinesis (Carmena et al., 1998; Nigg, 1998). The significance of the Arf/MKLP1 interaction is currently unknown, but it may be an event that occurs transiently at a specific stage of the cell cycle.

1.3.4.7 Arfophilin

Arfophilin is another putative Arf effector identified by the yeast two-hybrid system (Shin et al., 1999). Importantly, it was found to specifically interact with the GTP-bound form of Arf5, and did not interact with class I Arf isoforms. Subsequent experiments by the same investigators have recently revealed that Arfophilin also interacts with Arf6 in glutathione S-transferase (GST) pulldown experiments, although possibly via a distinct binding site (Shin et al., 2001). As with PICK1 and MKLP1, the physiological relevance of the interactions with Arf remain to be elucidated.

1.3.4.8 PICK1

PICK1 (protein interacting with C kinase 1) is another protein implicated as an immediate downstream Arf effector (Takeya et al., 2000). This is a PDZ-domain containing protein

that was originally identified by virtue of its interaction with protein kinase Cα in the yeast two-hybrid system (Staudinger et al., 1995). Interestingly, it contains a region homologous to the Arfaptins, but this does not bind Arfs as might be predicted (Takeya et al., 2000). However, the PDZ domain does appear to bind the C-termini of activated (Q71L mutants) class I, but not class II or III, mammalian Arfs, again in the yeast two-hybrid system (Takeya et al., 2000). PICK1 has been shown to localise to a perinuclear region (Staudinger et al., 1995), but again the significance or validity of the putative interaction with Arfs is unknown.

1.3.4.9 Modulation of the GTPase cycle by effector interactions

It has become apparent that Arf/effector interactions play direct roles in regulating the Arf GTPase cycle. In the case of Arf3 binding to Arfaptin 2, GGA1 and MKLP1, these interactions appear to increase the affinity for GTP *in vitro* (Zhu et al., 2000). This would, therefore, be predicted to prolong the interactions and any downstream events *in vivo*. Another report showed that the interaction of GGAs with Arf1-GTP inhibits GTP hydrolysis catalysed by ArfGAP1, and this would increase the duration of the interaction even more (Puertollano et al., 2001b). On the other hand, coatomer binding to Arf1 appears to enhance the GAP activity of ArfGAP1 1000-fold (Goldberg, 1999). So it seems that there is another level of complexity in the control of Arf function that is dependent on specific interactions with specific effectors. Indeed, it is conceivable that subtle differences could exist between different Arf isoforms interacting with the same effectors, and that these could potentially result in distinct cellular effects.

1.3.5 Arf6 – the odd one out?

Although Arf6 behaves essentially the same as all the other isoforms in *in vitro* assays such as the cholera toxin-stimulated ADP-ribosylation of G_s, or PLD activation, it is clearly different from the other five isoforms in that it does not localise to the Golgi complex. It localises to the plasma membrane in the GTP-bound state but there has been some debate as to whether it dissociates in the GDP-bound conformation like the other isoforms, and also whether it localises to intracellular endosomal locations. Initial immunoblot analysis of subcellular fractions suggested it localised uniquely to the plasma membrane irrespective of nucleotide status (Cavenagh et al., 1996). Other groups have, however, identified a cytosolic pool (Gaschet and Hsu, 1999; Yang et al., 1998), and the discrepancy is hard to reconcile. Ultrastructural and confocal microscopic investigations have revealed that mutants defective in GTP-hydrolysis and GTP-binding localise to the plasma

Fig. 1.3.6 **Cellular functions of ARF GTPases.**

A diagrammatic overview of the known functions and effectors of ARF GTPases. ARFs are activated by Sec7 domain-containing exchange factors that are often sensitive to brefeldin A (BFA) inhibition, and are inactivated by proteins containing ARF GAP domains. Downstream cellular events can be broadly divided into lipid metabolism, coat recruitment and cytoskeletal regulation, although there are no clear boundaries between these as they are all inter-related.

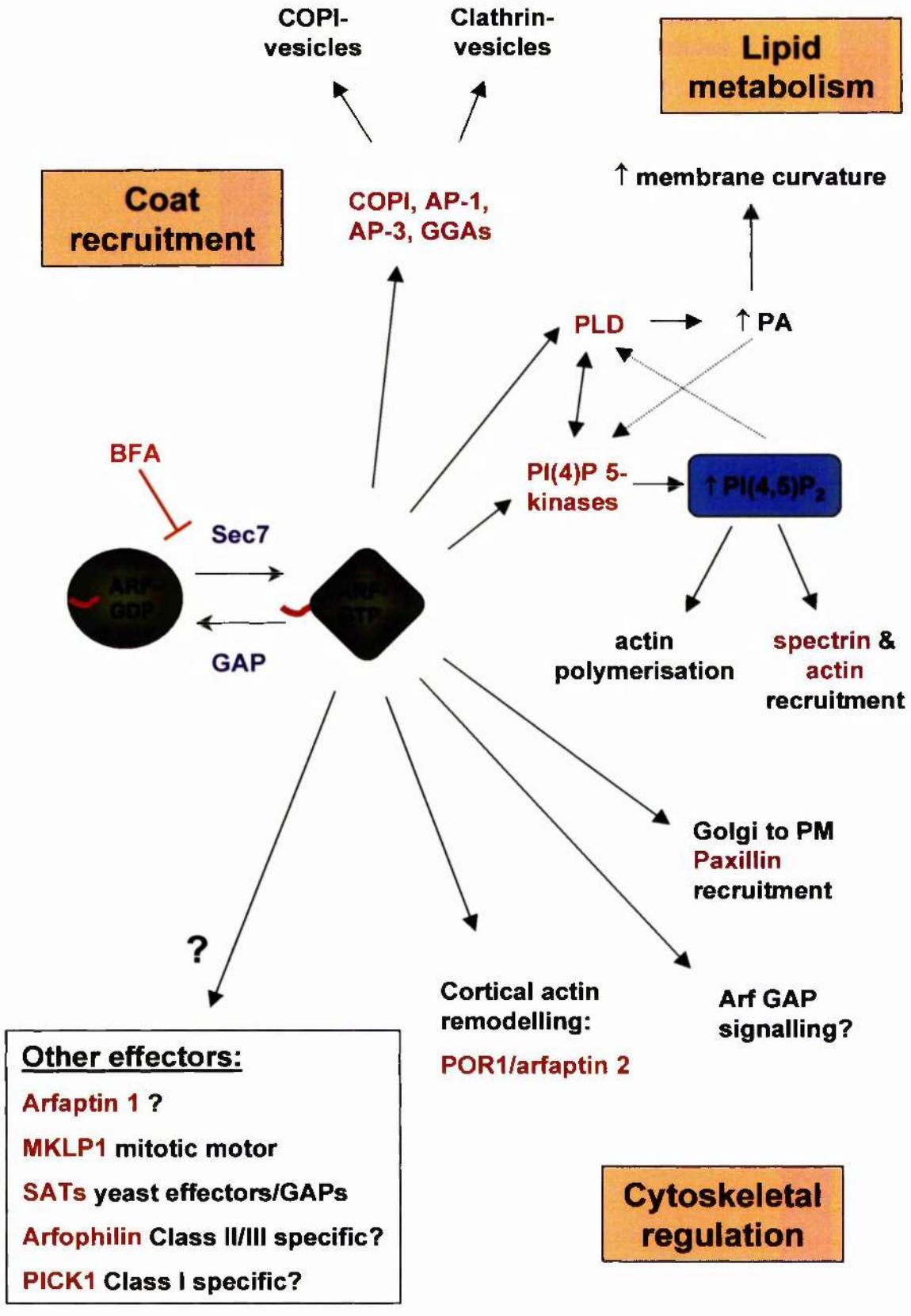
COPI-vesicles
Clathrin-vesicles
Lipid metabolism
Coat recruitment
COPI, AP-1, AP-3, GGAs
↑ membrane curvature
PLD
↑ PA
BFA
Sec7
PI(4)P 5-kinases
↑ PI(4,5)P2
ARF-GDP
ARF-GTP
GAP
actin polymerisation
spectrin & actin recruitment
Golgi to PM
Paxillin
recruitment
?
Cortical actin remodelling:
POR1/arfaptin 2
Arf GAP signalling?
Other effectors:
Arfaptin 1 ?
MKLP1 mitotic motor
SATs yeast effectors/GAPs
Arfophilin Class II/III specific?
PICK1 Class I specific?
Cytoskeletal regulation

membrane and recycling endosomes, respectively in cultured cells (D'Souza-Schorey et al., 1995; D'Souza-Schorey et al., 1998; Peters et al., 1995). Thus, it seems likely that Arf6-GDP is located in the endosomal compartment and then translocates to the plasma membrane upon GTP binding.

In terms of function, Arf6 has been implicated in the control of regulated exocytosis in chromaffin cells since it is associated with purified chromaffin granules and calcium-stimulated catecholamine exocytosis can be attenuated using a synthetic myristoylated peptide corresponding to the N-terminus of Arf6 but not with an analogous Arf1 peptide (Galas et al., 1997). A similar approach uncovered a potential role for Arf6 in regulated exocytosis in permeabilised 3T3-L1 adipocytes, since the same synthetic peptide could inhibit insulin-stimulated GLUT4 translocation (Millar et al., 1999). Another study in the same cell type using a virally-expressed Arf6D125N mutant (predicted to be an XTPase) as a dominant negative, saw no effect on GLUT4 trafficking although the basal and insulin-stimulated secretion of adipsin was apparently defective (Yang and Mueckler, 1999). Further studies in the same cell type reported inhibitory effects of the expression of the "GDP-locked" Arf6T27N mutant on endothelin-stimulated but not insulin-stimulated GLUT4 translocation (Bose et al., 2001). A role for Arf6 in endocytosis in CHO cells has also been proposed based on findings that Arf6 mutants could perturb the endocytosis and recycling of transferrin (D'Souza-Schorey et al., 1995). In polarised MDCK cells, Arf6 localises exclusively to the apical plasma membrane where both Arf6Q67L and Arf6T27N mutants stimulate clathrin-mediated endocytosis (Altschuler et al., 1999). Exactly how Arf6 regulates endocytosis/exocytosis is not known but it is likely to involve modulation of the cortical actin cytoskeleton through mechanisms that could involve phospholipase D activation and $PI(4,5)P_2$ generation.

Donaldson and colleagues have shown that aluminium fluoride treatment of cells overexpressing wild type Arf6 induces actin-rich protrusions of the plasma membrane (Radhakrishna et al., 1996) and that expression of Arf6T27N inhibits Rac-mediated membrane ruffling (Radhakrishna et al., 1999). More recently, these investigators have made a chimeric Arf protein consisting of the N-terminal half of Arf1 fused to the C-terminal half of Arf6. This chimera behaved like Arf6 in terms of subcelluar localisation and endosome to plasma membrane cycling in HeLa cells and did not affect Rac-induced membrane ruffling (Al Awar et al., 2000). However, it did inhibit the formation of actin-containing protrusions, suggesting that effects on membrane trafficking/Rac function and protrusion formation are functionally distinct (Al Awar et al., 2000).

Arf6 also appears to be involved in the desensitisation of G protein-coupled receptors such as the β2-adrenoceptor and the choriogonadotropin receptor since the process is inhibited by an Arf6 peptide (Mukherjee et al., 2000) and the GAP Git1 (Premont et al., 1998), while it is enhanced by overexpression of the GEF ARNO (Mukherjee et al., 2000). Receptor internalisation has long been known to involve β-arrestins that serve as adaptors between ligand-bound receptors and the clathrin endocytic machinery, and more recent evidence has shown that β-arrestin associates with ARNO and, following agonist stimulation, also with Arf6-GDP thereby facilitating guanine nucleotide exchange (Claing et al., 2001).

1.3.6 Other members of the Arf family

In addition to the Arfs, there are at least 3 yeast and 10 mammalian Arf-like proteins called Arls (Tamkun et al., 1991; Clark et al., 1993b; Schurmann et al., 1994; Zhang et al., 1995; Lowe et al., 1996) and a much larger protein called ARD1 that contains an 18 kDa Arf domain as well as an Arf GAP domain (Vitale et al., 1996). The Arls are also myristoylated GTP-binding proteins of approximately 20 kDa that are 40%-60% identical to each other or to other Arfs, but very little is known about their functions. The fact that mutation of the only *Drosphila* ARL is embryonically lethal, and cannot be rescued by upregulation of *ARF* genes, suggests separate but equally essential functions for the Arls (Tamkun et al., 1991). Unlike the Arfs, Arls have not been purified by an activity (e.g. cholera toxin ADP ribosylation of G_s, PLD activation) but they do exhibit some similarities. For example, overexpression in mammalian cells of a mutant Arl1 defective in GTP hydrolysis (Arl1Q71L) leads to a similar phenotype as that for Arf1Q71L, whereby Golgi morphology is disrupted in a manner reminiscent of BFA treatment (Van Valkenburgh et al., 2001). Yeast two-hybrid assays have also shown that ARL1-GTP can interact with some putative ARF effectors, such as Arfaptin 2/POR1 and MKLP1. Arl2 has been shown to be involved in microtubule nucleation at the centrosome by regulating the interaction of native tubulin with cofactor D (Bhamidipati et al., 2000).

The ARD1 protein has been described by Moss, Vaughan and colleagues (Vitale et al., 1996). It seems to have both Golgi and lysosomal targeting sequences conferred by the ARF domain and the GAP domain, respectively, but its function is unclear (Vitale et al., 2000a).

Other GTP-binding proteins that belong to the Arf family include the yeast proteins SAR1 and CIN4 although they only share 25%-35% identity with the ARFs and have clearly

distinct activities. *SAR1* was originally identified as a multicopy suppressor of a temperature-sensitive mutant of the *SEC12* gene that had been genetically identified as necessary for ER to Golgi transport in yeast (Nakano et al., 1988). There is only one SAR1 gene in yeast, while two Sar1 proteins (Sar1a and Sar1b) have been found in mammals (Kuge et al., 1994). Sec12p was found to be a guanine nucleotide exchange factor for Sar1p (Barlowe and Schekman, 1993) and the Sar1 GTPase cycle is now known to regulate the formation of COPII-coated vesicles (Barlowe, 2000). Cin4 was identified in a genetic screen for mutants defective in microtubule function (Hoyt et al., 1990; Stearns et al., 1990a) and it is most homologous to mammalian Arl2, also implicated in similar pathways.

1.3.7 Cross-talk between Arf and Rho family GTPases

Several lines of evidence suggest that Arf and Rho family GTPases act in concerted ways, and these should be considered when assessing Arf functions. They have been particularly pertinent in findings relating to Arf6- and Rac-induced cytoskeletal rearrangements. Firstly, Arfs and Rac1 both bind Arfaptin-2/POR1 (Kanoh et al., 1997; D'Souza-Schorey et al., 1997; Tarricone et al., 2001; Shin and Exton, 2001), and overexpression of a POR1 deletion mutant blocks Arf6-mediated cytoskeletal rearrangements (D'Souza-Schorey et al., 1997). Similarly, expression of dominant-negative mutants of Rac or Arf6 can abolish the cytoskeletal remodelling observed upon overexpression of EFA6, the Arf6 GEF (Franco et al., 1999). Thirdly, dominant-negative Arf6 expression can prevent Rac1-mediated membrane ruffling (Radhakrishna et al., 1999; Zhang et al., 1998b). Further evidence for a connection comes from the finding that the Arf GAP, PKL, links paxillin to PAK and PIX, which are components of Rac/Cdc42 pathways (Turner et al., 1999). Much of this cross-talk may be at the level of phosphoinositide signalling. Phosphatidylinositol 4-phosphate 5-kinase has been shown to directly interact with Rac-GTP (Tolias et al., 1995), to be activated by the Rho effector Rho-kinase (Oude Weernink et al., 2000), and to be an Arf6 effector that translocates to membrane ruffles and produces $PI(4,5)P_2$ synergistically with Arf6 and phosphatidic acid (Honda et al., 1999). Phosphatidic acid is itself produced by phospholipase D in response to both Rho and Arf proteins (Frohman and Morris, 1996). $PI(4,5)P_2$ itself regulates Arf activation via the recruitment of PH-domain containing GEFs and GAPs and also promotes the activation of Rho family members. In addition, $PI(4,5)P_2$ is required for other aspects of Rho family signalling such as the activation of N-WASP during Cdc42-stimulated actin polymerisation (Ma et al., 1998; Miki et al., 1996). Since a role for Arf6 in endocytosis has been demonstrated (D'Souza-

Schorey et al., 1995), this could be part of a mechanism coupling vesicle formation with actin rearrangements to facilitate vesicle trafficking. Also of interest is the finding that the tail of Cdc42 directly interacts with the γ-COP subunit of coatomer (Wu et al., 2000), whose assembly onto Golgi membranes is regulated by Arf (see section 1.1.4.1).

1.3.8 Aims of this study

An overwhelming body of evidence supports the central role of Arf proteins in the control of membrane traffic. However, there are still large gaps in our understanding of their precise cellular functions, and more recent developments regarding the actin cytoskeleton and ARFGAP signalling hint at how complex the situation really is. Particularly sparse is information as to the identities and/or functions of immediate downstream effectors, especially when compared to other small GTPases like Rab5.

What of the class II Arf isoforms: do they have specific effectors/functions, and if so, what are they? Previous work in the lab had shown that the addition of a myristoylated synthetic peptide corresponding to the unique N-terminus of Arf5 to permeabilised 3T3 L1 adipocytes inhibited insulin-stimulated translocation of the endosomal markers GLUT1 and the transferrin receptor to the plasma membrane (Millar et al., 1999). Analogous Arf1 or Arf6 peptides or a non-myristoylated peptide could not mimic this effect suggesting the existence of an Arf5-specific pathway (Millar et al., 1999). These findings inspired the work presented here and led us to try to identify novel Arf5 effector proteins. The preliminary aim was, therefore, to use the yeast two-hybrid system to identify novel class II Arf-interacting proteins, and this represents the focus of the first results chapter, Chapter 3. This strategy successfully identified two novel putative binding proteins and one of these, named Arfophilin-2, became the main focus of the two subsequent chapters. Chapter 4 deals with the initial characterisation of Arfophilin-2, including the cloning of the cDNA, the analysis of its expression in different tissues, and its subcellular distribution and pharmacological sensitivity in cultured cells. The aim of Chapter 5 was then to gain insight into the cellular function of Arfophilin-2, by examining the effects of overexpression or truncation of the protein, and by trying to establish the relationship between Arfophilin-2 and the Arfs themselves.

Chapter 2

Materials & Methods

2.1 Materials

All materials used in this study were of a high quality and were obtained from the following suppliers:

Amersham Pharmacia Biotech, Little Chalfont, Buckinghamshire, UK

Horseradish peroxidase (HRP)-conjugated donkey anti-rabbit IgG antibody

Horseradish peroxidase (HRP)-conjugated sheep anti-mouse IgG antibody

ECL Western blotting detection reagents

Glutathione sepharose 4B

Activated CH sepharose

Anachem Ltd., Luton, Bedfordshire, UK

30% acrylamide/bisacrylamide

Bio-Rad Laboratories Ltd, Hemel Hempstead, Hertfordshire, UK

N, N, N', N'-tetramethylethylenediamine (TEMED)

Boehringer Mannheim, Germany

Isopropyl-thio-ß-D-galactopyranoside (IPTG)

Tris

Brefeldin A

Protease inhibitor cocktail tablets: complete™ and complete-mini™

EXPAND™ High-Fidelity PCR kit

Clontech, Palo Alto, CA, USA

Human testis Matchmaker™ II library in pACT2

Human brain Matchmaker™ II library in pGAD10

Human multiple tissue Northen blots (MTNI and MTNII)

ExpressHyb hybridisation buffer

Human testis Marathon-Ready™ cDNAs

Human testis Protein Medley™ lysate

Dako, Ely, Cambridgeshire, UK

Horseradish peroxidase (HRP)-conjugated donkey anti-sheep IgG antibody

Difco Laboratories, Detroit, USA

Yeast nitrogen base (without amino acids)

Bacto-agar (for yeast work)

Fisher Scientific Ltd., Loughborough, Leicestershire, UK

Ammonium persulphate

Calcium chloride ($CaCl_2$)

Diaminoethanetetra-acetic acid, Disodium salt (EDTA)

Disodium hydrogen orthophosphate (Na_2HPO_4)

D-Glucose

Glycerol

Glycine

N-2-hydroxyethylpiperazine-N'-2-ethanesulphonic acid (HEPES)

Hydrochloric acid (HCl)

Isopropanol

Magnesium sulfate ($MgSO_4$)

Methanol

Potassium chloride (KCl)

Potassium dihydrogen orthophosphate (KH_2PO_4)

Sodium dodecyl sulphate (SDS)

Sodium chloride (NaCl)

Sodium dihydrogen orthophosphate dihydrate (NaH_2PO_4)

Sodium hydrogen carbonate ($NaHCO_3$)

Sucrose

Trichloroacetic acid

Tri-Sodium citrate ($Na_3C_6H_5O_7$)

Invitrogen, Groningen, The Netherlands

pCRII-TOPO^{TM} TA cloning kit

Bibby-Sterilin, Staffordshire, UK

IWAKI cell culture plastic ware: 6 well plates, 75 cm^2 flasks, 10 cm dishes

Graduated disposable pipettes

Kodak Ltd, Hemel Hempstead, Hertfordshire, UK

X-Omat S film

Life Technologies, Paisley, Scotland, UK

Dulbecco's modified Eagle's medium (without sodium pyruvate, with 4500mg/L glucose) (DMEM)

Modified Eagle's medium (MEM)

Hams F12 medium

Opti-MEM

Foetal bovine serum (FBS)

10000U/ml penicillin, 10000U/ml streptomycin

Trypsin/EDTA solution

Non essential amino acids

Lipofectamine reagent

1 kb DNA ladder

Agarose

Merck Ltd (BDH), Lutterworth, Leicestershire, UK

Magnesium chloride ($MgCl_2$)

Tween 20

Zinc cloride ($ZnCl_2$)

Molecular Probes, Oregon, USA

Alexa^{488}-conjugated donkey anti-mouse IgG secondary antibody

Alexa^{488}-conjugated donkey anti-rabbit IgG secondary antibody

Alexa^{594}- conjugated donkey anti-sheep IgG secondary antibody

Texas-Red^{TM}-Transferrin

MWG-Biotech, Germany

All oligonucleotide primers

NEN Dupont (UK) Ltd, Stevenage, Hertfordshire, UK

[α-^{32}P]-dCTP

New England Biolabs (UK) Ltd, Hitchin, Hertfordshire, UK

Prestained protein marker, broad range (6-175kDa)

Oxoid Ltd, Hampshire, UK

Bacteriological agar

Yeast extract

Tryptone

Pierce, Rockford, Illinois, USA

Slide-a-lyzer™ dialsysis cassettes

Premier Brands UK, Knighton Adbaston, Staffordshire, UK

Marvel powdered milk

Promega, Southampton, UK

All restriction enzymes (except Dpn 1)

Pfu polymerase

Taq polymerase

Nuclease-free water

Calf intestinal alkaline phosphatase

Deoxynucleotide triphosphates (dNTPs)

Qiagen, Crawley, West Sussex, UK

QIAprep™ spin miniprep kit

QIAprep™ maxiprep kit

Nickel NTA-agarose

Schleicher & Schuell, Dassel, Germany

Nitrocellulose membrane (pore size:0.45μM)

Shandon, Pittsburgh, PA, USA

Immu-mount™ mounting medium

Stratagene, La Jolla, CA, USA

Supercompetent XLI-blue *Escherichia coli*

Pfu Turbo™ polymerase (for Quikchange mutagenesis)

Dpn 1 restriction enzyme (for Quikchange mutagenesis)

Whatman International Ltd, Maidstone, UK

Whatman No.1 filter paper

Whatman No.3 filter paper

Whatman 3mm filter paper

Unless otherwise indicated, all remaining chemicals were supplied by Sigma Chemical Company Ltd, Poole, Dorset, UK.

Primary antibodies

Monoclonal anti transferrin receptor antibody was from Zymed Laboratories, Cambridge, UK. Monoclonal anti haemagluttinin antibody, anti Rab5, Rab11, Rho, Rac, EEA1 were all from Santa Cruz Biotechnology, Santa Cruz, California. Monoclonal anti Na/K ATPase was from Upstate Biotech, New York. Anti clathrin was from Transduction Laboratories, San Diego, CA, USA. Anti γ tubulin, α tubulin, and β COP were all from Sigma. Polyclonal anti GRASP55 and GRASP65 antibodies were a gift from Francis Barr (Max-Plank-Institute, Martinsreid, Germany). Margaret Robinson (University of Cambridge, UK) generously provided polyclonal antibodies to GGA1, RME1, AP-3δ and γ adaptin. Anti cellubrevin was a kind gift from David James, University of Queensland, Australia. Anti Arf6 was a gift from Julie Donaldson, NIH, Bethesda, USA. Anti-sortillin was from Nick Morris (University of Newcastle, UK). Antibodies to the CI-MPR and the CD-MPR were gifts from G. E. Lienhard (Dartmouth Medical School) and A. Hille-Rehfeld (Universitat Gottingen, Germany), respectively. Anti-syntaxin 6 polyclonal antibodies were produced in house by Kumudu Perera, against a recombinant His-tagged protein.

Escherichia coli strains

DH5α
XL1-blue
TOP10
JM109
BL21 DE3 (pLys)S
KC8

Saccharomyces cerevisiae strain for two-hybrid work

PJ69-2A was the only strain used in this study (James et al., 1996). It has the following genotype:

MATa, *trp1-901, leu2-3,112, ura3-52, his3-200, gal4Δ, gal80Δ, LYS::GAL1*$_{UAS}$*-GAL1*$_{TATA}$*-HIS3, GAL2*$_{UAS}$*-GAL2*$_{TATA}$*-ADE2*

General solutions

DNA loading buffer	40% (w/v) sucrose, 0.25% bromophenol blue
GST-tag buffer	100 mM HEPES, 200 mM KCl, pH 7.0
His-tag buffer	100 mM HEPES, 200 mM KCl, 5 mM imidazole, pH 8.0
Immunofluorescence buffer (IF)	PBS plus 0.2% fish skin gelatin and 0.1% donkey or goat serum [a different species to that in which the secondary antibodies were raised in]; freshly made and filtered through a Nalgene 0.2 μm vacuum type filter
Luria Broth (LB)	10% (w/v) tryptone, 5% (w/v) yeast extract, 10% (w/v) NaCl
Lysis buffer	25 mM HEPES, pH 7.5; 50 mM NaCl; 5 mM EDTA; 10% (v/v) glycerol; 1% (v/v) Triton X-100
Phosphate buffered saline (PBS)	136mM NaCl, 10mM NaH_2PO_4, 2.5mM KCl, 1.8mM KH_2PO_4, pH 7.4
SDS-PAGE electrode buffer	25mM Tris, 190mM glycine, 0.1% (w/v) SDS
SDS-PAGE sample buffer	93mM Tris-Cl pH6.8, 1mM sodium EDTA, 10% (w/v) glycerol, 2% (w/v) SDS, 0.002% (w/v) bromophenol blue, 20mM dithiothrictol
TAE	40 mM Tris-Acetate, 1 mM EDTA
TBST	20 mM Tris-HCl, pH 7.4; 150 mM NaCl; 0.08% (v/v) Tween-20
Transfer buffer	25 mM NaH_2PO_4, pH 6.5

2.2 Methods

General methods are given in this chapter, while more specific procedures or methods that are unique to a given chapter are presented in those chapters.

2.2.1 Molecular Biology

2.2.1.1 Amplification of DNA by Polymerase Chain Reaction (PCR)

All polymerase chain reactions (PCRs) were performed in thin walled PCR tubes in a Techne Progene thermocycler. Amplification of DNA from purified plasmid DNA was performed using Pfu polymerase enzyme (Promega), while PCR from cDNAs was performed using an EXPAND high-fidelity kit (Roche).

Reactions were set up on ice typically as follows:

10x polymerase buffer (with $MgCl_2$)	5 µl
nuclease-free water	to 50 µl
forward primer (4 pmol/ µl)	2.5 µl
reverse primer (4 pmol/ µl)	2.5 µl
dNTPs (10 mM each dCTP, dGTP, dATP, dTTP)	1 µl
template DNA (50-100 ng)	0.5 µl
polymerase	1 µl

The tubes were then briefly vortexed and pulsed in a microfuge, before thermal cycling was initiated. Typical cycling conditions were as follows:

	94°C	2 min	
x 25	94°C	15 sec	
	55°C	30 sec	
	68°C	2 min/kb (Pfu) or 1min/kb (Expand)	
	68°C	5 min	
	4°C	Hold	

The 55°C annealing temperature was sometimes decreased as low as 50 °C if initial attempts failed due to low primer melting temperatures. Following PCR cycling, half of the

reaction mixture was analysed by agarose gel electrophoresis (see below). All oligonucleotide primers were highly purified salt free (HPSF) grade (MWG-Biotech) and stocks were made at 100 pmol/µl in TE buffer (10 mM Tris-HCl, pH 8.0, 1 mM EDTA). These were then diluted to 4 pmol/µl in nuclease-free water when required.

2.2.1.2 Purification of PCR products

If a second round of PCR was to be performed, for example using nested primers, the first round PCR reaction was purified using a Qiagen PCR purification kit, according to the manufacturer's instructions and using the buffers supplied. Briefly, 25 µl of the reaction was mixed with 125 µl buffer PB and placed in a QIAspin column. This was then centrifuged in a microfuge at full speed for 1 min. The column was then washed in 750 µl buffer PE containing ethanol, and the column was spun and the flow-through was discarded. The column was then spun again to ensure the complete removal of the buffer and then placed in a sterile 1.5 ml microcentrifuge tube. 50 µl of buffer EB, warmed to 40°C, was then pipetted into the centre of the column and incubated for 1 min. The DNA was then collected in the microcentrifuge tube by centrifugation for 1 min. 5 µl of this would then be used as a template for a further round of PCR.

2.2.1.3 Agarose gel electrophoresis

For standard small 1% agarose gels, agarose was dissolved by boiling in 50 ml TAE buffer in a microwave oven. This was then allowed to cool to about 50-60°C before 1 µl of ethidium bromide (10 mg/ml) was added. This was mixed thoroughly and poured into a horizontal electrophoresis gel cartridge was an appropriate comb inserted. This was allowed to set at room temperature before being transferred to the electrophoresis tank containing TAE buffer. The comb was gently removed, samples in DNA loading buffer (30% (v/v) glycerol, 0.25% bromophenol blue) were applied to the wells, adjacent to a lane containing 0.5-0.75 µg 1 kb DNA ladder. Electrophoresis was carried out at 70 volts for 45-60 min or until the dye front had migrated sufficiently far to have allowed the resolution of the relevant DNA fragments. The gels were then visualised using an ultraviolet transilluminator and photographs were taken using a Mitsubishi video copy processor, where appropriate.

2.2.1.4 Gel extraction of DNA

A clean scalpel blade was used to excise required bands from agarose gels that were visualised under ultraviolet light. This was performed as quickly as possible to minimise DNA damage by ultraviolet irradiation. Gel slices were transferred to sterile 1.5 ml microcentrifuge tubes and DNA extraction was performed using a Qiagen gel purification kit, according to the manufacturer's instructions and using the buffers supplied. 600 µl of buffer QC was added to each gel slice and the tubes were incubated at 37°C for 10-15 minutes or until the agarose had completely dissolved. This was facilitated by periodic vortexing. The solution was then applied to a QIAspin column. This was then centrifuged in a microfuge at full speed for 1 min. The column was then washed in 750 µl buffer PE containing ethanol and the column was spun and the flow-through discarded. The column was spun again to ensure the complete removal of the buffer and was then placed in a sterile 1.5 ml microcentrifuge tube. 50 µl of buffer EB, warmed to 40 °C, was then pipetted into the centre of the column and incubated for 1 min. The DNA was then collected in the microcentrifuge tube by centrifugation for 1 min.

2.2.1.5 Adding 'A' base overhangs onto Pfu-amplified products

If Pfu-amplified PCR products were to be cloned into pCRII-TOPO for sequencing, mutagenesis and subcloning, they first had to be treated with Taq polymerase to add overhanging 'A' bases required for TA cloning. To do this, 5 µl of Taq buffer, 1 µl dNTPs (10 mM each dCTP, dGTP, dATP, dTTP) and 1 µl Taq polymerase were added to gel purified PCR products (<50 µl). These were mixed thoroughly and incubated at 72°C for 20 min.

2.2.1.6 TA cloning of PCR products

This was performed using the pCRII-TOPO kit (Invitrogen), according to the manufacturer's instructions. As a rule, 2 µl of purified PCR product containing overhanging 'A' bases was added to a sterile microcentrifuge tube and mixed with 0.5 µl of pCRII-TOPO vector. This was then incubated at room temperature for 5 min, before adding 0.5 µl of 'stop' solution (supplied with the kit). Meanwhile a vial of OneShot TOP10 competent *Escherichia coli* cells (Invitrogen) were thawed on ice. The 3 µl reaction mixture was then gently added to the cells and these were incubated on ice for 30 min. The cells were then heat-shocked for 30 sec at 42°C in a water bath, chilled on ice for

1 min and then incubated in 250 µl SOC medium (supplied by Invitrogen) for 1 h at 37°C. The cells were then plated onto LB agar plates containing 50 µg/ml kanamycin and incubated overnight at 37°C. Colonies were then picked, cultured overnight in LB containing 50 µg/ml kanamycin. Small-scale DNA preparations were then carried out and plasmids were analysed by restriction digestion and sequencing (see below).

2.2.1.7 DNA restriction digests

Approximately 500 ng plasmid DNA was used for diagnostic restriction digests (i.e. to determine the presence and/or orientation of an insert), while 2-4 µg were used for subcloning. Digests were routinely performed in 20 µl volumes, with 2 µl of an appropriate 10x buffer (taking into account the efficiency of both enzymes in double digests), 0.5-1 µl of each restriction endonuclease and the remaining volume made up with sterile water. Digests were incubated at 37°C for 2-3 h. If a cut vector was to be purified for a subsequent subcloning step, and especially if the subcloning was into a single restriction site, the digested vector would be de-phosphorylated with calf intestinal alkaline phosphatase (CIP) at this point to reduce the probability of religation in the absence of an insert. To do this, 2 µl of CIP buffer and 1 µl CIP enzyme were added to the ligation and incubated for a further 10 min at 37°C. Following the addition of 5x DNA loading buffer (30% (v/v) glycerol, 0.25% bromophenol blue), the digested DNA was then subjected to agarose gel electrophoresis as described above.

2.2.1.8 Ligations

Digested inserts and CIP-treated vectors were purified by agarose gel electrophoresis followed by gel extraction as described above. Ligation reactions were then set up in sterile microcentrifuge tubes using approximately a 3:1 molar ratio of insert:vector. These were mixed together with 2 µl ligase buffer and 1 µl T4 ligase in a final volume of 20 µl that was made up with sterile distilled water. The ligation reactions were then incubated either at room temperature for 2-3 h or overnight on an ice/water slurry. 5 µl of the reaction were then used to transform *Escherichia coli* strain DH5α or XL1-blue.

2.2.1.9 Preparation of competent *Escherichia coli*

10 ml sterile LB in a plastic universal tube was inoculated with *E. coli* from a glycerol stock and cultured overnight at 37°C with shaking at 300 rpm. 5 ml of this was then

subcultured into 100 ml LB in a sterile 500 ml flask and further grown at 37°C with shaking, until the optical density at 600 nm was 0.5 (typically about 3 h). The cells were then chilled on ice for 5 min and harvested by centrifugation in sterile 50 ml centrifuge tubes at 3000 rpm for 10 min in a Beckman benchtop centrifuge at 4°C. The supernatant was discarded and the cells were gently resuspended in a total of 40 ml sterile-filtered buffer 1 (30 mM KAc, 100 mM $RbCl_2$, 10 mM $CaCl_2$, 50 mM $MnCl_2$, 15% (v/v) glycerol; pH 5.8) using a sterile pipette. The cells were incubated on ice for a further 5 min and were then spun as before. All traces of the supernatant were removed and discarded and the cells were resuspended in a total of 4 ml sterile-filtered buffer 2 (10 mM MOPS, pH 6.5; 75 mM CaCl2; 10 mM $RbCl_2$ and 15% (v/v) glycerol). Following a further incubation of 15 min on ice, the cells were divided into 220 µl aliquots in pre-chilled sterile microcentrifuge tubes and stored at -80°C until required.

2.2.1.10 Transformation of *Escherichia coli*

Competent *E. coli* cells that had been made by the method in section 2.2.1.9 were thawed on ice and 50 µl per transformation were pipetted into sterile pre-chilled 1.5 ml microcentrifuge tubes. For each transformation, 5 µl of ligation reaction or 0.5 µl (50 ng) of purified plasmid DNA were added to the cells. These were gently mixed and incubated on ice for 15-30 min. The cells were then heat-shocked in a water bath at 42°C for exactly 90 sec, and then chilled on ice for 1 min. 450 µl of LB were then added to each tube and these were incubated at 37°C for 45 min. The cells were then spun down for 10 sec at full speed in a microfuge, 350 µl of LB were discarded and the cells were resuspended in the remaining 150 µl. They were then plated onto LB agar plates containing the appropriate antibiotic, and grown overnight inverted at 37°C. Competent *E. coli* cells that had been obtained from commercial suppliers were transformed according to the protocols provided by the suppliers.

2.2.1.11 Small-scale DNA preparations

Bacterial colonies were picked from selective LB agar plates and transferred to 3 ml LB (containing 100 µg/ml ampicillin or 50 µg/ml kanamycin, as appropriate) in 16 ml plastic tubes (Falcon). These were then grown overnight at 37°C with shaking at 300 rpm. DNA purification was then performed using a Qiagen miniprep kit, according to the manufacturer's instructions and using the buffers supplied. Briefly, the cells from 1.5 ml culture were collected by centrifugation for 5 min at full speed in microfuge. The

supernatant was discarded and the tube refilled with culture and spun again. Cell pellets were then resuspended in 250 µl buffer P1 (containing RNase A) by pipetting. 250 µl buffer P2 were then added and the tubes were mixed by inverting several times. These were left to incubate for 5 min at room temperature, after which time 350 µl buffer N3 were added and again mixed by inverting several times. The tubes were then centrifuged for 10 min at full speed in a microfuge and the supernatants were carefully decanted into Qiagen miniprep spin columns and spun at full speed for 1 min in microfuge. The flow-through was discarded and 750 µl buffer PE (with ethanol added as in the manufacturer's instructions) was added. The column was spun again and the flow-through was discarded. The column was spun a further time to ensure the complete removal of the buffer and it was then placed in a sterile 1.5 ml microcentrifuge tube. 50 µl of buffer EB, warmed to 40°C, was then pipetted into the centre of the column and incubated for 1 min. The DNA was then collected in the microcentrifuge tube by centrifugation for 1 min.

2.2.1.12 Large-scale DNA preparations

Large-scale DNA preparations were performed using a Qiagen plasmid maxi kit, following the high-copy plasmid protocol and using the buffers supplied by the manufacturers. Briefly, bacterial cultures of 100 ml were grown overnight in 500 ml flasks in LB containing the appropriate antibiotic for selection. The cells were then harvested by centrifugation at 3000 rpm for 10 min in 50 ml centrifuge tubes. The cells were resuspended in a total of 10 buffer P1 (containing RNase A) by pipetting. 10 ml buffer P2 were then added and mixed and this was left to lyse the cells for 5 min. The reaction was neutralised by the addition of 10 ml of chilled buffer P3. The flocculent precipitate formed was removed by centrifugation at 3000 rpm for 30 min followed by filtration through two layers of muslin. This supernatant was then applied to a P100 Qiagen column pre-equilibrated with 10 ml buffer QBT and was allowed to drain under gravity. The column was then washed with 30 ml buffer QC (with added ethanol according to manufacturer's protocol). The DNA was then eluted into a 50 ml tube by the addition of 15 ml buffer QF. 10.5 ml isopropanol was then added and well mixed and the precipitated DNA was collected by centrifugation at 3000 rpm for 30 min in a benchtop centrifuge. The supernatant was discarded and the pellet was washed in 4 ml 70% (v/v) ethanol. This was then removed and the pellet air-dried prior to being resuspended in 250 µl TE (10 mM Tris-HCl, pH 8.0, 1 mM EDTA). The DNA concentration and purity was then assessed spectrophotometrically.

2.2.1.13 Site-directed mutagenesis

This was essentially carried out according to the Quikchange method (Stratagene). Two oligonucleotide primers were designed with the desired mutation(s) present in the middle of the sequence. These primers were the reverse and complement of each other and were routinely 33 bp long. A PCR reaction was then set up on ice as follows:

10x Pfu-turbo buffer	5 µl
nuclease-free water	to 50 µl
forward primer (4 pmol/ µl)	2.5 µl
reverse primer (4 pmol/ µl)	2.5 µl
dNTPs (10 mM each dCTP, dGTP, dATP, dTTP)	1 µl
template DNA (50-100 ng)	0.5 µl
Pfu-turbo polymerase	1 µl

The tubes were then briefly vortexed and pulsed in a microfuge, before thermal cycling was initiated. Typical cycling conditions were as follows:

	95°C	30 sec
x 14	95°C	15 sec
	55°C	1 min
	68°C	2 min/kb template
	68°C	5 min
	4°C	Hold

Following this, 10 µl of the reaction was analysed by agarose gel electrophoresis to ensure amplification had occurred. 1 µl Dpn 1 restriction enzyme was then added to the remaining 40 µl and the parental *dam* methylated DNA was digested for 2 h at 37°C. 1 µl of the digest was then used to transform XL1-blue supercompetent cells (Stratagene), according to the suppliers protocols. The cells were plated on LB agar plates containing appropriate antibiotics and grown at 37°C for about 24 h. Colonies were then picked, cultured overnight in selective LB media and the DNA was extracted. Recovered plasmids were sequenced to ensure the presence of the desired mutations and the absence of undesired ones.

2.2.1.14 DNA sequencing

The University of Glasgow Molecular Biology Support Unit performed all DNA sequencing using Big Dyes kits (PE biosystems) and an ABI Prism 377 sequencer. This was performed for all constructs that were produced following PCR steps to ensure that no undesired mutations had been introduced.

2.2.2 Mammalian Cell culture

2.2.2.1 Cells and culture conditions

Human embryonic kidney HEK 293 cells, human cervical carcinoma HeLa cells and Chinese hamster ovary (CHO) cells were generous gifts from Dr. Pam Scott (University of Glasgow). HEK 293 cells were cultured in Dulbecco's modified Eagle's medium (DMEM) supplemented with 10% (v/v) foetal calf serum (FCS) and L-glutamine; HeLa cells were cultured in minimal Eagle's medium (MEM) supplemented with 10% (v/v) foetal calf serum (FCS) and non-essential amino acids; and CHO cells were grown in Hams F12 medium supplemented with 10% (v/v) foetal calf serum (FCS) and 1% (v/v) penicillin and streptomycin. These media are referred to as complete growth media. All cells were grown on Iwaki plasticware at 37°C in a humidified atmosphere containing 5% CO_2 and the media were replaced every 2-3 days if the cells did not require passaging (see below). Cells were cultured in 75 cm^2 flasks for maintenance.

2.2.2.2 Trypsinisation and passage of cells

When cells had reached 80-90% confluency, the media were aspirated and the cells were rinsed with 3-4 ml sterile PBS warmed to 37°C. This was then aspirated and 2 ml trypsin/EDTA was added and evenly distributed over the entire base of the flask. Following a 3 min incubation at 37°C, the cells were dislodged by gentle tapping of the flask, and the cells were then separated by gentle pipetting. The cells were then transferred to a fresh flask containing the desired volume of fresh complete growth media, mixed well, and were distributed to the appropriate culture vessels (6 well plates, 10 cm dishes, more flasks) as required. Cells were generally diluted 1:5 or 1:10 in this manner. For cells destined for confocal microscopy, glass coverslips were flamed in ethanol briefly to ensure sterility prior to placing them in 6 well plates ready for seeding cells.

2.2.2.3 Freezing down and resurrecting cells

Cells trypsinised from one 75 cm^2 flask as described above were added to 12 ml of appropriate growth medium in a 16 ml sterile centrifuge tube. They were then spun at 2000 x g for 3 min. The medium was aspirated and the cells were resuspended in 1 ml complete growth medium containing 10% dimethyl sulphoxide (DMSO) and transferred to a 1.8 ml polypropylene cryo-vials. These vials were then wrapped in multiple layers of tissue paper and placed at -80°C overnight to freeze slowly before being transferred to a liquid nitrogen storage vat.

To resurrect cells from liquid nitrogen storage, vials were rapidly thawed by incubation at 37°C in a water bath. Any cell clumps were dispersed by pipetting and the cells were transferred to a flask containing 15 ml complete growth medium that had been previously equilibrated in the incubator at 37°C for about 1 h. The growth media were changed the following day to remove the DMSO.

2.2.2.4 Cell transfections

Cell transfections were carried out using Lipofectamine reagent (Life Technologies, Gibco, Paisley, UK), according to the manufacturer's recommendations. Typically, cells were plated the day before transfection and the transfections were performed on cells that were between 40-60% confluent. Per 6 well plate or 10 cm dish, 7.5 µg maxiprep DNA (see section 2.2.1.12) were diluted in 600 µl Optimem (Life Technologies) in a sterile 50 ml centrifuge tube and 30 µl Lipofectamine were diluted in a separate 600 µl Optimem. The Lipofectamine/Optimem mixture was then added drop-wise to the DNA/Optimem mixture. This was then incubated for 30 min at room temperature. Meanwhile, the cells were rinsed in 1 ml/well or 5 ml/10 cm dish Optimem at 37°C. 4.8 ml warm Optimem was then added to the DNA/Lipofectamine mixture and this was dispensed onto the cells (1 ml per well or 6 ml per 10 cm dish). The cells were then returned to the incubator for 3-6 h, after which time an equal volume of complete growth medium containing a total of 20% (v/v) FCS was added to give a final concentration of 10% FCS. Cells were typically harvested or used 18-22 h post-transfection (i.e. post the addition of the DNA/Lipofectamine mixture).

2.2.2.5 Incubation of cells with fluorescent transferrin and drugs

Cells to be treated with drugs or fluorescent transferrin, were first quiesced for 2 h by replacing the complete growth media with serum free media. After this time, drugs such as

brefeldin A (20 μg/ml for 10 min; Boehringer Mannheim), nocodazole (50 ng/ml for 1 h; Sigma) or wortmannin (100 ng/ml; Sigma) were added and the cells returned to the incubator for the appropriate time. Control experiments using the vehicle alone (methanol or DMSO) were conducted in parallel. Cells were then washed in ice-cold PBS and processed for immunofluorescence as described below in section 2.2.3.1. Similarly, Texas-red transferrin (1 μg/ml; Molecular Probes) was incubated with the quiesced cells for a specified time (5 or 30 min). The cells were then either washed extensively in cold PBS prior to fixation, or washed in complete growth media containing 1 mg/ml iron-saturated transferrin (Sigma) for a specified chase time. The cells were then fixed as described below.

2.2.3 Immunofluorescence and confocal microscopy

2.2.3.1 Fixing cells and processing them for immunofluorescence

The transfection media were aspirated and the cells were washed twice with 2 ml/well ice cold PBS and all traces were removed by aspiration. 2 ml methanol at -20°C were then added to each well and these were then incubated at -20°C for 5 min. The methanol was aspirated and the coverslips were washed 3 times in cold PBS and twice in IF buffer (PBS containing 0.2% fish skin gelatin and 0.1% donkey or goat serum [whichever species the secondary antibodies were raised in]; freshly made and filtered through a Nalgene 0.2 μm vacuum type filter). The cells were left in the second IF buffer wash for 10-15 min. Meanwhile primary antibody dilutions were prepared. These were generally diluted 1:100 to 1:200 in IF buffer (except α-tubulin 1:3200; γ-tubulin 1:300; actin-Cy3 conjugate 1:1000). Coverslips were then placed cells-down onto a 100 μl drop of antibody solution on parafilm. These were incubated for 1 h at room temperature, then returned to the 6 well plates for 5 x washes in IF buffer. Secondary antibodies were then prepared in IF buffer at a dilution of 1:200 and coverslips were again incubated for 1 h cells-down onto 100 μl placed on parafilm. The coverslips were again washed 5 times in IF buffer and were mounted onto a small drop of Immu-mount (Shandon, Pittsburgh, USA) on glass slides. These were then allowed to harden overnight and were kept in the dark until analysed by confocal microscopy.

2.2.3.2 Confocal microscopy

Mounted coverslips were analysed using a 63x Zeiss oil immersion objective on a Zeiss Axiovert fluorescence microscope (Carl Zeiss, Germany) equipped with a Zeiss LSM4 laser confocal imaging system. Images were captured using either (or both) of 488 nm or 543 nm lasers with appropriate filter sets for collection of GFP/Alexa^{488}/FITC signals (band-pass 505-520 nm) or Alexa^{594}/TRITC signals (long-pass 590 nm). Data files were saved in .TIF format and analysed using Photoshop 5.5 software (Adobe).

2.2.4 Biochemical Procedures

2.2.4.1 Protein assays

Protein concentration was measured using the Bradford method (Bradford, 1976). Coomassie Brilliant Blue G-250 (35 mg) was dissolved in 50 ml of 95% (v/v) ethanol and 60 ml 85% (w/v) orthophosphoric acid was added. The mixture was made up to 1 L with distilled water, filtered through Whatman 541 grade filter paper and stored protected from light. For protein determinations, 1 ml of this reagent was added to 100 µl of sample and the absorbance measured at 595 nm against a reference sample which contained 1 ml of reagent and 100 µl of buffer or water as appropriate. Readings were compared to those of a standard curve obtained from analysing samples containing 1 to 5 µg bovine serum albumin (BSA).

2.2.4.2 SDS-PAGE

Sodium dodecyl suphate polyacrylamide gel electrophoresis (SDS-PAGE) was carried out using Bio-Rad mini-PROTEAN II gel apparatus and either 10 or 15 well combs. The percentage of acrylamide in each gel ranged from 8% to 15%, according to the molecular weight of the proteins of interest. All reagents were of electrophoresis grade.

A resolving gel was prepared using 30% acrylamide/bisacrylamide, 1.5 M Tris-HCl (pH 8.8) (to a final concentration of 375mM), 10% (w/v) SDS (to a final concentration of 0.1%), polymerised with 10% (w/v) ammonium persulphate (to a final concentration of 0.1%) and TEMED (to a final concentration of 0.019%). This gel was allowed to polymerise overlaid with water and leaving enough space for the wells plus about 1.5 cm of stacking gel. The stacking gel was prepared using 30% acrylamide/bisacrylamide, 1M Tris-HCl (pH 6.8) (to a final concentration of 125mM), 10% (w/v) SDS (to a final

concentration of 0.1%), polymerised with 10% (w/v) ammonium persulphate (to a final concentration of 0.1%) and TEMED (to a final concentration of 0.05%). This was then applied on top of the resolving gel, with a comb in place and allowed to polymerise.

Protein samples were resuspended in 1x SDS PAGE sample buffer (93mM Tris-Cl pH6.8, 20mM dithiothreitol [added immediately before use], 1mM sodium EDTA, 10% (w/v) glycerol, 2% (w/v) SDS, 0.002% (w/v) bromophenol blue) and were routinely boiled for 2-3 min in a water bath. The samples were then loaded onto the wells in the stacking gel, adjacent to broad-range (Mr 6-175 kDa) pre-stained molecular weight markers (New England Biolabs). Gels were electrophoresed in electrode buffer (25mM Tris, 190mM glycine and 0.1% (w/v) SDS) at 60 mA for about 1 h or until the dye front had reached the bottom of the gel.

2.2.4.3 Coomassie staining of SDS-PAGE gels

Following the separation of proteins by SDS-Polyacrylamide Gel Electrophoresis, a 0.25% Coomassie blue stain solution was prepared. For this 10ml of glacial acetic acid was mixed with 90ml of a methanol:H_2O (1:1 v/v) mixture and 0.25g of Coomassie Brilliant Blue R were added. This stain was then filtered through Whatman number 1 filter paper. The gel was submerged in the stain for about 1 h then rinsed and destained with the same acetic acid, methanol:H_2O mixture (without the Coomassie dye). Destaining was for at least 3 h with frequent changes of destain buffer or overnight. The gels were then placed between clear polythene sheets and scanned to provide digital records.

2.2.4.4 Transfer of proteins to nitrocellulose

Proteins were separated by SDS-PAGE as described above. A sponge pad, two sheets of Whatman 3 mm filter paper and a sheet of nitrocellulose membrane (pore size 0.45mM), cut to size and previously soaked with transfer buffer (25mM NaH_2PO_4, pH 6.5) were placed on the black plate of a Bio-Rad Trans Blot gel cassette holder. The gel was then placed on top of the nitrocellulose membrane and any air bubbles were gently removed. The "sandwich" was completed with two more sheets of filter paper and a sponge pad as before. Transfer was carried out using a Bio-Rad mini or Bio-Rad trans-blot electrophoretic cell containing transfer buffer at a constant current of 300 mA for 3 h or overnight at 60 mA. The efficiency of transfer was then assessed by staining the nitrocellulose with Ponceau S solution (Sigma).

2.2.4.5 Immunoblotting

Following transfer, non-specific binding sites on the nitrocellulose membrane were blocked by shaking for at least 1 h in 5% (w/v) dried skimmed milk in TBST buffer (20mM Tris, 150mM NaCl, 0.02% Tween-20, pH 7.4). The nitrocellose membrane was then heat-sealed in polythene tubing together with primary antibody in 1% (w/v) dried skimmed milk in TBST buffer at the appropriate dilution and shaken for at least 2 h at room temperature. Following five washes with TBST buffer over a period of 1 h, the membrane was incubated with shaking in 1% (w/v) dried skimmed milk in TBST buffer containing the appropriate secondary antibody, (HRP-linked IgG) at a 1:1000 dilution for 1 h at room temperature. The membrane was then washed a further five times over a period of 1 h.

The detection of antigen/primary/secondary antibody complexes on the nitrocellulose blots was then performed using the enhanced chemiluminescence method (ECL, Amersham). Equal volumes of Amersham "detection reagent 1" and "detection reagent 2" (typically 2 ml of each) were mixed and placed onto the membrane for about 1 min. The blot was then dabbed dry with some tissue paper and wrapped in cling film. This was then placed in a light tight cassette and exposed to Kodak film in a dark room for varying exposure times. The film was developed using an X-OMAT automatic processor.

2.2.4.6 Immunoprecipitations

Using a rubber policeman, cells were collected in ice-cold lysis buffer (25 mM HEPES, pH 7.5; 50 mM NaCl; 5 mM EDTA; 10% (v/v) glycerol; 1% (v/v) Triton X-100 containing complete protease inhibitor cocktail; 250 µl/well of a 6 well plate). They were then triturated several times using a pipette, transferred to 1.5 ml microcentrifuge tubes and incubated on ice for 15 min. The tubes were then spun at full speed for 10 min in a microcentrifuge chilled to 4°C. The supernatants were transferred to fresh screw-cap microcentrifuge tubes and the triton-insoluble pellets were discarded. Approximately 5 µg primary antibody/ preimmune serum were then added to 500 µl of lysate and the tubes were rotated end over end for 2 h at 4°C. Meanwhile protein A/ protein G-sepharose beads were washed three times in lysis buffer and a 50% slurry was made in the same buffer. 25 µl of this was then added to each tube and these were rotated for a further 1 h. The tubes were then spun in the microfuge for 1 min and the supernatants were carefully removed and transferred to separate tubes. The beads were washed four times with 1 ml of lysis buffer by resuspension and centrifugation. All traces of buffer were removed fter the final

spin and 50 µl high urea buffer (8 M urea; 5% (w/v) SDS; 200 mM Tris-HCl pH 6.8; 0.1 mM EDTA; 0.5 mg/ml bromophenol blue; 10% (v/v) β-mercaptoethanol) were added to the beads. These were vortexed for 15 sec, pulsed in a microfuge, boiled for 2-3 min, pulsed again and the supernatants were removed and the proteins were resolved by SDS-PAGE.

2.2.4.7 Recombinant protein production

An *E. coli* colony harbouring an appropriate plasmid was picked from a freshly grown selective LB agar plate and used to inoculate 10 ml of LB containing appropriate antibiotics. This was grown overnight at 37°C with shaking at 250 rpm. The following day, the 10 ml culture was used to inoculate 1 L LB plus antibiotics in a 5 L flask. This was grown at 30°C with shaking until the optical density at 600 nm had reached about 0.5-0.6. IPTG was then added to a final concentration of 0.5-1 mM and the culture was induced for 5 h. The cells were then harvested in 250 ml tubes in a Beckman JA-14 rotor by centrifugation at 5000 rpm for 15 min. The cell pellets were resuspended by pipetting in 40 ml His-tag buffer (100 mM HEPES, 200 mM KCl, 5 mM imidazole, pH 8.0) or GST-tag buffer (100 mM HEPES, 200 mM KCl, pH 7.0) depending on the type of recombinant protein to be purified. This was transferred to a 50 ml centrifuge tube and spun at 3500 rpm in a benchtop centrifuge for 20 min. The supernatant was discarded and the cell pellet was frozen on dry ice and kept at -20°C overnight.

2.2.4.8 Recombinant protein purification

The cell pellet was thawed and resuspended in 20 ml ice-cold His-tag buffer (containing complete protease inhibitor cocktail and 1 mM PMSF) or GST-tag buffer (containing complete protease inhibitor cocktail and 1 mM PMSF) depending on the type of recombinant protein to be purified. 1 ml of 10 mg/ml lysosyme in the same buffer was then added and the tube was inverted several times and vortexed to ensure proper mixing. This was then incubated on ice for 30 min until the contents had become very viscous due to cell lysis. The lysate was then sonicated four times for 30 sec each using a 0.8 mm tapered Dawa Ultrasonics probe at 50 watts with a 30 sec pause between sonications. The lysate was then clarified by centrifugation for 15 min at 10,000 rpm in a Beckman JA-20 rotor at 4°C. The lysate was then transferred to a 50 ml centrifuge tube containing 2.5 ml of washed nickel NTA-agarose (for His-tagged proteins; Qiagen) or glutathione-sepharose 4B (for GST-fusion proteins; Pharmacia) beads. The tube was sealed with parafilm and placed

on a roller mixer for 2 h at 4°C. Following centrifugation at 2000 rpm for 5 min in a benchtop centrifuge, the supernatant was removed and the beads were washed five times in 50 ml His-tag buffer (for His-tagged proteins) or PBS (for GST-fusion proteins). The beads were transferred to a column consisting of a 5 or 10 ml syringe barrel plugged with a small disc of Whatman filter paper. 5 ml of His-tag elution buffer (His-tag buffer containing 200 mM imidazole, pH 7.0) or GST-tag elution buffer (10 mM reduced glutathione in 50 mM Tris, pH 8.0) were then added to the column and 1 ml fractions were collected from the bottom of the column. The protein concentrations of the fractions were determined as described in section 2.2.4.1 and those containing the most protein were pooled and dialysed into PBS using slide-a-lyzer dialysis cassettes (Pierce). The purity of the protein was assessed by SDS-PAGE followed by Coomassie staining of the gel (see sections 2.2.4.2 and 2.2.4.3).

Chapter 3

A yeast two-hybrid screen for Arf5 effectors

Introduction

3.1.1 ADP ribosylation factors

The ADP ribosylation factor (Arf) family of small molecular weight GTP-binding proteins forms one branch of the Ras superfamily. It is itself further subdivided into Arfs and Arf-like protcins called Arls. There are six known mammalian Arf isoforms (Arf1-6) categorised into three classes based on sequence homology and size. Class I Arfs include Arfs 1, 2 & 3, class II comprises Arfs 4 & 5 while Arf6, the least conserved family member, is the sole member of class III. There are also a number of Arls so far described but these have been less well studied. As with all Ras-like GTPases, Arfs cycle between active and inactive conformations when GTP- and GDP-bound, respectively, and these states can be mimicked by point mutations (Fig. 3.1.1). Arfs have almost no detectable intrinsic GTPase activity, and hence GTP hydrolysis is catalysed by accessory GTPase activating proteins (GAPs) and GDP/GTP exchange is mediated by guanine nucleotide exchange factors (GEFs), which contain Sec7 domains (reviewed in Donaldson and Jackson, 2000). Upon GTP binding, conformational changes occur such that the Arf N-termini, which are the regions with the greatest sequence diversity, become exposed allowing for interactions with membranes and downstream effector molecules. Importantly, Arfs are myristoylated on position 2 glycine residues and these moieties are required for *in vitro* and *in vivo* activities. Arfs generally cycle on and off membranes depending on their nucleotide status and this is central to their function (see section 1.3).

Arf6 is the most divergent member of the family in terms of primary amino acid sequence. It also differs from the other Arfs in that in its active state, it is located at the plasma membrane, where it regulates endosomal recycling to the plasma membrane (D'Souza-Schorey et al., 1995), GLUT4 exocytosis and adipsin secretion in adipocytes (Millar et al., 1999; Yang and Mueckler, 1999), and clathrin endocytosis (Altschuler et al., 1999). It also seems to be a major player in the regulation of the cortical actin cytoskeleton (see section 1.3.5). By contrast, Arfs 1-5 are reported to reside intracellularly in and around the Golgi complex. Of these isoforms, Arf1 is by far the best characterised and its role in coatomer and clathrin coat formation is very well documented (Schekman and Orci, 1996; Brodsky et al., 2001). All Arf isoforms are virtually indistinguishable in a number of assays including the ADP-ribosylation of Gs catalysed by cholera toxin, the activation of phospholipase D, the recruitment of coat complexes to Golgi membranes and the rescue of lethal *arf1*$^{-}$*/arf2*$^{-}$ double mutation in *Saccharomyces cerevisiae* (Boman and Kahn, 1995).

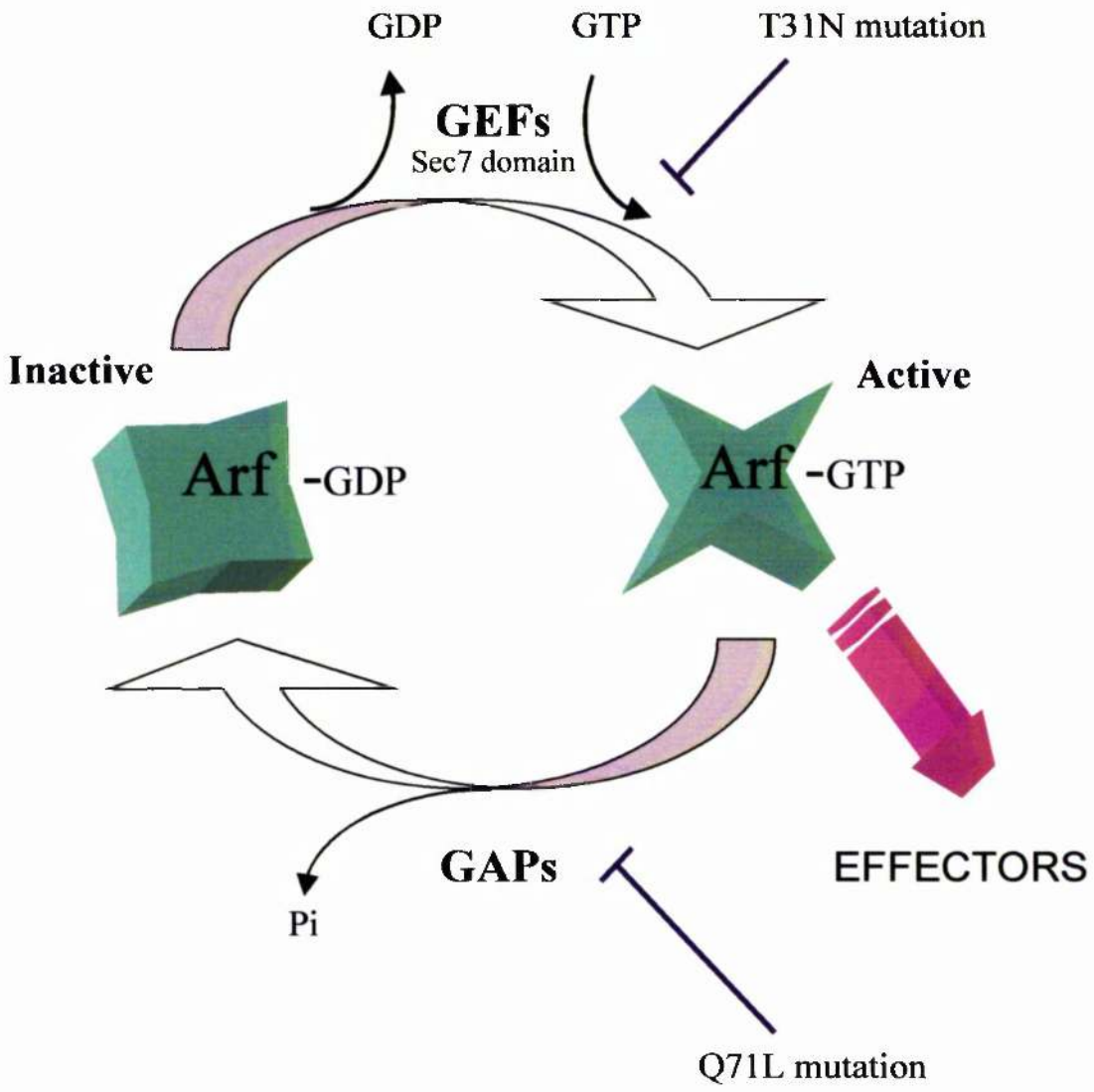

Fig. 3.1.1 **The Arf GTPase cycle.**
Inactive cytosolic Arfs are activated by GDP/GTP exchange catalysed by exchange factors containing Sec7 domains (GEFs). This causes a conformational change allowing interaction with downstream effector molecules and membrane association via an N-terminal myristoyl moiety. GTP hydrolysis is then catalysed by GTPase activating proteins (GAPs) returning the Arf to its inactive form. GTP binding is defective in T31N mutants (T27N for Arf6) resulting in a GDP-locked form, whereas a Q71L mutation (Q67L for Arf6) results in a GTPase deficient GTP-locked form.

It had generally been accepted by many researchers that the class I and II Arfs have overlapping or redundant roles since, for example, Arf1 and Arf5 are equally effective at recruiting the adaptor AP-1 to purified Golgi membranes (Liang and Kornfeld, 1997). While this may be true for some assays, there is recent evidence to suggest that there are probably some class-specific functions as well. Firstly, an Arf GEF, GBF1, was cloned from CHO-K1 cells and shown to exhibit specificity for Arf5 *in vitro*, suggesting a unique Arf5 pathway (Claude et al., 1999). Secondly, a yeast two-hybrid screen led to the discovery of Arfophilin, a class II/III-specific and GTP-dependent Arf interacting protein (Shin et al., 1999; Shin et al., 2001). Furthermore, work from this laboratory showed that the addition of a myristoylated synthetic peptide corresponding to the unique N-terminus of Arf5 to permeabilised 3T3 L1 adipocytes inhibited insulin-stimulated GLUT1 and transferrin receptor translocation to the plasma membrane (Millar et al., 1999). Analogous Arf1 or Arf6 peptides could not mimic this effect, again suggestive of an Arf5-specific pathway (Millar et al., 1999). Also consistent with the notion that class I and II Arfs are not completely interchangeable and perform some distinct functions is the finding that the PDZ domain of PICK1 specifically interacts with GTP-bound class I Arfs but not class II Arfs (Takeya et al., 2000).

3.1.2 The yeast two-hybrid system

The yeast two-hybrid system was first described just over a decade ago (Fields and Song, 1989), and it has since become a widely used tool for detecting protein-protein interactions. It is an exceptionally powerful technique as it can be used to screen whole cDNA libraries from any organism and can rapidly provide cloned cDNAs of proteins interacting with a chosen protein of interest. The GAL4 system is perhaps the most widely used two-hybrid system and it is based on the fact that the GAL4 yeast transcription factor is comprised of two separable domains, a DNA binding domain that recognises a specific upstream activating sequence (UAS) and a transcriptional activation domain that recruits the cellular transcription machinery. These two domains can be expressed from plasmids in yeast as proteins fused to putative interacting partners of interest, proteins X and Y. If proteins X and Y do interact, they bring the two GAL4 domains into sufficient proximity to one another to allow transcription of any genes under the control of a GAL4 UAS promoter. Yeast reporter strains have been engineered to have auxotrophic amino acid biosynthesis genes under the control of such promoters. Therefore, these yeast strains are only able to survive on media lacking the particular amino acids when there is an

interaction between proteins X and Y. A simplified diagram of the yeast two-hybrid system is shown in Fig. 3.1.2.

Yeast two-hybrid screens have helped uncover many interactions and pathways involved in intracellular protein trafficking (reviewed in Stephens and Banting, 2000). They have been particularly successful when functional relevance has been built into the screening strategy. One such example was a screen for proteins that interacted with the cytosolic acidic cluster domain of furin. It was known that this domain was reversibly phosphorylated and that this was involved in the trafficking of the protein. Therefore, a screen was performed by using a bait consisting of a mutant furin domain mimicking the phosphorylated form and then counter-screening with a mutant corresponding to the non-phosphorylated form, and looking for a loss of interaction with the latter. This strategy yielded PACS-1, which does indeed mediate the trafficking of furin in a phosphorylation-dependent manner (Wan et al., 1998). Another well-planned screen identified TIP47 as a cargo selection device involved in mannose-6-phosphate receptor trafficking (Diaz and Pfeffer, 1998). Here the authors looked for proteins that would interact with the cytosolic tails of both the cation-dependent and -independent isoforms, which are structurally unrelated.

Systematic and large-scale yeast two-hybrid screening to identify any binary interacting partners has already been performed (reviewed in Uetz and Hughes, 2000) and one particular study using *Saccharomyces cerevisiae* open-reading frames identified 957 putative interactions involving 1004 different yeast proteins (Uetz et al., 2000). While this is a useful strategy for rapidly producing maps of putative protein-protein interactions, such an approach would fail to uncover many important interactions. One type of interaction that would be missed would be that of Ras-like GTPases interacting with their effectors. Because of the transient, GTP-dependent nature of such interactions *in vivo*, they cannot usually be detected in the two-hybrid system using the GTPases in their wild type conformations. Nevertheless, when tailored to specific small G proteins, the yeast two-hybrid system has been instrumental in identifying their downstream effector molecules (see Table 3.1.1 for some examples). This has been aided by the fact that there are known mutations that mimic GTP and GDP bound conformations, that were originally identified in Ras but analogous ones are found throughout the family, including the Arfs (Kahn et al., 1995). By definition, an effector molecule should only interact with a GTP-liganded G protein, so these mutations offer excellent intrinsic controls that can be incorporated into the screening strategy to discount potential false-positives. As these mutations can often have toxic effects on the yeast host, however, very low-level expression plasmids are

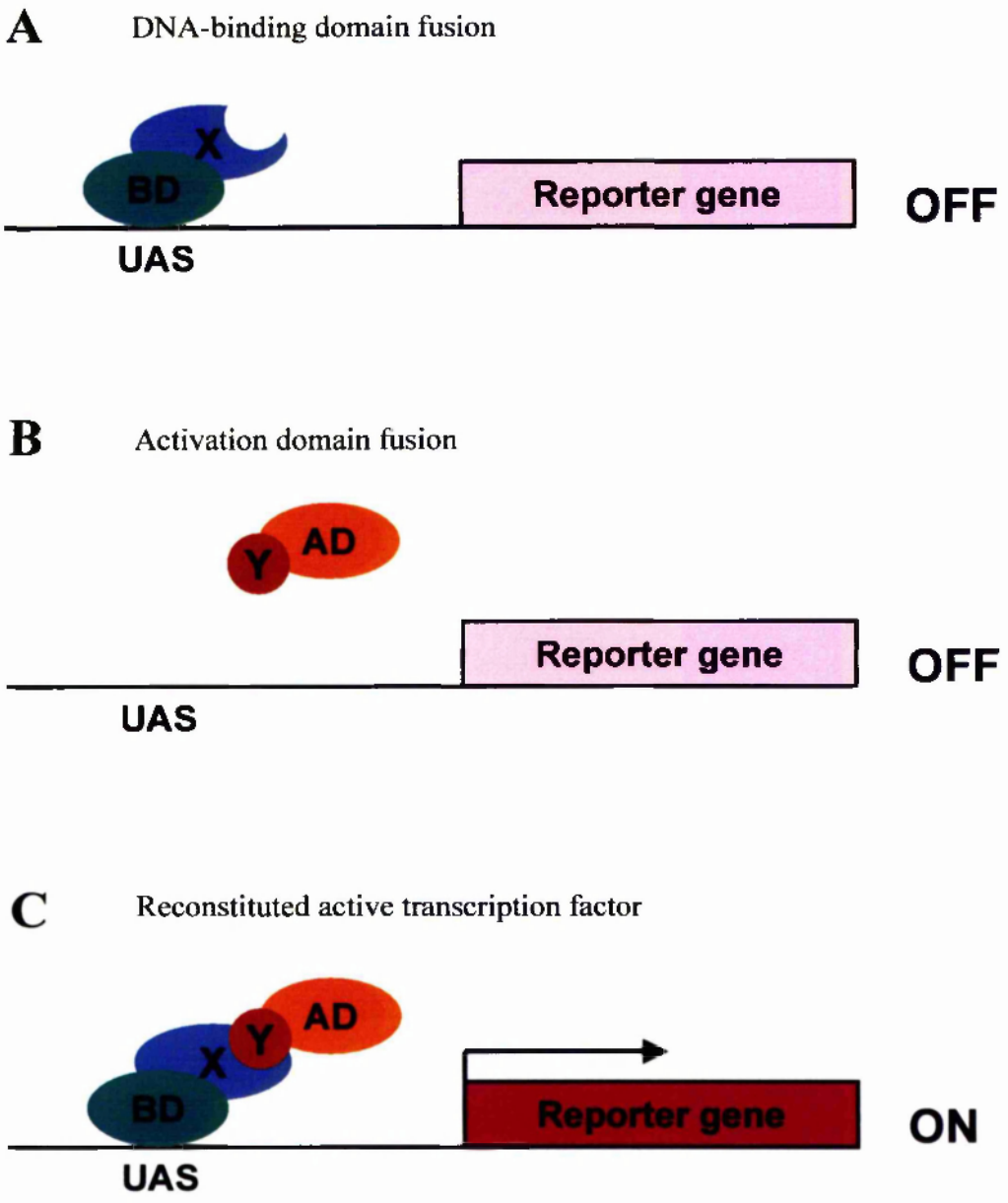

Fig. 3.1.2 **The principle of the yeast two-hybrid system.**

DNA-binding domain (BD) and transcription activation domain (AD) fusion proteins are engineered and expressed from plasmids in a yeast reporter strain. **A**. The BD fused to protein X binds to upstream activating sequences (UAS) but cannot itself activate transcription. **B**. The AD fused to protein Y is similarly unable to activate transcription in the absence of a DNA-binding domain. **C**. Interaction between proteins X and Y reconstitutes a functional transcription factor resulting in transcription of reporter genes, such as *HIS3* or *LacZ*, providing a read-out for the interaction. *(Adapted from Stephens & Banting, 2000).*

preferable if not essential. Another important consideration is the removal of prenylation motifs, such as the C-terminal CAAX motif in Rab proteins, as these can interfere with the targeting of the fusion proteins, which must of course enter the nucleus for the system to work. When properly implemented, such screens have successfully identified many binding partners for Rabs, Arfs/Arls, Rho family GTPases, Ran and Ras itself (see Table 3.1.1 for some examples for the Arf, Rab and Rho families).

Arfs are ubiquitous and abundant proteins, but the current repertoire of Arf effectors seems rather small. As this is especially the case for the class II Arfs, it was decided to perform a yeast two-hybrid screen for Arf5 effectors using the constitutively active Arf5Q71L mutant as bait. The specific aim of this chapter was, therefore, to perform such a screen and identify putative effectors based on selective interactions with the Q71L but not the T31N mutant of Arf5. A further aim was to assess the specificity of any interacting proteins for the different Arf isoforms, again using the two-hybrid system.

GTPase	Putative Effector	References
Arf	Arfaptin 1 & 2	Kanoh et al, 1997
	MKLP1	Boman et al, 1999
	GGA 1-3	Boman et al., 2000
Class I Arfs	PICK1	Takeya et al., 2000
Arf5	Arfophilin	Shin et al., 1999
Arl6	Sec61β	Ingley et al., 1999
Rab1	GM130	Weide et al., 2001
Rab3	Rabin3	Brondyk et al., 1995
Rab4	Rabip4	Cormont et al., 2001
	cytoplasmic dynein light chain-1	Bielli et al., 2001
Rab5	Rabaptin5	Stenmark et al., 1995
	Rabaptin5β	Gournier et al., 1998
	Rab5ip	Hoffenberg et al., 2000
Rab6	Rabkinesin-6	Echard et al., 1998
Rab7	Rab7-RIPL	Cantalupo et al., 2001
Rab8	Rab8ip	Ren et al., 1996
	FIP-2	Hattula and Peranen, 2000
Rab9	p40	Diaz et al., 1997
Rab11	Rab11BP/Rabphilin-11	Zeng et al., 1999; Mammoto et al., 1999
	Myosin Vb	Lapierre et al., 2001
Rho	rhotekin	Reid et al., 1996
	rhophilin	Watanabe et al., 1996
Rho/Rac1	citron	Madaule et al., 1995
Cdc42	WASP	Aspenstrom et al., 1996
	Cip4	Aspenstrom, 1997
	SPECs	Pirone et al., 2000
Rho/Rac/Cdc42	kinectin	Hotta et al., 1996
Rac	Plexin-B	Driessens et al., 2001

Table 3.1.1 **Putative small GTPase effectors identified by yeast two-hybrid screening.**

Some examples of putative effector proteins for small Ras-like GTPases of the Arf, Rab and Rho families that have been identified by yeast-two hybrid screening. While this is not an exhaustive list, it demonstrates the power of the technique in this particular application.

3.2 Materials & Methods

3.2.1 Yeast media

YPD powder was purchased from Sigma and dissolved in distilled water according to the manufacturer's instructions. This was sterilised by autoclaving and allowed to cool. A 0.2% (w/v) sterile-filtered solution of adenine hemisulphate (Sigma) was prepared and used to make YPAD which had a final concentration of 0.003% adenine. For agar plates (containing 20 g/L agar), the sterilised media were allowed to cool to 55-60°C before the addition of adenine and subsequent pouring.

Quadruple-dropout synthetic selection media consisted of 0.67% (w/v) yeast nitrogen base (Difco), 2% (w/v) glucose and 0.01% (w/v) each of alanine, arginine, asparagine, aspartic acid, cysteine, glutamine, glutamic acid, glycine, inositol, isoleucine, lysine, methionine, phenylalanine, proline, serine, threonine, tyrosine and valine and 0.001% para-aminobenzoic acid (all from Sigma). Leucine and histidine were added as appropriate to give final concentrations of 0.002% and 0.001%, respectively. The media were sterilised by autoclaving and allowed to cool. If required, a 0.2% (w/v) sterile-filtered solution of adenine hemisulphate (Sigma) was then added to a final concentration of 0.003%. For agar plates (containing 20 g/L agar), the sterilised media were allowed to cool to 55-60°C before the addition of adenine and subsequent pouring.

3.2.2 Constructing the bait plasmids

Murine Arf5Q71L and Arf5T31N cDNAs were obtained from Dr. J. Tavare (University of Bristol). These were then PCR amplified using *Pfu* polymerase and primers `5'-GGGagatctCCATGGGCCTCACGGTGTCCGCG-3'` (*BglII* site in small letters, initiating codon in bold) and `5'-GGGctcgagTCAGCGCTTTGACAGCTCGTGGGA-3'` (*XhoI* site in small letters, STOP codon in bold). The resulting products were TA cloned into pCRII-TOPO, sequenced and subcloned into the *BamHI* and *SalI* sites of pGBT9, all according to the methods in chapter 2 and producing plasmids pGBT9-Arf5Q71L and pGBT9-Arf5T31N (see the appendix).

3.2.3 Small-scale yeast transformations

Yeast reporter strain PJ69-2A (Clontech) was cultured on YPAD agar plates, with a fresh plate being streaked out every three weeks. A match head sized ball of yeast cells were used to inoculate a starter culture in 25 ml of sterile YPAD medium in a 100 ml flask that was grown overnight at 30 °C with shaking at 200 rpm. This starter culture was then used to inoculate 200 ml of YPAD in a 1 L flask to give a starting OD_{600} of between 0.1-0.2. This was then further cultured at 30 °C with shaking at 200 rpm until the OD_{600} reached 0.5-0.6 (typically 3-4 h). At this point the cells were harvested by centrifugation at 2000 rpm for 5 min at room temperature in 50 ml Falcon tubes in a Beckman bench-top centrifuge. The pelleted cells were resuspended and pooled in 50 ml sterile water and spun again. All traces of water were removed and the cells were resuspended in 1.5 ml freshly prepared sterile 100 mM LiAc in 1 x TE buffer. 100 µl of cells were then added to sterile 1.5 ml centrifuge tubes containing 10 µl of salmon sperm carrier DNA (Sigma) at a concentration of 10 mg/ml and also containing 1 µl of each plasmid to be transformed. These were then briefly mixed by vortexing and 0.6 ml freshly prepared sterile 5% PEG-3350/100 mM LiAc solution was added to each tube. After a 10 second vortex, these were incubated at 30 °C for 30 min with shaking at 300 rpm. 70 µl of DMSO were then added to each tube and these were mixed by inversion and then heat-shocked for 15 min at 42 °C in a water bath. The tubes were then placed on ice for 1 min and centrifuged for 5 seconds in a microcentrifuge. The supernatants were removed by aspiration and the cell pellets were resuspended in 0.5 ml sterile TE. 200 µl from each transformation were then plated onto the appropriate synthetic medium selective for the transformed plasmids (lacking leucine and tryptophan if pGBT9 and pACT2 plasmids were co-transformed). After 3 or 4 days of growth at 30 °C, colonies were picked with sterile yellow pipette tips and restreaked onto selective media also lacking histidine (triple dropout, TDO) or histidine and adenine (quadruple dropout, QDO) to look for the reconstitution of transcriptional activation and hence interactions.

3.2.4 Yeast two-hybrid screening

A schematic of the two-hybrid system used in this study is given in Fig 3.2.1 The screens were performed essentially according to the TRAFO protocol (Agatep et al., 1998; Parchaliuk et al., 1999) (see also http://www.umanitoba.ca/faculties/medicine/units/human_genetics/gietz/2HS.html). Since greater transformation efficiency is achieved if sequential transformation is performed, a bait strain containing pGBT9-Arf5Q71L was

produced by performing a small-scale transformation, as described above, and it was selected for on medium lacking tryptophan. This was then cultured overnight at 30 °C with shaking at 200 rpm in 50 ml SC media lacking tryptophan to maintain the presence of the plasmid. This was then sub-cultured into 150 ml YPAD medium to give an OD_{600} of 0.1 (5 x 10^6 cells/ml) and grown until the OD_{600} reached 0.4 (2 x 10^7 cells/ml). The cells were then harvested and washed as in section 3.2.3, and resuspended in fresh 100 mM LiAc in TE to give a total volume of 4 ml. This was then divided into 6 aliquots of 0.6 ml in 15 ml sterile Falcon centrifuge tubes. To these were added, and in the following order, 960 µl 50% PEG-3350, 216 µl 1 M LiAc, 300 µl salmon sperm carrier DNA (at a concentration of 2.0 mg/ml, boiled for 5 min and chilled on ice for 5 min), and 204 µl of water containing 60, 600, or 6000 ng of human testis or human brain cDNA libraries in pACT2 and pGAD10 vectors, respectively (both from Clontech). These were then vigorously vortexed for 10 seconds and incubated at 30 °C for 30 min. This was followed by a 15 min heat-shock at 45 °C in a water bath. During this time, the tubes were gently agitated every 1-2 min to ensure even heat distribution. The tubes were then chilled on ice for 2 min and centrifuged briefly to pellet the cells. All of the supernatant was removed and the cells were resuspended in 2 ml sterile water. 2 µl from each transformation were added to 100 µl of water and plated onto a -leu/-trp plate to monitor the transformation efficiency, while the remaining cells were pooled according to the library that was transformed and these were then each plated onto a total of six 150 mm triple dropout selection plates lacking histidine as well as leucine and tryptophan. These plates were then incubated at 30 °C for 3-6 days and any colonies appearing during this time were picked and restreaked onto fresh triple and quadruple dropout plates awaiting further analysis.

3.2.5 Extraction of DNA from yeast cells

Crude DNA extractions were performed as follows on the yeast clones of interest. A match head sized ball of cells scraped from a fresh plate were resuspended in 1 ml of water in a 1.5 ml centrifuge tube. These were then pelleted by centrifugation at 10,000 g for 2 min and resuspended in 0.5 ml buffer S (10 mM K_2HPO_4, pH 7.2; 10 mM EDTA; 50 mM β-mercaptoethanol; 50 µg/ml zymolase). Following incubation at 37 °C for 30 min, 100 µl of lysis buffer (25 mM Tris-HCL, pH 7.5; 25 mM EDTA; 2.5% (w/v) SDS) were added. The tubes were then vortexed and incubated for a further 30 min at 65 °C. Then 166 µl of 3 M potassium acetate were added to each tube and these were mixed by inversion and incubated on ice for 10 min. The tubes were then spun in a microcentrifuge for 10 min at

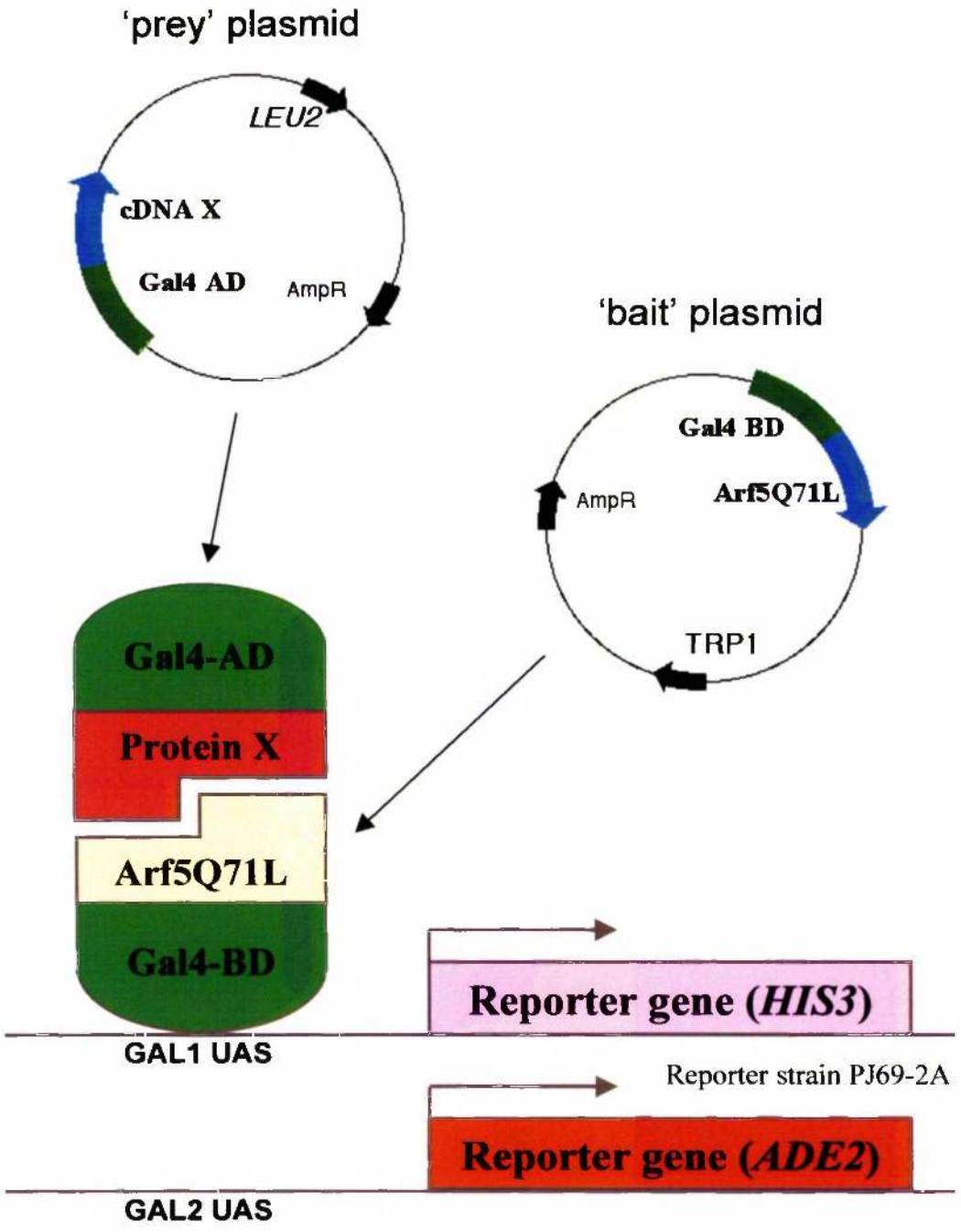

Fig. 3.2.1 **Schematic of the yeast two-hybrid system used in this study.**

The yeast strain PJ69-2A has two reporter genes *HIS3* and *ADE2* under the control of a GAL4 promoter. Arf5Q71L fused to the GAL4 DNA binding domain (BD) is expressed from a plasmid (pGBT9) that also contains a *TRP1* marker. Putative interacting proteins (X) are expressed as fusions to the GAL4 activation domain (AD) from a plasmid containing a *LEU2* selectable marker. If a protein X interacts with Arf5Q71L, the GAL4 transcription factor is reconstituted and the yeast can grow on media lacking histidine and adenine.

full-speed, the supernatants were aspirated and discarded and the pellets were washed with 1 ml 70% ethanol. The pellets, containing a mixture of genomic and plasmid DNA, were then air dried and resuspended in 40 µl distilled water.

3.2.6 Recovery of prey plasmids

As both the bait plasmid pGBT9 and the prey plasmids pACT2/pGAD10 have ampicillin resistance as their selectable marker for growth in *Escherichia coli*, it was necessary to recover the prey plasmids of interest by using nutritional selection. KC8 strain of *Escherichia coli* requires leucine to be added to growth medium, so transformants containing the pACT2 or pGAD10 plasmids (which have a yeast *LEU2* marker) should grow on media lacking leucine, while transformants containing the pGBT9 plasmid should not. 50 µl of electrocompetent KC8 cells were then placed at the bottom of pre-chilled sterile electroporation cuvettes (Bio-Rad) together with 1 µl extracted yeast DNA. These were then electroporated in a Bio-Rad Genepulser at 2.5 Mv with the capacitance set at 25. The cells were then gently recovered in 1 ml LB broth and incubated for 1 h at 37 °C without agitation. The cells were then pelleted by centrifugation at 4000 rpm for 1 min in a microcentrifuge, resuspended in 50 µl of sterile water and plated onto M9 minimal media agar plates lacking leucine. Colonies appearing after 24-30 h of growth at 37 °C were picked and cultured overnight in 3 ml LB broth containing 100 µg/ml ampicillin. Small-scale DNA preparations were then performed according to the protocol in section 2.2.1.11 and the purified plasmids were digested with *BglII* and *EcoRI* to verify that the correct plasmids had been rescued and also to verify the sizes of the inserts within those plasmids.

3.2.7 Retransformation of recovered plasmids

Following the rescue of the pACT2/pGAD10 prey plasmids encoding the putative Arf5-interacting proteins, it was necessary to retransform these back into the yeast strain together with the bait pGBT9-Arf5Q71L plasmid to ensure that the yeast were indeed growing as a result of the plasmids and not due to some mutation or anomaly. At the same time, the prey plasmids were also retransformed together with the pGBT9-Arf5T31N plasmid to check whether interactions were specific for the GTP-bound mutant and not the GDP-bound mutant, as would be predicted for any effector protein. All transformations were carried out exactly as in section 3.2.3.

3.2.8 Immunoblot analysis of yeast proteins

Immunoblot analysis was also performed of the yeast expressing the putative positives as GAL4 activation domain fusion proteins. Samples for SDS-PAGE were prepared as follows: match head sized balls of cells from fresh plates were resuspended in 1 ml water in 1.5 ml microcentrifuge tubes. 100 µl 1.85 M NaOH containing 7.5% (v/v) β-mercaptoethanol were then added, and the tubes were incubated on ice for 10 min. 150 µl of 55% (w/v) trichloroacetic acid were then added and the tubes were further incubated for 10 min on ice. These were then centrifuged at full-speed for 10 min at 4°C. The supernatants were discarded and the precipitated proteins were resuspended in 200 µl HU buffer (8 M urea; 5% (w/v) SDS; 200 mM Tris-HCl pH 6.8; 0.1 mM EDTA; 0.5 mg/ml bromophenol blue; 10% (v/v) β-mercaptoethanol). The samples were then boiled for a few min and a few microlitres of 1M Tris-base were added if the solutions turned yellow. 20 µl of each sample were run on 10% or 15% SDS-PAGE gels and immunoblotted using a monoclonal anti-haemagglutinin (HA) antibody (Santa Cruz, F7 probe), all according to the protocols in section 2.2.4. This antibody recognises a HA epitope situated between the GAL4 activation domain and any protein fused to it encoded by the pACT2 vector.

3.2.9 Sequence analysis

Prey plasmids that appeared to confer GTP-dependent interactions with Arf5, were digested with BglII to determine the sizes of the inserts, and subjected to automated sequencing. This was initially performed according to the procedure outlined in section 2.2.1.14 using a primer designed against the GAL4 activation domain sequence `5'-TACCACTACAATGGAT-3'`. Internal forward and reverse sequencing primers were then designed and used to sequence the whole inserts. Sequences obtained were then analysed in Editview and by BLAST searching against the public non-redundant and EST databases (at http://www.ncbi.nlm.nih.gov/blast/).

3.2.10 Cloning and mutagenesis of other Arf proteins

Bovine Arf1Q71L and Arf1N126I (another dominant negative GTP-binding defective mutant) were amplified by PCR from pre-existing plasmids obtained from Dr. S. Cockcroft (University College London), using primers `5'-ggatccCCATGGGGAACATCTTCGCCAACC-3'` (*BamHI* site in small letters) and `5'-ctcgagTCACTTCTGGTTCCGGAGCTG-3'` (*Xho I* site in small letters) and subcloned into the *BamHI* and *SalI* sites of pGBT9 exactly as described

for Arf5 in section 3.2.1. Arf6Q67L and Arf6T27N pGBT9 constructs were similarly generated by amplifying the ORFs from plasmids obtained from Dr. J. Donaldson (NIH, Bethesda), using primers 5'-GGGagatctCC**ATG**GGGAAGGTGCTATCCAAA-3' (*Bgl II* site in small letters, start codon in bold) and 5'-GGGctcgag**TTA**AGATTTGTAGTTAGAGGTTAA-3' (*Xho I* site in small letters, stop codon in bold).

Arf2 was amplified by two rounds of PCR from a murine Marathon-Ready cDNA library (Clontech) using primers 5'-GggatccC**CATG**GGGAATGTCTTTGAAAAGCTGTTTAA AAGCC-3' (*BamHI* site in small letters, start codon in bold) and 5'-Gctcgag**TCA** CTTCTGGTTTTTGAGCTGGTTGGAGAG-3' (*Xho I* site in small letters, stop codon in bold). Arf3 and Arf4 cDNAs were amplified from a human foetus Marathon-Ready library (Clontech) using primers 5'-GggatccC**CATG**GGCAATATCTTTGGAAACCTTCTCAAG-3' (*BamHI* site in small letters, start codon in bold) and 5'-Gctcgag**TCA**CTTCTTGTTTTTGAGCTGATTGGCCAG-3' (*Xho I* site in small letters, stop codon in bold), and 5'-GggatccC**CATG** GGCCTCACTATCTCCTCCCTCTTCTCC-3' (*BamHI* site in small letters, start codon in bold) and 5'-Gctcgag**TTA**ACGTTTTGAAAGCTCATTTGACAGCCAGTC-3' (*Xho I* site in small letters, stop codon in bold), respectively. These were then TA cloned into pCRII-TOPO vector (Invitrogen) and subjected to QuikChange site-directed mutagenesis to produce the active/ inactive mutants, all according to the protocols described in Chapter 2. These were then sequenced and subcloned into the *BamHI* and *Sal I* sites of pGBT9. The pairs of mutagenic primers used to produce the indicated mutants were as follows, with changes in bold:

Arf2Q71L: 5'-TGGGATGTTGGTGGCCTGGACAAAATTAGACCT-3'
3'-ACCCTACAACCACCGG**A**CCTGTTTTAATCTGGA-5'

Arf2T31N: 5'-GATGCAGCTGGCAAAAA**C**ACGATCTTGTACAAA-3'
3'-CTACGTCGACCGTTTTT**G**TGCTAGAACATGTTT-3'

Arf3Q71L: 5'-TGGGATGTGGGTGGCCTGGACAAGATTCGACCC-3'
3'-ACCCTACACCCACCGG**A**CCTGTTCTAAGCTGGG-5'

Arf3T31N: 5'-GATGCCGCAGGAAAGAA**C**ACCATCCTATACAAG-3'
3'-CTACGGCGTCCTTTCTT**G**TGGTAGGATATGTTC-5'

Arf4Q71L: 5'-TGGGATGTTGGTGGTCTAGATAGAATTAGGCCT-3'
3'-ACCCTACAACCACCAG**A**TCTATCTTAATCCGGA-5'

Arf4T31N: 5'-CATCCTGCTGGCAAGAA**C**ACCATTCTGTATAAA-3'
3'-CTACGACGACCGTTCT**T**GTGGTAAGACATATTT-5'

3.2.11 Production of Arf4/Arf5 chimeras

This work was performed jointly with Sam Yarwood, and an outline of the strategy used to produce the Arf4/Arf5 chimeras is given in Fig. 3.2.1. Constructs containing Arf4Q71L and Arf4T31N in the pCRII vector, that were obtained in section 3.2.9, were subjected to a further round of site directed mutagenesis to introduce an *Acc I* restriction site at position 276 of the ORFs. This required a single base substitution (T-C) at position 280, a mutation that would not affect the amino acid composition of the resulting polypeptide. The primers used were 5'-CCCAGGGTCTTATTTTTGTGGTAGACAGCA ACGATCGTGAAAGAATTCAG-3' and 5'-CTGAATTCTTTCACGATCGTTGCTGTCTACCACAAAAATAAG ACCCTGGG-3' and the presence of the desired mutation and the absence of undesired ones were verified by automated sequencing. Arf5Q71L and Arf5T31N cDNAs also in pCRII had pre-existing *Acc I* sites at the same position and all four constructs had been TA cloned in the same orientation into the vector, such that the 5' end of the ORFs were nearer the T7 promoter than the SP6 promoter. This then allowed the isolation of *Kpn I* and *Acc I* digested 5' ends, which could then be swapped and religated to produce N5-Arf4Q71L, N5-Arf4T31N, N4-Arf5Q71L and N4-Arf5T31N (see Fig. 3.2.1, and the appendix). These chimeric cDNAs were then subcloned into the *BamHI* and *Sal I* sites of pGBT9. All DNA manipulations were using the standard molecular biology procedures outlined in Chapter 2.

1

```
Human Arf4 MGLTISSLFSRLFGKKQMRILMVGLDAAGKTTILYKLKLGEIVTTIPTIGFNVETVEYKN 60
Human Arf5 MGLTVSALFSRIFGKKQMRILMVGLDAAGKTTILYKLKLGEIVTTIPTIGFNVETVEYKN 60

Human Arf4 ICFTVWDVGGQDRIRPLWKHYFQNTQGLIFVVDSNDRERIQEVADELQKMLLVDELRDAV 120
Human Arf5 ICFTVWDVGGQDKIRPLWRHYFQNTQGLIFVVDSNDRERVQESADELQKMLQEDELRDAV 120

Human Arf4 LLLFANKQDLPNAMAISEMTDKLGLQSLRNRTWYVQATCATQGTGLYEGLDWLSNELSKR 180
Human Arf5 LLVFANKQDMPNAMPVSELTDKLGLQHLRSRTWYVQATCATQGTGLYDGLDWLSHELSKR 180
```

2

A Arf4

Acc I

5′-CCCAGGGTCTTATTTTTGTGGTAGACAGCAAGCATCGTGAAAGAATTCAG-3′

3′-GGGTCCCAGAATAAAAACACCATCTGTCGTTCGTAGCACTTTCTTAAGTC-5′

B

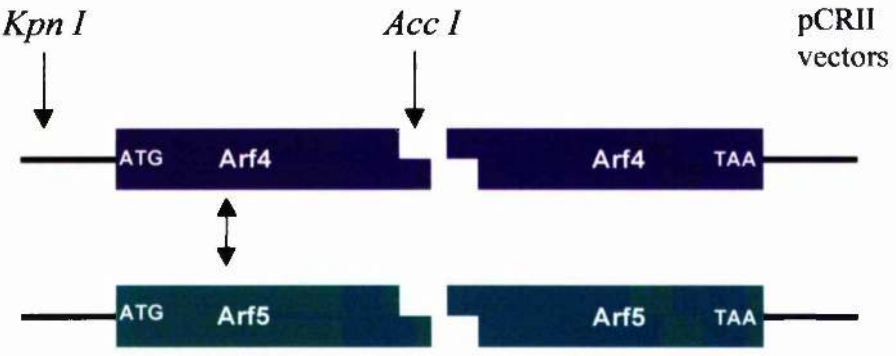

C

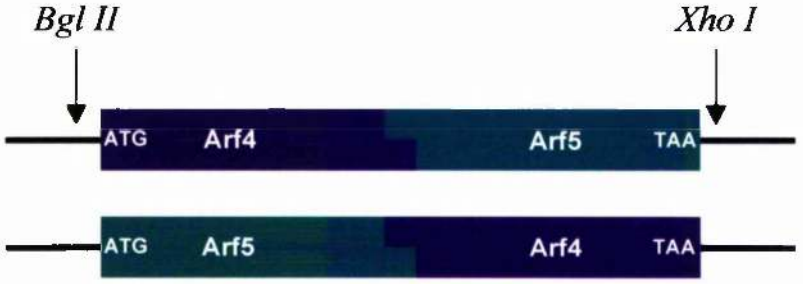

Fig. 3.2.2 **The construction of Arf4/Arf5 chimeras.**

Panel 1: Amino acid sequence alignment of Arf4 and Arf5. The 18 non-identical residues are in bold and the position where the N-termini were swapped is underlined. Panel 2: Strategy for producing chimeras. A, oligonucleotide primers used to produce a silent mutation at base 276 (in bold) of the Arf4 ORF to introduce an *Acc I* restriction site (underlined). B, Arf4(276C) and Arf5 pCRII plasmids were then digested with *Kpn I* and *Acc I*. C, The resulting inserts were then swapped and ligated to the other vector sequences to produce chimeric Arf cDNAs. These were then subcloned into pGBT9 using the *Bgl II* and *Xho I* sites as indicated. Although not shown, the entire procedure was performed using both T31N and Q71L mutants of Arf4 and Arf5. These DNA manipulations were performed jointly with S. Yarwood.

3.3 Results

Arf5 constitutively active (Q71L) and dominant negative (T31N) mutants were subcloned into vector pGBT9 in frame with the GAL4 DNA binding domain, as described in section 3.2.1. This vector uses a truncated *ADH* promoter that gives rise to very low-level expression in yeast, which is necessary to reduce the toxic effects that would otherwise be apparent upon constitutively active Arf expression (Deitz et al., 1996). It was then necessary to check that the expression of the constructs did not allow growth on media selective for an interaction, in the presence of the 'empty' prey plasmid pACT2, since any growth would render the screen unworkable. This was performed in the reporter strain PJ69-2A which has two reporter genes under the control of GAL4: *HIS3* and *ADE2*. This allows for two levels of stringency for selecting for an interaction: medium stringency by monitoring growth on media lacking histidine, and high stringency requiring the activation of both genes. The plasmids were co-transformed as described in section 3.2.3 and no growth was observed on media lacking histidine showing that the constructs did not allow auto-activation (data not shown). Immunoblots of yeast transformed with these plasmids were also performed using a monoclonal antibody against the GAL4 DNA-binding domain to check for expression of the fusion constructs. This revealed bands with apparent molecular weights of approximately 40 kDa, as expected (data not shown).

At the outset, the intention was to perform large-scale screens but as it turned out, this was not necessary. Pilot scale screens were performed by producing a bait strain, pGBT9-Arf5Q71L in PJ69-2A and then transforming this with human brain and testis libraries in pGAD10 and pACT2, respectively. This gave rise to approximately 60,000 transformants that were plated onto synthetic media lacking leucine, tryptophan and histidine (triple dropout) to select for the plasmids and any interactions. Colonies appearing within 5 days of growth at 30 °C, were then picked and restreaked onto the same media, and media also lacking adenine (quadruple dropout) as a higher stringency selection for interactions. At this stage there were 3 colonies from the brain screen and 23 colonies from the testis screen. DNA was then recovered from the yeast and the prey plasmids were isolated as described in sections 3.2.5 and 3.2.6. These were then retransformed into PJ69-2A yeast together with pGBT9-Arf5Q71L or pGBT9-Arf5T31N constructs and plated onto -Leu/Trp plates. The resulting co-transformants were then streaked onto triple and quadruple dropout selection media to ascertain whether the *HIS3* and *ADE2* reporter genes were activated. One plasmid from the brain library (designated clone B1) and eight from the testis library (clones T3, T4, T9, T12, T14, T17 and T20) allowed growth under these conditions when

co-transformed with the pGBT9-Arf5Q71L construct but not with the pGBT9-Arf5T31N dominant negative construct (see Figs. 3.3.1-3.3.5 and Table 3.3.1). The plasmids conferring these specific interactions were then digested with *BglII* to determine the insert sizes, and were sequenced using a plasmid-specific primer as described in section 3.2.8 and analysed by BLAST searching. The results are summarised in Table 3.3.1.

Immunoblot analyses of the yeast expressing the different GAL4-activation domain fusion proteins were also performed to check for the expression and sizes of the proteins produced. This revealed that T4, T14, T17 and T20 clones expressed fusion proteins of approximately 100 kDa (Fig. 3.3.6), while T9 only encoded a protein of about 35-40 kDa. Curiously, no fusion protein was detected in cells transformed with the T3 plasmid (Fig. 3.3.6). The size of the B1 clone fusion protein was not determined as the pGAD10 vector, unlike pACT2, does not encode a HA epitope.

From the testis screen, clone T3 encoded the full open-reading frame of Arfaptin 2/POR1 including some 5' and 3' UTR sequences. Interestingly, the 5' UTR contained a 40 bp insert not present in the Genbank entries and also contained a single in-frame stop codon near the GAL4-AD/testis cDNA fusion junction.

A third plasmid recovered from the testis screen, T12, encoded the C-terminal half of a protein present in the database as two proteins of slightly different length (accession numbers AB029343 and XM_041760) but whose function is unknown. It is named HCR for "α-helical coiled-coil rod homologue". The gene is on chromosome 6 near the HLA (human leukocyte antigen) locus where many major histocompatibility complex genes are found, but no other information was available at the time.

Five additional clones from testis (T4, T9, T14, T17, T20) had inserts of varying size ranging from 900-2000 bp but that were all identical at their 3' ends, with T4 and T20 having the longest insert and T9 the shortest. BLAST analysis against the non-redundant database revealed that these came from a novel gene on human chromosome 17, aided by the fact that the genomic region had been fully sequenced. Further analysis revealed that the protein encoded by this gene shared significant homology in its C-terminus with the C-terminal Arf-binding domain of KIAA0665/Arfophilin (63% identity and 79% homology; see Fig. 3.3.7, and in greater detail in Chapter 4), although the N-termini were divergent. It was, therefore, decided to name this novel protein Arfophilin-2. BLAST analysis also revealed homology between both Arfophilins and other metazoan proteins, but this will be addressed in Chapter 4.

clone	approx. cDNA insert size (bp)	GAL4-AD fusion protein size (kDa)	BLAST search results	Accession numbers
B1	900	N.D.	3' end of Kiaa0665/Arfophilin	NM_014700
T3	1600	not visible	Arfaptin 2 complete ORF	U52522
T4	2000	100	unknown but identical to regions of a chromosome 17 genomic clone	AC003101
T9	900	35	same as T4 but shorter cDNA	AC003101
T14	2000	100	same as T4	AC003101
T17	2000	100	same as T4	AC003101
T20	2000	100	same as T4	AC003101
T12	1000	60	Protein of unknown function: "α-helix coiled-coil rod homologue"	AB029343 (2270 bp) XM_041760 (2348 bp)

Table 3.3.1 **Summary of positive clones obtained by yeast two-hybrid screening for Arf5 effectors.**

The different clones that conferred specific interactions with Arf5Q71L and not with Arf5T31N are shown. B1 is the only one from the brain library while all the others are of testis origin. Approximate sizes of cDNA insert and GAL4-activation domain (AD) fusion proteins are shown, as are summarised BLAST search results against the non-redundant database. Relevant accession numbers of identical sequences present in the database are also given. N.D. not determined.

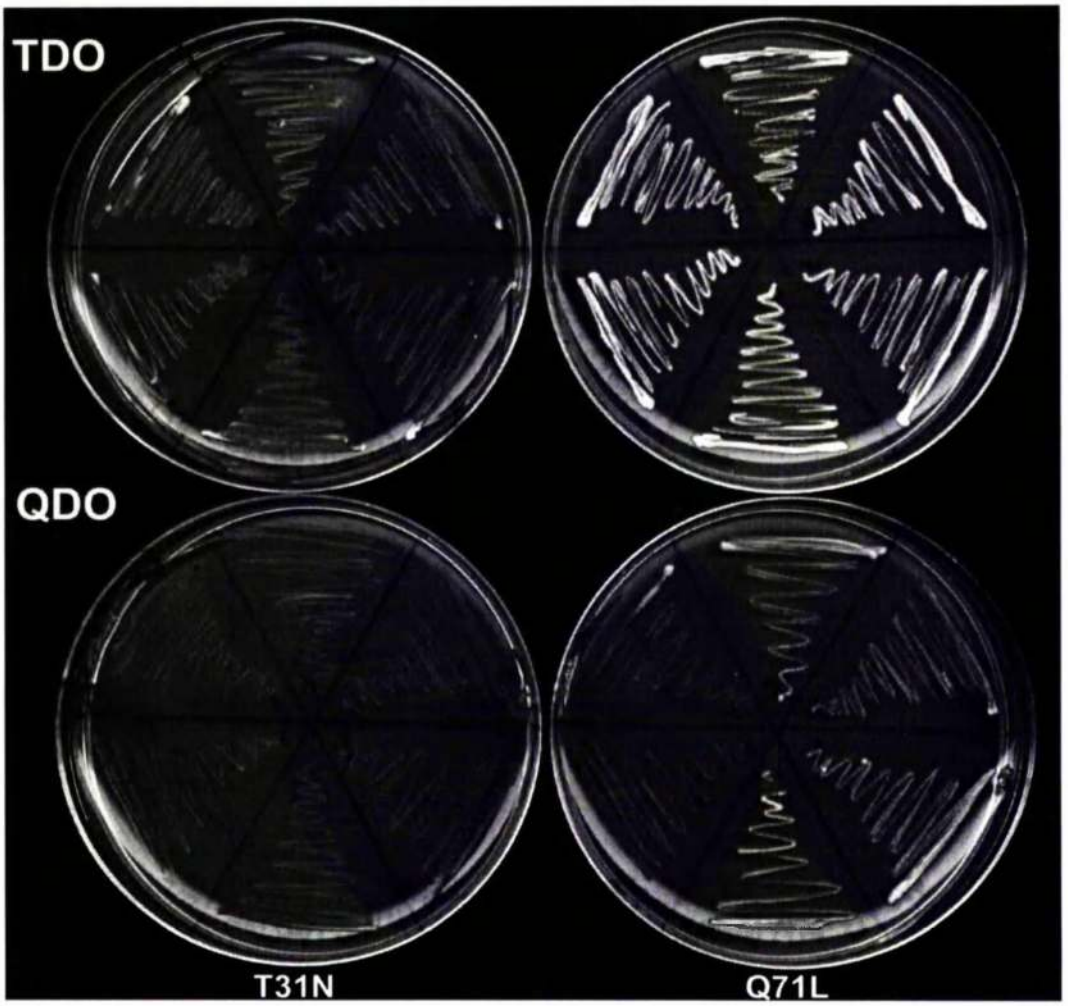

Fig. 3.3.1 **Yeast two-hybrid interaction assay between T3 and Arf5 Q71L and T31N mutants.**

Plasmid pACT2-T3 (encoding full-length Arfaptin 2/POR1) recovered from the two-hybrid screen, was co-transformed into yeast strain PJ69-2A with pGBT9-Arf5Q71L or pGBT9-Arf5T31N and plated onto synthetic media lacking leucine and tryptophan to select for the plasmids. After 3 days of growth at 30 °C, six independent colonies were then restreaked onto triple dropout medium lacking histidine (TDO; top plates) and quadruple dropout medium also lacking adenine (QDO; bottom plates), to select for an interaction with two levels of stringency. These were then grown for a further 3 days at 30 °C, and then scanned to produce the image above. Yeast co-expressing Arf5Q71L are displayed on the right, while those expressing Arf5T31N are on the left. This experiment was performed three times with similar results.

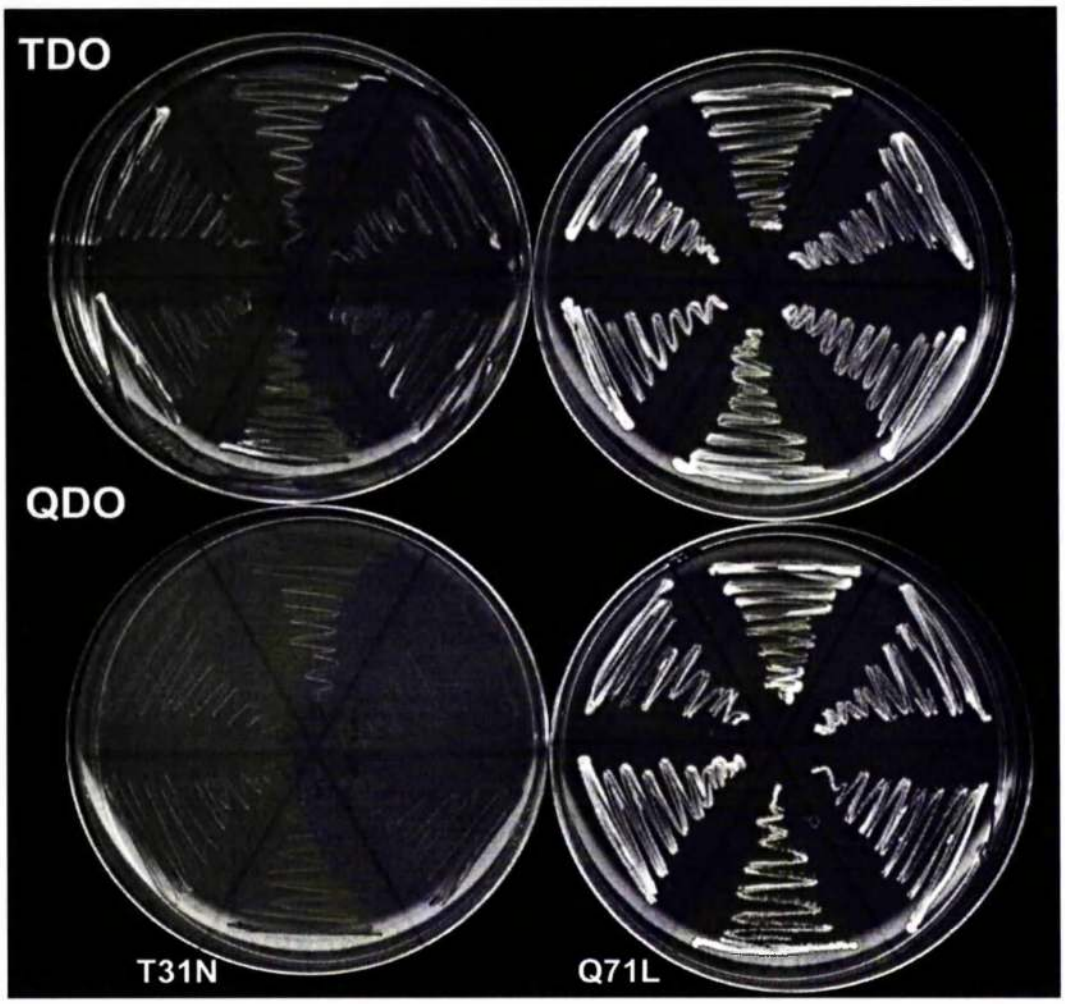

Fig. 3.3.2 **Yeast two-hybrid interaction assay between T4 and Arf5 Q71L and T31N mutants.**

Plasmid pACT2-T4 (encoding the C-terminal 556 residues of arfophilin-2) recovered from the two-hybrid screen, was co-transformed into yeast strain PJ69-2A with pGBT9-Arf5Q71L or pGBT9-Arf5T31N and plated onto synthetic media lacking leucine and tryptophan to select for the plasmids. After 3 days of growth at 30 °C, six independent colonies were then restreaked onto triple dropout medium lacking histidine (TDO; top plates) and quadruple dropout medium also lacking adenine (QDO; bottom plates), to select for an interaction with two levels of stringency. These were then grown for a further 3 days at 30 °C, and then scanned to produce the image above. Yeast co-expressing Arf5Q71L are displayed on the right, while those expressing Arf5T31N are on the left. This experiment was performed three times with similar results.

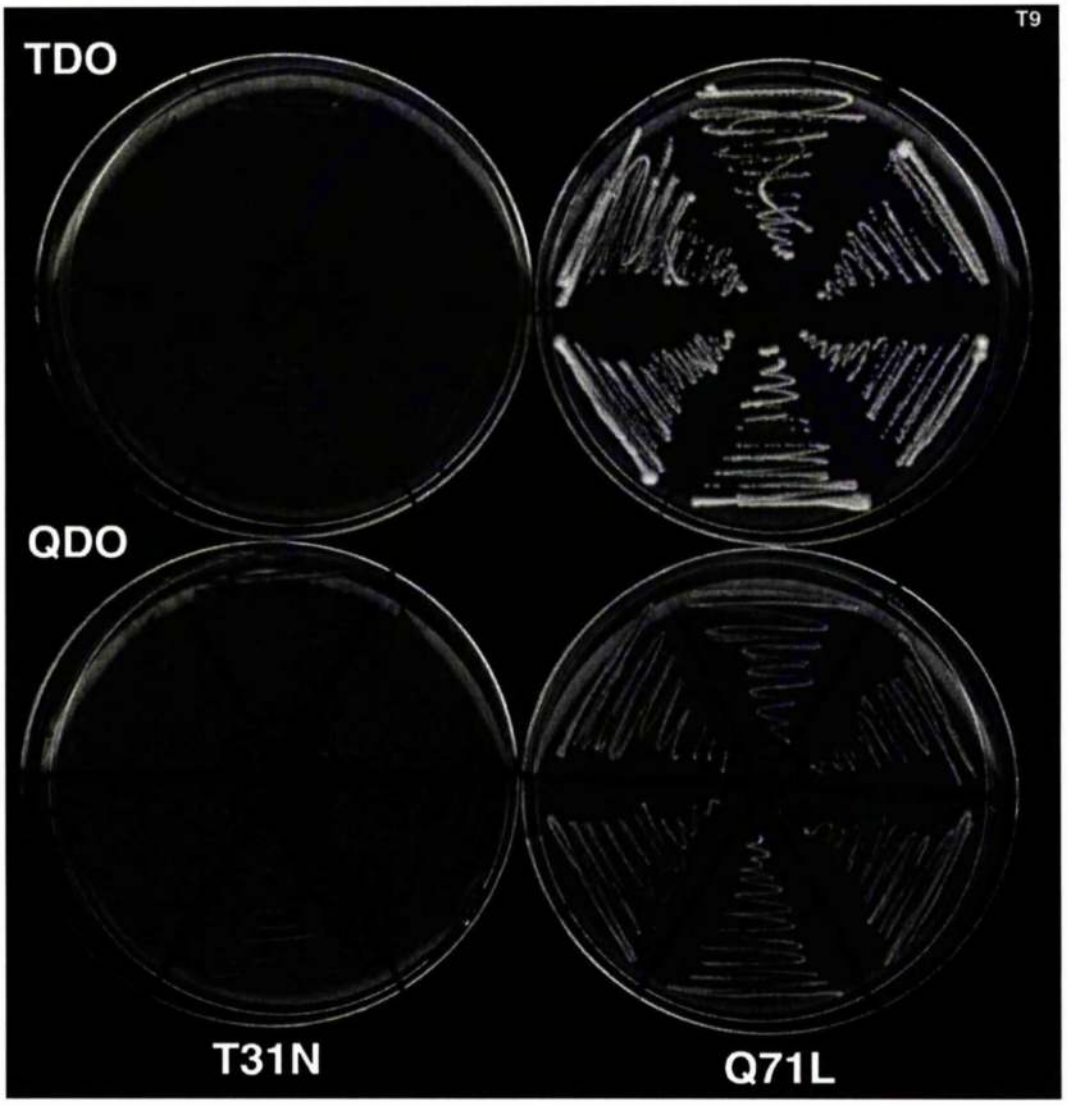

Fig. 3.3.3 **Yeast two-hybrid interaction assay between T9 and Arf5 Q71L and T31N mutants.**

Plasmid pACT2-T9 (encoding the C-terminal 200 residues of arfophilin-2) recovered from the two-hybrid screen, was co-transformed into yeast strain PJ69-2A with pGBT9-Arf5Q71L or pGBT9-Arf5T31N and plated onto synthetic media lacking leucine and tryptophan to select for the plasmids. After 3 days of growth at 30 °C, six independent colonies were then restreaked onto triple dropout medium lacking histidine (TDO; top plates) and quadruple dropout medium also lacking adenine (QDO; bottom plates), to select for an interaction with two levels of stringency. These were then grown for a further 3 days at 30 °C, and then scanned to produce the image above. Yeast co-expressing Arf5Q71L are displayed on the right, while those expressing Arf5T31N are on the left. This experiment was performed three times with similar results.

Fig. 3.3.4 **Yeast two-hybrid interaction assay between T12 and Arf5 Q71L and T31N mutants.**

Plasmid pACT2-T12 (encoding the C-terminal half of protein AB029343/α-helix coiled-coil rod homologue [HCR]) recovered from the two-hybrid screen, was co-transformed into yeast strain PJ69-2A with pGBT9-Arf5Q71L or pGBT9-Arf5T31N and plated onto synthetic media lacking leucine and tryptophan to select for the plasmids. After 3 days of growth at 30 °C, six independent colonies were then restreaked onto triple dropout medium lacking histidine (TDO; top plates) and quadruple dropout medium also lacking adenine (QDO; bottom plates), to select for an interaction with two levels of stringency. These were then grown for a further 3 days at 30 °C, and then scanned to produce the image above. Yeast co-expressing Arf5Q71L are displayed on the right, while those expressing Arf5T31N are on the left. This experiment was performed three times with similar results.

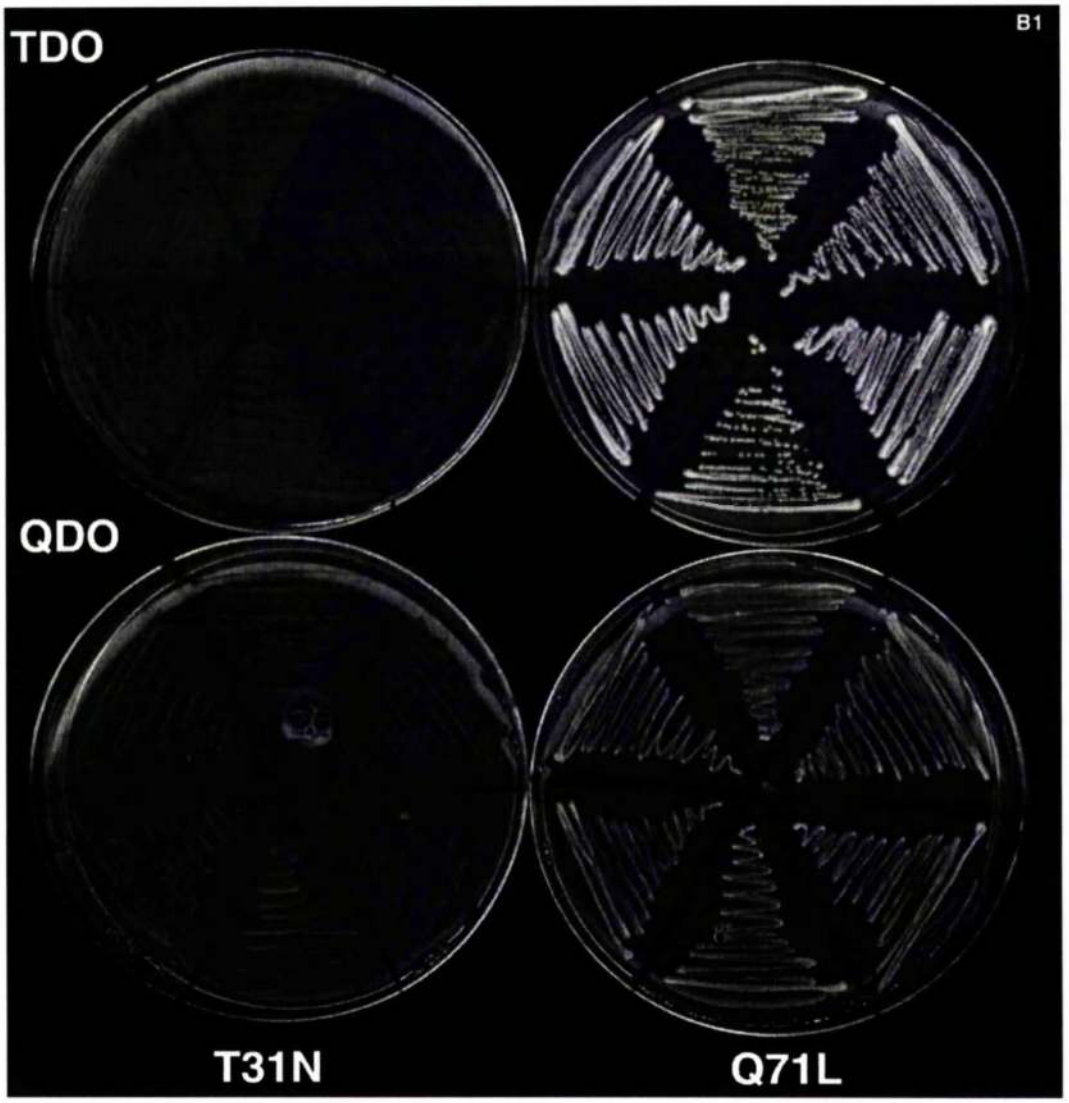

Fig. 3.3.5 **Yeast two-hybrid interaction assay between B1 and Arf5 Q71L and T31N mutants.**

Plasmid pGAD10-B1 (encoding residues 557-756 of KIAA0665/Arfophilin) recovered from the two-hybrid screen, was co-transformed into yeast strain PJ69-2A with pGBT9-Arf5Q71L or pGBT9-Arf5T31N and plated onto synthetic media lacking leucine and tryptophan to select for the plasmids. After 3 days of growth at 30 °C, six independent colonies were then restreaked onto triple dropout medium lacking histidine (TDO; top plates) and quadruple dropout medium also lacking adenine (QDO; bottom plates), to select for an interaction with two levels of stringency. These were then grown for a further 3 days at 30 °C, and then scanned to produce the image above. Yeast co-expressing Arf5Q71L are displayed on the right, while those expressing Arf5T31N are on the left. This experiment was performed three times with similar results.

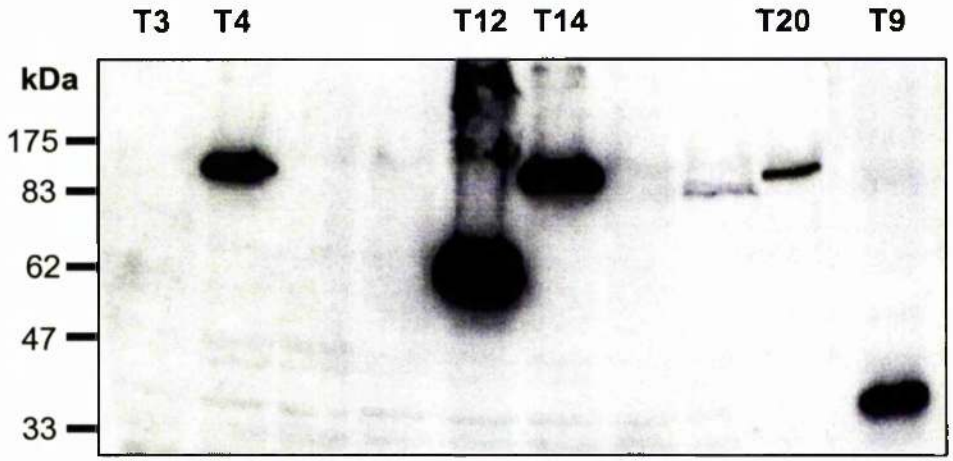

Fig. 3.3.6 **Immunoblot analysis of yeast expressing putative Arf5-interacting GAL4 activation domain fusion proteins.**

PJ69-2A yeast cells were transformed with the pACT2 plasmids indicated at the top and total protein extracts were prepared by trichloroacetic acid precipitation as described in section 3.2.4. 20 μl from each sample were subjected to SDS-PAGE on a 15% polyacrylamide gel, followed by immunoblotting with an anti-haemagluttinin antibody against an epitope situated between the GAL4 activation domain and any polypeptide fused to it. The Gal4 activation domain has an apparent molecular weight of 20-25 kDa. T3 encodes Arfaptin 2/POR1 although no fusion protein was detected (see text), and plasmids T4, T9, T14 and T20 all encode arfophilin-2. T12 represents HCR (α-helix coiled-coil rod homologue). The positions of molecular weight markers (in kDa) are indicated on the left.

```
Score =  150 bits (380), Expect = 1e-36
Identities = 92/147 (63%), Positives = 116/147 (79%), Gaps = 2/147 (1%)

Arfo1: 612 QRDKEATQELIEDLRKQLEHLQLLKLEAEQ-RRGRSSSMGLQEYHSRARESELEQEVRRL 670
           Q+++EATQELIEDLRK+LEHLQ+ KL+ E+  RGRS+S GL E+++RARE ELE EV+RL
Arfo2: 410 QKEREATQELIEDLRKELEHLQMYKLDCERPGRGRSASSGLGEFNARAREVELEHEVKRL 469

Arfo1: 671 KQDNRNLKEQNEELNGQIITLSIQGAKSLFST-AFSESLAAEISSVSRDELMEAIQKQEE 729
           KQ+N  L++QN++LNGQI++LS+  AK+LF+    ++SLAAEI + SRDELMEA+++QEE
Arfo2: 470 KQENYKLRDQNDDLNGQILSLSLYEAKNLFAAQTKAQSLAAEIDTASRDELMEALKEQEE 529

Arfo1: 730 INFRLQDYIDRIIVAIMETNPSILEVK- 756
           INFRL+ Y+D+II+AI++ NPSILE+K
Arfo2: 530 INFRLRQYMDKIILAILDHNPSILEIKH 556
```

Fig. 3.3.7. **BLAST alignment of Arfophilin-1 and Arfophilin-2 C-termini.**

The BLASTP output for the extreme C-terminal Arf-binding domains of Kiaa0665/Arfophilin (Arfo1) and the novel Arfophilin-2 (Arfo2) is shown. They are 63% identical with 79% homology. The region corresponds to the minimum Arf5 binding domain of Arfophilin as determined by deletion analysis in (Shin *et al.*, 1999). The N-termini are more divergent (see Chapter 4 for more detailed analyses).

Given the high degree of sequence similarity between the Arfs (see Fig 1.3.1 in Chapter 1), it was deemed important to test how specific the interactions were for Arf5. Therefore, murine Arf2 and human Arfs 3 and 4 were cloned from cDNA libraries, subjected to site-directed mutagenesis to produce Q71L and T31N point mutants, and subcloned into the pGBT9 yeast two-hybrid bait vector as described in section 3.2.9. Arf1 and Arf6 mutants were similarly subcloned into the same vector from pre-existing plasmids. These were then tested for auto-activation and also against plasmids T3 (Arfaptin 2), B1 (Arfophilin), T20 (Arfophilin-2) and T12 (unknown coiled-coil protein) in the yeast two-hybrid system as before. Slight auto-activation was observed with pGBT9-Arf6Q67L but not with any of the other constructs (not shown). Fig. 3.3.8 shows the positives co-transformed with these constructs on triple and quadruple dropout media. No colonies grew in the presence of any of the dominant negative T-N mutants. Colonies expressing Arfaptin 2 grew very well with the activated class I Arfs, less well with Arfs 5 and 6, and hardly at all with Arf4. Conversely, Arfophilin did not allow growth with the class I Arfs on either selection medium, but did with the class II and III isoforms even on the high stringency quadruple dropout medium. It appeared to prefer Arf5, then Arf6 and Arf4 the least of all (Fig. 3.3.8). Arfophilin-2 showed similar specificity although growth with Arf4 was even less pronounced and this construct did not allow growth on quadruple dropout selection. Arfophilin-2 also appeared to have a preference for Arf6 over Arf5 (Fig. 3.3.8). However, it should be noted that direct comparison between Arfophilin-1 and Arfophilin-2 in these experiments may not be entirely feasible since the fusion proteins are of varying lengths and the vectors are not identical. The T12/HCR protein only allowed growth with the Q71L mutant of Arf5.

Further investigation was prompted by the fact that T12 seemed specific for Arf5 and did not interact with Arf4, which is over 90% identical. Since the Arf N-termini are known to be important sites of interaction with effectors, Arf4/Arf5 chimeras were generated to see whether the Arf5 N-terminus, which differs from that of Arf4 in only seven out of the first hundred amino acid residues, was responsible for the interaction. N4-Arf5 encoded Arf5 with the N-terminus of Arf4, while N5-Arf4 encoded Arf4 with the N-terminus of Arf5 (see section 3.2.10 and Fig. 3.2.2). The corresponding Q71L and T31N mutants of these chimeras were then tested, again in the yeast two-hybrid system, against the T12 protein and also against Arfaptin 2 (plasmid T3) and Arfophilin-2 (plasmid T20). Both N4-Arf5Q71L and N5-Arf4Q71L constructs allowed growth on selective media when cotransformed with Arfaptin 2 or Arfophilin-2 (Fig. 3.3.9). However, in the case of the T12/HCR protein, growth was only observed with the N5-Arf4Q71L construct and not with the N4-Arf5Q71L construct. It was also apparent that N5-Arf4 mimicked Arf5 and

N4-Arf5 mimicked Arf4 when cotransformed with Arfophilin-2 (compare Figs. 3.3.8 and 3.3.9).

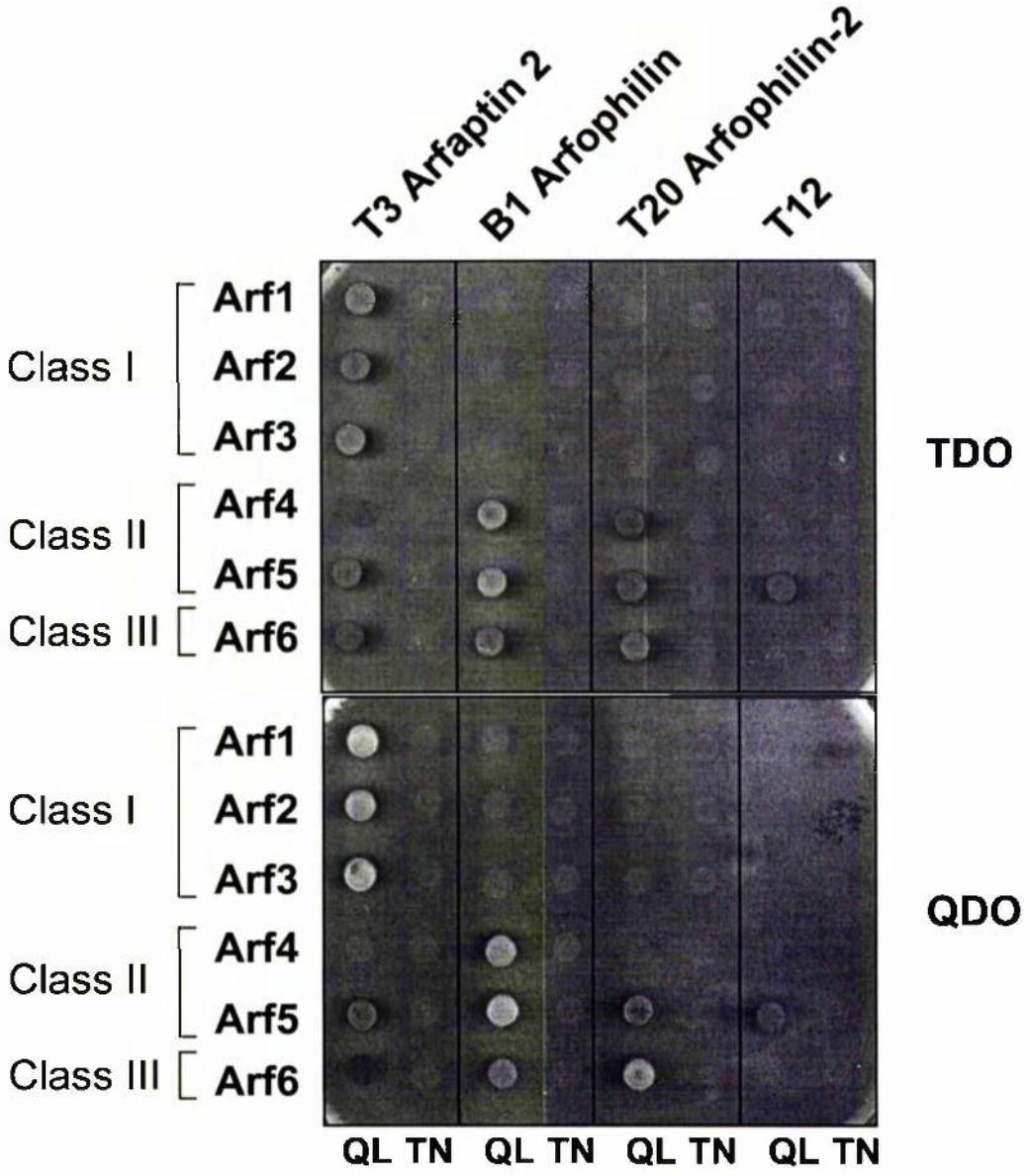

Fig. 3.3.8 **Specificity of interactions for different Arf isoforms using the yeast two-hybrid system.**

GAL4 activation domain plasmids T3 (Arfaptin 2/POR1), B1 (Arfophilin), T20 (Arfophilin-2) and T12 in pACT2 recovered from the two-hybrid screen, were co-transformed into yeast strain PJ69-2A with Q-L and T-N mutants of all six mammalian Arfs in pGBT9. The yeast were plated onto synthetic media lacking leucine and tryptophan to select for the plasmids. After 3 days of growth at 30 °C, six independent colonies from each co-transformation were then pooled in 1 ml of sterile water, diluted 100 fold and 10 μl from each were pipetted onto triple dropout medium lacking histidine (TDO; top panel) and quadruple dropout medium also lacking adenine (QDO; bottom panel), to select for interactions with two levels of stringency. These were then grown for a further 3 days at 30 °C, and scanned producing the images above. This experiment was performed three times with similar results.

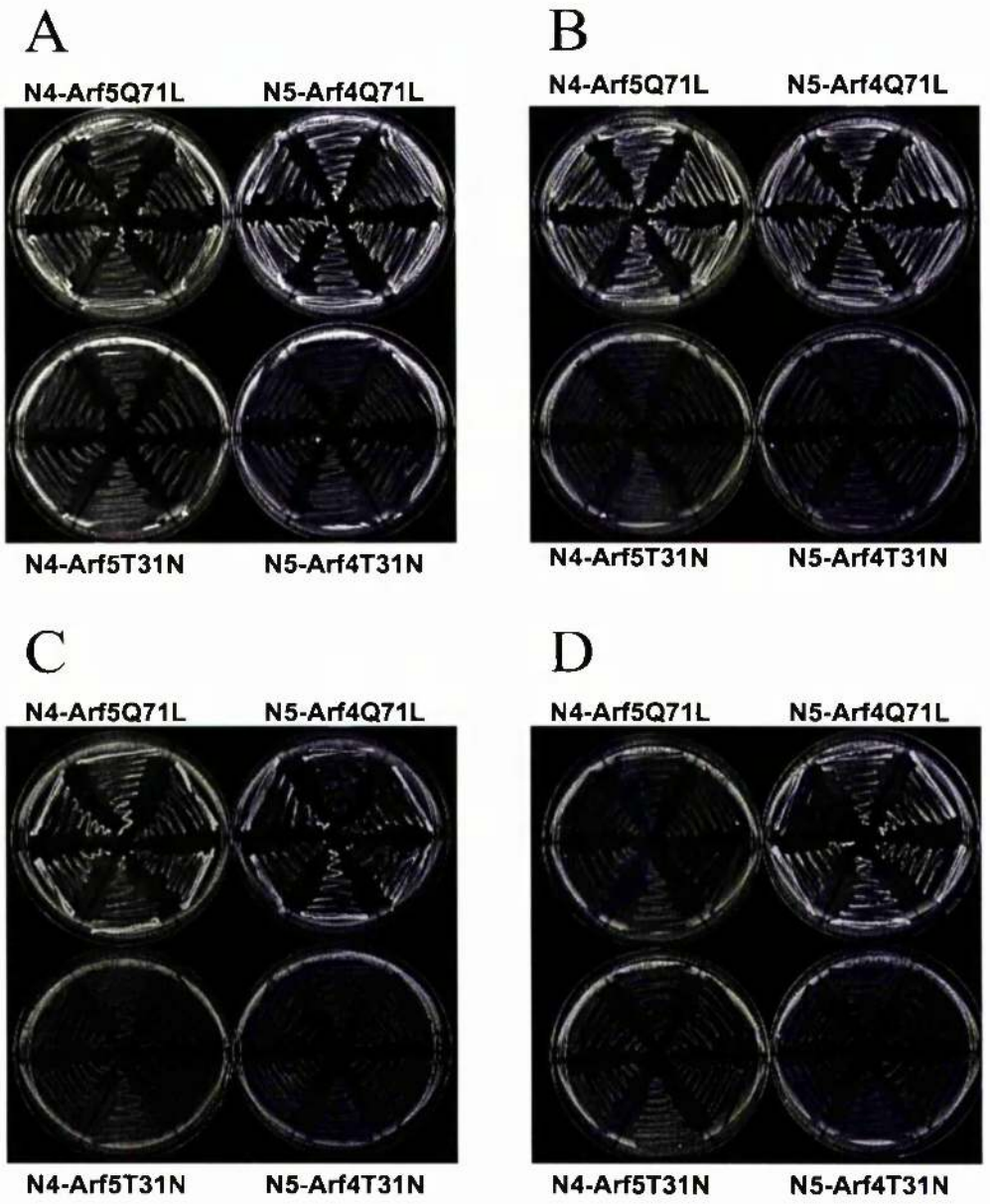

Fig. 3.3.9 **Yeast two-hybrid analysis of interactions between Arf4/Arf5 chimeras and the positives recovered from the Arf5 screen.**

Arf4/Arf5 chimeras containing both Q71L and T31N mutations were produced and subcloned into pGBT9 as described in section 3.2.10. These were then co-transformed into yeast strain PJ69-2A with plasmids T3 (A, Arfaptin 2/POR1), B1 (B, Arfophilin), T20 (C, Arfophilin-2) and T12 (D). The cells were then grown on synthetic media lacking leucine and tryptophan to select for the plasmids, and after 3 days of growth at 30 °C, six independent colonies were then restreaked onto triple dropout medium lacking histidine to select for two-hybrid interactions. These were then grown for a further 3 days at 30 °C, and scanned to produce the images above. These experiments were performed jointly with S. Yarwood and were repeated twice with comparable results.

3.4 Discussion

This chapter describes the use of the yeast two-hybrid system to screen for novel Arf5 interacting proteins. The screening strategy was specifically geared towards identifying effector proteins that would only interact with Arf5 in a GTP-bound and not a GDP-bound conformation. This in-built control was a powerful way of eliminating many false positives, as was the required activation of two reporter genes. In some respects, it may have been preferable to perform the screen with Arf5Q71L fused to the N-terminus of the GAL4 DNA-binding domain, as this would have provided a free Arf5 N-terminus, which is known to be an important site for some Arf/effector interactions. Nevertheless, the strategy used proved to be effective, perhaps aided by the sensitivity of the two-hybrid system. Even small pilot-scale screens yielded very interesting results including the discovery of a completely novel protein, Arfophilin-2, and an uncharacterised one, HCR.

The fact that Arfaptin 2 was recovered was particularly encouraging as it indicated that the screen was functioning efficiently. This protein was originally identified by two groups and named Arfaptin 2 by one (Kanoh et al., 1997) and POR1 by the other (van Aelst et al., 1996), although the latter protein lacked the first 38 amino acids. The former group identified it in a yeast two-hybrid screen for Arf3 effectors along with Arfaptin 1 that is 60% identical and 81% homologous. The other group reported it to bind Rac1-GTP and therefore called it Partner of Rac1 (POR1). They then went on to show that POR1 also interacted with Arf6 in a GTP-dependent manner and that Arf6 and Rac1 work in opposing pathways through POR1 in the regulation of the cortical actin cytoskeleton (D'Souza-Schorey et al., 1997). There appears to be some discrepancy as to the specificity of Arfaptin 2/POR1 for the different Arf isoforms. D'Souza-Schorey and colleagues reported it to be an Arf6 effector and they confirmed the interaction using *in vitro* binding assays (D'Souza-Schorey et al., 1997). Exton's group, however, showed that the protein interacts much more strongly with the class I Arfs and only very weakly with Arf6 in the yeast two-hybrid system and in biochemical interaction assays (Shin et al., 1999). A third group have since reported similar findings (Van Valkenburgh et al., 2001), and the results presented here are also consistent with Arfaptin 2 being predominantly a class I Arf effector. The Rac-GTP interaction now seems questionable as a recent study involving yeast two-hybrid and GST pulldown methodologies showed negligible binding to this form of Rac, but significant binding to Rac-GDP (Shin and Exton, 2001). The 40 bp insert present in the 5'end of the T3 Arfaptin 2 clone is interesting. Although it would not be predicted to give rise to a different protein product, since it is in the 5'UTR and lacks an ATG initiation

codon, it may represent a transcript that is alternatively regulated. In any case it was not the result of a cloning anomaly since Arfaptin 2 ESTs containing the extra sequence are present in the databases, and indeed this isoform has just been reported by others who cloned it from pancreatic cDNAs (Shin and Exton, 2001). The presence of an in-frame stop codon very close to the GAL4/Arfaptin-2 fusion boundary was bewildering. The only explanation as to why an interaction was detected seems to be that suppressor tRNAs in the yeast must have allowed a small amount of Arfaptin-2 to be translated. In theory, only two molecules need to be translated to allow activation of the two reporter genes so a small amount of 'read-through' is all that would be required. Consistent with a very low level of expression was the fact that no fusion protein was detected in immunoblot analysis (see Fig. 3.3.6). Another equally alarming phenomenon that has been reported in the literature is that out-of-frame fusions can produce functional proteins in yeast (Fromont-Racine et al., 1997). Collectively, these findings suggest that stop codon suppression and translational frameshifting are significant mechanisms of protein expression in yeast and should be taken into account when analysing two-hybrid prey sequences.

It was also very encouraging to recover KIAA0665/Arfophilin in the screen, as this had just been published as a class II-specific Arf effector (Shin et al., 1999). However, the authors of this paper had not tested whether Arfophilin interacted with Arf6, but had speculated that it probably did not, given that Arf6 is the most divergent isoform of the family. More recently, they have published that it does indeed interact with Arf6 (Shin et al., 2001). Intriguingly, the C-terminus of Arfophilin seems to bind different regions of Arf5 and Arf6, implying that there may be two distinct binding sites within the Arfophilin C-terminus (Shin et al., 2001). It would be interesting to see whether these interactions are mutually exclusive, and whether the same is true for Arfophilin-2. The results presented here are consistent with an Arf6 interaction with both Arfophilin-1 and Arfophilin-2, although the fact that slight auto-activation was observed with the pGBT9-Arf6Q67L construct, means that this cannot be heavily relied on. Neither Arfophilin-1 nor Arfophilin-2 has been tested for interactions with other members of the Arf family, such as the Arls or ARD1. Recent two-hybrid studies have shown that Arl1 does share some effectors with Arfs (Van Valkenburgh et al., 2001), but these were all proteins that showed no specificity within the true Arfs, such as MKLP1 and Arfaptin 2. Given the Arf specificity observed with the Arfophilins it seems unlikely that they will interact with less conserved members of the family, but this possibility should nonetheless be explored. The minimum Arf5 binding site on Arfophilin was limited to the extreme C-terminal 144 amino acids by deletion analysis, and the Arf5 N-terminus was shown to mediate the interaction (Shin et al., 1999). Our findings are wholly consistent with these for both Arfophilin and

Arfophilin-2. The shortest Arfophilin-2 cDNA recovered (clone T9) encoded 200 amino acids, and the Arfophilin clone (B1) encoded 199 amino acids. Furthermore, the Arf5 N-terminus also mediates the interaction with Arfophilin-2 since N5-Arf4 behaved like Arf5 and N4-Arf5 behaved like Arf4 in the two-hybrid assay, with a stronger interaction being apparent in the former. The fact that so many Arfophilin-2 positives were recovered (5 from only 60,000 transformants) was promising since it suggested that this was a 'true' positive likely to be of physiological importance, and also that testes must surely express the gene at very high levels.

The discovery of the T12/HCR coiled-coil protein as a putative Arf5 interacting protein was also intriguing. The fact that N5-Arf4 acquired the ability to interact while N4-Arf5 lost it again suggests the N-terminus of Arf5 is required for the interaction. Arf4 and 5 only differ in seven amino acids at their N-termini and some of these are highly conserved such as position 12 which is either leucine or isoleucine (see Fig 3.2.2). The most likely single residue conferring the Arf5 specificity is at position 7, which is serine in Arf4 and alanine in Arf5, since this is the least conserved difference. It would be relatively straightforward to mutate this residue and determine whether this is the case. It must be stressed that despite the controls built into the screening strategy, this T12/Arf5 interaction needs to be confirmed by some other, non-yeast-based, method such as by "pulldown" or co-immunoprecipitation experiments. The same is of course true for Arfophilin-2, although in this case it is not so crucial given that it is highly homologous to Arfophilin, which has itself been confirmed as a *bona fide* interacting protein (Shin et al., 1999). If the T12/Arf5 interaction is physiologically relevant, however, it could have very interesting implications suggestive not only of unique class II Arf functions, but also of unique functions within the class itself. During the writing of this thesis, it was drawn to my attention that this gene had in fact been studied in a molecular genetic context, as a candidate gene for psoriasis (Asumalahti et al., 2000).

Owing to time constraints and the need to prioritise, it was decided that subsequent work would focus on the novel Arfophilin-2 protein rather than the T12 protein, given that no functional studies have been performed on the Arfophilins and that these are more likely to be true effectors. The next steps in this regard were to try to clone the full open reading frame of the Arfophilin-2 cDNA and to gather as much information as possible relating to the expression, distribution and function of the gene and its product(s). The next two chapters seek to address such issues.

Chapter 4

The cloning and initial characterisation of Arfophilin-2

4.1 Introduction

As described in Chapter 3, a yeast two-hybrid screen for Arf5 effectors using a human testis library identified a novel gene homologous to Arfophilin-1, which we named Arfophilin-2. The aims of this chapter were to clone the full Arfophilin-2 cDNA, to examine its tissue distribution, and to raise specific Arfophilin-2 antibodies to allow the subcellular distribution of native protein to be examined.

4.1.1 Arfophilin-1 (KIAA0665)

Arfophilin-1, for which there has only been two publications to date, was identified by virtue of its GTP-dependent interaction with Class II, but not Class I, Arfs in the yeast-two hybrid system (Shin et al., 1999). This interaction was confirmed biochemically in GST-Arf5 pull-down assays of Arfophilin-1 overexpressed in CHO cells, and it was shown that the Arf N-termini and the Arfophilin-1 C-terminal 144 amino acids were responsible for this interaction. Furthermore, association of overexpressed Arfophilin-1 with intracellular membranes was shown to increase upon incubation with Arf5 bound to GTPγS and to decrease in the presence of Arf5 bound to GDPβS. Collectively, these data argue strongly that Arfophilin-1 is a *bona fide* Class II Arf effector protein. However, no analysis of endogenous Arfophilin-1 protein was performed and no information relating to its cellular function was put forward.

The gene encodes a polypeptide of 756 amino acid residues with a calculated molecular mass of 82.4 kDa. The sequence also corresponds to that of KIAA0665 protein identified in large-scale cDNA sequencing projects (see http://www.kazusa.or.jp/huge/gfpage/KIAA0665/). Notable features that were reported include the presence of predicted coiled coils and leucine zipper motifs in the C-terminal Arf-binding domain (Shin et al., 1999); see also Fig. 4.3.10 later in the chapter). Northern blot analysis revealed that the gene was expressed predominantly in heart and skeletal muscle, but lower levels were also reported in kidney, pancreas, brain, placenta and liver (Shin et al., 1999).

More recently, the same investigators have published a report indicating that Arf6 also binds to Arfophilin-1 *in vitro*, but that a different region of the Arf is required, suggesting the existence of two Arf binding sites (Shin et al., 2001). Again, no functional data were presented.

4.2 Materials & Methods

4.2.1 Cloning 5' ends of Arfophilin-2 by RACE PCR

A 5' Rapid Amplification of cDNA Ends (RACE) protocol was used to identify the 5'end of the Arfophilin-2 cDNA. A schematic representation of the whole cloning strategy is given in Fig. 4.2.1. A pair of nested primers was designed against the sequence of a human EST (accession number AI570483) known to represent part of an Arfophilin-2 cDNA. The chosen sequences were 5'-CCTCGACCCTTTCATGCCGAACACCC-3' (GSP1) and 5'-CCTTGAAGTTGATTCTCCCCAGGTCGTTGG-3' (GSP2) and these were analysed by BLAST against the non-redundant database (with an expected value of 1000), to ensure that they were identical to the genomic sequence and also that they were specific for this sequence. Importantly, the melting temperature of GSP1 was 71.0 °C, slightly higher than that of the Clontech AP1 primer, allowing 'touchdown PCR' to be performed to increase the chances of specific amplification (Don et al., 1991). A 50 µl reaction was set up in a thin-walled PCR tube on ice as follows:

Expand buffer 2 (Roche)	5 µl
Nuclease free H_2O (Promega)	37 µl
AP1 primer (Clontech)	1 µl
GSP1 (4 pmol/µl)	2.5 µl
Human testis Marathon-Ready cDNAs (Clontech)	2.5 µl
dNTP mix (10 mM each, Promega)	1 µl

This tube was then placed in a Techne Progene PCR machine set with the following cycling parameters:

94.0 °C	2 min	
94.0 °C	15 sec	5 cycles
72.0 °C	4 min	
94.0 °C	15 sec	5 cycles
70.0 °C	4 min	
94.0 °C	15 sec	30 cycles
68.0 °C	4 min	
68.0 °C	4 min	
4.0 °C	hold	

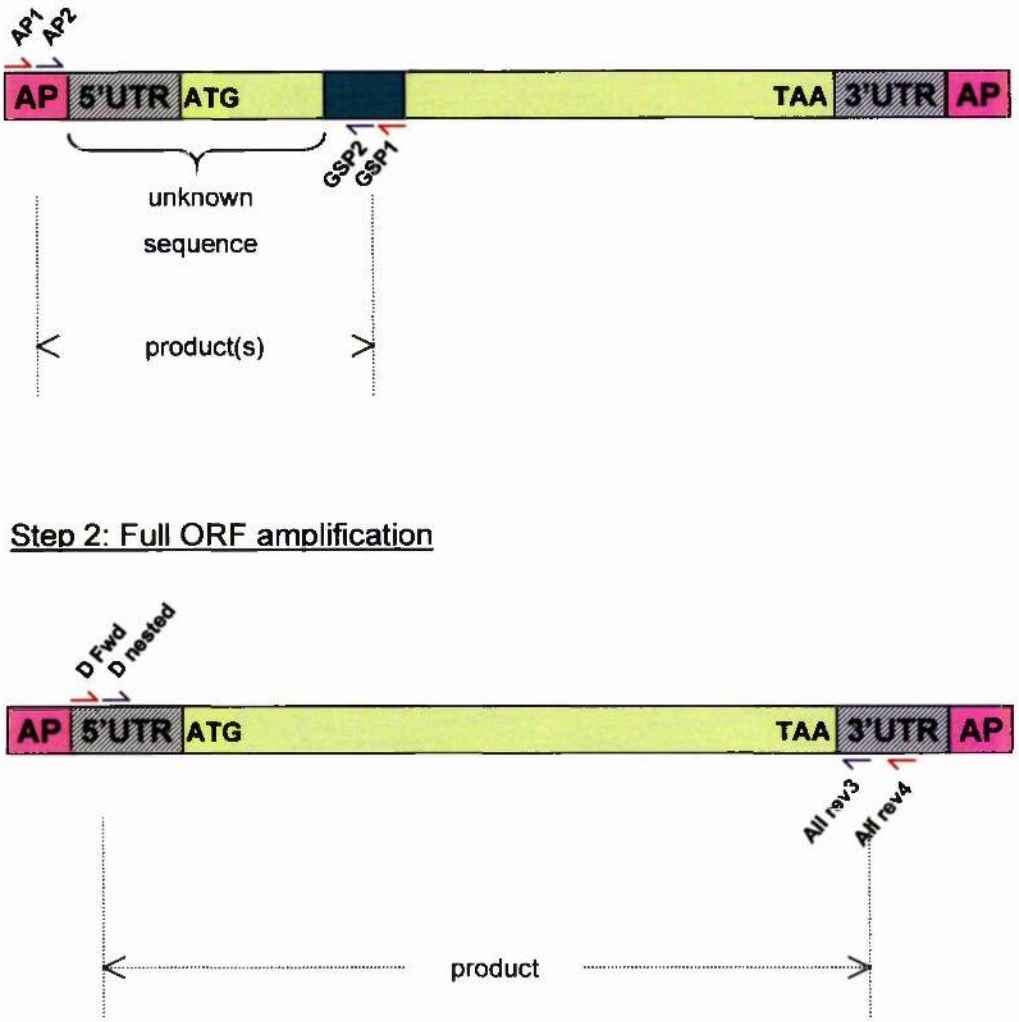

Fig. 4.2.1 **Overview of Arfophilin-2 cloning strategy.**

5'RACE using adaptor (AP, in purple) primers (AP1 and AP2) and nested gene-specific primers (GSP1 and GSP2) was performed to specifically amplify the 5' end of the arfophilin-2 cDNA from adaptor-ligated full-length cDNAs (top panel). The region in dark green represents the exons containing the EST AI570483 sequence.

A subsequent step using nested primers designed to the 5'UTR (D Fwd and D nested) and 3'UTR (All rev4 and All rev3) then amplified the full open reading frame (ORF, bottom panel).

In both steps, the outer primers (in red) were used in a first round PCR reaction, which was then used as the template for second round reactions using the nested inner primers (in blue), allowing specific amplification of the products indicated.

After the first minute at 94 °C, the program was paused, 1 µl of Expand enzymes (Roche) was added, and the cycling was resumed. Once finished, 25 µl of the reaction mixture was purified as described in section 2.2.1.2 and 5 µl of this was used as a template in the second round PCR reaction using the nested AP2 and GSP2 primers. This was performed using the standard PCR protocol described in section 2.2.1.1. 25 µl of reaction mixture from each round of PCR were then electrophoresed on a 1% agarose gel, alongside a 1 kb ladder. Two bands (350 bp and 700 bp) were excised from the gel, purified, TA cloned into pCRII-TOPO and sequenced, all according to the methods described in section 2.2.1.

4.2.2 Cloning the full Arfophilin-2A open reading frame

Having obtained specific 5' RACE products containing putative Arfophilin-2 start codons and 5' UTRs, it was necessary to amplify the full ORFs from cDNAs (see Fig 4.2.1 for schematic overview of the stategy). To do this, nested primers were designed against the 5' and 3' UTRs. The outer primers used were `5'-GTGGTACCTTATCGAAGCCCAGGCAG-3'` (D Fwd) and `5'-GAGGCCCGGCTTAGGCCTGCATCCTTGGGC-3'` (AII rev4) and again these had melting temperatures of over 70 °C to allow several initial rounds of high-temperature, specific amplification. The PCR conditions used were identical to those of the 5' RACE reactions section 4.2.1. A second round reaction was then performed using standard PCR conditions as described in section 2.2.1.1 and two inner nested primers `5'-CGCTCTCTCGGCATGCGACCTGTGCAG-3'` (D nested) and `5'-gtcgacTTAGTGTTTGATCTCGAG GATGGAGGG-3'` (AII rev3; *Sal I* site in small letters). 25 µl of reaction mixture from each round of PCR were then electrophoresed on a 1% agarose gel, alongside a 1 kb ladder. A single band of 2.1 kb was excised from the gel, purified, TA cloned into pCRII-TOPO and sequenced, all according to the methods in section 2.2.1.

4.2.3 Northern blot analysis of Arfophilin-1 and -2 expression

Human multiple tissue northern blots (MTN I and MTN II) were purchased from Clontech. These each had 2 µg/lane of poly(A)+ RNA (i.e. mRNA) isolated from eight different tissues pooled from several individuals. The RNA had been electrophoresed on formaldehyde gels and transferred to nylon membranes by the manufacturers. Northern analysis of Arfophilin-2 was performed first. A cDNA probe was produced by amplifying the 3' 1 kb of the Arfophilin-2 ORF by PCR using *Taq* polymerase, plasmid T20 pACT2 (see the appendix) as template, and primers `5'-CAGCTCATGCACAGCAGCAACTTCAGC-3'` (AII north fwd) and `5'-CAGCCAGCCCCGTGCCTTAGTGTTTG-3'`(AII north rev). The resulting

product was run on an agarose gel and subsequently purified as described in section 2.2.1.4. Approximately 200 ng of this was then incubated overnight at 37 °C with 3 µl (specific activity 3000 Ci/mmol) [α-^{32}P]-dCTP (NEN Dupont), 0.2 mM each unlabeled dATP, dGTP, dTTP plus 1 µl of Klenow enzyme (Promega) in Klenow buffer to produce a radiolabelled probe. The following day, the membranes were pre-hybridised in 25 ml ExpressHyb buffer (Clontech) at 68°C for 30 minutes in a Hybaid rotary hybridisation oven. Meanwhile the probe was purified to remove any unincorporated isotope using a G-20 column made from a 1 ml syringe barrel plugged with a small amount of glass wool. The column was packed and spun twice in a benchtop centrifuge at 2000 rpm for 2 minutes to remove all liquid. It was then placed in a clean 1.5 ml screw cap microcentrifuge tube, the labelled probe was added to the top and the column was spun once again. The purified labelled probe was then denatured by heating to 95°C for 5 min and placed on ice for 5 min. It added directly to the ExpressHyb buffer (Clontech) and mixed before incubating with the membranes for 3 hours at 68°C. The blots were then washed twice for 20 min each in buffer 1 (300 mM NaCl, 30 mM sodium citrate, pH 7.0, 0.05% SDS) at room temperature and once in buffer 2 (15 mM NaCl, 1.5 mM sodium citrate, pH 7.0, 0.1% SDS) at 50°C for a further 20 min. The blots were then wrapped in saran wrap, sealed in polythene and exposed to autoradiography film at -70 °C for 3 days using a cassette with two intensifier screens. The film was then developed using a Kodak XO-MAT system. The blots were stripped by washing twice in stripping buffer (5 mM Tris.Cl, pH 8; 0.2 mM EDTA, 0.05% (w/v) Na pyrophosphate, 0.002% (w/v) polyvinyl-pyrolidone, 0.002% (w/v) bovine serum albumin, 0.002% (w/v) ficoll) at 70 °C and for 20 min each and the efficacy of stripping was monitored by autoradiography. The blots were then exposed to film again for 3 days to verify that the probe had indeed been removed. Northern analysis was then repeated using an analogous probe amplified from KIAA0665 clone using primers 5′-CCTGACCATGGAGGCCCTGGAGGAC-3′ (AI north fwd) and 5′-CTGCCTCTACTTGACCTCCAGG TTG-3′ (AI north rev). These blots were exposed for 1 week at at -70 °C using a cassette with two intensifier screens and developed as before.

4.2.4 Construction of untagged Arfophilin-2 expression plasmids

5'RACE PCR amplified two Arfophilin-2 5' ends, product A and product B (see Fig. 4.3.3.2 for sequences), and these were TA cloned into pCRII as described in section 4.2.1. These plasmids were then used as templates for PCR reactions to specifically amplify the putative 5' ends of the putative ORFs. The primers used were 5'-CcgaattcATGCATAGAGC GCTCAGAACAGTGCCTGGC-3' and 5'-CCgaattcATGGCTGATACTGACCCCAGGGTGAGGG-3' (*EcoR1* sites in small letters) for product A and product B, respectively. These were used in conjunction with the GSP2 primer originally used in the 2nd round RACE reaction and the PCR was performed using the EXPAND kit as described in section 2.2.1.1. The resulting products were then digested with *EcoR1* (incorporated in the primers) and *BamH1* (an internal site in both) and these were ligated into the same sites of pEGFPN1. The resulting plasmids were digested with *BamH1* and treated with calf intestinal alkaline phosphatase as described in section 2.2.1.7. They were then used to accept a *BamH1* fragment consisting of the entire Arfophilin-2A ORF (including the stop codon) obtained in section 4.2.2. Further restriction analysis was performed to verify the presence and correct orientation of the inserts. A plasmid containing product A fused to the Arfophilin-2 3' sequence was designated Arfophilin-2A and the one containing sequence derived from product B was designated Arfophilin-2B. A schematic overview of the subcloning procedure is given in Fig. 4.2.4. For an untagged Arfophilin-2A construct, the entire ORF was amplified (including the stop codon) from the plasmid obtained in section 4.2.2 using primers 5'-CCggatccccATGAAAGGGTGCGAGGAGCTGCTGAAGG-3' (*BamH1* site in small letters) and 5'-gtcgacTTAGTGTTTGATCTCGAGGATGGAGGG-3' (*Sal I* site in small letters). The resulting product was gel purified, digested with *BamH1* and *Sal 1*, gel purified again and then ligated into the *Bgl II* and *Sal I* sites of pEGFPN1, although no fusion protein would be produced due to the presence of the TAA stop codon. All DNA manipulations were performed according to the molecular biology protocols described in section 2.2.1.

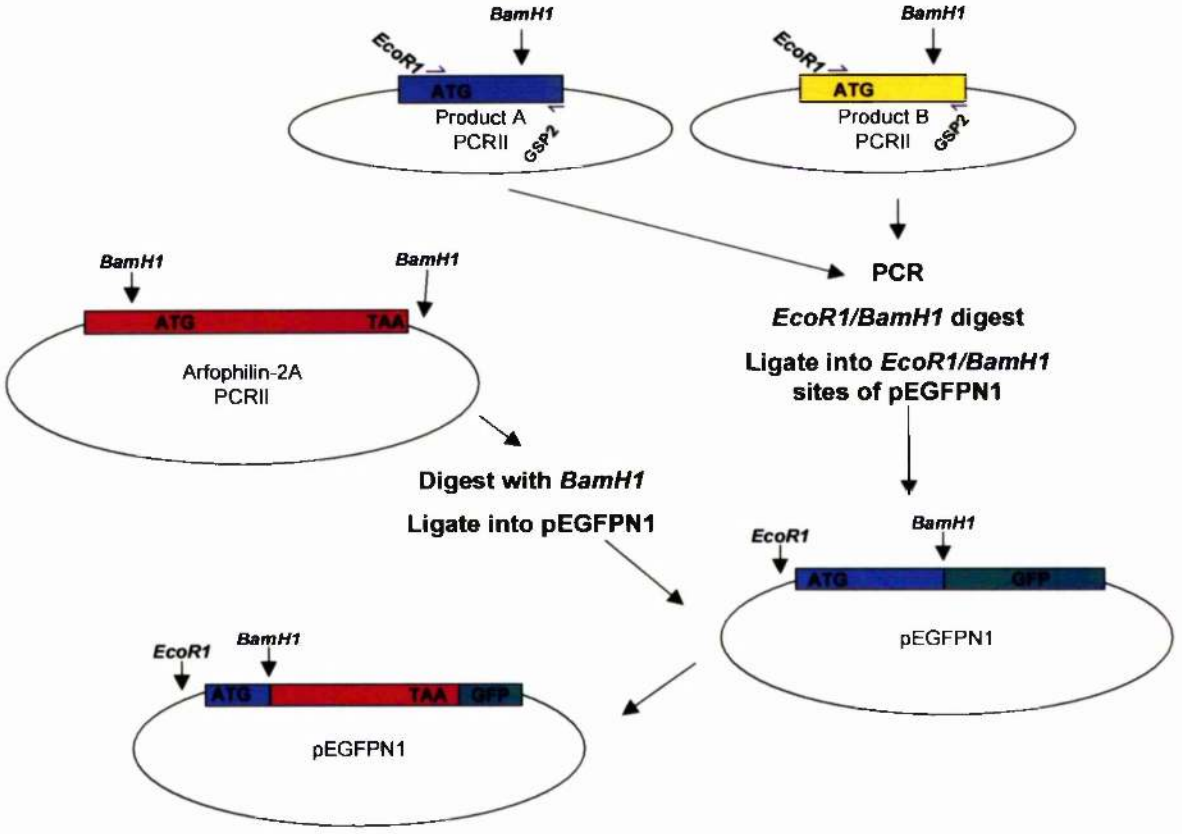

Fig. 4.2.4 **Construction of Arfophilin-2B and -2C untagged constructs.**

The 5' ends of the putative Arfophilin-2B and -2C splice variants (products A and B) were amplified by RACE PCR and cloned into pCRII as described in section 4.2.1. These were then used as templates for PCR using primers designed to include the ATG putative initiation codons and incorporating EcoR1 restriction sites. These primers were used together with the GSP2 primer used in the 2nd round RACE reaction (see section 4.2.1). The resulting products were digested with EcoR1 and BamH1 and ligated into the same sites of pEGFPN1 (Clontech). The full Arfophilin-2A ORF and 5'UTR, cloned into pCRII as described in section 4.2.2, was then digested with BamH1, treated with alkaline phosphatase, and ligated into the BamH1 sites of the pEGFPN1 vectors previously obtained. The correct orientation of the insert was verified by further restriction digestion, and the amplified 5' ends were sequenced to ensure no mutations had been introduced. Note that the GFP protein would not be translated due to the presence of the Arfophilin-2 stop codon. For simplicity, only one of the two constructs is shown.

4.2.5 Production of polyclonal Arfophilin antisera

4.2.5.1 Production of recombinant Arfophilin-2 antigen

A 1.2 kb BglII fragment was subcloned directly from the yeast two-hybrid T20 pACT2 (see the appendix) vector into the *BamH1* site of pQE32 (Qiagen) using the standard techniques described in chapter 2. This fragment corresponded to the 3' 1 kb of coding sequence together with the 3'UTR and was predicted to encode the C-terminal 330 amino acids of Arfophilin-2 that would be in frame with an N-terminal hexahistidine tag provided by the vector. The presence and correct orientation of the insert was verified by further restriction digestion. The resulting AII_{330} pQE32 vector (see the appendix) was then transformed into chemically competent *Escherichia coli* strain BL21 DE3pLysS and selected for on LB-agar containing 100 μg/ml ampicillin. A single colony was then used to produce and subsequently purify the recombinant His-Arfophilin-2ΔN from 1 L of culture grown at 30°C according to the methods in section 2.2.4.7 and 2.2.4.8. The resulting purified protein was analysed on a Coomassie-stained SDS-PAGE gel and also by immuno-blotting using monoclonal RGS-His antibody (Qiagen) as described in section 2.2.4.

4.2.5.2 Production of recombinant Arfophilin-1 antigen

A 900 bp BglII fragment was subcloned directly from yeast two-hybrid B1 pGAD10 vector (see the appendix) into the BamH1 site of pQE31 (Qiagen) using standard techniques described in chapter 2. This fragment corresponded to the 3' 600 bp of coding sequence together with the 3'UTR and was predicted to encode an N-terminal hexahistidine tag fused to the C-terminal 200 amino acids of Arfophilin-1. Production and purification of the recombinant protein was performed exactly as for Arfophilin-2.

4.2.5.3 Inoculation of animals and collection of sera

All antibody production was performed by Diagnostics Scotland under the direction of Dr. M. Chambers, Law Hospital, Carluke, Lanarkshire, Scotland.

Briefly, rabbit R1123 was inoculated twice at one month intervals, each time with approximately 150 μg of recombinant Arfophilin-1 antigen in 150 μl of PBS and about 30 ml of serum was recovered after two months. This was followed by two booster injections

of antigen and two further bleeds in the subsequent two months, with the final bleed being an exsanguination.

For the production of Arfophilin-2 antibodies, sheep S638A was inoculated twice at one month intervals, each time with 250 μg of recombinant Arfophilin-2 antigen and about 400 ml serum was recovered after one month. This was followed by three booster injections of antigen and two further bleeds in the subsequent two months.

In both cases, samples of pre-immune serum were collected from the animals prior to the initial inoculation.

4.2.5.4 Production of His-Arfophilin-1_{330} and His-Arfophilin-2_{330} from pET28b vector

The 3' 1 kb of Arfophilin-1 ORF was amplified by PCR using *Pfu* polymerase (Promega), and oligonucleotide primers `5'-ggatccGCTCTCCAGCAAGAAGGTGGCAAGG-3'` (*BamHI* site in small letters), and `5'-gtcgacGACCTTCCTGCCT`**`CTA`**`CTTGACCTCCA-3'` (*SalI* site in small letters, STOP codon in bold) from the KIAA0665 clone kindly provided by Dr Ohara (Kazusa sequencing project, Japan). The analogous region of Arfophilin-2 was similarly amplified from T20 pAC12 plasmid using oligonucleotide primers `5'-ggatccCTCCAGCACGGCCTTTGGACGGCAGCTC-3'` (*BamHI* site in small letters), and `5'-gtcgac`**`TTA`**`GTGTTTGATCTCGAGGATGGAGGG-3'` (*SalI* site in small letters, STOP codon in bold). The resulting products were purified from agarose gel slices, treated with *Taq* polymerase for 20 minutes at 72 °C to add 'A' overhangs and TA-cloned using the pCRII-TOPO vector system (Invitrogen) as described in more detail in section 2.2.1.6. These were then sequenced using M13 forward and reverse primers to ensure no PCR-induced mutations were present. These plasmids were then digested with BamHI and SalI and the released inserts were purified and subcloned into the same sites in pET28b (Novagen) giving rise to plasmids AI_{330} pET28b and AII_{330} pET28b (see the appendix).

These Arfophilin pET28b constructs were then each transformed into competent *Escherichia coli* strain BL21 DE3 and selected for on LB-agar containing 50 μg/ml kanamycin. Single colonies were then used to produce and subsequently purify by affinity chromatography the recombinant proteins from 1 L cultures grown at 37°C according to the methods in section 2.2.4. The resulting purified proteins were analysed on a Coomassie-stained SDS-PAGE gel.

4.2.5.5 Preparation of Arfophilin-2 affinity column

1 g of activated CH-sepharose 4B (Pharmacia) was put into a 20 ml Econo-pak column (Bio-rad) and mixed with 15 ml 1 mM HCl. This was eluted and the column washed with a further 200 ml 1 mM HCl followed by 20 ml coupling buffer (0.1 M $NaHCO_3$, pH 8.0). Approximately 3 mg of purified His-Arfophilin-2_{330} produced from the pET28b vector was then added to 20 ml coupling buffer, the pH was adjusted to 8.0, and this was then added to the stoppered column. The column was left overnight rotating end over end at room temperature. It was then left to drain before being rotated for a further hour at room temperature in 20 ml blocking buffer (100 mM Tris/HCl, pH 8.0). This was then drained from the column, reapplied, and the column was then washed with 200 ml TBS containing 0.1% v/v Tween-20 before proceeding directly to the antibody purification steps described below.

4.2.5.6 Affinity purification of Arfophilin-2 antibodies

20 ml of sheep S638A first bleed serum was diluted three-fold in TBS containing 0.1% v/v Tween-20 and loaded three times onto the Arfophilin-2 affinity column. The bound antibodies were then washed with 300 ml of TBS/Tween containing 400 mM NaCl to remove non-specifically bound proteins. The antibodies were then eluted from the column with 20 ml of 50 mM glycine/HCl pH 2.5, and 1 ml fractions were collected in eppendorf tubes containing 50 µl of 1.5 M Tris/HCl pH 8.0 to neutralise the pH. 13 µl from each fraction were then boiled in SDS-PAGE sample buffer, electrophoresed on a 15% polyacrylamide gel and the proteins stained with Coomassie brilliant blue. The peak fractions containing the antibodies were pooled, the protein concentration was estimated using the Bradford assay (see section 2.2.4.1), and the antibody was divided into 250 µl aliquots and stored at -80 °C until required. The column was recycled by washing with 100 ml 10x TBS/Tween and stored at 4 °C in 15 ml TBS/Tween containing 0.02% sodium azide as a preservative.

4.2.6 Production of rat testis lysate for western blotting

A testicle was removed from a 14 week old Wistar Kyoto strain rat following sacrifice. It was frozen in liquid nitrogen and then broken up and powdered in a small volume of liquid nitrogen with a ceramic pestle and mortar that had been chilled on dry ice. Approximately 1 g of powdered testicle was then transferred to 5 ml ice-cold lysis buffer (25 mM HEPES, pH 7.5; 50 mM NaCl; 5 mM EDTA; 10% (v/v) glycerol; 1% (v/v) Triton X-100) containing complete protease inhibitor cocktail (Roche). This was then subjected to 20 strokes in a glass/Teflon homogeniser and incubated on ice for 10 minutes. The lysate was then clarified by centrifugation at full speed for 10 minutes in a microcentrifuge at 4°C. Supernatant containing 20 μg of total protein as determined by the Bradford method (see section 2.2.4.1), was loaded onto SDS-PAGE gels for subsequent immuno-blot analysis according to the methods described in section 2.2.4. Human testis lysate (10 mg/ml) was purchased already in SDS-PAGE sample buffer from Clontech.

4.2.7 Subcellular fractionation of HeLa cells

HeLa cells cultured in 10 cm dishes were grown to approximately 75% confluency. They were then rinsed twice with ice-cold HES buffer (255mM sucrose, 20mM HEPES, 1mM EDTA, pH 7.4.) and all traces of the buffer were removed. The cells from each dish were then harvested in 750 μl HES containing complete protease inhibitor cocktail (Roche) using a rubber policeman. Cells from ten dishes were pooled and homogenised with 20 strokes in a glass/teflon homogeniser, chilled on ice. The homogenate was then spun at 18,000 x g for 20 min in a refrigerated microcentrifuge, to give the low-speed pellet (P1). The supernatant was removed and transferred to a fresh tube and centrifuged at 100,000 x g in a Beckman TLA-100 rotor for 1 h at 4°C. This yielded the high-speed pellet (P2) and the supernatant (S) represented the cytosolic fraction. The P1 and P2 pellets were resuspended in 200 μl of HES buffer with protease inhibitors. Equal amounts of total protein from each fraction were then subjected to SDS-PAGE followed by immunoblotting as described in section 2.2.4

4.2.8 Separation of HeLa cell membranes by sucrose density gradient centrifugation

A 1.8 M solution of sucrose was made in HE buffer (20 mM HEPES, pH 7.4, 1 mM EDTA). This was then diluted with more HE buffer to give solutions of 0.6 M, 0.8 M, 1.0 M, 1.2 M, 1.4 M and 1.6 M sucrose. 1.7 ml of the 0.6 M sucrose solution was added to the bottom of a Beckman 13 ml Ultra-Clear^{TM} 14x95 mm tube centrifuge tube. 1.7 ml of each sucrose solution were then sequentially applied to the bottom of the tube by underlaying increasing concentrations of sucrose under the previous layers. This was done using a pasteur pipette fitted to a 5 ml syringe and this was gently slid down the side of the tube, taking care not to disturb the layers already present. This tube was then sealed with parafilm and kept upright at 4°C overnight to allow a linear gradient to form. Six 10 cm dishes of dividing HeLa cells (about 75% confluent) were rinsed twice in ice-cold HES buffer (255mM sucrose, 20mM HEPES, 1mM EDTA, pH 7.4.) and each plate was then scraped in 400 µl HES containing complete protease inhibitor cocktail (Roche) using a rubber policeman. The cells were pooled and spun at 2000 rpm for 2 min in a refrigerated microcentrifuge. The supernatant was discarded and the cells were resuspended in 600 µl HES containing complete protease inhibitor cocktail. They were then homogenised in a 1 ml glass homogeniser and spun again at 200 rpm for 3 min at 4°C. The supernatant was removed and added to the top of the sucrose gradient, and this was spun at 4°C for 6 h at 33,000 rpm in a Beckman SW-40 rotor. 1 ml fractions were then removed from the top of the gradient and placed into chilled microcentrifuge tubes containing 20 µl 50x protease inhibitor cocktail. Samples from each fraction were then diluted in SDS-PAGE sample buffer and subjected to SDS-PAGE and immunoblotting as described in section 2.2.4.

4.3 Results

4.3.1 Bioinformatic analysis of the Arfophilin-2 gene

As described briefly in Chapter 3, nucleotide BLAST analysis (Altschul et al., 1990) against the non-redundant database revealed that the Arfophilin-2 cDNA sequences recovered from the yeast two-hybrid screen were identical to regions of human chromosome 17q11.2. In particular, the sequences were found on two overlapping fully sequenced PAC and BAC clones, whose GenBank accession numbers are AC003101 and AC004526, respectively, and which constitute part of contig NT_010799.5. A graphical overview of the cytological position of the gene is shown in Fig. 4.3.1.1. BLAST analysis against the human EST database also revealed that while there are many Arfophilin-2 ESTs, nearly all are clustered at the 3' end (in Unigene cluster Hs3454) and only one (accession number AI570483) extended our sequence in the 5' direction. In addition, this EST was lacking the extreme 5' exon of the yeast two-hybrid T20 clone, suggesting alternative splicing (see Fig. 4.3.3.2). Primers were designed to this EST sequence and used to amplify the entire 3' end of the Arfophilin-2 open reading frame from testis cDNAs (not shown). Interestingly, the major product obtained lacked the 10th from last exon of the cDNA recovered in the two-hybrid screen, indicating further alternative splicing. The EST sequence itself was found to span an intron of approximately 100 kb making computer analysis of the whole gene sequence problematic. A 158 kilobase portion (two thirds of the gene and about the maximum size that can be analysed) was therefore assembled *in silico* from clones AC004526 (bases 180000-297878) and AC003101 (bases 68953-109000) to include the entire 5' end up to and including the eleventh from last exon (which appears to be present in all splice variants, see Fig. 4.3.3.2). This sequence was then analysed using Nix (at http://www.hgmp.mrc.ac.uk): a computer program that employs multiple bioinformatic packages and displays them in one easy-to-interpret interface. The programs it runs include Grail, Genemark, Genscan, Fgenes, HMMGene, Fex, MZEF and Hexon, which are exon prediction programs that use different algorithms, in addition to BLAST against multiple databases. The output from such analysis is shown in Figure 4.3.1.3. Several important observations are apparent. Firstly, the end of the neurofibromatosis type 1 gene (*NF1*) is at the start of the sequence and this obviously sets a limit as to where the start of the Arfophilin-2 gene must be. Secondly, the EST (accession number AI570483) corresponds to sequences around position 70000 bp (and 155000 bp) and nearly all the programs predict exons containing the same sequence. This means that the Arfophilin-2 gene must begin further back along the chromosome in the centromeric direction. Thirdly, there is an excellent candidate promoter complete with TATA box at

about position 126000 of the genomic sequence used as input. This is only a few kilobases upstream from the start of the yeast two-hybrid clone T20 sequence and lies adjacent to a CpG island: a strong indication for the start of a gene. For comparison, a similar Nix analysis was performed using a sequence assembled from the region of 16p13.3 containing

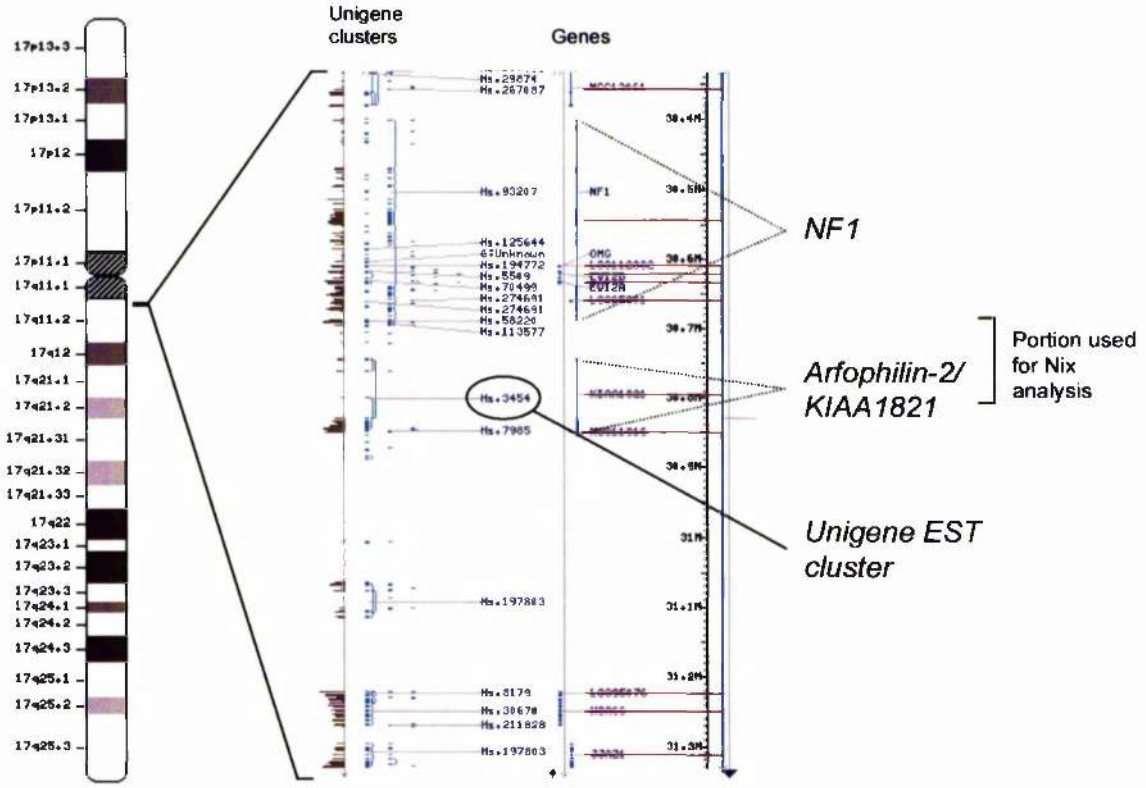

Fig. 4.3.1.1 **Schematic overview of the position of the Arfophilin-2 gene on human chromosome 17.**

Shown is a representation of human chromosome 17 (left-hand side) and a magnified view of the q11.2 region containing the *NF1* and *Arfophilin-2* genes which are indicated (right-hand side). Also indicated are the positions of a Unigene EST cluster (Hs3454) corresponding to Arfophilin-2 and the position of the sequence used for Nix analysis. A scale bar in Megabases is shown. The images were obtained from the genome resources available at http//:www.ncbi.nlm.nih.gov.

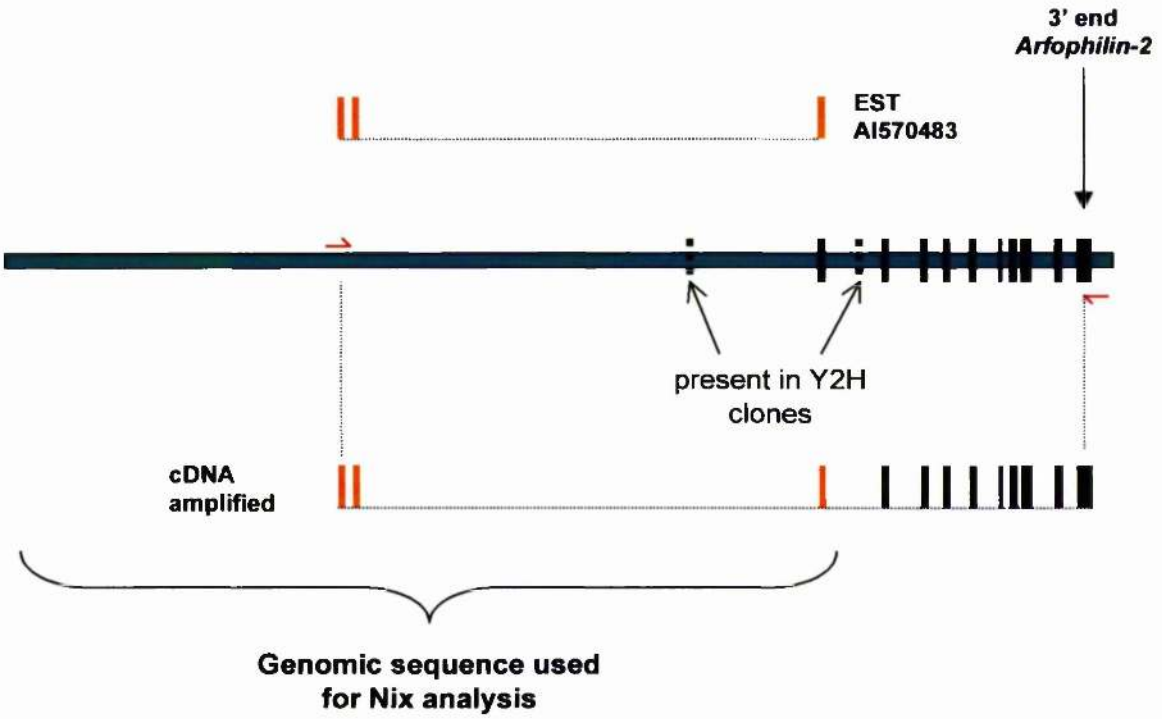

Fig. 4.3.3.2 **Overview of the chromosomal region (17q11.2) containing the Arfophilin-2 5' end.**

A 200 kb portion of human chromosome 17q11.2 is shown (in green), with the approximate positions the 3' Arfophilin-2 exons deduced from the cDNA sequences recovered in the two-hybrid screen denoted by black bars. The position of sequences derived from ESTAI570483 are also shown (orange bars). Primers designed to the sequences denoted by the red arrows were used to amplify, from testis, the cDNA shown at the bottom. This lacked two exons that were recovered in the two-hybrid clones (dotted black bars). The 158 kb portion of genomic sequence used for Nix analysis is shown.

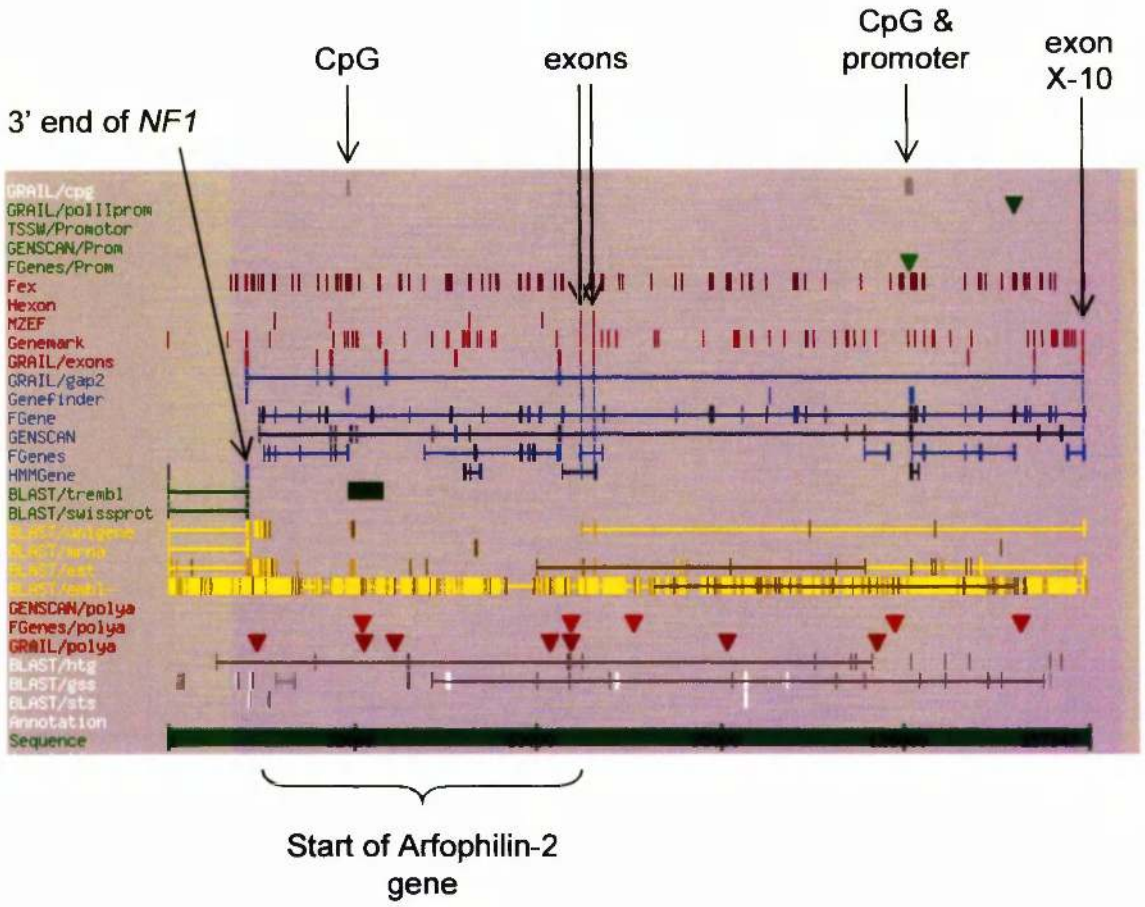

Figure 4.3.1.3 **Analysis of the human genomic sequence containing the 5' end of the Arfophilin-2 gene.**

Shown is a graphical overview of a Nix output for the forward strand of a ~158 kb genomic sequence (see green bar at the bottom for scale) assembled from fully sequenced overlapping BAC/PAC clones AC004526 and AC003101 corresponding to position 17q11.2 of the human genome. This sequence included the 10th from last exon (x-10) of the Arfophilin-2 gene, as determined by analysing the cDNA sequences recovered in the yeast two-hybrid screen. The different programs run by Nix are named on the left and regions predicted by the programs are denoted by bars and arrowheads at the appropriate positions along the sequence. Important features are indicated by arrows and include the end of the NF1 gene, exons known to encode Arfophilin-2 from cDNA sequencing and EST data (that are also predicted by most of the programs), CpG islands and putative promoter. The region which must contain the true start of the gene is also indicated.

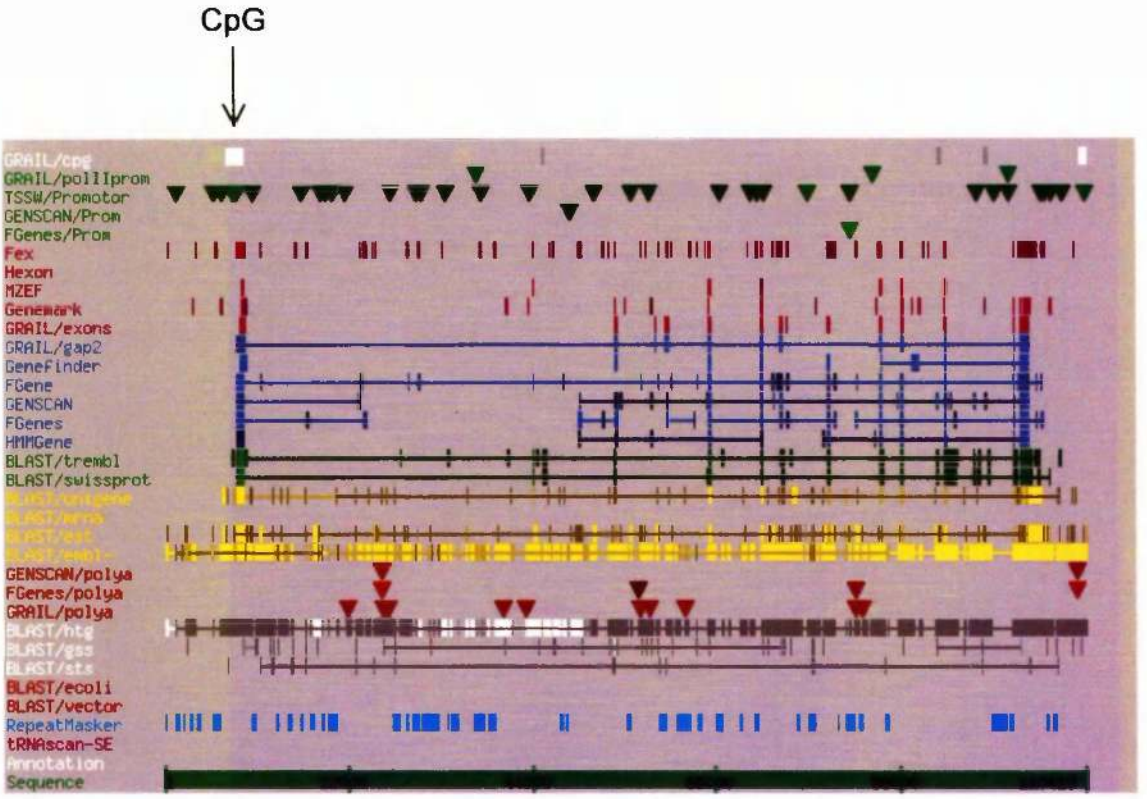

Figure 4.3.1.4 **Analysis of the human genomic sequence containing the KIAA0665/Arfophilin-1 gene.**

Shown is a graphical overview of a Nix output for the forward strand of a ~110 kb genomic sequence from human chromosome 16p13.3. The different programs are named on the left and regions predicted by the programs are denoted by bars and arrowheads at the appropriate positions along the sequence. Note that the gene starts around a prominent CpG island and that many of the programs predict the same exons.

the KIAA0665/Arfophilin-1 gene (bases 15000-260418 of clone AE006463). The output is shown in Fig. 4.3.1.4 and it reveals that the gene is smaller in size, that there is a large CpG island near the 5' end, and that many of the programs predict the exons with greater accuracy.

4.3.2 Molecular cloning of human Arfophilin-2

Numerous attempts at amplifying the 5' end(s) of Arfophilin-2 by RACE PCR using different combinations of nested primers designed against the common 3' sequence proved unsuccessful, as were several attempts at cloning an open reading frame predicted by Genscan starting around the CpG island. Therefore, it was decided to attempt 5' RACE from human testis cDNAs using primers designed to the exons encoding EST AI570483, in the knowledge that this would not yield every 5' end that exists (see Fig. 4.2.1 for an overview of the strategy). This led to the amplification of two distinct but specific products of ~350 bp and ~700 bp, designated Product A and Product B in Fig. 4.3.2.1 (panel A), respectively. Both aligned with the correct genomic sequence and their sequences are shown in Fig. 4.3.2.2. Both were predicted to encode distinct N-terminal splice variants when theoretically assembled with the known 3' sequence. Furthermore, the presence of upstream in-frame STOP codons suggested that the initiation codons were present. Forward primers designed against the predicted 5' untranslated regions of these were then designed and used in nested PCR to amplify the complete open reading frames. However, this was only successful for the amplification of Arfophilin-2A (Fig 4.3.2.1, panel B) despite various annealing temperatures being employed with the other set of primers. The 5' end of Arfophilin-2A differed slightly from the initial RACE product in that it lacked the exon with the predicted initiating codon (see Figs. 4.3.2.2 and 4.2.2.3 for sequences and Fig. 4.3.2.4. for a diagrammatic representation). As there were still upstream stop codons, this meant that a different start site would be predicted in this isoform, resulting in a slightly smaller protein. The full sequence of the Arfophilin-2A mRNA and its predicted protein product is given in Fig. 4.3.2.3.

As described in section 4.2.2, it was possible to assemble predicted Arfophilin-2B and -2C open reading frames by fusing the 5' ends amplified by RACE to the 3' Arfophilin-2A sequence via a *BamH1* site present in the overlapping sequence (see Figs. 4.3.2.2 & 4.3.2.3 for the position). However, it is noted that caution is required when interpreting data obtained with these constructs since it is not certain that they exist *in vivo* as exon usage may differ with these variants. Thus the only open reading frame that we can be completely confident of is that of Arfophilin-2A.

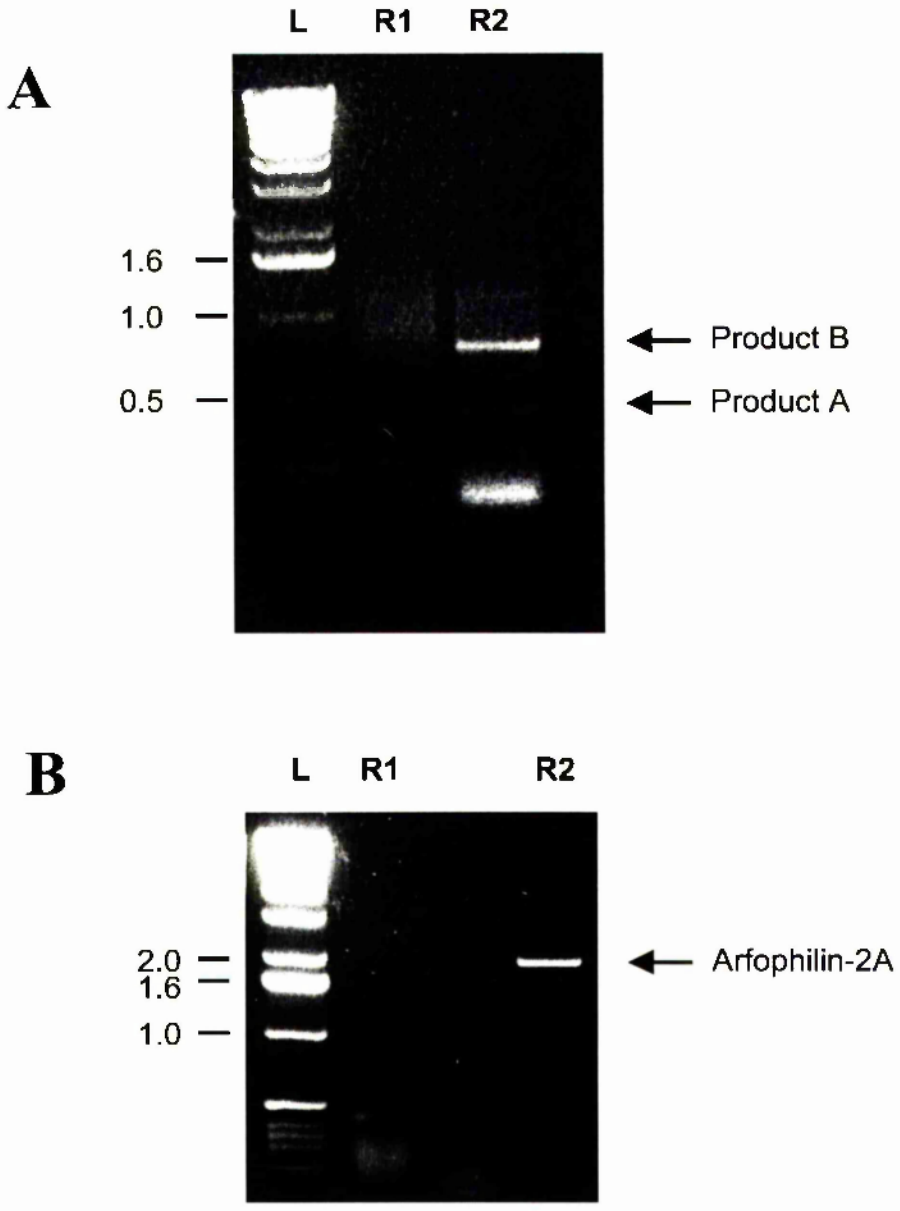

Figure 4.3.2.1 **Amplification of Arfophilin-2 from testis cDNAs.**

Panel **A**: Two rounds (R1 and R2) of PCR were performed in 5'RACE reactions using nested adaptor and gene specific primers as described in section 4.2.1. This amplified the two specific products A and B as indicated. These were then cloned and sequenced (see Fig. 4.3.2.2).

Panel **B**: PCR reactions were performed using nested primers designed from the sequence obtained from 5'RACE product A along with primers designed to the 3'UTR of Arfophilin-2, resulting in the amplification of Arfophilin-2A as indicated. This was cloned and sequenced (see Fig. 4.3.2.3).

25 μl of 50 μl reactions were run on 1% agarose gels alongside 0.75 μg of 1 kb DNA ladder (L). The positions and sizes (in kb) of DNA markers are indicated.

Product A

```
1    CGCAGTGGTACCTTATCGAAGCCCAGGCAGAGCCCGCTCTCTCGGCATGCGACCTGTGCAGTCACTCAGGGATTAGTG   78
79   CTCTGGGGTTGCCTTCTTGAAATTCGTGGTAATGTTCCCCTTTGCCCTGGGCGCCACTAATTGCGGAGCTGGTCCTGG  156
157  GCCCGGGGCTCCTGACTCCTCCAGGAGGCTTTCCACAACCACATACCCCCTCTACCAGTGGCCTACCCAGGGTGGTGG  234
235  CGAGGATTAAACAAATTCATATGCATAGAGCGCTCAGAACAGTGCCTGGCACAAAGGAAGGCTCGCTAAGCATTTGCT  312
                          M  H  R  A  L  R  T  V  P  G  T  K  E  G  S  L  S  I  C  F

313  TTGATTCCCGTGGAAAACTTGTGAAATATTTGGATCCCAACGACCTGGGGAGAATCAACTTCAAGG  376
       D  S  R  G  K  L  V  K  Y  L  D  P  N  D  L  G  R  I  N  F  K
```

Product B

```
1    GTAAATTATGATGAACCCACCGGGCAGAATGTGTTACAGCCACTAACAACGTGGGTTGTACACACCAAGCAGCATGGA   78
79   AACTGTTTCTGTCCTACCTCCTGTTACACGGGAGAGAAACTCTCCAACCTCAGGGATGGCTGACTCTGCCAGGTGAAA  156
157  ACTTACTTCCTTATTCATCTAACACTCTTCATTGAAGTGCAAGGTACAAATAGAACAGAAAAGTTCATCAGCCACCAG  234
235  TGTCCATCTCAGTGAGTTTCCCCATCTAGCCAGCACCTGGAACAAGAAATAGAACAAGAGAAATGGTGGGATTTCTGG  312
313  GTCATTTACAATGAGTTTGTGTCTGTTTTGTGTGAAAGAAACCAATTTTAAAACATCGGCAGAGCCTCGGCTTTCATT  390
391  GTGCAGTCCCTGGGGGAAGGAGGCTCGGCCCCTGAAGCCGTGTGCTCAGGGAGGGTGTGCTCAGGGAGGAGCCGGTGT  468
469  TGGCTCTGCTTTTCTTTGCCCGAGTTGTCTGTCACCATGGGGAGAATAAAGTGGCCCCATGGCTGATACTGACCCCAG  546
                                                          M  A  D  T  D  P  R

547  GGTGAGGGTAAGAGGACTGGGCGGGGACACTGGTGTCCCTCCCTCCCTCCCAGCCTCCCCACCCAGCTCCCTGAGTCT  624
       V  R  V  R  G  L  G  G  D  T  G  V  P  P  S  L  P  A  S  P  P  S  S  L  S  L

625  TCGGGAGATCCTTGGGTGTCTCACACCTGTCCCTGCTTCATTCCCACAGGTGGAAAAACTTGTGAAATATTTGGATCC  702
       R  E  I  L  G  C  L  T  P  V  P  A  S  F  P  Q  V  E  K  L  V  K  Y  L  D  P

703  CAACGACCTGGGGAGAATCAACTTCAAGG  731
       N  D  L  G  R  I  N  F  K
```

Fig. 4.3.2.2 cDNA and predicted amino acid sequences of Arfophilin-2 5'RACE products.

The cDNA and predicted amino acid sequences of the products A and B amplified by 5' RACE from testis cDNAs are shown. In frame stop codons are underlined, the sequence of the nested (GSP2) primer used in the RACE reactions is boxed and the BamH1 site used for assembling Arfophilin-2B and Arfophilin-2C is in red.

```
1    CGCAGTGGTACCTTATCGAAGCCCAGGCAGAGCCCGCTCTCTCGGCATGCGACCTGTGCAGTCACTCAGGGATTAGTG   1
79   CTCTGGGGTTGCCTTCTTGAAATTCGTGGTAATGTTCCCCTTTGCCCTGGGCGCCACTAATTGCGGAGCTGGTCCTGG  156
157  GCCCGGGGCTCCTGACTCCTCCAGGAGGCTTTCCACAACCACATACCCCCTCTACCAGTGGCCTACCCAGGGTGGAAA  234
235  AACTTGTGAAATATTTGGATCCCAACGACCTGGGGAGAATCAACTTCAAGGACTTTTGCCGGGGGGTGTTCGCCATGA  312
                                                                        M  K

313  AAGGGTGCGAGGAGCTGCTGAAGGATGTGCTGTCGGTGGAGAGCGCGGGGACGCTGCCGTGCGCGCCAGAGATCCCAG  390
       G  C  E  E  L  L  K  D  V  L  S  V  E  S  A  G  T  L  P  C  A  P  E  I  P  D

391  ACTGCGTGGAGCAGGGCAGCGAGGTCACAGGCCCCACCTTTGCTGATGGCGAGCTCATCCCCAGGGAACCCGGCTTTT  468
       C  V  E  Q  G  S  E  V  T  G  P  T  F  A  D  G  E  L  I  P  R  E  P  G  F  F

469  TTCCCGAGGACGAGGAGGAGGCTATGACGCTGGCGCCACCTGAGGGCCCCCAGGAGTTGTACACAGACAGCCCCATGG  546
       P  E  D  E  E  E  A  M  T  L  A  P  P  E  G  P  Q  E  L  Y  T  D  S  P  M  E

547  AGAGCACTCAGAGCCTGGAGGGGTCTGTCGGGAGTCCTGCCGAGAAGGACGGGGGACTTGGGGGCCTGTTTCTGCCAG  624
       S  T  Q  S  L  E  G  S  V  G  S  P  A  E  K  D  G  G  L  G  G  L  F  L  P  E

625  AAGACAAGTCCCTGGTCCACACTCCATCCATGACGACCTCAGACCTTTCTACACACTCCACCACCTCGCTCATCAGCA  702
       D  K  S  L  V  H  T  P  S  M  T  T  S  D  L  S  T  H  S  T  T  S  L  I  S  N

703  ATGAGGAGCAGTTTGAAGACTATGGGGAGGGTGACGATGTGGACTGTGCCCCCAGCAGCCCTTGCCCCGATGATGAGA  780
       E  E  Q  F  E  D  Y  G  E  G  D  D  V  D  C  A  P  S  S  P  C  P  D  D  E  T

781  CCAGGACCAACGTCTACTCGGACCTGGGGTCTTCGGTGTCTTCCAGTGCGGGGCAGACGCCTAGGAAAATGCGGCACG  858
       R  T  N  V  Y  S  D  L  G  S  S  V  S  S  S  A  G  Q  T  P  R  K  M  R  H  V

859  TGTACAACAGCGAATTGCTAGATGTTTACTGCTCTCAATGCTGCAAGAAAATCAACCTGCTCAATGACTTGGAAGCCC  936
       Y  N  S  E  L  L  D  V  Y  C  S  Q  C  C  K  K  I  N  L  L  N  D  L  E  A  R

937  GACTGAAAAACCTGAAGGCCAACAGCCCCAACCGAAAGATCTCCAGCACGGCCTTTGGACGGCAGCTCATGCACAGCA 1014
       L  K  N  L  K  A  N  S  P  N  R  K  I  S  S  T  A  F  G  R  Q  L  M  H  S  S

1015 GCAACTTCAGCAGCAGCAATGGCAGCACCGAAGACCTGTTCCGGGACAGCATTGACTCTTGCGACAATGACATCACAG 1092
       N  F  S  S  S  N  G  S  T  E  D  L  F  R  D  S  I  D  S  C  D  N  D  I  T  E

1093 AGAAGGTAAGCTTCCTGGAAAAGAAGGTGACAGAGCTGGAGAATGACAGCCTGACCAATGGGGACCTGAAGAGCAAGC 1170
       K  V  S  F  L  E  K  K  V  T  E  L  E  N  D  S  L  T  N  G  D  L  K  S  K  L

1171 TGAAGCAAGAGAACACACAGCTGGTGCACAGGGTGCATGAGCTGGAGGAGATGGTGAAGGATCAGGAGACCACGGCCG 1248
       K  Q  E  N  T  Q  L  V  H  R  V  H  E  L  E  E  M  V  K  D  Q  E  T  T  A  E

1249 AGCAGGCTCTGGAGGAGGAGGCGCGGCGCCACCGCGAGGCCTACGGCAAGCTGGAGAGGGAGAAGGCTACCGAGGTGG 1326
       Q  A  L  E  E  E  A  R  R  H  R  E  A  Y  G  K  L  E  R  E  K  A  T  E  V  E

1327 AGCTGCTCAATGCCAGGGTGCAGCAGTTGGAGGAAGAAAATACAGAGCTTAGAACAACAGTGACTCGGCTCAAGTCTC 1404
       L  L  N  A  R  V  Q  Q  L  E  E  E  N  T  E  L  R  T  T  V  T  R  L  K  S  Q

1405 AAACAGAGAAACTGGATGAGGAGCGGCAGCGCATGTCTGACCGTCTGGAGGACACCAGCCTGCGGCTCAAAGATGAGA 1482
       T  E  K  L  D  E  E  R  Q  R  M  S  D  R  L  E  D  T  S  L  R  L  K  D  E  M

1483 TGGACCTGTACAAGCGCATGATGGACAAGCTGCGACAGAACCGCCTTGAGTTCCAGAAGGAGCGGGAGGCGACGCAGG 1560
       D  L  Y  K  R  M  M  D  K  L  R  Q  N  R  L  E  F  Q  K  E  R  E  A  T  Q  E

1561 AGCTCATCGAGGACTTGCGGAAGGAGCTGGAGCACCTGCAGATGTACAAGCTGGACTGCGAGCGGCCAGGCAGGGGCC 1638
       L  I  E  D  L  R  K  E  L  E  H  L  Q  M  Y  K  L  D  C  E  R  P  G  R  G  R

1639 GCAGTGCCTCCTCTGGCCTAGGCGAGTTCAATGCCAGGGCCCGCGAGGTGGAGCTCGAGCACGAGGTCAAGCGGCTCA 1716
       S  A  S  S  G  L  G  E  F  N  A  R  A  R  E  V  E  L  E  H  E  V  K  R  L  K

1717 AGCAGGAGAATTATAAGCTGCGGGATCAGAACGACGACTTGAATGGGCAGATTTTGAGCCTCAGCCTCTACGAAGCAA 1794
       Q  E  N  Y  K  L  R  D  Q  N  D  D  L  N  G  Q  I  L  S  L  S  L  Y  E  A  K

1795 AAAACCTCTTTGCTGCCCAGACTAAAGCCCAGTCTCTGGCTGCGGAGATAGACACCGCCTCGCGCGATGAGCTAATGG 1872
       N  L  F  A  A  Q  T  K  A  Q  S  L  A  A  E  I  D  T  A  S  R  D  E  L  M  E

1873 AAGCCCTGAAGGAGCAGGAGGAGATCAACTTCCGGCTGAGGCAGTACATGGACAAGATTATCCTCGCCATCCTGGACC 1950
       A  L  K  E  Q  E  E  I  N  F  R  L  R  Q  Y  M  D  K  I  I  L  A  I  L  D  H

1951 ACAATCCCTCCATCCTCGAGATCAAACACTAAGGCACGGGGCTGGCTGCAAGAGCAGCCTTAGGACCCTGGGACCAAG 2028
       N  P  S  I  L  E  I  K  H  •

2029 GGCAGACCCTGCCCAAGGATGCAGGCCTAAGCCGGGCCTCACACTCACACTGTAAATGTCTCTCTGGCCACCATGAAA 2106
2107 AAAAAAAAAAAAAAA                                                               2121
```

Fig 4.3.2.3 cDNA and predicted amino acid sequences of Arfophilin-2A. The 2121 bp cDNA and predicted 557 amino acid protein are shown. The two in frame stop codons are underlined. The BamH1 restriction site used for assembling Arfophilin-2B and -2C is in red.

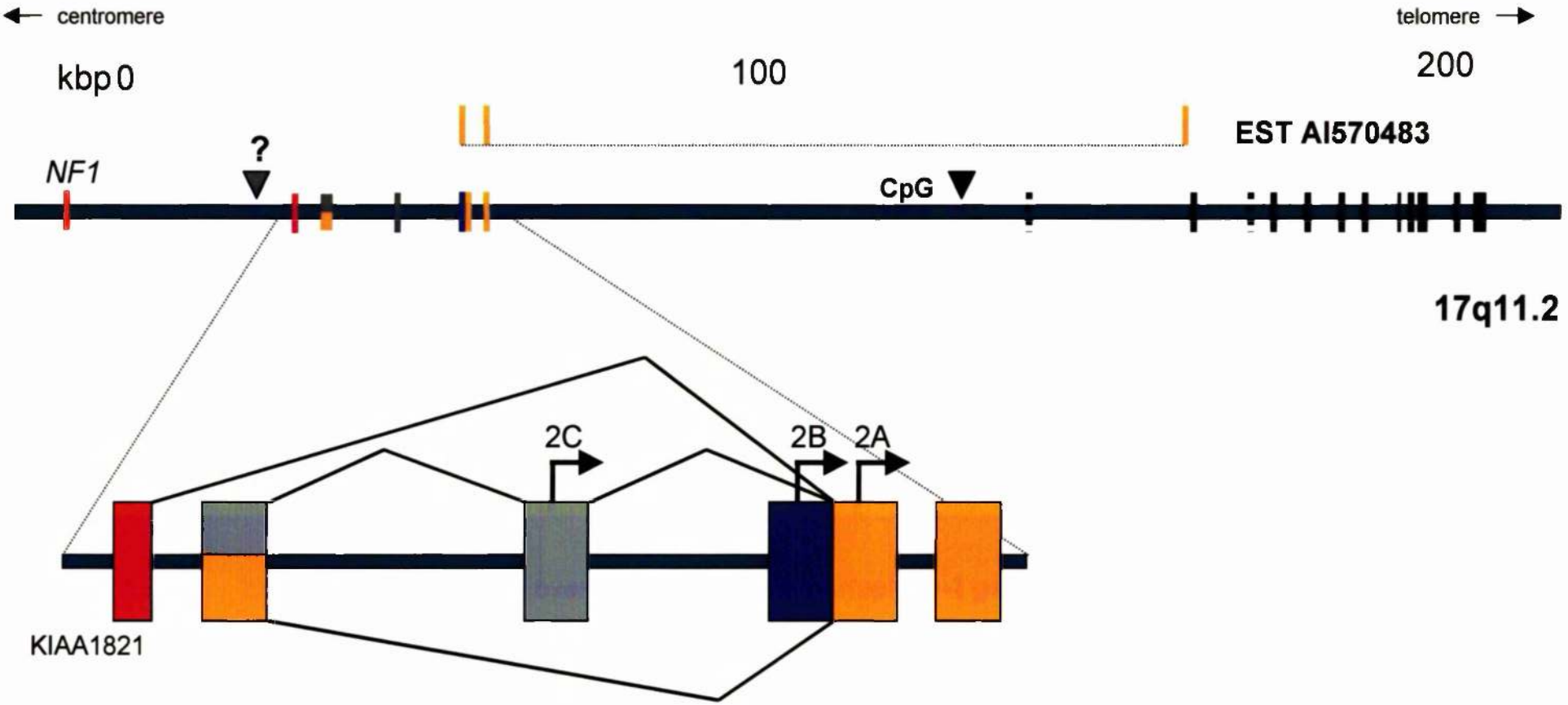

Figure 4.3.2.4 **Diagrammatic overview of the human Arfophilin-2 gene.**

Shown are approximately 200 kilobases of human chromosome 17q11.2 (in green) with the approximate positions of Arfophilin-2 exons. The black exons were recovered in the yeast-two hybrid screen and all evidence available suggests that the solid black exons are present in all splice variants whereas the dotted and coloured exons are only present in some variants. The 3'end of the NF1 gene is indicated by a red box. A magnified view of the 5' end of the gene is also shown together with the starts of the open reading frames. Putative promoter sites are indicated by triangles, and one of these is near a CpG island.

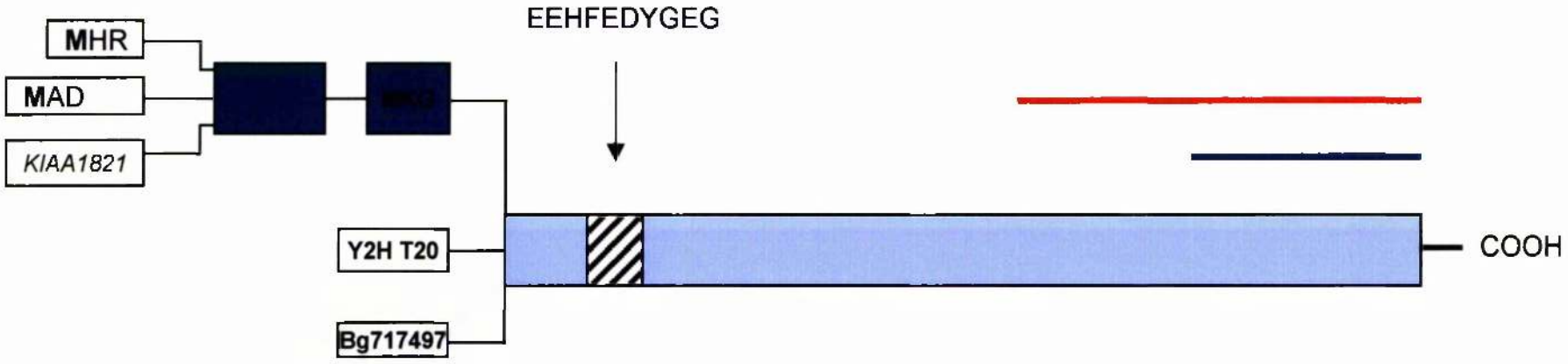

Figure 4.3.2.5 **Diagrammatic overview of Arfophilin-2 splice variants**

Shown are putative splice variants of human Arfophilin-2 deduced from sequences obtained from PCR of testis cDNAs and from analysis of EST databases (not strictly to scale). Initiating methionine residues are shown in bold for Arfophilin-2A (MKG), -2B (MAD) and -2C (MHR). Bg717497 represents the accession number of an EST used to predict one variant. Y2H T20 refers to sequence derived from the longest clone recovered in the yeast two-hybrid screen. Sequences common to all variants are in purple; sequences common to Arfophilins-2B, -2C and KIAA1821 are shown in green, and the hatched box represents sequence derived from an exon that can be spliced out in some variants. EEHFEDYGEG represents an amino acid sequence encode by this exon that is conserved in Arfophilin-1 (see text).Also indicated are the approximate positions of the Arf binding domain (blue line) and the region used to subsequently generate antibodies (red line).

4.3.3 Bioinformatic analysis of Arfophilin-2 protein sequence

Having successfully cloned one Arfophilin-2 splice variant and having predicted the sequences of two others with reasonable confidence, more rigorous bioinformatic analysis of the deduced amino acid sequences was warranted. This was performed using Pix, which like Nix, provides a single output for multiple programs (see Fig. 4.3.3.1). This revealed that Arfophilin-2 is hydrophilic, is unlikely to have any signal sequences or transmembrane domains, but has a high probability of forming coiled-coils in its C-terminus just like Arfophilin-1 (Fig. 4.3.3.1). Also, like Arfophilin-1, it has leucine zipper motifs in its C-terminus (Fig. 4.3.3.1). These consist of five or more leucine residues spaced seven residues apart and are common modules in DNA-binding transcription factors. They are also present in numerous other proteins and often mediate dimerisation (reviewed in Busch and Sassone-Corsi, 1990). For a full sequence alignment of Arfophilin-1 with Arfophilin-2A, see Fig. 4.3.3.2. It also became obvious that proteins homologous to both Arfophilins existed in *Drosophila melanogaster* and *Caenorhabditis elegans*. More specifically, the extreme C-termini of the Arfophilins were homologous to the extreme C-terminus of a *Drosophila* protein called Nuclear Fallout (Nuf; see Fig 4.3.3.3). This is a very interesting protein (described later in section 5.1.1) that is also predicted to have coiled-coils. Similarly, the same region of the Arfophilins showed homology to the central portion of hypothetical *C. elegans* protein F55C12.1 (see Fig. 4.3.3.4), which also has a predicted leucine zipper motif near the Arfophilin-homology domain (not shown). Indeed all of these proteins contain a domain of ~70 residues catalogued in the protein domain (ProDom) database as PD031147. They also appeared to have the PD000002 domain typical of muscle and non-muscle myosin heavy chain tails and tropomyosin. However, this is primarily a reflection of the coiled-coil structures present in these domains, rather than any real sequence homology.

BLAST analysis of the N-termini of the Arfophilins did not uncover any interesting features. While Arfophilin-1 and -2 are quite divergent in their N-termini (see Fig. 4.3.3.2), there is a well conserved motif present (amino acid sequence EE[H/Q]FEDYGEG; see Fig. 4.3.3.2). Intriguingly, this is encoded by the 10^{th} from last exon of Arfophilin-2, the exon that can be spliced out in some variants (see Fig. 4.3.2.5).

Searching the non-human EST databases using the tBLASTn program revealed that there are Arfophilin homologues in *Mus musculus*, *Rattus norvegicus*, *Sus scrofa*, *Bos taurus*, *Xenopus laevis*, *Danio rerio*, and *Oryzias latipes*, in addition to *Caenorhabditis elegans* and *Drosophila melanogaster* as already mentioned. A subset of the results from such

analysis is shown in Fig. 4.3.3.5. Also of note is the fact that there are no apparent Arfophilin orthologues in the *Saccharomyces cerevisiae* genome.

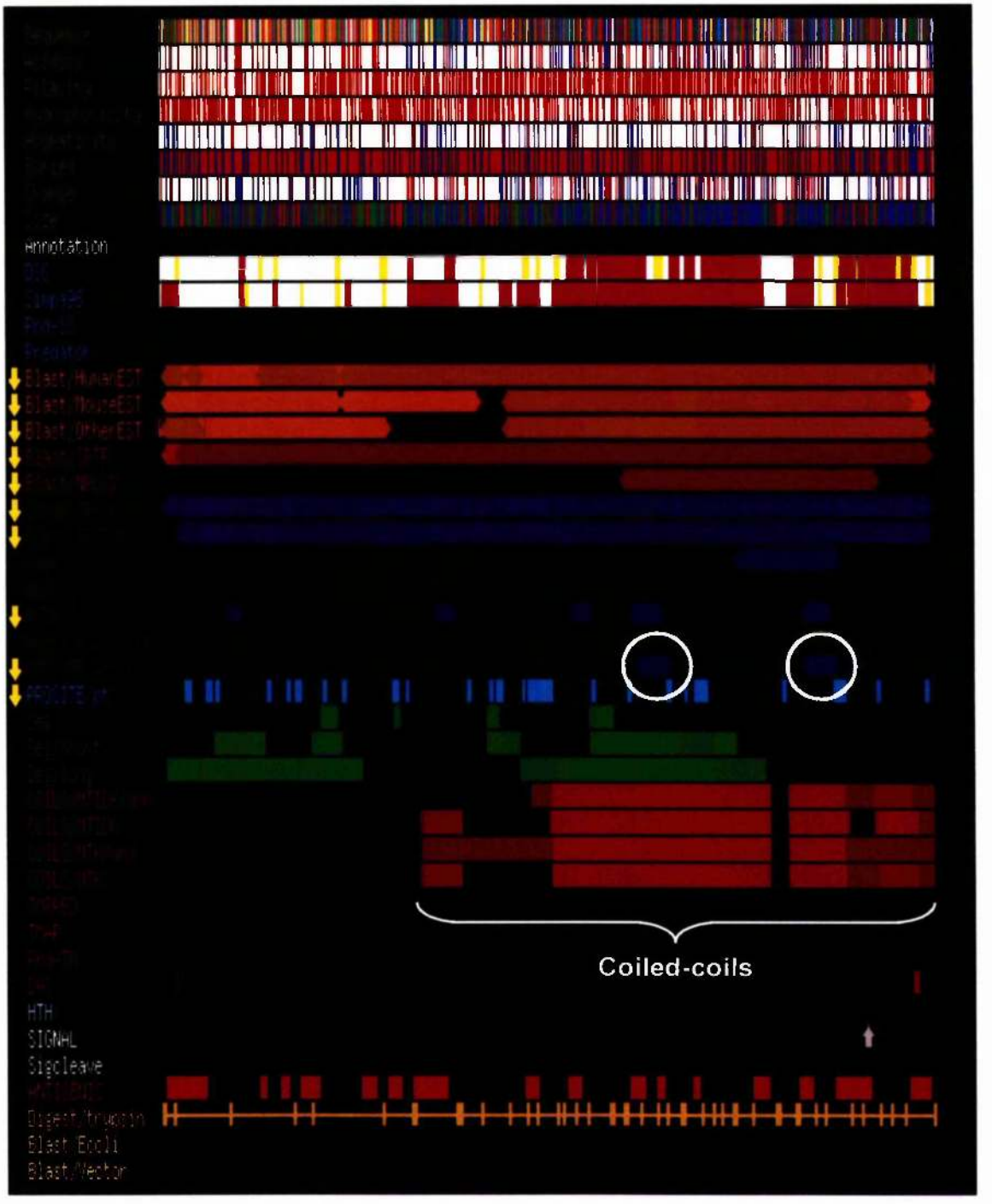

Figure 4.3.3.1 **Analysis of human Arfophilin-2 predicted amino acid sequence.**

Shown is the graphical overview of a Pix output for the 557 amino acid sequence of Arfophilin-2A. The different programs are indicated on the left. Of particular note are the predicted coiled-coil regions in the C-terminal half of the protein. The leucine zipper motifs are circled.

```
Hs_Arfo1        MASAPPASPPGSEPPGPDPEPGGPDGPGAAQLAPGPAELRLGAPVGGPDPQSPGLDEPAP 60


Hs_Arfo1        GAAADGGARWSAGPAPGLEGGPRDPGPSAPPPRSGPRGQLASPDAPGPGPRSEAPLPELD 120

Hs_Arfo1        PLFSWTEEPEECGPASCPESAPFRLQGSSSSSHRARGEVDVFSPFPAPTAGELALEQGPGS 180
Hs_Arfo2A       ---------------------------MKGCEELLKDVLSVESAGTLPCAPEIPDCVEQGS 34


Hs_Arfo1        PPQPSDLSQTHPLPSEPVGSQEDGPRLRAVFDALDGDGDGFVRIEDFIQFATVYGAEQVK 240
Hs_Arfo2A       EVTGPTFADGELIPREPGFFPEDE--------------------EEAMTLAPPEGPQEL- 73
                    . ::: . :* **    **                      *: : :*.  *.:::

Hs_Arfo1        DLTKYLDPSGLGVISFEDFYQGITAIRNGDPDGQCYGGVASAQDEEPLACPDEFDDFVTY 300
Hs_Arfo2A       ----YTDSPMESTQSLEG-SVGSPAEKDGG-----LGGLFLPEDK----------SLVHT 113
                    * *..  .. *:*.   * .* ::*.      **:  .:*:           .:*

Hs_Arfo1        EANEVTDSAYMGSESTYSECETFTDEDTSTLVHPELQPEGDADSAGGSAVPSECLDAMEE 360
Hs_Arfo2A       PSMTTSDLSTHSTTSLISNEEQFEDYGEG----------DDVDCAPSSPCPDDETRTNVY 163
                 :  .:* :  .: *  *: * * * . .          .*.*.* .*. *.:   :

Hs_Arfo1        PDHGALLLLPGRPHPHGQSVITVIGGEEHFEDYGEGSEAELSPETLCNGQLGCSDPAFLT 420
Hs_Arfo2A       SDLGSSVSSSAGQTPR---KMRHVYNSELLDVYCSQCCKKIN---LLN-DLEARLKNLKA 216
                .* *: :  ..   *:    :  : ..* :: * . .  ::.   * * :* .    : :

Hs_Arfo1        PSPTKRLSSKKVARYLHQSG--ALTMEALEDPSPELMEGPEEDIADKVVFLERRVLELEK 478
Hs_Arfo2A       NSPNRKISSTAFGRQLMHSSNFSSSNGSTEDLFRDSIDSCDNDITEKVSFLEKKVTELEN 276
                 **.:::**. ..* * :*.  : :  : **   : ::. ::**::** ***::* ***:

Hs_Arfo1        DTAATGEQHSRLRQENLQLVHRANALEEQLKEQELRACEMVLEETRRQKELLCKMEREKS 538
Hs_Arfo2A       DSLTNGDLKSKLKQENTQLVHRVHELEEMVKDQETTAEQALEEEARRHREAYGKLEREKA 336
                *: :.*: :*:*:*** *****.: *** :*:**  * : : **:**::*   *:****:

Hs_Arfo1        IEIENLQTRLQQLDEENSELRSCTPCLKANIERLEEEKQKLLDEIESLTLRLSEEQENKR 598
Hs_Arfo2A       TEVELLNARVQQLEEENTELRTTVTRLKSQTEKLDEERQRMSDRLEDTSLRLKDEMDLYK 396
                 *:* *::*:***:***:***: .. **:: *:*:**:*:: *.:*. :***.:* :  :

Hs_Arfo1        RMGDRLSHERHQFQRDKEATQELIEDLRKQLEHLQLLKLEAEQ-RRGRSSSMGLQEYHSR 657
Hs_Arfo2A       RMMDKLRQNRLEFQKEREATQELIEDLRKELEHLQMYKLDCERPGRGRSASSGLGEFNAR 456
                ** *:* ::* :**:::************:*****: **:.*:  ****:* ** *:::*

Hs_Arfo1        ARESELEQEVRRLKQDNRNLKEQNEELNGQIITLSIQGAKSLFS-TAFSESLAAEISSVS 716
Hs_Arfo2A       AREVELEHEVKRLKQENYKLRDQNDDLNGQILSLSLYEAKNLFAAQTKAQSLAAEIDTAS 516
                *** ***:**:****:* :*::**::*****::**:  **.**:  : ::******.:.*

Hs_Arfo1        RDELMEAIQKQEEINFRLQDYIDRIIVAIMETNPSILEVK- 756
Hs_Arfo2A       RDELMEALKEQEEINFRLRQYMDKIILAILDHNPSILEIKH 557
                *******:::********::*:*:**:**:: ******:*
```

Figure 4.3.3.2 **Sequence alignment of Arfophilins 1 and 2A.**

A clustal alignment of *Homo sapiens* (Hs) Arfophilin-1 and Arfophilin-2A is shown. Identical residues are donated by asterisks, highly conserved residues by double dots and conserved residues by single dots. The leucine zipper motifs consisting of at least five leucine residues spaced seven residues apart are shown in blue, and the minimum Arf-binding domain (according to Shin et al., 1999) is underlined. Note also the conserved motif EE[H/Q]FEDYGEG (in red) in a region that is otherwise not well-conserved. This is encoded by an exon that can be spliced out in some Arfophilin-2 splice variants.

Figure 4.3.3.3 **Amino acid sequence alignment of Human Arfophilins and *Drosophila* Nuf.**

Shown is a Clustal alignment of the extreme C-terminal ~340 amino acid residues of human Arfophilin-1 (Hs_Arfo1), Arfophilin-2 (Hs_Arfo2) and *Drosophila* Nuf (Dm_Nuf). Asterisks (*) denote identical residues, double dots (:) denote highly conserved residues and single dots (.) denote conserved residues.

```
Hs_Arfo1          KEATQELIEDLRKQLEHLQLLKLEAEQ-RRGRSSSMGLQEYHSRARESELEQEVRRLKQD 673
Hs_Arfo2          REATQELIEDLRKELEHLQMYKLDCERPGRGRSASSGLGEFNARAREVELEHEVKRLKQE 472
Dm_Nuf            KKSTEELMLELGRELQRAREESGARAM----------PTTSPESIRLEELHQELEEMRQK 408
Ce_F55C12.1       ------------------------------------------KAKVAELMKEKEEMTDQ 264
                                                             :  ** :* ..: :.

Hs_Arfo1          NRNLKEQNEELNG-------QIITLSIQGAKSLFST-AFSESLAAEISSVSRDELMEAIQ 725
Hs_Arfo2          NYKLRDQNDDLNG--------QILSLSLYEAKNLFAAQTKAQSLAAEIDTASRDELMEALK 525
Dm_Nuf            NRTLEEQNEELQATMLTNQATMLTNGVEQGRHLLNG--TLNSLAQELEEMSQAQLQQAFQ 466
Ce_F55C12.1       ----------------------LLATSVERGRSLIAD--TP-SLADELAGGDSSQLLDALR 300
                                       ::: .:  .: ':      *** *:   .  :* :*::

Hs_Arfo1          KQEEINFRLQDYIDRIIVAIMETNPSILEVK----- 756
Hs_Arfo2          EQEEINFRLRQYMDKIILAILDHNPSILEIKH---- 557
Dm_Nuf            EKEDENVRLKHYIDTILLNIVENYPQLLEVKPMERK 502
Ce_F55C12.1       EQEICNQKLRVYINGILMRVIERHPEILEI------ 330
                  ::*  * :*: *:: *:: :::  *.:**:
```

Figure 4.3.3.4 **Amino acid sequence alignment of Human Arfophilins, *Drosophila* Nuf and hypothetical *C. elegans* proteins.**

Shown is a Clustal alignment of the extreme C-terminal ~340 amino acid residues of human Arfophilin-1 (Hs_Arfo1), Arfophilin-2 (Hs_Arfo2), *Drosophila* Nuf (Dm_Nuf) and residues 247-330 of hypothetical *C. elegans* protein (Ce_F55C12.1). Asterisks (*) denote identical residues, double dots (:) denote highly conserved residues and single dots (.) denote conserved residues. The last 70 residues constitute domain PD031147 in the ProDom database.

```
>gi|5910150|gb|AW049621.1|AW049621 Mus musculus cDNA clone
 Length = 363
 Score =  117 bits (294), Expect = 2e-26
 Identities = 57/70 (81%), Positives = 62/70 (88%) Frame = +2

Arfo2A: 1   MKGCEELLKDVLSVESAGTLPCAPEIPDCVEQGSEVTGPTFADGELIPREPGFFPEDEEE 60
           MKGCEELLKDVLSVESAGTLPC+P+IPDCVEQGS+ +G T  DGE +PREP FF EDEEE
Sbjct:  158 MKGCEELLKDVLSVESAGTLPCSPDIPDCVEQGSDFSGST--DGEQLPREPDFFQEDEEE 331

Arfo2A: 61  AMTLAPPEGP 70
           AMTLA PEGP
Sbjct:  332 AMTLALPEGP 361
```

```
>gi|11663880|gb|BF554150.1|BF554150 Rattus norvegicus cDNA clone
 Length = 460

 Score =  174 bits (442), Expect = 2e-43
 Identities = 87/110 (79%), Positives = 95/110 (86%), Gaps = 1/110 (0%)
 Frame = -3

Arfo2A: 1   MKGCEELLKDVLSVESAGTLPCAPEIPDCVEQGSEVTGPTFADGELIPREPGFFPEDEEE 60
           MKGCEELLKDVLSVESAGTLPC+P+IPDCVEQGS+ +G T+ADGEL+PREPGFF EDEEE
Sbjct:  332 MKGCEELLKDVLSVESAGTLPCSPDIPDCVEQGSDFSGSTYADGELLPREPGFFQEDEEE 153

Arfo2A: 61  AMTLAPPEGPQELYTDSPMESTQSLEGSVGSPA-EKDGGLGGLFLPEDKS 109
           AMTL  PEGPQEL  DSPMES+Q  EGSV SP  EK+  LGGLFLPED S
Sbjct:  152 AMTLTLPEGPQELDMDSPMESSQGPEGSVRSPVEEKEPELGGLFLPEDTS 3
```

```
>gi|11074765|gb|BF191396.1|BF191396 2389?2 Sus scrofa cDNA 5'.
 Length = 534
 Score =  166 bits (419), Expect = 8e-41
 Identities = 82/119 (68%), Positives = 90/119 (74%), Gaps = 2/119 (1%)
 Frame = +1

Arfo2A: 27  PDCVEQGSEVTGPTFADGELIPREPGFFPEDEEE--AMTLAPPEGPQELYTDSPMESTQS 84
           P   +QGSEV  PTFADGEL+PREPGFFPEDE+E  AMTLAPPEGPQEL  + PMEST+S
Sbjct:  109 PASGDQGSEVPDPTFADGELLPREPGFFPEDEDEDEAMTLAPPEGPQELDMEGPMESTRS 288

Arfo2A: 85  LEGSVGSPAEKDGGLGGLFLPEDKSLVHTPXXXXXXXXXXXXXXLISNEEQFEDYGEGD 143
           L+GS+G PAEKD GLG LFLPEDKS VHTP               L+SNEEQFEDYGE D
Sbjct:  289 LDGSLGMPAEKDAGLGSLFLPEDKSRVHTPPMTTSDLSTHSTTWLVSNEEQFEDYGEAD 465
```

Fig. 4.3.3.5 **Results of tBLASTn searches of Arfophilins 1 and 2 against non-human ESTs (continued overleaf).**

Arfophilin-2A (Arfo2A, this page) and Arfophilin-1 (Arfo1, next page) amino acid sequences were aligned against the non-human EST database translated in all reading frames (tBLASTn program). Shown are some of the high-scoring outputs shown aligned with the Arfophilin family member with which they exhibit the greatest homology.

```
EM:BF606409 BF606409 273444 MARC 3BOV Bos taurus cDNA
Length = 471
Score =  247 bits (624), Expect = 6e-64
Identities = 125/156 (80%), Positives = 134/156 (85%)Frame = +3

Arfo1: 545 QTRLQQLDEENSELRSCTPCLKANIERLEEEKQKLLDEIESLTLRLSEEQENKRRMGDRL 604
          Q RLQQLDEENSELRSCTPCLKANIERLEEEKQKLLDEIE L++RLS+EQEN+R++GDRL
Sbjct: 3   QARLQQLDEENSELRSCTPCLKANIERLEEEKQKLLDEIEELSVRLSDEQENRRKLGDRL 182

Arfo1: 605 SHERHQFQRDKEATQELIEDXXXXXXXXXXXXXXXXRRGRSSSMGLQEYHSRARESELE 664
          SHERHQFQRDKEATQELIED               RRGRSSS GLQEYHSR RESELE
Sbjct: 183 SHERHQFQRDKEATQELIEDLRKQLEHLQLFKLEAEQRRGRSSSAGLQEYHSRTRESELE 362

Arfo1: 665 QEVRRLKQDNRNLKEQNEELNGQIITLSIQGAKSLF 700
          QEVRRLKQDNR+LKEQN+ELNGQII LSIQGA+SLF
Sbjct: 363 QEVRRLKQDNRSLKEQNDELNGQIINLSIQGARSLF 470
```

```
EM:AL585583 AL585583 Gallus gallus mRNA; expressed sequence tag
Length = 402
Score =  201 bits (506), Expect = 4e-50
Identities = 103/115 (89%), Positives = 111/115 (95%)Frame = -2

Arfo1: 642 RRGRSSSMGLQEYHSRARESELEQEVRRLKQDNRNLKEQNEELNGQIITLSIQGAKSLFS 701
          RRGRSSSMGLQEY+SR RE+ELEQE+ +LKQDNR+LKEQN+ELNGQII LSIQGAK+LFS
Sbjct: 347 RRGRSSSMGLQEYNSRTRETELEQEINQLKQDNRSLKEQNDELNGQIINLSIQGAKNLFS 168

Arfo1: 702 TAFSESLAAEISSVSRDELMEAIQKQEEINFRLQDYIDRIIVAIMETNPSILEVK 756
           +FSESLAAEISSVSRDELMEAIQKQEEINFRLQDYIDRIIVAIMETNPSILEVK
Sbjct: 167 ASFSESLAAEISSVSRDELMEAIQKQEEINFRLQDYIDRIIVAIMETNPSILEVK 3
```

```
EM:BI064697 BI064697 normalized chicken fat cDNA library Gallus gallus cDNA
Length = 548
Score =  129 bits (320), Expect = 3e-28
Identities = 78/161 (48%), Positives = 86/161 (52%)Frame = +3

Arfo1: 110 PRSEAPLPELDPLFSWTEEPEECGPASCPESAPFRLQGSSSSHRARGEVDVFSPFPAPTA 169
          P    P P LDP   W E   E  P   PES      G+                  PA  A
Sbjct: 144 PARPPPAPPLDPGPRWDEAGPEADPEPEPESELEAEPGAE---------------PALWA 278

Arfo1: 170 GELALEQGPGSPPQPSDLSQTHPLPSEPVGSQEDGPRLRAVFDALDGDGDGFVRIEDFIQ 229
           E A    P +PP               G  ED PRLR VFDALD DGDGFVR+E+F+Q
Sbjct: 279 AEPAAGTPPWAPPGRG-------------GCPEDEPRLRPVFDALDRDGDGFVRVEEFVQ 419

Arfo1: 230 FATVYGAEQVKDLTKYLDPSGLGVISFEDFYQGITAIRNGD 270
          FAT YGAEQVK+LTKYLDPSGL VISFEDF++GI AI  GD
Sbjct: 420 FATAYGAEQVKELTKYLDPSGLXVISFEDFHRGIXAIXXGD 542
```

```
EM:AU170919 AU170919 Oryzias latipes cDNA, clone:br6952.
Score =  120 bits (299), Expect = 8e-26
Identities = 65/89 (73%), Positives = 74/89 (83%), Gaps = 3/89 (3%)Frame = +3

Arfo1: 668 RRLKQDNRNL---KEQNEELNGQIITLSIQGAKSLFSTAFSESLAAEISSVSRDELMEAI 724
          RR    NR      +  N+ELNGQII LSIQGAK+L S +FS+SLAAEI+SVSR ELME +
Sbjct: 81  RRSNGSNRTTAL*RSFNDELNGQIINLSIQGAKTLMSASFSDSLAAEINSVSRVELMETV 260

Arfo1: 725 QKQEEINFRLQDYIDRIIVAIMETNPSILEVK 756
           KQEEIN+RLQDYID+IIVAIME NPSILEVK
Sbjct: 261 HKQEEINYRLQDYIDKIIVAIMECNPSILEVK 356
```

```
EM:AW280381 AW280381 fj39c06.y1 zebrafish adult brain Danio rerio
Score = 61.3 bits (146), Expect = 7e-08
Identities = 27/62 (43%), Positives = 41/62 (65%), Gaps = 1/62 (1%)Frame = +1

Arfo1: 206 RLRAVFDALDGDGDGFVRIEDFIQFATVYG-AEQVKDLTKYLDPSGLGVISFEDFYQGIT 264
          +L+ VFD  D D DG++R+E F+     +G  ++VK   KYLDP+  G I+F+DF  G+
Sbjct: 58  KLKEVFDVCDEDADGYIRVEHFVDLGLQFGQGDEVKKFAKYLDPNAHGRINFKDFCHGVF 237

Arfo1: 265 AIR 267
          AI+
Sbjct: 238 AIK 246
```

```
EM:AW636537 AW636537 bl47h10.w1 Xenopus laevis cDNA clone PBX0047H10
Score = 58.6 bits (139), Expect = 5e-07
Identities = 34/95 (35%), Positives = 61/95 (63%), Gaps = 12/95 (12%)

Arfo1: 662 ELEQEVRRLKQDNRNLKEQNEELNGQIITLSIQGAKSLFSTAFSE-----------SLA 709
          E E+E +RL  +N++L+E NE+L   ++   +Q     F     E            S+A
Sbjct: 169 ECEREKQRLADENQSLREINEDLQDALL---VQNGSVCFPYRTHEENSHSKPGSPVHSIA 339

Arfo1: 710 AEISSVSRDELMEAIQKQEEINFRLQDYIDRIIVAIMETNPSILEVK 756
           EI   ++ ++  A+ +Q+EIN RL+ Y+DR+I+ ++E +P +LE+K
Sbjct: 340 EEIDVCTQQQI-SALNEQKEINRRLRQYLDRVILTVLEKDPGLLEIK 477
```

4.3.4 Tissue expression of human Arfophilin mRNAs

Northern blot analyses of both Arfophilins-2 and -1 were performed to determine their expression profiles and also to see what size transcripts were present and whether these were in good agreement with the sizes of cDNAs obtained from testis. Commercially bought, standardised, multiple-tissue blots containing 2 μg per lane of polyA+ RNA recovered from 16 different tissues pooled from several individuals were used. The cDNA probes used corresponded to the extreme 3' 1 kb of the open reading frames and they were both expected to hybridise with all splice variants of their respective genes, based on analysis of the EST databases. The Arfophilin-2 blots were performed first, stripped of probe, and then re-blotted for Arfophilin-1. Although an Arfophilin-1 northern blot has been previously published (Shin et al., 1999), it was deemed necessary to repeat this with more tissues including testis since we predicted that Arfophilin-2 would be highly expressed in this tissue given the high number of positives recovered from such a small-scale yeast two-hybrid screen. It was also necessary to check that the probes did not cross-hybridise.

As can be seen in Fig. 4.3.4 (panel A) Arfophilin-2 is indeed highly overexpressed in testes. Three transcripts are apparent with a major one ~2.4 kb in length, a less pronounced one of ~4.4 kb, and a minor one of ~ 5-6 kb. The ~2.4 kb band is in excellent agreement with the sizes of Arfophilins-2A, -2B and -2C, which are predicted to be between 2.1 and 2.6 kb. A much larger band running at about 7-10 kbp was also detected in skeletal muscle. Upon inspection of longer exposures, a low level but ubiquitous expression of the 4.4 kbp transcript was observed (Fig. 4.3. 4; panel B).

Arfophilin-1 is also highly expressed in testes with major 5-6 kb and minor ~ 4.4 kb transcripts being apparent (Fig. 4.3. 4; panel C). The larger of the two is also present at lower levels in ovary, skeletal muscle and kidney, while the smaller appears to be the predominant form in kidney. Skeletal muscle and heart also express large (7-10 kb) Arfophilin-1 mRNAs. These findings are not wholly consistent with the published data (Shin et al., 1999), which showed Arfophilin-1 expression almost exclusively in heart and skeletal muscle, despite the fact that the authors had identified the gene in a screen of kidney cDNAs. The reason for this discrepancy is unclear especially as the blot they used was of the same type, from the same supplier and the probe was only marginally (200 bp) longer, and corresponded to the same region of the open reading frame.

Note that the major testis Arfophilin-2 band is absent in the Arfophilin-1 blot, and that the major kidney Arfophilin-1 band is absent in the Arfophilin-2 blot, showing that, under the conditions used, the probes were specific with no significant cross-hybridisation.

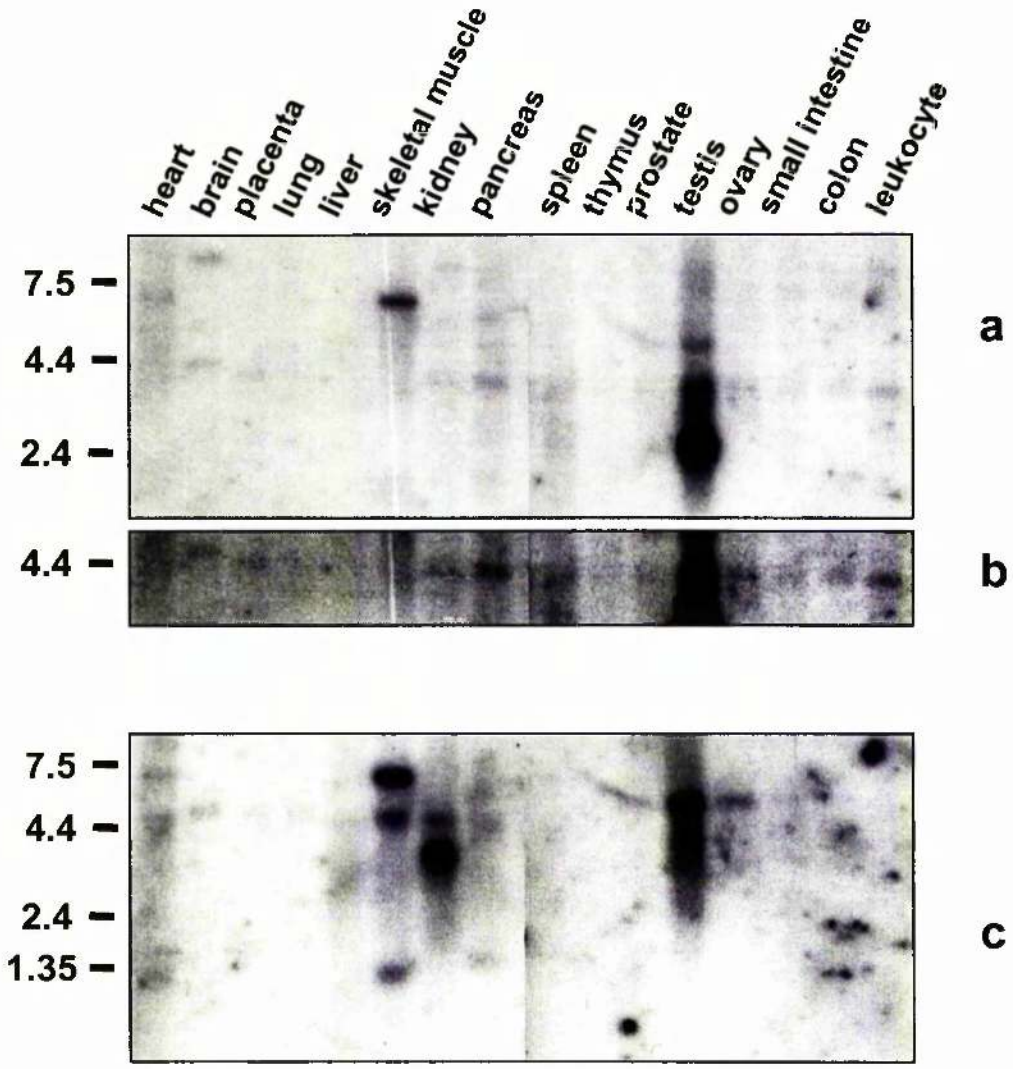

Figure 4.3.4 Tissue expression profiles of human Arfophilins 1 & 2.

Northern analysis of Arfophilin-2 (*panels a and b*) and Arfophilin-1 (*panel c*) using human multiple-tissue blots as indicated was performed using probes corresponding to the 3' 1kb of the respective open reading frames. Both genes are highly expressed in testes. In addition, strong signals are apparent for Arfophilin-1 in skeletal muscle and kidney. Longer exposure revealed a 4.4kb Arfophilin-2 transcript present in nearly all the tissues (*panel b*). Note the lack of significant cross-hybridisation between probes. Approximate sizes of transcripts in kbp are indicated on the left-hand side.

4.3.5 Production and initial characterisation of Arfophilin antisera

We sought to produce specific antibodies to allow us to determine in which cells Arfophilins were expressed and then to try to uncover their subcellular distributions and possible roles within those cells. Recombinant proteins were produced in *Escherichia coli*, purified, and used to inoculate a rabbit and a sheep to produce Arfophilin-1 and Arfophilin-2 polyclonal antibodies, respectively. The use of two different species was a conscious decision to allow for comparative analyses of products from the two different genes in future experiments.

Since the antisera we raised were from recombinant proteins comprising the regions of Arfophilin-1 and Arfophilin-2 with the greatest homology, it was necessary to test the specificity of each antibody and determine whether affinity purification against the other isoform would be required to obtain isoform-specific antibodies. To this end, hexahistidine-tagged Arfophilin-1 and -2 recombinant proteins were produced corresponding to their respective C-terminal 330 amino acid residues - the same size as the original Arfophilin-2 antigen. It was found that the pET28b vector (Novagen) gave superior results compared to the pQE vectors (Qiagen) in that a single major band of the correct predicted molecular mass was produced for each protein as opposed to the multiple ladders of bands previously observed with the pQE vector (not shown).

As can be seen in Fig. 4.3.5 (panel A), Arfophilin-2 immune serum, but not preimmune serum, only recognised the Arfophilin-2 recombinant protein and not the analogous Arfophilin-1 protein in immuno-blot analysis. This shows that antibodies were successfully produced, that they are specific for Arfophilin-2 and that they do not recognise the His-tag present in both proteins. Equal protein was present in each lane, as determined by both Bradford assay and Ponceau staining (not shown).

Arfophilin-2 antibodies were then affinity purified using the same His-tagged Arfophilin-2 produced from the pET vector in order to increase specific and decrease non-specific staining necessary for certain applications. Fig. 4.3.5 (panel B) is of a polyacrylamide gel stained with Coomassie brilliant blue showing the purified IgG fractions eluted from the affinity column. Fractions 4-13 were pooled, separated into aliquots and stored at -80°C prior to use in the experiments described below. The protein concentration was 0.24 mg/ml.

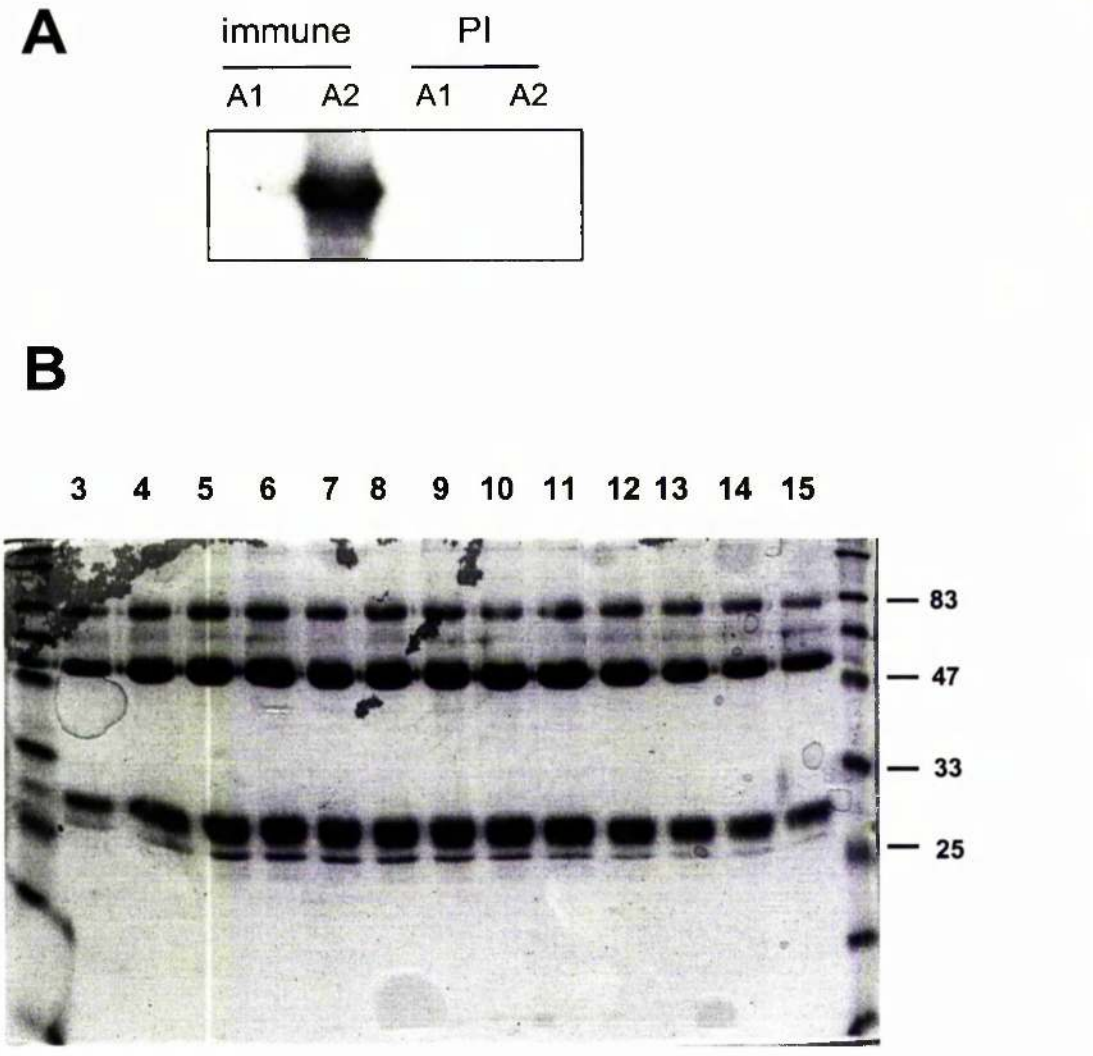

Figure 4.3.5 **Anti-Arfophilin-2 polyclonal antibodies.**

Panel A: 1 μg of recombinant His-Arfophilin-1 (A1; C-terminal 330 residues) and His-Arfophilin-2 (A2; C-terminal 330 residues) were run on a 10% SDS PAGE gel, transferred to nitrocellulose, and immuno-blotted with crude Arfophilin-2 immune serum according to the methods described in section 2.2.4. A duplicate blot was also performed using pre-immune serum (PI).

Panel B: Purified IgGs were eluted from an Arfophilin-2 affinity column and collected in 1 ml fractions. 13 μl of each fraction were boiled in sample buffer and loaded onto a 15% SDS-PAGE gel. Following electrophoresis, the gel was stained with Coomassie and then destained, to reveal the IgG light chains (lower bands) and heavy chains (intermediate bands). The positions and sizes (in kDa) of molecular weight markers are shown on the right). Fractions 4-13 were later pooled and the protein concentration was found to be 0.24 mg/ml.

The rabbit polyclonal antibody to Arfophilin-1 has not yet been characterised or affinity purified. The crude serum was, however, used in an immunoblot of recombinant Arfophilin proteins and also in immunofluorescence of cells transfected with an Arfophilin-1 construct. Positive signals were observed compared to pre-immune serum indicating that the animal did indeed produce antibodies, but it remains to be seen how specific they are for Arfophilin-1 (data not shown).

4.3.6 Endogenous Arfophilin-2 protein expression

The purified anti-Arfophilin-2-specific antibody was used to analyse the native protein by immunoblot analysis. Lysates from human and rat testes as well as cultured HeLa, HEK 293 and CHO cells were run on SDS-PAGE gels, transferred to nitrocellulose and probed for Arfophilin-2 using the antibody at a concentration of 50 ng/ml. This revealed a single major band with an apparent molecular mass of ~83 kDa in all the cells of human origin examined: testis, HeLa and HEK 293 (Fig. 4.3.6; panel A), although the commercially obtained human testis preparation consistently produced a smear that may have masked less intense bands (Fig. 4.3.6, panel A, 2nd lane). This suggests that despite the three distinct transcripts on the northern blot, only one protein seems to be made in testes. Rat testis and CHO cell lysates, on the other hand, showed no immunoreactivity with the Arfophilin-2 antibody (Fig. 4.3.6, panel A), suggesting that the epitopes do not reside in well-conserved regions of Arfophilin-2.

Given the lack of immunoreactivity, CHO cells were used for the heterologous expression and subsequent western blotting of untagged Arfophilin-2 constructs, to allow direct comparison of the electrophoretic mobility of each putative protein with the native ones in testis or HeLa cells. The results of such analysis are also shown in Fig 4.3.6 (panel A), where it can be seen that untagged, heterologously expressed Arfophilin-2A migrates the same as the native proteins on an 8% polyacrylamide gel. It runs at 83 kDa despite having a calculated molecular mass of 61 kDa. The constructs encoding putative Arfophilin-2B and -2C, however, each produced two bands that were spaced about 10 kDa apart. The reason for this is unclear but none of these bands migrated exactly as the endogenous proteins (Fig. 4.3.6; panel A). These data suggest that Arfophilin-2A is the major (or only) variant expressed in testes and HeLa cells.

Immunoprecipitation experiments were also carried out to further characterise the affinity-purified antibodies. One such experiment is shown in Fig. 4.3.6 (panel B) where it can be seen that the endogenous protein running at 83 kDa can be precipitated from a HeLa cell

lysate using the antibody coupled to protein G-sepharose beads. Furthermore, this is a specific antibody/ antigen interaction since preimmune serum cannot reproduce the result.

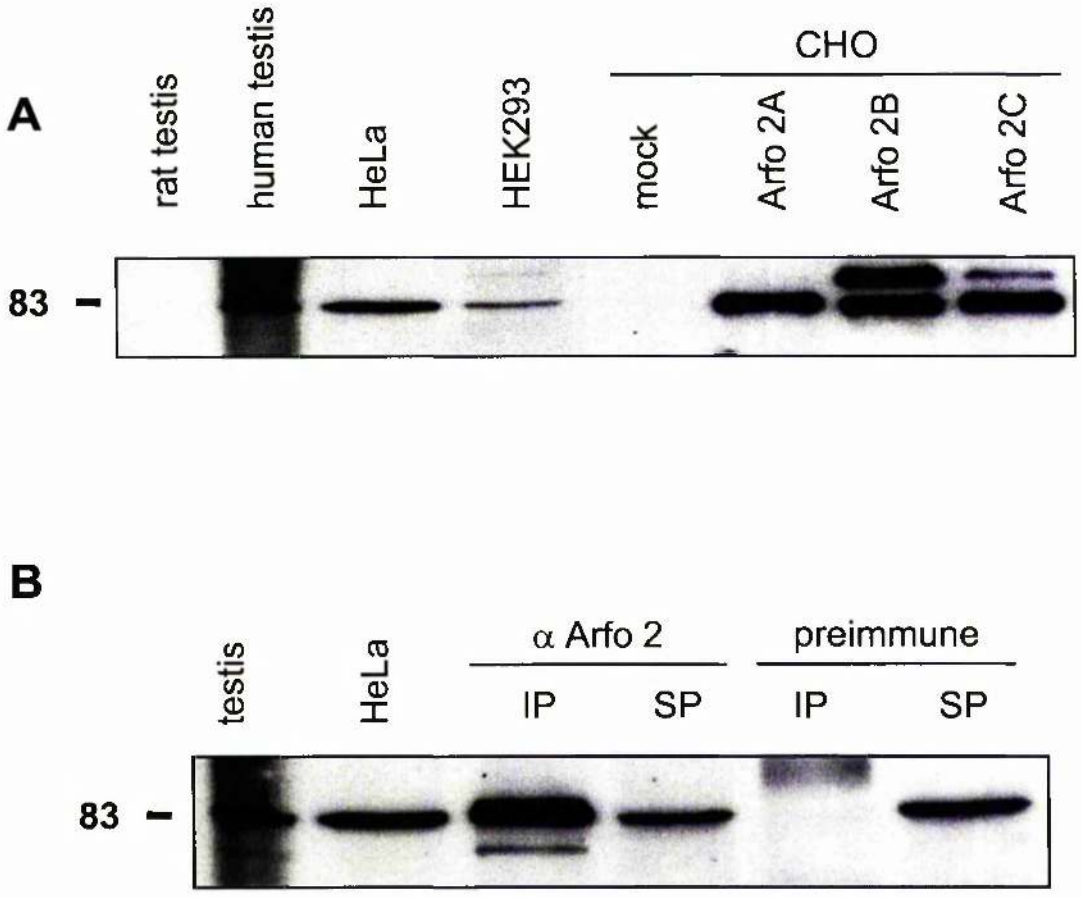

Fig. 4.3.6 **Immunoblotting and immunoprecipitation using the affinity purified Arfophilin-2-specific antibody.**

Panel A: Lysates from rat testis, human testis, HeLa cells and HEK 293 cells were run on an 8% SDS-PAGE gel alongside mock-transfected (mock) and untagged Arfophilin-2A/2B/2C-transfected (Arfo2) CHO cells (all 20 µg per lane except transfected cells which had only 1 µg). The proteins were transferred to nitrocellulose and immunoblotted with the affinity-purified Arfophilin-2-specific antibody (50 ng/ml) according to the methods in section 2.2.4. The position of the 83 kDa molecular weight marker is indicated.

Panel B: HeLa cell lysates were subjected to immunoprecipitation using the Arfophilin-2 antibody (α Arfo 2; 10 µg/ml) coupled to protein G-sepharose, according to the method described in section 2.2.4.6. As a control, an equivalent amount of preimmune serum was used. Proteins associated with the beads (IP) and the supernatants (SP) were resolved on an 8% SDS-PAGE gel alongside 20 µg each of human testis and HeLa cell lysate. These were then transferred to nitrocelluose and immunoblotted with the same Arfophilin-2 antibody. The position of the 83 kDa molecular weight marker is indicated.

4.3.7 Subcellular localisation of endogenous Arfophilin-2 in interphase HeLa cells

The data presented thus far have clearly established that Arfophilin-2 is expressed at the protein level in HeLa cells. Therefore, I used immunofluorescence and confocal microscopy to determine its subcellular localisation in this cell type; with a view to begin to understand what cellular function(s) it may be performing. As a first step to test its efficacy and specificity in such experiments, the affinity purified Arfophilin-2 antibody was used on its own to label fixed HeLa cells on coverslips. The results can be seen in Fig. 4.3.7.1, where diffuse cytosolic staining as well as perinuclear staining is apparent (upper panels). All the signals were abolished when the antibody was pre-incubated with antigen demonstrating that the staining patterns are specific for Arfophilin-2 (lower panel).

Double immunofluorescence labelling was then performed using the Arfophilin-2 antibody in conjunction with antibodies to a range of other marker proteins. Representative confocal images from these experiments are shown in Fig. 4.3.7.2. Co-staining for filamentous actin (F-actin, panels a-c) clearly defines the outline of the cells, as does staining for microtubules (MTs; panels d-f) using an α-tubulin antibody, and this allows good visualisation of the perinuclear Arfophilin-2 pool. Further analysis revealed that this staining was coincident with staining for the CI-MPR (Fig. 4.3.7.2, panels g-i) and to a lesser extent, the CD-MPR (Fig. 4.3.7.2, panels j-l) which both traffic between the TGN, late endosomes and the plasma membrane. It also partially colocalised with βCOP (Fig. 4.3.7.2, panels m-o), a constituent of the COPI coatomer complex, and was adjacent to GRASP65 (Fig. 4.3.7.2, panels p-r), a Golgi cisternal stacking protein enriched in the medial Golgi (Barr et al., 1997). Colocalisation was not observed, however, with other proteins such as the AP-3 adaptor complex (Fig. 4.3.7.3, panels a-c) or GGA1 (Fig. 4.3.7.3, panels d-f). Similarly, no obvious overlap was apparent with the endosomal transferrin receptor (TfR, Fig. 4.3.7.3, panels g-i) or RME1 (Fig. 4.3.7.3, panels j-l). Upon further investigation, it was noted that there was also a minor centrosomal pool of Arfophilin-2 as evidenced by partial colocalisation with γ-tubulin (Fig. 4.3.7.3, panels m-o) which is found at the hub of the microtubule-nucleating centre. This pattern of staining was so striking that centrosomes could easily be identified without the need for observing γ-tubulin labelling, and it was specific as prior incubation of the antibody with antigen abolished it (not shown). It was also noted that the Arfophilin-2 antibody stained peripheral structures resembling focal adhesions or filopodia (for example, see arrowheads in panel l of Fig. 4.3.7.2).

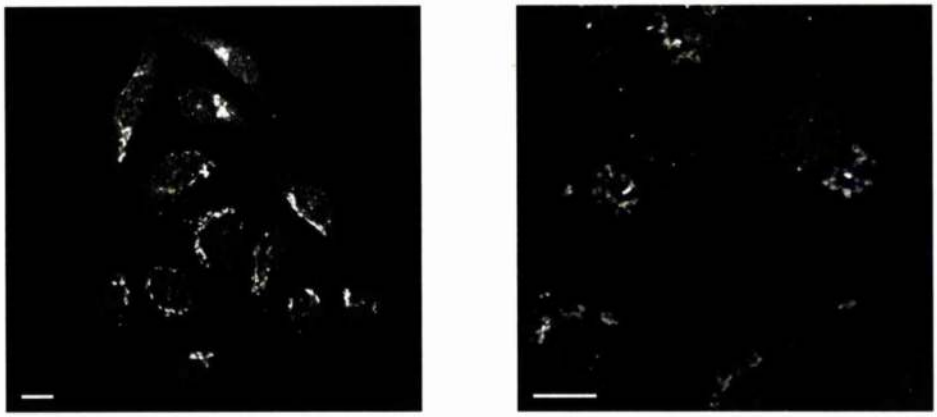

- antigen

- antigen

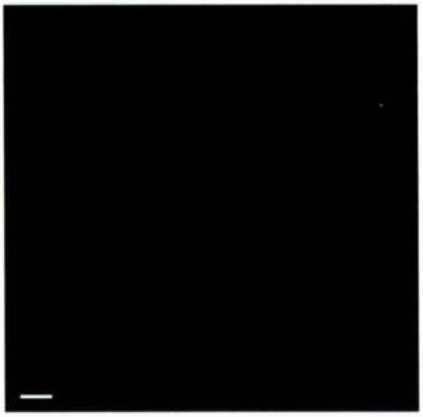

+ antigen

Figure 4.3.7.1 **Affinity purified Arfophilin-2 antibodies are specific for the antigen in immunofluorescence.**

HeLa cells grown on coverslips were fixed and processed for immunofluorescence using the affinity purified Arfophilin-2 antibodies at a dilution of 1:100 (240 ng/ml), followed by an Alexa^{594}-conjugated anti-sheep antibody, all according to the protocols described in section 2.2.3. The top two panels show representative confocal images of the stained cells. The bottom panel shows the effect of preincubating the antibody with 5 µg of recombinant His-Arfophilin-2 antigen for 30 min at room temperature. Scale bars, 10 µm.

Fig. 4.3.7.2 **Subcellular localisation of endogenous Arfophilin-2 in HeLa cells.**

HeLa cells grown on glass coverslips were washed in PBS and fixed in methanol at -20°C. They were then processed for immunofluorescence using the purified sheep anti-Arfophilin-2 antibody (Arfo 2; 1:200) in conjunction with a Cy3-conjugated anti-actin antibody (a-c), and antibodies to α tubulin to label microtubules (MTs, d-f), CI-MPR (g-i), CD-MPR (j-l), βCOP (m-o) and GRASP65 (p-r). Alexa^{594}-anti-sheep and Alexa^{488}-anti-rabbit/mouse secondary antibodies were then used as appropriate and the coverslips were mounted. Shown are representative confocal images. The arrowheads in panel l indicate peripheral Arfophilin-2 staining in focal adhesions. Scale bars, 10 µm.

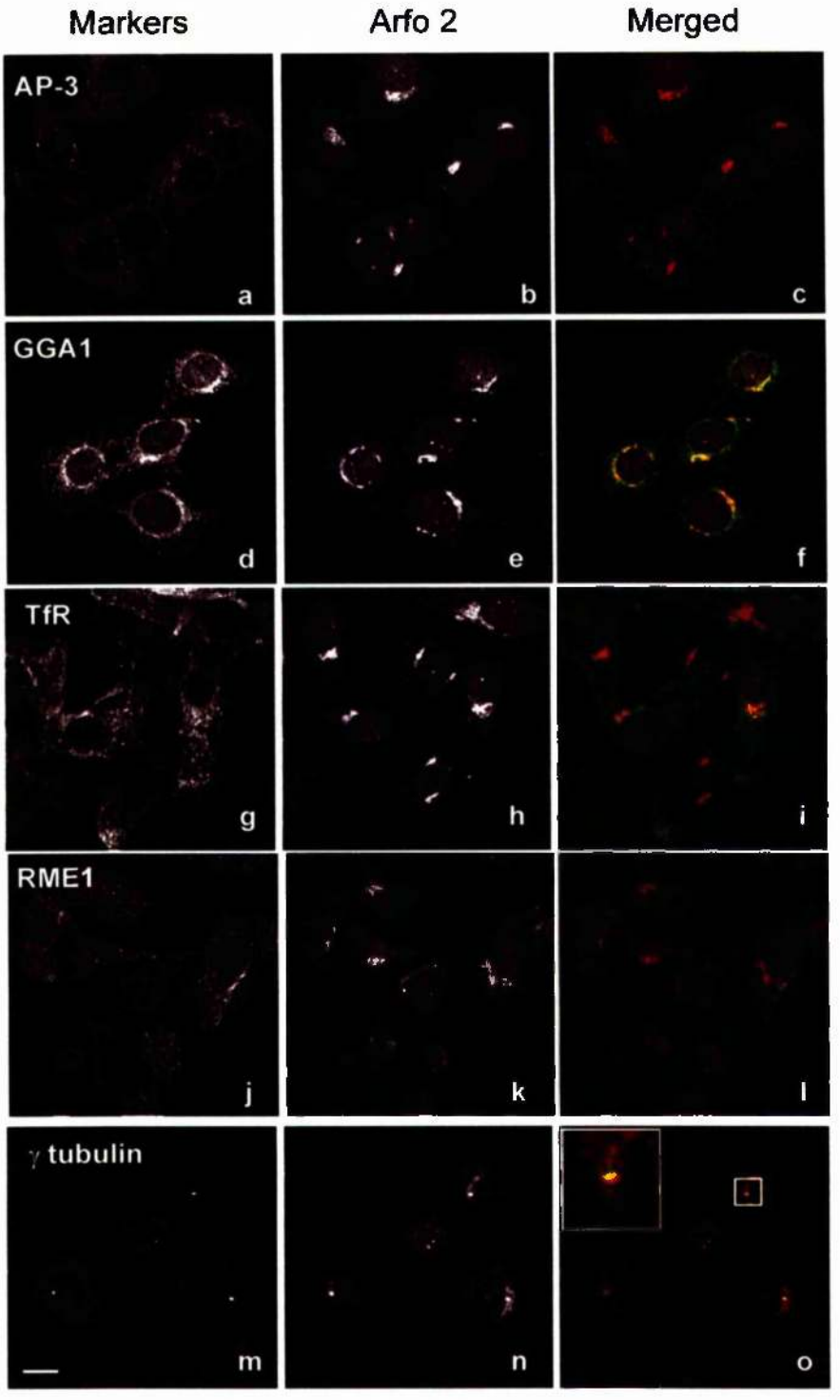

Fig. 4.3.7.3 **Subcellular localisation of endogenous Arfophilin-2 in HeLa cells (continued).**

HeLa cells grown on glass coverslips were washed in PBS and fixed in methanol at -20°C. They were then processed for immunofluorescence using the purified sheep anti-Arfophilin-2 antibody (Arfo 2; 1:200) in conjunction with antibodies against AP-3 (a-c), GGA1 (d-f), TfR (g-i), RME1 (j-l) and γ tubulin (m-o) that were all used at a 1:200 dilution. Alexa^{594} anti-sheep and Alexa^{488} anti-rabbit/mouse secondary antibodies were then used and the coverslips were mounted. Shown are representative confocal images. The inset in panel o is an enlargement of the boxed region where partial colocalisation between Arfophilin-2 and γ tubulin staining is apparent. Scale bar, 10 μm.

4.3.8 Subcellular localisation of endogenous Arfophilin-2 in dividing HeLa cells

The centrosomal localisation of Arfophilin-2 was particularly intriguing given the fact that the homologous Nuf protein cycles on and off this organelle and is believed to function there at various stages of the *Drosophila* syncytial cell cycle (Rothwell et al., 1998). Given this information, a preliminary experiment was performed looking at the distribution of Arfophilin-2 in mitotic cells. An asynchronous population of HeLa cells on glass coverslips was fixed and processed for immunofluorescence using α-tubulin and Arfophilin-2 antibodies and care was taken not to wash off the mitotic cells. Dividing cells were then located and confocal images were taken. Although diffuse staining throughout the cytosol was apparent, Arfophilin-2 appeared concentrated at the spindle poles during metaphase (Fig. 4.3.8 panels a-c) and anaphase (panels d-f) and some cells exhibited Arfophilin-2 staining at the midbody during late telophase/cytokinesis (panels g-i).

4.3.9 The effects of drug treatment on endogenous Arfophilin-2 localisation

Further studies were performed to investigate the effects of the drugs nocodazole and brefeldin A (BFA) on Arfophilin-2 distribution. The former is a microtubule-disrupting agent known to result in shortened Golgi stacks (reviewed in Thyberg and Moskalewski, 1985), while the latter causes a collapse of the Golgi into the endoplasmic reticulum by inhibiting Arf activation by BFA-sensitive GEFs (see section 1.1.1.3). In control cells, as previously mentioned, Arfophilin-2 colocalises with the CI-MPR in the TGN region (Fig. 4.3.9, panels a-c). Upon BFA treatment (20 μg/ml for 10 min), both proteins are dispersed, with Arfophilin-2 staining appearing very diffuse (Fig. 4.3.9, panels d-f). Nocodazole treatment (50 ng/ml for 1 h) also disrupted the localisations of both proteins (Fig. 4.3.9, panels g-i), although Arfophilin-2 remained in punctate structures. While some colocalisation between the two proteins persisted following microtubule disruption, it was noticeably reduced (see inset in panel i, Fig. 4.3.9). Conversely, neither BFA nor nocodazole treatment appeared to have any effect on the distribution of the centrosomal Arfophilin-2 staining (Fig. 4.3.9, panels j-o). In nocadazole-treated cells, Arfophilin-2 immunoreactivity at the cell periphery was also apparent, as previously seen (see arrowheads panels i and o, Fig. 4.3.9). Cells were also treated for 1 h with 100 nM wortmannin but this had no discernible effect on Arfophilin-2 localisation suggesting that this is not dependent on phosphatidyl inositol 3 kinase activity (data not shown).

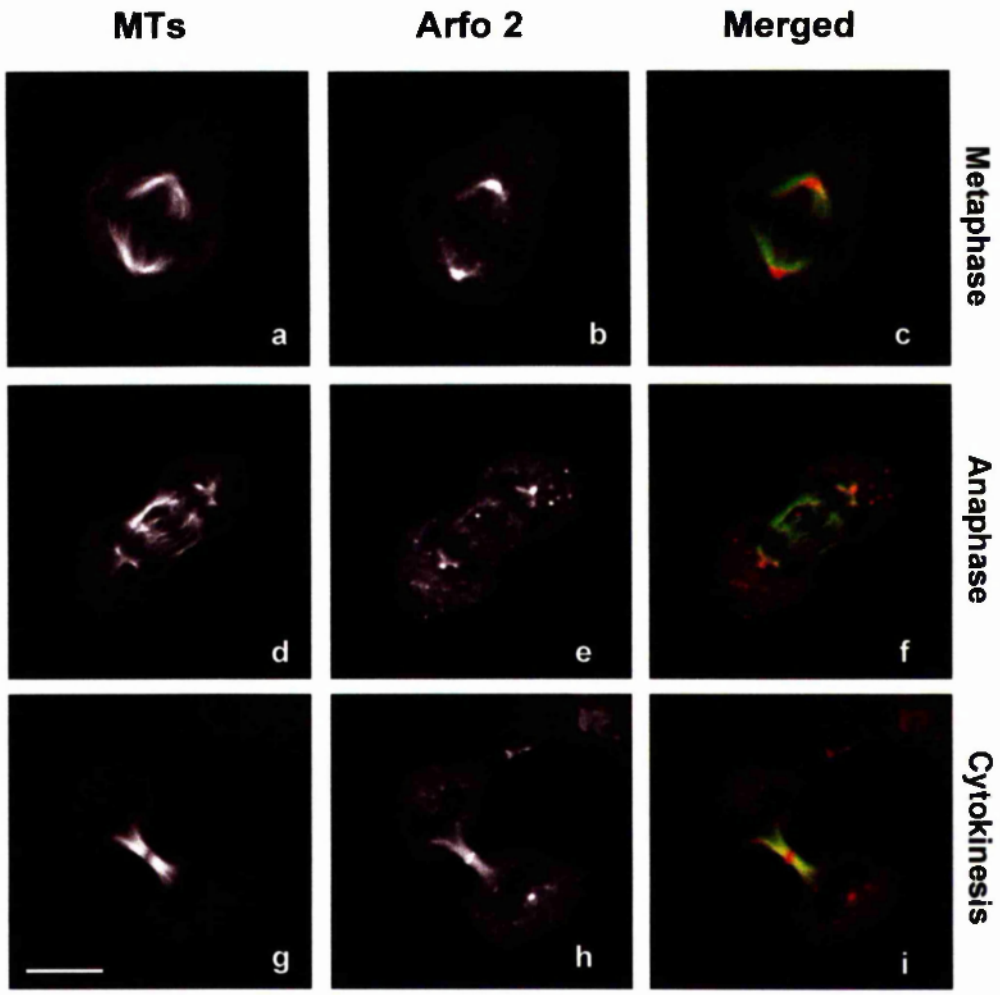

Figure 4.3.8 **Distribution of Arfophilin-2 in mitotic HeLa cells.**

Asynchronous Hela cells (30-50% confluent) grown on coverslips were fixed and processed for immunofluorescence using the affinity purified Arfophilin-2 antibodies (Arfo 2; centre panels and RED in the merged images) in conjunction with an α-tubulin antibody to stain microtubules (MTs; left hand panels and GREEN in the merged images). Representative images of cells in metaphase (panels a-c), anaphase (panels d-f) and late telophase/cytokinesis (panels g-i) are shown. Scale bar, 10 μm.

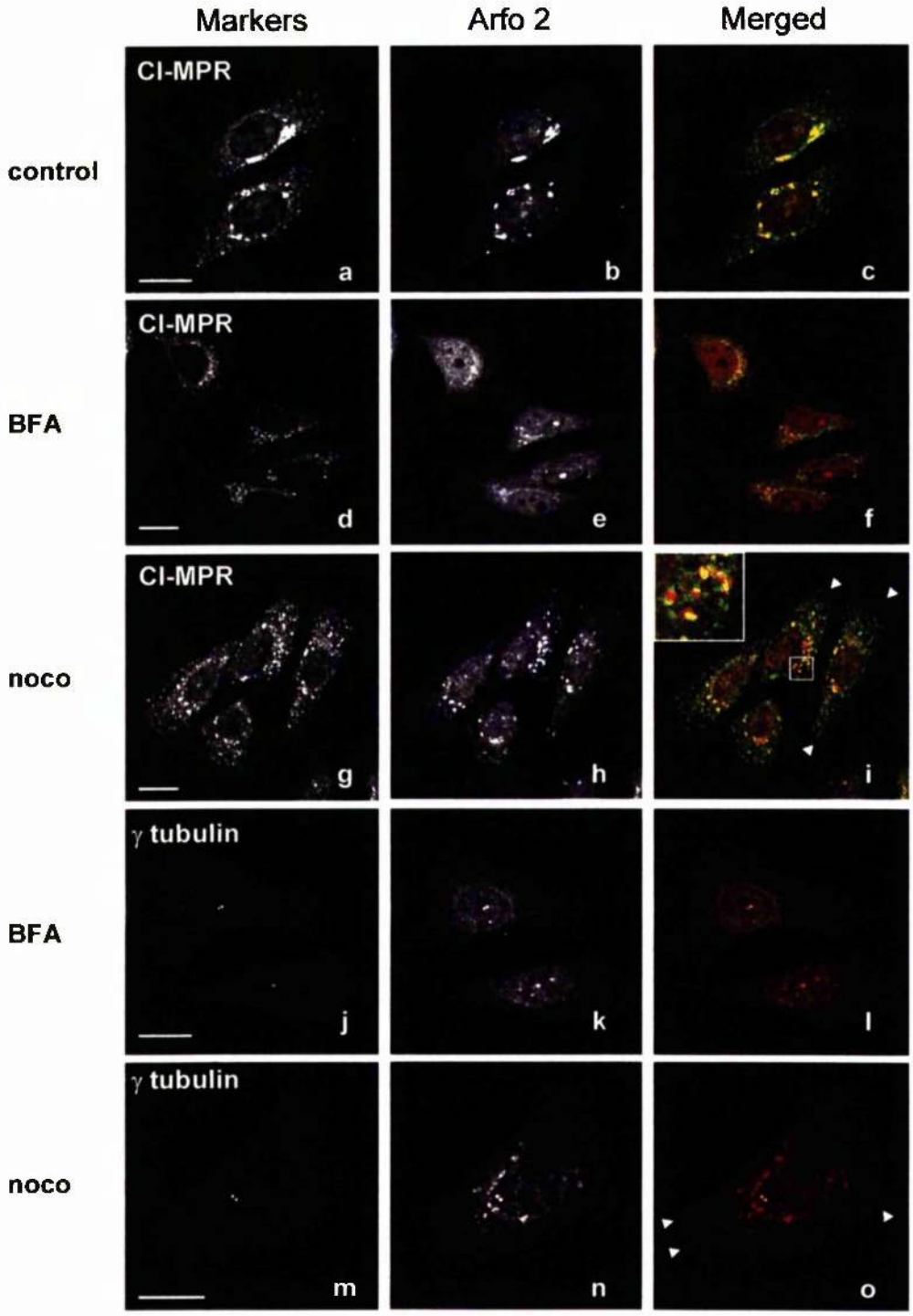

Fig. 4.3.9 **The effects of drug treatment on endogenous Arfophilin-2 localisation**

HeLa cells grown on glass coverslips were incubated in serum free media for 2 h and then treated with DMSO (control, 1 h, panels a-c), brefeldin A (BFA; 20 µg/ml for 10 min, panels d-f and j-l) or nocodazole (noco; 50 ng/ml for 1 h, panels g-i and m-o). The cells were washed in PBS, fixed in methanol and processed for immunofluorescence using the purified sheep anti-Arfophilin-2 antibody (Arfo 2; 1:200) in conjunction with antibodies against CI-MPR (a-i), or γ tubulin (j-o). Alexa^{594}-anti-sheep and Alexa^{488}-anti-rabbit/mouse secondary antibodies were then used. Shown are representative confocal images obtained. The inset in I represents a magnification of the boxed region. The arrowheads in panels i and o point to peripheral Arfophilin-2 staining. Scale bars, 10 µm.

4.3.10 Biochemical analysis of Arfophilin-2 in HeLa cells.

The distribution of endogenous Arfophilin-2 in HeLa cells was also determined using biochemical fractionation approaches. In one approach, crude subcellular fractionations were performed to isolate low-(P1) and high-(P2) speed pellets and soluble proteins (S) and these were then subjected to immunoblot analysis using a variety of antibodies to cellular markers as well as the Arfophilin-2 antibody. The results of these experiments can be seen in Fig. 4.3.10.1. The P1 fraction contains the majority of Arf6 and the Na/K ATPase, suggesting that the plasma membrane is enriched in this fraction. The majority of GRASP65 and GGA1 were also present in the low speed pellet suggesting that a large proportion of the Golgi may also be in this fraction. By contrast, Arfophilin-2 was predominantly found in the high-speed P2 pellet with lower amounts in the cytosolic S fraction and a small amount in the P1 pellet. Syntaxin 6, a t-SNARE implicated in TGN/endosomal traffic; RME-1, a regulator of the recycling endosomes; cellubrevin/VAMP3, an endosomal v-SNARE; and γ-tubulin, were all similarly more abundant in this Arfophilin-2-enriched high-speed fraction. The transferrin receptor was present in roughly equal amounts in both membrane fractions consistent with its recycling through the endosomal system to and from the plasma membrane. Collectively these data show that Arfophilin-2 exists in both cytosolic and membrane-associated pools, and suggest that the latter predominantly resides in a compartment distinct from the plasma membrane and Golgi, but enriched in endosomal markers. Furthermore, since the early endosomal markers EEA1 and Rab5 appeared more abundant in the P1 fraction, it is likely that the majority of membrane-associated Arfophilin-2 is in a later subcompartment(s) of the endocytic system. These experiments were repeated using cells that had been treated with wortmannin and with cells that had been permeabilised and incubated with GTPγS, but neither of these conditions appeared to affect the subcellular distribution of Arfophilin-2 (data not shown).

Another approach was to take a post-nuclear HeLa cell homogenate and to separate it on a 0.6 M to 1.8 M linear sucrose density gradient. Fractions recovered from such separation were then analysed by immuno-blotting for different cellular markers and for Arfophilin-2. This also revealed a cytosolic pool of Arfophilin-2 present in fraction 1 at the top of the gradient (Fig 4.3.10.2), and the membrane-associated pool was also found near the top of the gradient in fractions 2 and 3 consistent with the previous experiments. The Na/K ATPase plasma membrane marker was enriched in fractions 5 and 6 as these membranes are denser. EEA1, RME-1, γ-tubulin, βCOP, CI-MPR and syntaxin 12 all seemed fairly

enriched in the lower density membranes nearer the top of the gradient. Of these, only syntaxin 12 appeared to have a similar distribution to Arfophilin-2.

Interestingly, there are 2 distinct proteins cross-reacting with the GGA1 antibody and these can be separated on the sucrose gradient with one peak at the top and the other in denser fractions more like those of the plasma membrane. The two species also migrate differently on gels. It would be interesting to know what they represent as no real differences between the GGAs have thus far been reported. They could potentially be products of different GGA genes, or they could be distinct GGA1 splice variants or they could have undergone different post-translational modification.

Considering the immunofluorescence data and the biochemical fractionation data as a whole, Arfophilin-2 in HeLa cells resides in cytosolic and membrane-associated pools in the vicinity of the *trans*-Golgi network and also at the centrosome.

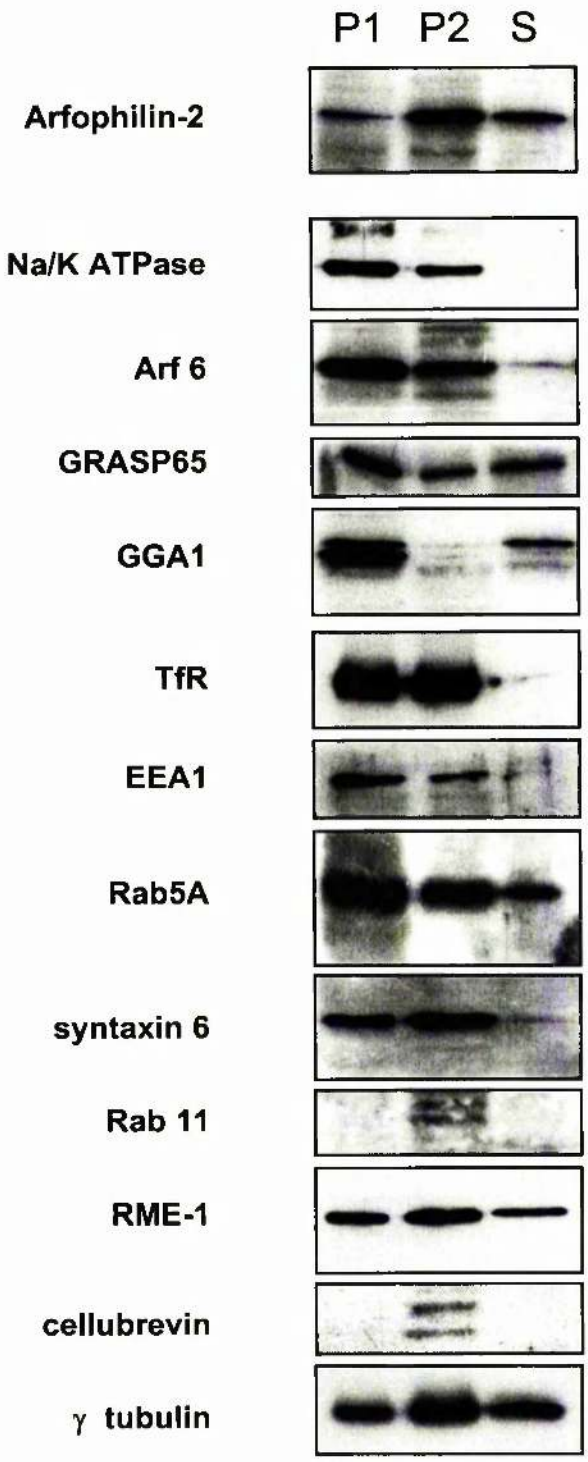

Fig.4.3.10.1 **Immunoblot analysis of HeLa subcellular fractions.**

HeLa cells grown in 10 cm dishes were scraped into HES buffer and homogenised as described in section 4.2.7. The cell homogenate was then subjected to centrifugation at **18,000** g for **20** min to produce the P1 pellet. The supernatant was further centrifuged at 100,000 x g for 1 h to yield a P2 pellet and a cytosolic (S) fraction. The P1 and P2 pellets were resuspended in buffer and 20 µg protein per lane of each fraction were resolved on 8-15% SDS-PAGE gels, as appropriate. The proteins were transferred to nitrocellulose and immunoblotted with the antibodies indicated on the left, according to the methods outlined in section 2.2.4.

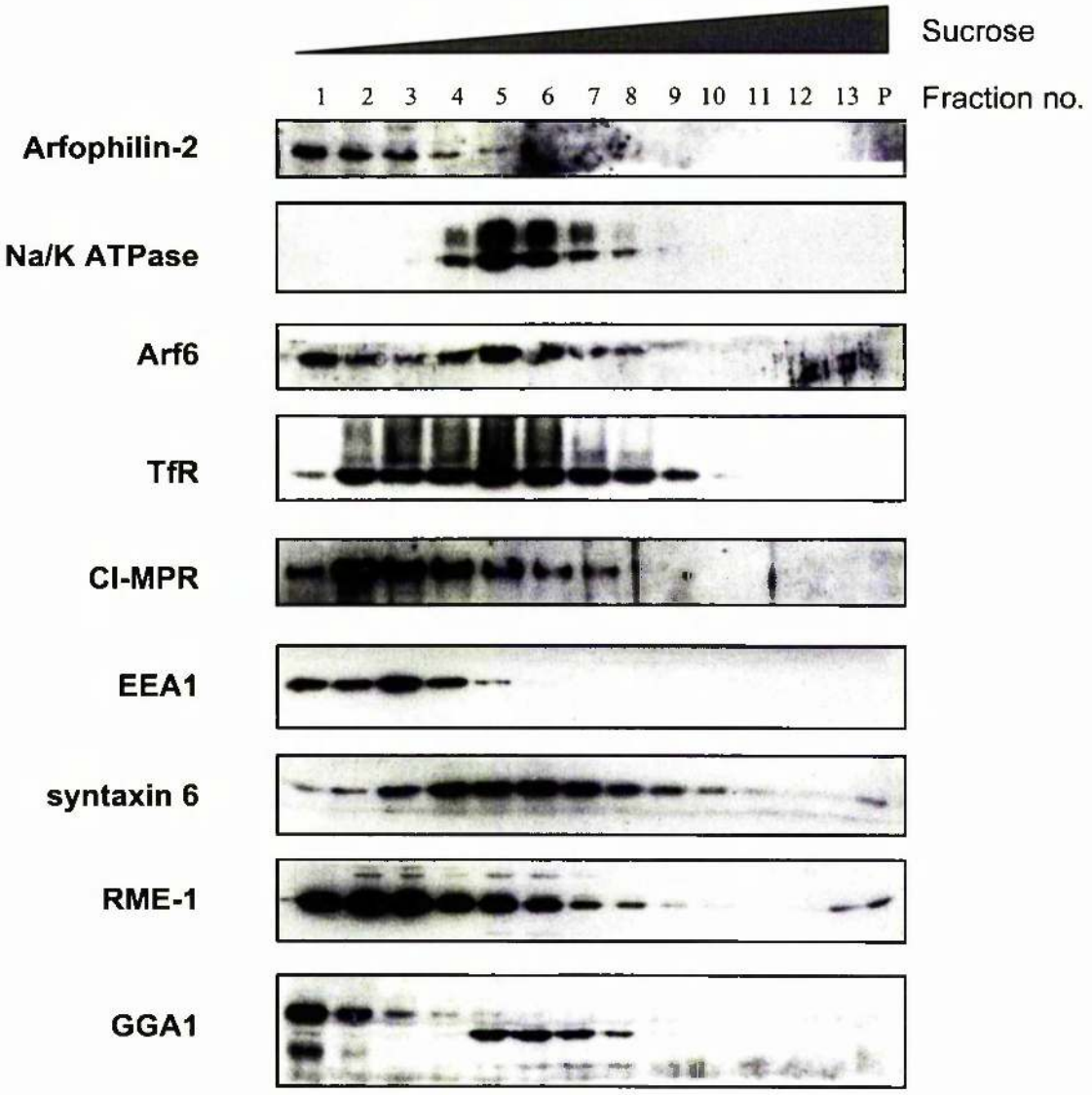

Fig.4.3.10.1 **Immunoblot analysis of HeLa proteins separated on a linear sucrose density gradient.**

HeLa cells grown in 10 cm dishes were scraped into HES buffer and homogenised as described in section 4.2.8. The cell homogenate was then applied to a 0.6 M to 1.8 M linear sucrose density gradient and spun at 33,000 rpm for 6 h in a Beckman SW-40 rotor. 1 ml fractions were taken from the top of the gradient (starting with fraction 1) and equal volumes of the fractions (20 µl) were subjected to SDS-PAGE on 8-15% polyacrylamide gels, as appropriate. The proteins were transferred to nitrocellulose and immunoblotted with antibodies against the proteins indicated on the left, all according to the methods outlined in section 2.2.4.

4.4 Discussion

The results presented in this chapter have described the molecular cloning and initial characterisation of human Arfophilin-2, following its identification in the previous chapter.

By analysing and comparing the sequences of the genomic region, ESTs and the cDNAs recovered in the Arf5 yeast two-hybrid screen, it has become apparent that the Arfophilin-2 gene is moderately large (about 200 kilobases) and encodes multiple splice variants. Whether the predicted Arfophilin-2A, -2B and -2C mRNAs actually produce distinct proteins is yet to be determined. Potentially, they could differ only in their 5' UTRs, or they could result in distinct protein products. It is important to remember that only Arfophilin-2A was amplified in its entirety and that the assembled Arfophilin-2B and -2C constructs may not exist *in vivo*. For example, these 5' ends may only exist if the 10^{th} from last exon is spliced out. On the other hand, the two exons found in the T20 yeast two-hybrid clone that were absent in other amplified cDNAs clearly indicate that alternative splicing resulting in distinct protein products does indeed occur. One of these exons encodes the amino acid sequence EE[H/Q]FEDYGEG present in both Arfophilins 1 and 2, and this could be an interesting regulatory motif. From the Nix analysis, it seems likely that there is a promoter around the CpG island (in addition to one further upstream), although numerous attempts at RACE cloning the 5' UTR of such a species have so far failed. If there are two promoters driving the expression of the Arfophilin-2 gene, it would be interesting to see whether they are differentially regulated, for example in different tissues or at different stages of the cell cycle.

The BLAST searches against the non-human EST databases revealed that there are many ESTs that are almost identical to the 3' end of Arfophilin-1 but not Arfophilin-2, and that there are also some that are virtually identical to the 5' end of Arfophilin-2A, but not Arfophilin-1. This either suggests that both genes may be present in some of these species, or that there are single genes having 5' ends more like Arfophilin-2 and 3' ends more like Arfophilin-1. BLAST analysis also revealed that there are no significantly homologous genes in the *Saccharomyces cerevisiae* genome. This implies that the Arfophilins have evolved more recently and hence are more likely to participate in specialised cellular events in metazoans, unless of course there are functional homologues that cannot be identified on the basis of sequence analysis alone. It is of note that yeast lack Class II Arf isoforms, and indeed homologues of several other proteins important in membrane trafficking in metazoans such as RME-1. The 70 amino acid conserved protein domain

(PD031147) at the C-termini of the Arfophilins and Nuf presumably serves an important function for it to have been conserved through evolution. Interestingly, it contains a motif SLAxEL (where x is any amino acid) that is present in all species examined that could perhaps be a serine phosphorylation site. All of the proteins also appear to have coiled-coil structures in and around this region. Coiled-coils are often present at sites of protein-protein interaction, for example in the formation of SNARE complexes during membrane fusion (see section 1.1.7).

The proximity of the Arfophilin-2 gene to the neurofibromatosis type 1 (*NF1*) gene is interesting. *NF1* encodes a putative Ras GEF and has an unusually high mutation rate (3 x 10^{-5} to 1 x 10^{-4}, Vogel and Motulsky, 1997), which is why neurofibromatosis type 1 is one of the most common autosomal dominant conditions. A subset of patients actually have a complete gene deletion resulting in a very severe phenotype including dysmorphism, mental retardation and the early onset of a large number of neurofibromas (see Riva et al., 2000 and references therein). Fluorescent *in situ* hybridisation analysis of some such patients has revealed that, centromerically from the *NF1* gene, there is a common deletion breakpoint but that telomerically, the position of the break is variable (Riva et al., 2000). These latter breaks would affect, to varying degrees, the Arfophilin-2 gene, whose existence is unknown to researchers in the neurofibromatosis field and which may aid in explaining the lack of a genotype-phenotype correlation in the condition. It could be potentially useful to study these patients with respect to Arfophilin-2, although interpreting which effects are due to the disruption of which of the two genes may be problematic.

During the latter stages of the work presented in this thesis, two mRNA sequences corresponding to that of Arfophilin-2 appeared in the GenBank and HUGE databases. They had come from large-scale cDNA sequencing projects and encoded the protein designated as KIAA1821 (accession numbers AB058724 and XM_050101). This protein is identical to the predicted Arfophilins-2B and -2C except in the first 27 amino acids. The extreme 5' end of the KIAA1821 cDNA sequence encoding these amino acids does not appear to align with the genomic sequence in BLAST analysis and is, therefore, questionable. In addition, it is unlikely that the full ORF is present as there is no apparent 5'UTR containing in-frame stop codons. If the complete ORF is present, however, it would encode a protein identical to that of Arfophilin-2A. The sequences also differ in that they have a 3'UTR of ~5 kb, much larger than the ones present in testis. Semi-quantitative RT-PCR performed at the kazusa sequencing project using primers within the 3'UTR revealed the highest expression in brain, the tissue from which it was cloned with no expression apparent in testis (see http://www.kazusa.or.jp/huge/gfpage/KIAA1821/). The northern

analysis performed here is more informative as it uses a probe to the coding sequence and not to the variable UTR. It seems likely that the large transcripts apparent on the northern blot in brain, heart and skeletal muscle are due to similarly large 3' UTRs. These have been linked to decreased mRNA stability particularly if AU-rich elements are present and this may influence the protein levels accordingly in these tissues (reviewed in Guhaniyogi and Brewer, 2001).

The significance of the apparent overexpression of Arfophilin-2 mRNAs (and Arfophilin-1) in testes is not presently known. It will be interesting to determine whether this is due to a unique testis-specific function or whether this is a reflection of the high degree of mitotic and meiotic cell division occurring in testes compared to the other tissues examined which are terminally differentiated. The notion of a role in cell division is attractive given the homology with Nuf and also given the localisation of Arfophilin-2 at the spindle poles and the midbody in dividing cells. This, however, will be discussed in greater depth in the next chapter. Whether Arfophilin protein levels are actually different between tissues has not been addressed. From immunoblot analysis, similar levels of Arfophilin-2 appear to be present in testis and in HeLa cells with markedly lower amounts in HEK 293 cells. HeLa cells are derived from a carcinoma, and consistent with elevated expression, an Arfophilin-1 EST (xs176) has been reported to be overexpressed during the development of pancreatic cancer (Gress et al., 1996).

The Arfophilin-2 polyclonal antibody characterised in this chapter is a powerful tool for future studies of Arfophilin-2. It has proved to be a good reagent for immuno-blotting and immunofluorescence and also to be capable of immunoprecipitating the native protein from cell lysates. Importantly, it has shown that heterologously expressed Arfophilin-2A migrates exactly as the native protein in testis, HeLa, HEK 293 cells indicting that the full open reading frame has been cloned. By separating HeLa cell homogenates by centrifugation, it has also been possible to see that native Arfophilin-2 is both cytosolic and associated with intracellular membranes devoid of plasma membrane markers.

Indirect immunofluorescence microscopy has also provided much information regarding the subcellular distribution of Arfophilin-2. In particular, a major brefeldin A-sensitive pool has been localised to the TGN region of the cell. This localisation would be consistent with a role for Arfophilin-2 in Arf5-mediated events. However, minor but specific staining was also observed at the centrosome and in peripheral structures such as focal adhesions or actin-rich protrusions. Plasma membrane localisation would be more in keeping with a role in Arf6 signalling, since this is where the activated Arf6 resides (D'Souza-Schorey et al.,

1995; Cavenagh et al., 1996; see also section 1.3.5). Given that Exton's group has shown Arfophilin-1 binding to both of these Arf isoforms (Shin et al., 1999, 2001), it is tempting to speculate that, depending on the cellular context, the Arfophilins could be dual class II and class III effectors. Arf5 appears to require the N-terminal alpha helix for the interaction with Arfophilin-1 (Shin et al., 1999) while Arf6 seems to bind independently of the N-terminus via a more central region (Shin et al., 2001). This implies that there are two distinct binding sites in the Arfophilin-1 C-terminal 144 residues, and it is conceivable that each interaction could mediate distinct downstream events. Indeed, the Arfophilins may function as linkers between Arf5 and Arf6, rather like the proposed role for Arfaptin 2/POR1 in Arf6 and Rac signalling (refer to sections 1.3.4.5 and 1.3.7). It would be interesting to see whether Arf5 and Arf6 binding is mutually exclusive, and also whether the two Arfophilins exhibit any preferences for the two Arf isoforms.

The centrosomal pool of Arfophilin-2 needs further characterisation. There are well-documented methods for purifying centrosomes (Blomberg-Wirschell and Doxsey, 1998; Mitchison and Kirschner, 1986) and these should be employed to confirm that Arfophilin-2 is indeed associated with these organelles.

It will be extremely interesting in future work to discover whether Arfophilin-1 exhibits any similarities or differences compared to Arfophilin-2. Once the antiserum is affinity purified, similar experiments can be performed to see in which cells it is produced, where it is localised, and also to test whether the predicted open-reading frame encodes a protein that migrates the same as native protein(s) on SDS-PAGE gels. Furthermore, since we raised antibodies in different species, it should be possible to examine the distributions of both Arfophilins relative to each other in the same cells by immunofluorescence. Hopefully both reagents will be useful for other applications such as microinjection, immunogold electron microscopy and immunocytochemistry. Antibody injection is a potential way of perturbing Arfophilin function in live cells and is one avenue worth exploring. Similarly, immunogold electron microscopy would allow much higher resolution images to be taken and this could help further pinpoint Arfophilin localisation.

Although, Arfophilin-2 was identified by virtue of its selective interaction with Arf5Q71L in the yeast-two hybrid system, this interaction has not yet been confirmed biochemically. Initial attempts were hampered by the fact that *E. coli* would not produce GST-Arfophilin-2 from a pGEX-5X vector or His-tagged Arfophilin-2 from a pQE vector. In both cases translation appeared to stop prematurely resulting in a ladder of protein when run on SDS-PAGE gels. Many different growth conditions and *E. coli* strains were tried to no avail.

Several approaches were attempted unsuccessfully, including GST pulldowns and co-immunoprecipitations (see Table 4.4.1 below).

beads	protein produced in?	interacting protein?	produced in?	detected using?
GSH-GST-Arf5Q71L	*E. coli*	HA-Arfophilin-2	HeLa or CHO cells	anti-HA
GSH-GST-Arfo2 (330)	*E. coli*	Arf5Q71LHA	CHO cells	anti-HA
GSH-GST-Arfo2 (152)	*E. coli*	Arf5Q71LHA	CHO cells	anti-HA
GSH-GST-Arf5Q71L	*E. coli*	His-Arfo2(330)	*E. coli*	anti-His
His-Arfo2(330)	*E. coli*	GSH-GST-Arf5Q71L	*E. coli*	anti-GST
Protein G-sepharose-anti-HA-Arf5Q71LHA	HeLa cells	Arfo2 (endogenous)	HeLa cells	anti-Arfo2
Protein G-sepharose-anti-Arfo2-Arfo2	HeLa cells (endogenous)	Arf5Q71LHA	HeLa cells	anti-HA
Protein G-sepharose-anti-Arfo2-Arfo2	CHO cells	Arf6 (endogenous)	CHO cells	anti-Arf6

Table 4.4.1 **Summary of Arf/Arfophilin-2 biochemical interaction assays attempted.**

Various pulldown/co-immunoprecipitation approaches were employed unsuccessfully to try to confirm the Arf5/Arf6 interaction with Arfophilin-2, using both native and recombinant proteins. Numbers in brackets refer to the number of C-terminal amino acids used in truncated forms of Arfophilin-2. * GTPγS was included in these experiments to try to 'lock' the endogenous Arf in the active GTP-bound conformation. Following 1 h incubations at 4°C, the beads were washed and associated proteins were removed by boiling in SDS-PAGE sample buffer. Samples were then processed for immunoblotting using the antibodies indicated in the right hand column.

Bacterially expressed Arfophilin-2 may be lacking important post-translational modifications necessary for the interaction, or the proteins may be incorrectly folded. It would be useful to repeat the Exton lab procedure, whereby GST-tagged Arfophilin was produced in CHO cells (Shin et al., 1999). Otherwise, other eukaryotic systems such as baculovirus expression or *in vitro* translation using a reticulocyte lysate system could prove fruitful. Also potentially problematic is the fact that the Arfophilin-2 antiserum was raised against the portion containing the Arf-binding domain. This may hamper co-immunoprecipitation experiments. Similarly, while a GAL4 DNA-binding domain fusion at the N-terminus of Arf5 may permit an interaction in the yeast two-hybrid system, an N-terminal GST-tag may not allow the interaction in pulldown assays. Despite the lack of data from these important experiments, it seems highly likely that Arfophilin-2 is a true Arf binding protein given that Arfophilin-1 has been shown to be (Shin et al., 1999, 2001) and given that they are 63% identical (and 79% conserved) in their C-terminal Arf-binding domains.

In summary, chapter 4 has shown that Arfophilin-2 is an endogenous cytosolic and membrane-associated protein in HeLa cells. It exhibits the same electrophoretic mobility as the cloned Arfophilin-2A and, by immunofluorescence microscopy, it localises around the trans-Golgi network and the centrosome in this cell line. HeLa cells represent a good model system to study, as they are likely to express the appropriate cellular machinery required for Arfophilin-2 function.

The next step is to try to elucidate what the function of Arfophilin-2 might be. One approach to address this is to construct chimeric proteins whereby full-length and truncated forms of Arfophilin-2 are fused to GFP, and to express them in cells and monitor their behaviour. This type of experiment is described in the following chapter.

Chapter 5

Functional characterisation of Arfophilin-2

5.1 Introduction

As described in chapter 3, a yeast-two hybrid screen for Arf5 effectors identified a novel protein that we named Arfophilin-2. The cloning and initial characterisation of Arfophilin-2 was then presented in chapter 4, where the native protein was examined in HeLa cells and shown to reside in cytosolic and membrane-associated pools, and to localise around the *trans*-Golgi network and the centrosome. The main aim of this chapter is to expand on these findings and to provide insight into the cellular function(s) of Arfophilin-2. One specific aim includes the generation, expression and analysis of GFP-Arfophilin-2 fusion proteins. Another aim is to pursue the finding that Arfophilins share sequence homology with nuclear fallout, a well-characterised *Drosophila* protein, and to examine whether any functional homology can be uncovered. A third aim is to investigate the relationship between Arfophilins and Arfs in a cellular context by making use of mutant forms of Arf.

5.1.1 Nuclear fallout

In addition to the observed homology with KIAA0665/Arfophilin, it was apparent that Arfophilin-2 also shared significant homology with a hypothetical *Caenorhabditis elegans* protein and *Drosophila melanogaster* nuclear fallout (Sullivan et al., 1993).

Nuclear fallout is an essential maternal-effect gene, whose product is required for cellularisation (Rothwell et al., 1998; Rothwell and Sullivan, 2000). This process is a dramatic variation of animal cell cytokinesis (Schejter and Wieschaus, 1993; Miller and Kiehart, 1995) that transforms a one-cell syncytium into a multicellular embryo by the synchronous encapsulation of approximately 6000 cortical nuclei with one continuous plasma membrane furrow. The furrow invaginates between adjacent nuclei and at right angles to the cell surface before widening along its base to seal each nucleus off from the inner cytoplasm. Furrow progression is dependent on an actomyosin-based contractile mechanism that also requires other elements such as anillin, septins and formin homology proteins (Glotzer, 2001). Golgi derived membrane secretion and syntaxin-mediated fusion with the plasma membrane are also key events, as in cytokinesis (Glotzer, 2001).

Nuclear fallout encodes a highly phosphorylated coiled-coil protein of 502 amino acids, whose subcellular localisation changes in a cell-cycle-regulated fashion (Rothwell *et al.*, 1998). During the late syncytial divisions, it is generally cytoplasmic but concentrates at the centrosomes during prophase. It is also found at the centrosomes throughout cellularisation where it is believed to load vesicles onto microtubules for transport to the

furrows (Rothwell et al., 1999). In *nuf*-mutant embryos, the recruitment of cortical actin is disrupted as is the localisation and phosphorylation of another protein required for cortical furrow formation, discontinuous actin hexagon (Dah) (Rothwell et al., 1999; Zhang et al., 2000). Interestingly, the sequence of Dah is homologous to the dystrobrevin family of proteins and the carboxyl terminal portion of the dystrophin molecule. A working model for Nuf and Dah function, as proposed by Sullivan and colleagues, the principal investigators of these proteins, is given in Fig. 5.1.1.

Later in the chapter, evidence will be provided suggesting that Arfophilins and *nuclear fallout* are functionally related, and the implications for membrane trafficking and cytokinesis will be discussed.

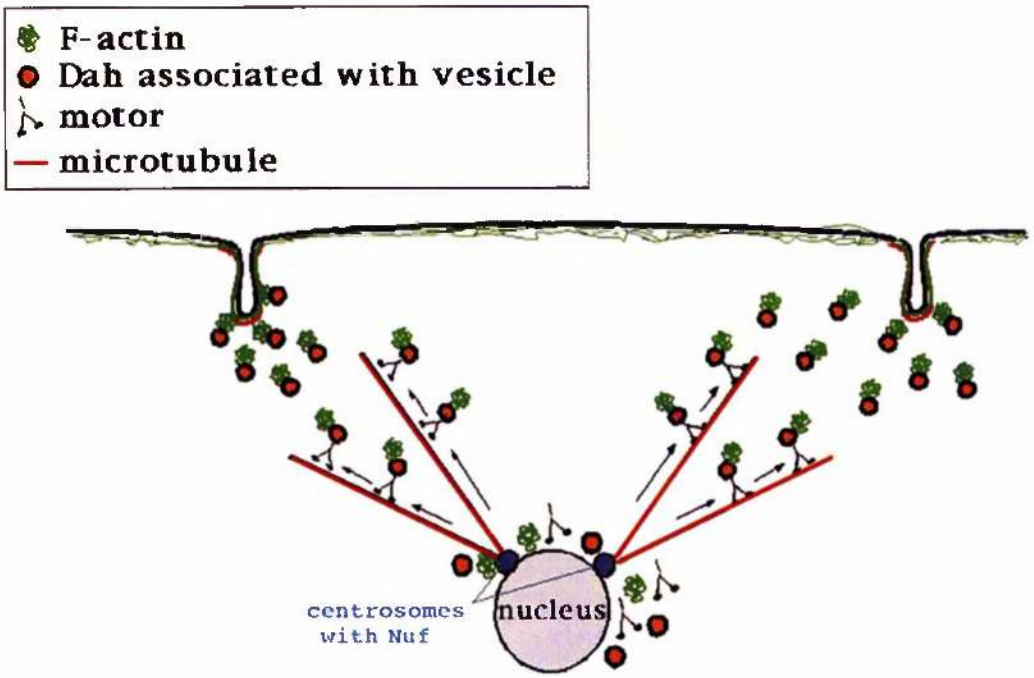

Fig. 5.1.1 **Working model proposed by Sullivan and colleagues for Nuf function in the *Drosophila* embryo.**

A model proposing that Nuf acts at the centosome to load vesicles for transport to the cortex. Side by side particles of actin and Dah are shown being transported together, as a unit. Furrow invagination may occur through vesicle fusion in a process requiring the Dah membrane-associated protein. *Reproduced from Rothwell et al., 1999.*

5.2 Materials and Methods

Arf5T31N-HA and Arf5Q71L-HA mammalian expression constructs were generous gifts from Jeremy Tavaré (University of Bristol) and the Arf6T27N-HA construct was kindly provided by Julie Donaldson (NIH, Bethesda, USA). The wild-type Arf5-FLAG mammalian expression plasmid was previously generated in this laboratory and has been described elsewhere (Campbell, 1999).

5.2.1 Generation of Arfophilin constructs for over-expression

Several Arfophilin-1 and Arfophilin-2 mammalian expression constructs were generated (see Fig. 5.2.1 for a diagrammatic overview, and the appendix for plasmid maps). The plasmid T20 pACT2 (see the appendix) recovered in the yeast two hybrid screen had three *Bgl II* restriction sites, one just between the GAL4 activation domain and the HA tag, an internal one in the Arfophilin-2 ORF 990 bases from the stop codon, and one immediately after the Arfophilin-2 3'UTR. This plasmid was, therefore, partially digested for 20 min with *Bgl II* and the DNA fragments were separated by agarose gel electrophoresis as described in section 2.2.1. This allowed the isolation of a partially digested fragment in which the internal *Bgl II* site was uncut. This was gel extracted and ligated into the *BamH1* site of pCDNA3.1mycHis (Invitrogen) and the *Bgl II* site of pEGFPC2 (Clontech), giving rise to construct A (Arfo-2_{T20} pCDNA3) and construct B (Arfo-2_{T20} pEGFPC2), respectively. The cut vectors were treated with calf intestinal alkaline phosphatase (Promega) and gel purified prior to ligation and all procedures were according to the general molecular biology protocols described in section 2.2.1. The presence and correct orientation of the inserts were verified by further restriction digestion (not shown). The HA epitope excised from the pACT2 vector contained an ATG initiation codon and immunoblot analysis using an antibody to the HA tag revealed that both proteins were efficiently translated in transfected HeLa cells (not shown). For the production of construct C in Fig. 5.2.1 (Arfo-2_{330} pEGFPC2), plasmid T20 pACT2 was digested to completion with *Bgl II* and the resulting ~1.3 kb band (representing the 3' kilobase of the ORF and the 3'UTR of Arfophilin-2) was gel purified and also ligated into the *Bgl II* site of pEGFPC2. Again the presence and correct orientation of the insert was verified by further restriction digestion. The analogous Arfophilin-1 construct (D in Fig. 5.2.1; Arfo-1_{330} pEGFPC2) was obtained by PCR and subsequent subcloning into pEGFPC2. Briefly, the 3' 1 kb of the Arfophilin-1 ORF was amplified using *Pfu* polymerase and primers `5'-ggatccGGCTCTCCAGCAAGAAGGTGGCAAGG-3'` (*BamH1* site in small) and `5'-gtcgacGACCTT`

CCTGCCT**CTA**CTTGACCTCCA-3' (*Sal I* site in small, stop codon in bold) from KIAA0665 clone (in pBluescript SK^+, obtained from Dr. Ohara, Kazusa sequencing project, Japan). This was then treated with *Taq* polymerase to add A base overhangs, TA cloned into pCRII-TOPO as described in sections 2.2.1.5 and 2.2.1.6, and sequenced to ensure no mutations were present. This plasmid was then digested with *BamH1* and *Sal I* and the released fragment was gel purified and ligated into the *Bgl II* and *Sal I* sites of pEGFPC2.

Constructs I, J and K in Fig. 5.2.1 (untagged Arfophilin-2A, -2B and -2C, respectively) were described in section 4.2.4. To generate constructs E, G and H in Fig. 5.2.1 (encoding eGFP fused to the N-termini of Arfophilin-2A, -2B and -2C, respectively), the Arfophilin-2 (putative) ORFs were excised from constructs I, J and K by digestion with *EcoR1* and *Sal I*. These were then gel purified and ligated into the *EcoR1* and *Sal I* sites of pEGFPC2

5.2.2 Generation of GFP-Nuf mammalian expression construct

A Nuf cDNA (kindly provided by Dr. W. Sullivan, UCSC, Santa Cruz, USA) was used as template in a PCR reaction using the EXPAND kit (see section 2.2.1.1) and primers 5'-ggatccGC**ATG**GCACCAATGCCCCGAATTCAGTTAC-3' (*BamHI* site in small letters, ATG in bold) and 5'-gtcgac**CTA**CTTTCGCTCCATGGGCTTGACTTCCAG-3' (*Sal I* site in small letters, stop codon in bold). The resulting ~1.5 kb product was TA cloned into pCRII-TOPO according to the methods described in section 2.2.1.6 and sequenced to ensure no mutations had been introduced during amplification. The Nuf ORF was then excised from the pCRII vector by restriction digestion with *BamHI* and *Sal I* and then subcloned into the *Bgl II* and *Sal I* sites of pEGFPC2 (see appendix).

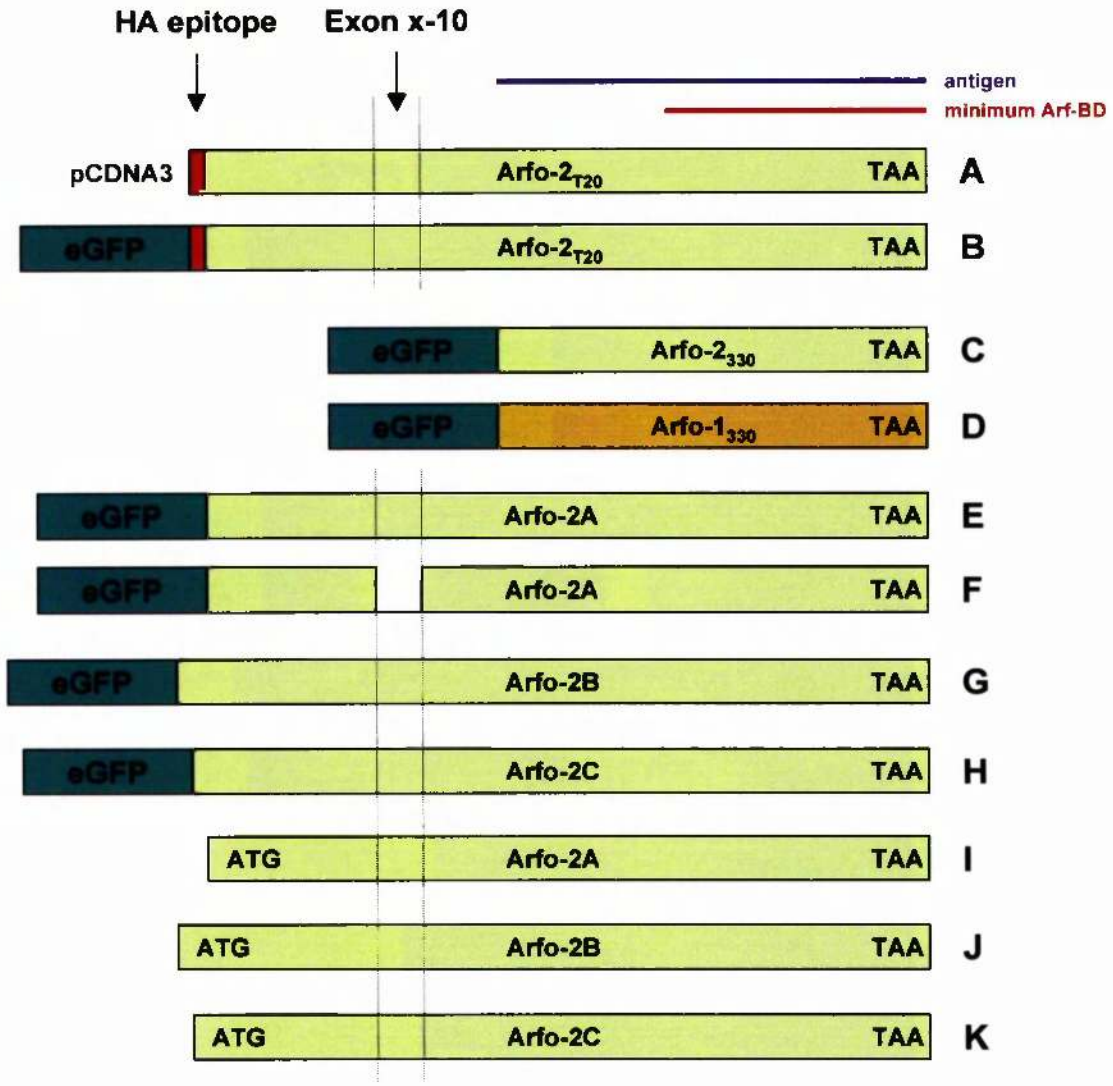

Fig. 5.2.1 **Diagrammatic overview of Arfophilin mammalian expression constructs**

Shown are protein products encoded by constructs A-K. Construct A was in vector pCDNA3.1 while constructs B-K were in pEGFP-N or -C vectors (see text for more details). eGFP in dark green corresponds to enhanced green fluorescent protein. Arfo-2_{T20} (constructs A and B) represents the longest clone recovered in the yeast two-hybrid screen, directly subcloned including HA epitope tag (in red). C and D represent the C-terminal 330 amino acids of Arfophilin-2 and Arfophilin-1, respectively, fused to the C-terminus of eGFP. Construct F represents Arfophilin-2A lacking the 10th from last exon. E, G & H represent full-length Arfophilins-2A/-2B/-2C, respectively, fused to the C-terminus of eGFP (described in section 4.2.4). I, J & K are full-length untagged Arfophilin-2A/-2B & -2C constructs, respectively. The approximate positions and sizes of the minimal Arf-binding domain (Arf-BD) and the portion of Arfophilin-2 used for antibody production are given at the top of the diagram.

5.2.3 Generation of GFP-Arfophilin-2 stable cell lines

Sparsely populated (~10-15% confluency) HeLa, HEK 293 and CHO cells growing in 10 cm dishes (three each) were transfected with Arfo-2330 pEGFPC2 (encoding the C-terminal 330 amino acids of Arfophilin-2 fused to the C-terminus of enhanced GFP; construct C in Fig. 5.2.1) according to the Lipofectamine method described in section 2.2.2.4. Nineteen hours post-transfection the media were replaced with the appropriate complete growth media (containing 10% foetal calf serum, see section 2.2.2.1 for precise compositions) to which sterile-filtered G418 sulphate (Sigma) had been added to a final concentration of 600 µg/ml. These G418-containing complete growth media were used for all subsequent culture of these cells and the media were replaced every 2-3 days. Cells were grown at 37°C in a humidified atmosphere containing 5% CO_2, as with the wild type cells. After 1 to 2 weeks, the G418-resistant cells from each cell type were trypsinised (see section 2.2.2.2), pooled, spun at 2000 x g for 3 min at room temperature, and resuspended in 20 ml complete growth media containing 600 µg/ml G418 sulphate. The cells were then serially diluted in the same media in sterile 96 well plates (Iwaki, 100 µl/well) using a multi-channel pipette. The cells were returned to the incubator and grown for a further 3-4 weeks. During this time, the cells were monitored for the presence of single colonies in the wells and for GFP fluorescence associated with those colonies using a Zeiss Axiovert fluorescence microscope. None of the HeLa transfectants exhibited any GFP fluorescence, while many CHO and HEK 293 colonies did. These were allowed to reach confluency, at which point they were trypsinised using 100 µl/well trypsin/EDTA (Gibco, Life Technologies, Paisley, UK) and transferred to 25 cm2 flasks. Once these reached near confluency, the cells were further passaged into several 75 cm2 flasks (see section 2.2.2.2). When sufficient cells had grown, several flasks of the different G418-resistant, GFP-Arfophilin-2-expressing clones were frozen down (see section 2.2.2.3), while others were maintained for subsequent experiments.

5.3 Results

5.3.1 Subcellular localisation of overexpressed GFP-Arfophilin-2 chimeras

In an attempt to shed light on the cellular role of Arfophilin-2, constructs were engineered to encode chimeric proteins fused to enhanced green fluorescent protein (GFP). Initially these were made by fusing the 3' ends of Arfophilin-2 recovered in the yeast two-hybrid screen to the 3' end of GFP in pEGFP-C vectors, but this was then extended to include full-length sequences. All of the constructs are described in section 5.2.1 and graphically represented in Fig. 5.2.1. These were then transiently transfected into HeLa and CHO cells and the resulting overexpressed proteins were monitored by laser scanning confocal microscopy. In addition to the GFP fluorescence, known cellular compartments were labelled using a panel of antibodies to different marker proteins in indirect immunofluorescence experiments similar to the ones described in chapter 5. These analyses revealed that, in both cell types, GFP-Arfophilin-2 localised to a tight peri-nuclear compartment that surrounded the centrosome marker protein γ-tubulin (HeLa cells Fig. 5.3.1.1A, panels a-c; CHO cells not shown). More strikingly, transfected cells displayed a dramatic accumulation of transferrin receptors (TfRs) and the recycling endosomal marker Rab 11 in the same peri-centriolar region, while adjacent untransfected cells exhibited much more diffuse staining for these proteins (Fig. 5.3.1.1A, panels d-i). A similar change in distribution was also observed for GGA1 (Fig. 5.3.1.1A, panels j-l). By contrast, the distributions of a variety of other proteins were unaffected by GFP-Arfophilin-2 expression. These included Golgi proteins such as GRASP 55 (Fig. 5.3.1.1A, panels m-o) and GRASP 65 (not shown), β COP coatomer protein (Fig. 5.3.1.1B, panels a-c), adaptor proteins AP-1 (γ adaptin subunit, Fig. 5.3.1.1B, panels d-f) and AP3 (δ subunit, Fig. 5.3.1.1B, panels g-i), and both isoforms of the mannose-6-phosphate receptors (Fig. 5.3.1.1B, panels j-o). Similarly early endosomal marker proteins such as Rab 4, EEA1 and the glucose transporter GLUT1 showed no apparent alterations in distribution (Fig. 5.3.1.1C, panels a-i), and nor did clathrin (Fig. 5.3.1.1C, panels j-l) or the small GTPase Rac (Fig. 5.3.1.1C, panels m-o). Other proteins involved in membrane trafficking events, such as RME1, TGN38, sortilin, PACS-1, PLD1, dynamin II, Rab5 and Rho also appeared to be unaffected, although the antibodies to some of these were poor for immunofluorescence (data not shown). Nevertheless, these data as a whole suggested that GFP-Arfophilin-2 overexpression was specifically interfering with some aspect of the recycling endosomes. All the experiments shown in Figs. 5.3.1.1A-C were performed

using constructs B or F from Fig. 5.2.1, but similar results were seen for all constructs containing the C-terminal 330 amino acids or more.

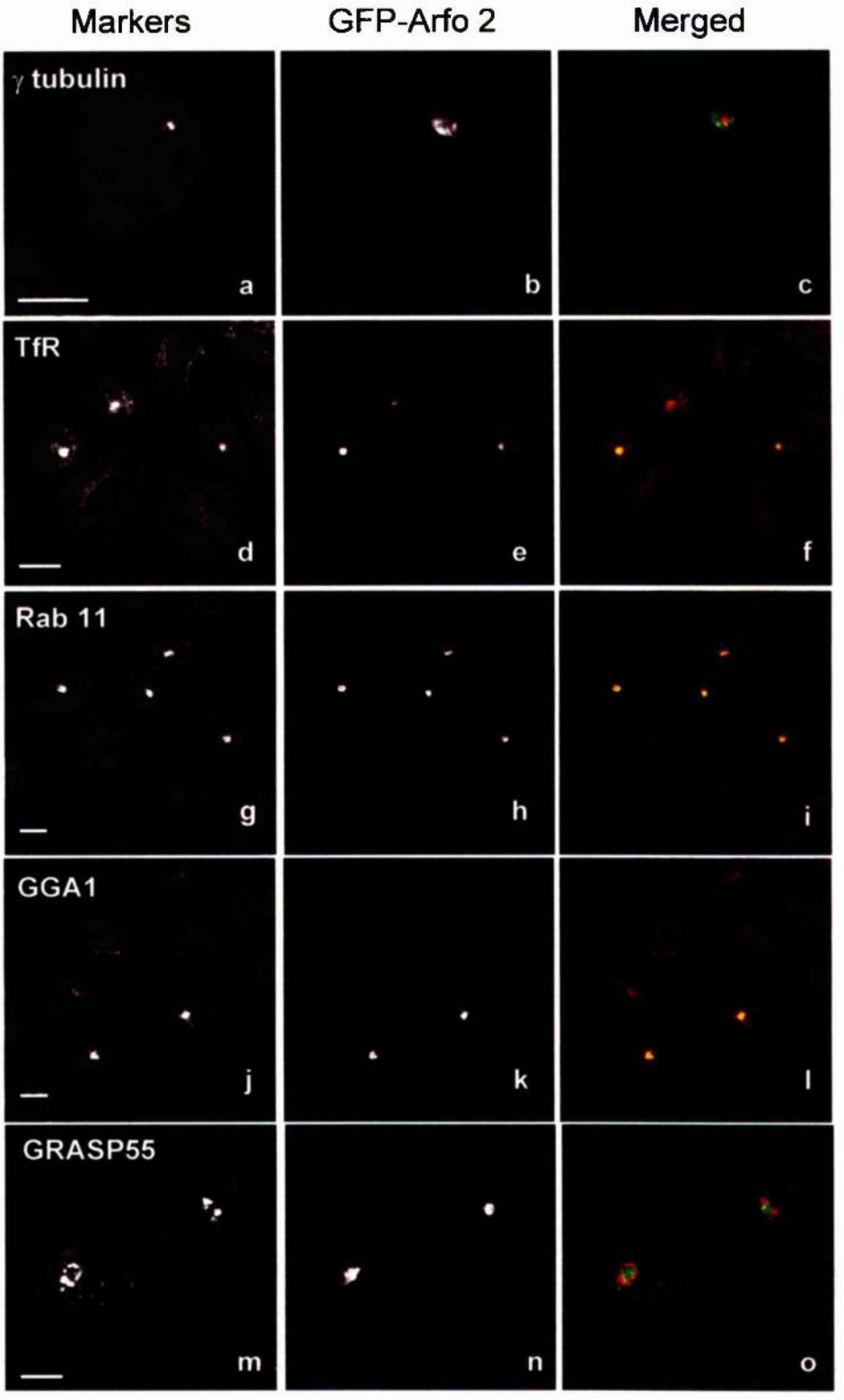

Fig. 5.3.1.1A **Localisation of GFP-Arfophilin-2 in HeLa cells.**

HeLa cells transiently expressing GFP-Arfophilin-2 (Arfo2; shown in the centre panels and GREEN in right-hand panels) were fixed in methanol 18 h after transfection and processed for immunofluorescence using primary antibodies against γ tubulin (**a-c**), TfR (**d-f**), Rab11 (**g-i**), GGA1 (**j-l**) and GRASP 55 (**m-o**). Confocal images were taken and the marker proteins are shown on the left-hand panels and RED in the merged images. Scale bars, 10 μm.

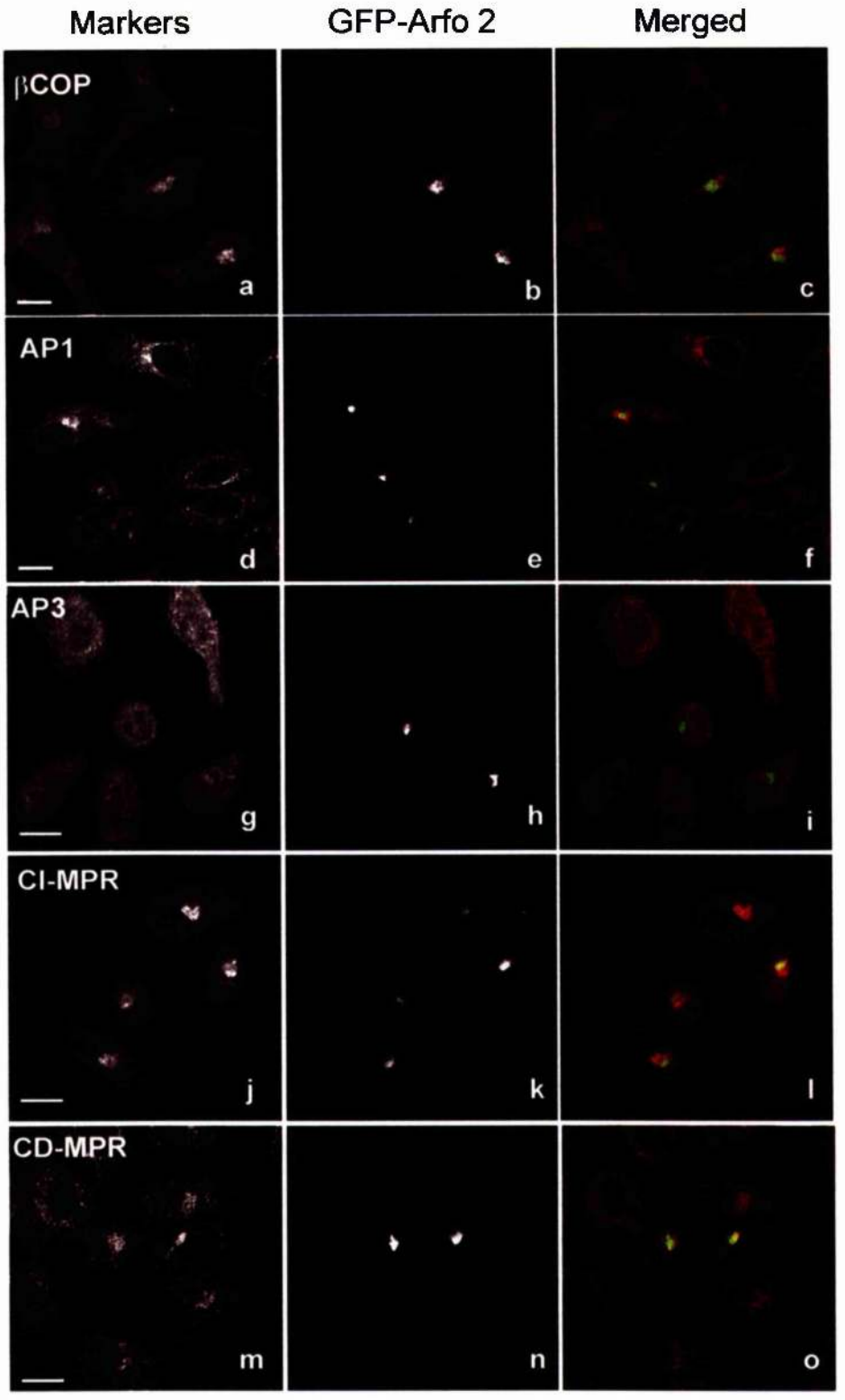

Fig. 5.3.1.1B **Localisation of GFP-Arfophilin-2 in HeLa cells.**

HeLa cells transiently expressing GFP-Arfophilin-2 (Arfo2; shown in the centre panels and GREEN in right-hand panels) were fixed in methanol 18 h after transfection and processed for immunofluorescence using primary antibodies against β COP (**a-c**), AP1 (γ adaptin; **d-f**), AP3 (δ subunit; **g-i**), CI-MPR (**j-l**) and CD-MPR (**m-o**). Confocal images were taken and the marker proteins are shown on the left-hand panels and RED in the merged images. Scale bars, 10 μm.

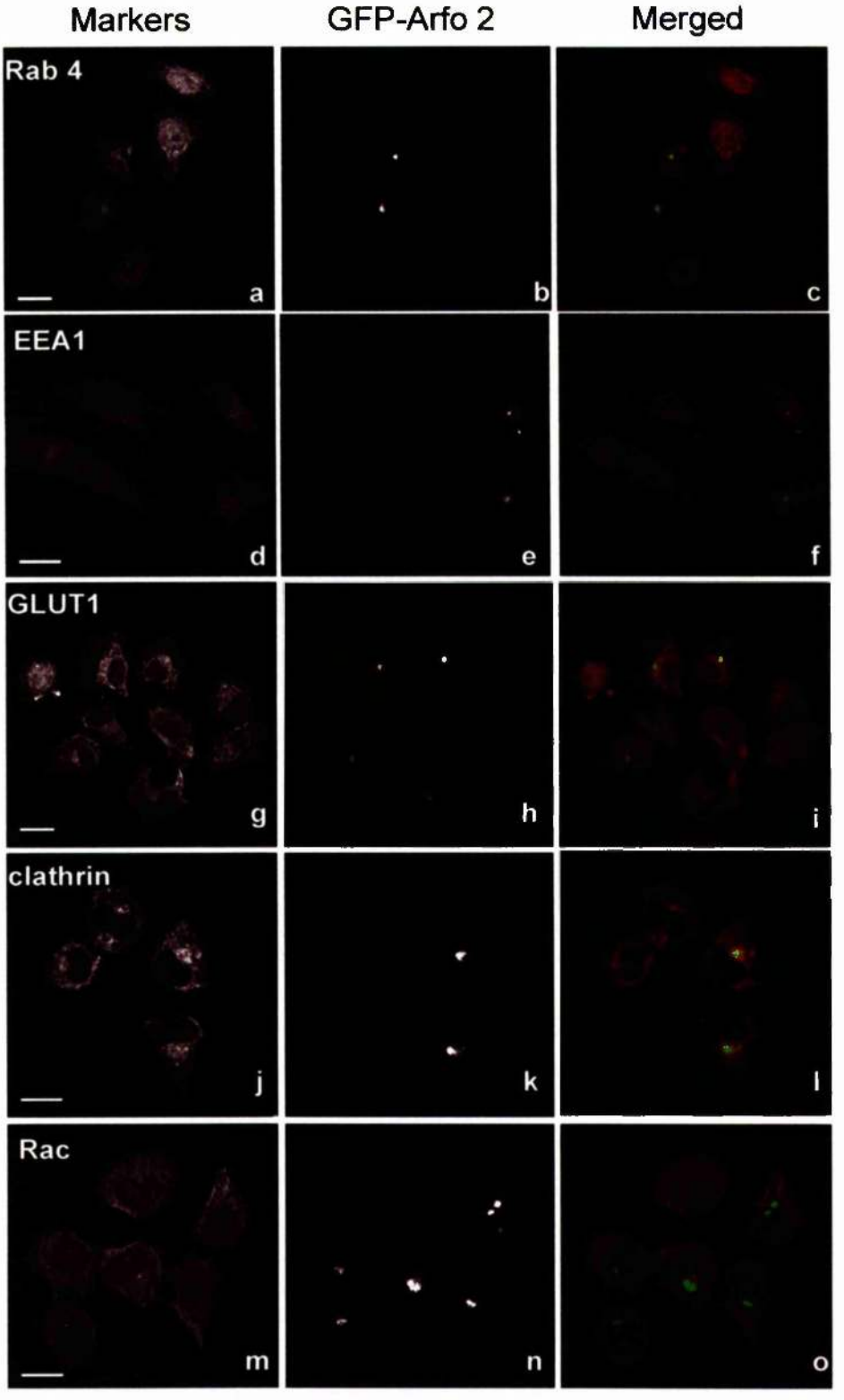

Fig. 5.3.1.1C **Localisation of GFP-Arfophilin-2 in HeLa cells.**

HeLa cells transiently expressing GFP-Arfophilin-2 (Arfo2; shown in the centre panels and GREEN in right-hand panels) were fixed in methanol 18 h after transfection and processed for immunofluorescence using primary antibodies against Rab4 (**a-c**), EEA1 (**d-f**), GLUT1 (**g-i**), clathrin (**j-l**) and Rac1 (**m-o**). Confocal images were taken and the marker proteins are shown on the left-hand panels and RED in the merged images. Scale bars, 10 μm.

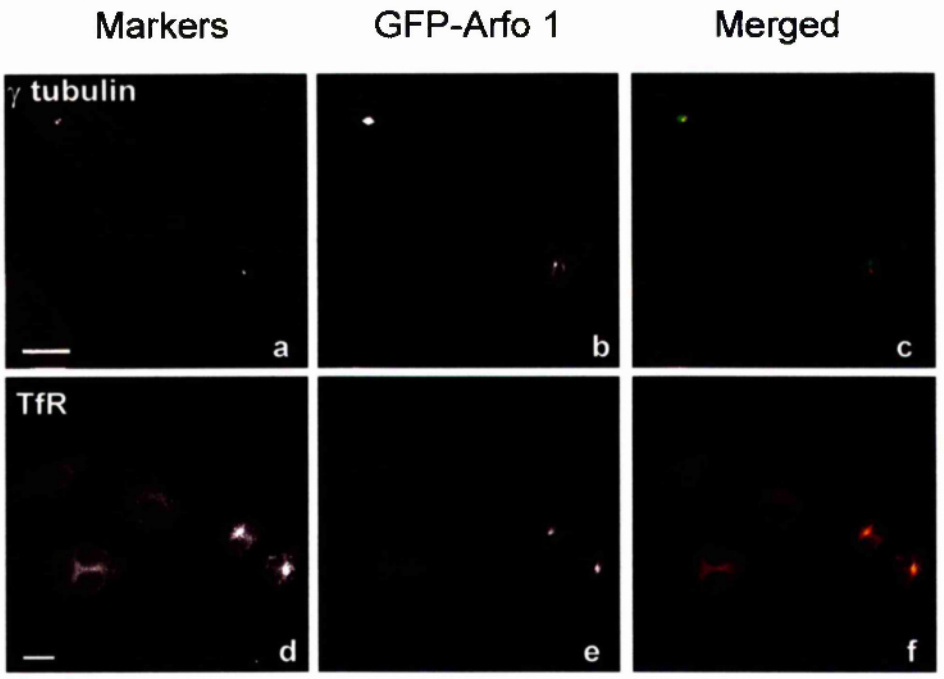

Fig. 5.3.1.2 **Localisation of GFP-Arfophilin-1 in HeLa cells.**

HeLa cells transiently expressing GFP-Arfophilin-1 (GFP-Arfo1; construct D in Fig. 5.2.1; shown in the centre panels and in GREEN in right-hand panels) were fixed in methanol 18 h after transfection and processed for immunofluorescence using primary antibodies against γ tubulin (**a-c**) and the transferrin receptor (TfR; **d-f**). Confocal images were taken and the marker proteins are shown on the left-hand panels and RED in the merged images. Scale bars, 10 μm.

Similar experiments were also performed using the construct encoding GFP fused to the C-terminal 330 amino acid residues of Arfophilin-1 (construct D in Fig. 5.2.1). Although this fusion protein was less extensively studied, it also localised around the centrosome (Fig. 5.3.1.2, panels a-c) and specifically caused an accumulation of TfRs in the same region (Fig. 5.3.1.2, panels d-f).

5.3.2 Analysis of TfR trafficking in GFP-Arfophilin-2 expressing cells

In light of these findings, experiments were performed to determine whether the profound morphological effects on TfR distribution were due to a specific block in its exit from recycling endosomes or whether the compartment had simply become concentrated in a smaller physical space whilst still able to function. To this end, it was determined whether the GFP-Arfophilin-2 and TfR-positive compartment was accessible to fluorescently labelled transferrin added to the culture medium, and if so, whether this could be chased out of the compartment with unlabelled transferrin. Within 5 min of uptake at 37°C, substantial colocalisation between the GFP chimeras and Texas-red transferrin was observed (Fig. 5.3.2.1, panels a-c), demonstrating that TfRs from the cell surface were able to traffic efficiently to the compartment. After a 30 min uptake, the GFP-Arfophilin-2 compartment was brightly stained with Texas-red transferrin (Fig. 5.3.2.1, panels a-c) and a steady decrease in transferrin fluorescence was observed over the chase time in both transfected and untransfected cells (Fig. 5.3.2.1, panels g-r). By 90 min nearly all the labelled transferrin had disappeared (Fig. 5.3.2.1, panels d-r).

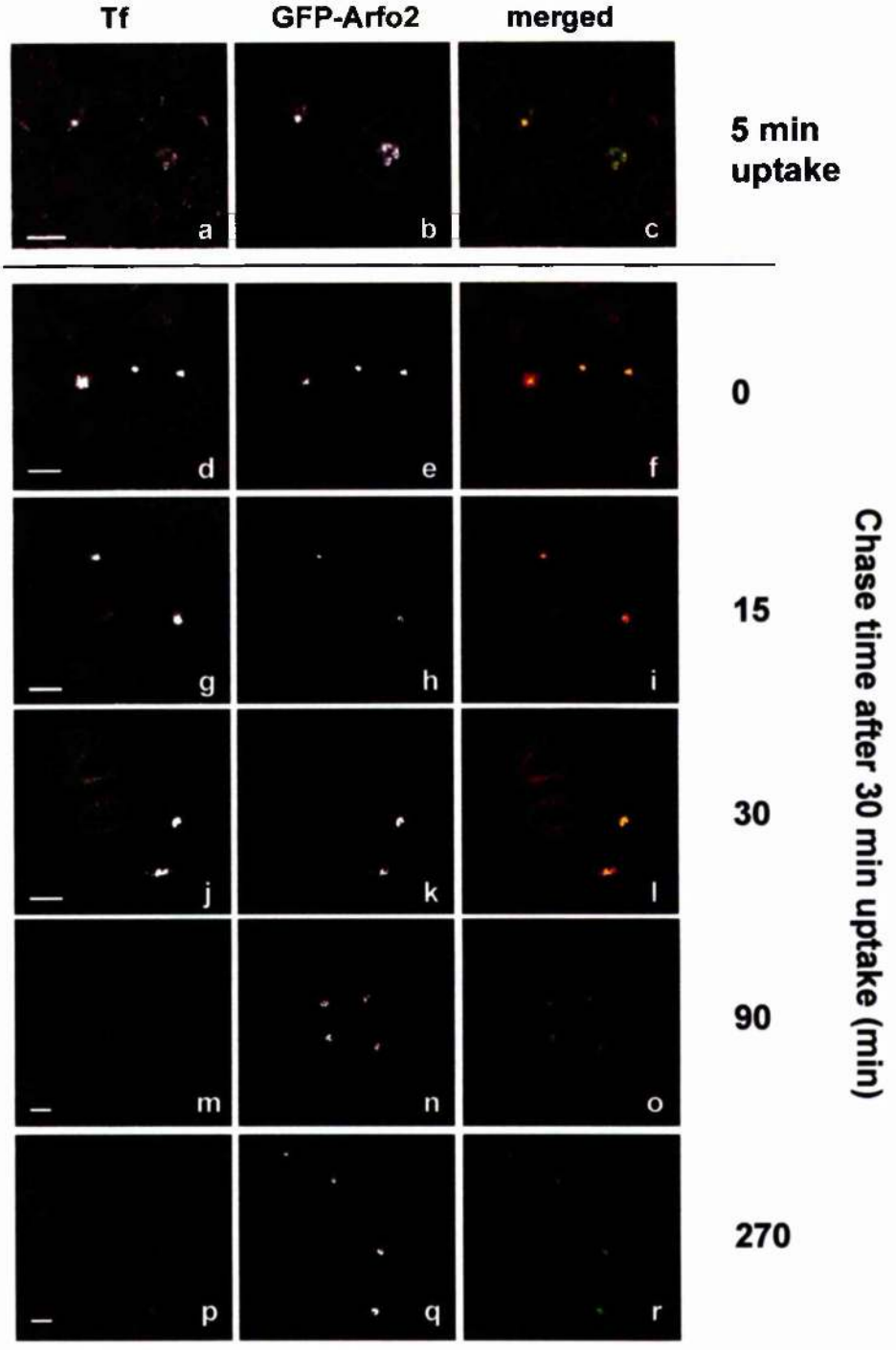

Fig. 5.3.2.1 **Effects of GFP-Arfophilin-2 overexpression on fluorescent transferrin trafficking in HeLa cells.**

HeLa cells transiently expressing GFP-Arfophilin-2 (Arfo2; shown in the centre panels and GREEN in right-hand panels) were serum starved for 1 h then incubated with 1 μg/ml Texas Red-transferrin either for 5 min (**a**,**b** and **c**) or for 30 min (**d**-**r**). Those incubated for only 5 min were washed and fixed immediately while those incubated for 30 min were washed and further incubated in complete medium containing serum and 100 μg/ml unlabelled transferrin for the times indicated (in minutes). These cells were then washed in ice-cold PBS, fixed in methanol and confocal images were taken. Transferrin fluorescence is shown in panels **a**,**d**,**g**,**j**,**m** & **p** and in RED in the merged images. Scale bars, 10 μm.

5.3.3 Sensitivity of GFP-Arfophilin-2 to drug treatment

The effects of the fungal metabolite brefeldin A, the actin monomer-stabilising agent latrunculin A and the microtubule disrupting drug nocodazole on the distribution of GFP-Arfophilin-2 were assessed. In contrast to the effect on the endogenous protein (see Fig. 4.3.7.4, panels a-f), a 10 min brefeldin A treatment (20 μg/ml) had no obvious effect on the localisation of GFP-Arfophilin-2 despite markedly scattering GRASP 55 immunoreactivity (Fig. 5.3.3.1, panels a-f). Moreover, GGA1 colocalisation persisted under these conditions (Fig. 5.3.3.1, panels g-i), as did colocalisation with the transferrin receptor and Rab11 (not shown). Similarly, 200 μM latrunculin A did not alter GFP-Arfophilin-2 distribution but did lead to gross changes of the actin cytoskeleton as evidenced by diffuse staining and the lack of discernible actin filaments (Fig. 5.3.3.2, panels a-f). Conversely, a 1 h 50 ng/ml nocodazole treatment did disperse GFP-Arfophilin-2 from its peri-centrosomal location, resulting in large punctae present throughout the cytoplasm (Fig 5.3.3.3, panels d-f), demonstrating that the integrity of the microtubule cytoskeleton is required for its localisation. This dispersal was reversible since the fusion protein returned to the microtubule organising centre within 1 h following a washout of the drug (Fig. 5.3.3.3, inset in panel f). Furthermore, analysis of TfR and GGA1 immunofluorescence following nocodazole treatment showed that colocalisation with GFP-Arfophilin-2 was maintained under these conditions (Fig. 5.3.3.3, panels g-l), suggesting that all three molecules were intimately associated with one another. Rab 11, however, could not be detected in the dispersed punctae (data not shown), although the Santa Cruz Rab11 antibody is not particularly sensitive.

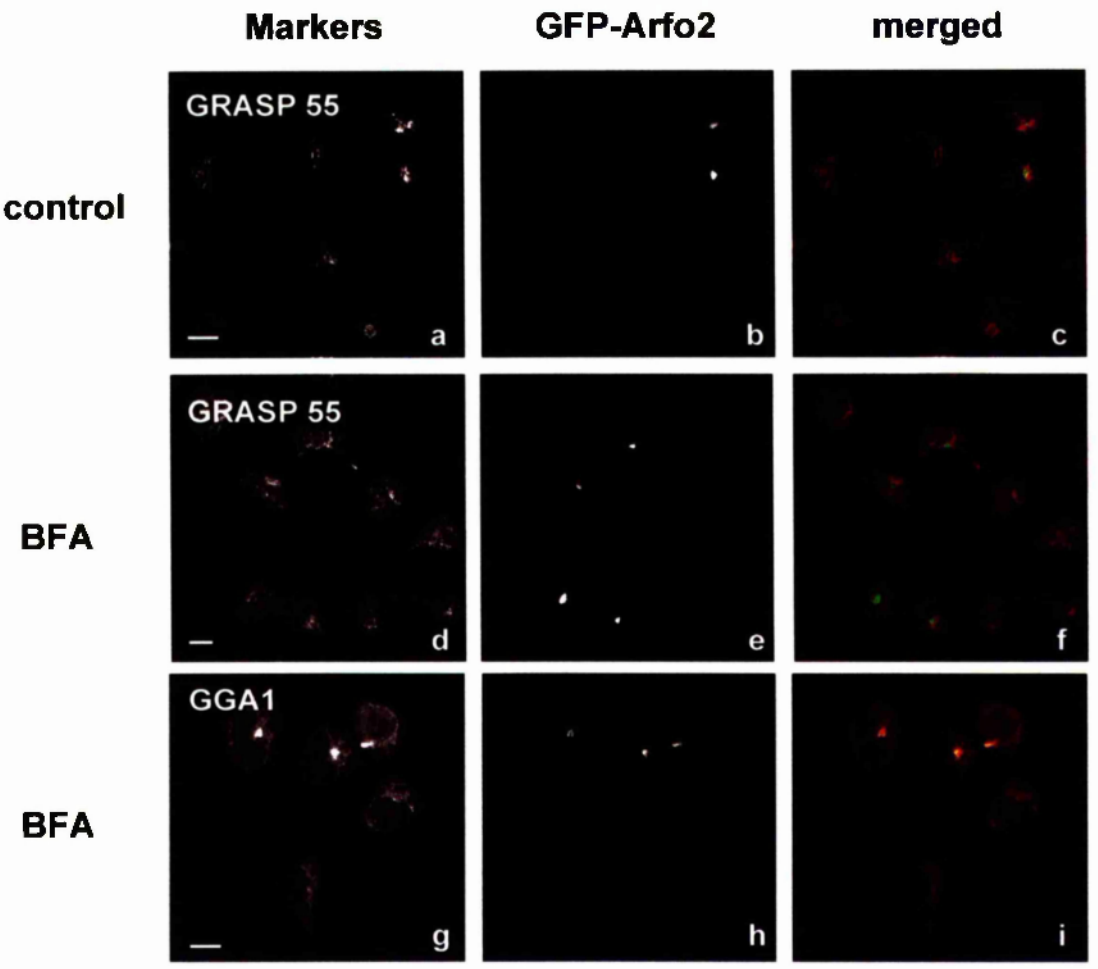

Fig. 5.3.3.1 Effect of Brefeldin A treatment on GFP-Arfophilin-2 localisation.

HeLa cells on coverslips were transiently transfected with GFP-Arfophilin-2 (GFP-Arfo2). 18 h post-transfection, the cells were incubated in serum free medium for 2 h and then with 20 μg/ml Brefeldin A (BFA, **d-i**) or vehicle control (**a-c**) for 10 min. Cells were then fixed in ice-cold methanol and processed for immunofluorescence using αGRASP55 (**a**,**d**, RED in **c**,**f**) and αGGA1 (**g**, RED in **i**) primary antibodies. GFP fluorescence is in GREEN in the merged images. Scale bars, 10 μm.

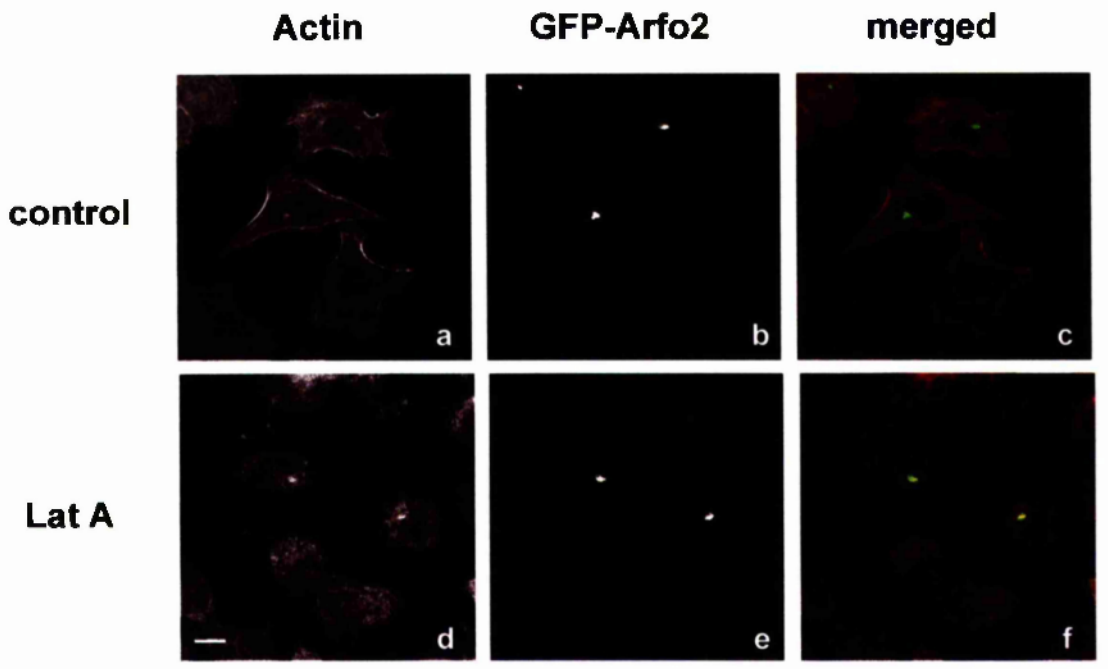

Fig. 5.3.3.2 Effect of disruption of the actin cytoskeleton on GFP-Arfophilin-2 localisation.

HeLa cells on coverslips were transiently transfected with GFP-Arfophilin-2 (Arfo2). 18 h post-transfection, the cells were incubated in serum free medium for 2 h and then with 200 µM latrunculin A (Lat A, **d-f**) or vehicle control (**a-c**) for 10 min. Cells were then fixed in ice-cold methanol and incubated with a Cy3-conjugated monoclonal anti-actin antibody (left hand panels, RED in merged images). Confocal images are shown with GFP fluorescence is GREEN in the merged images. Scale bar, 10 µm.

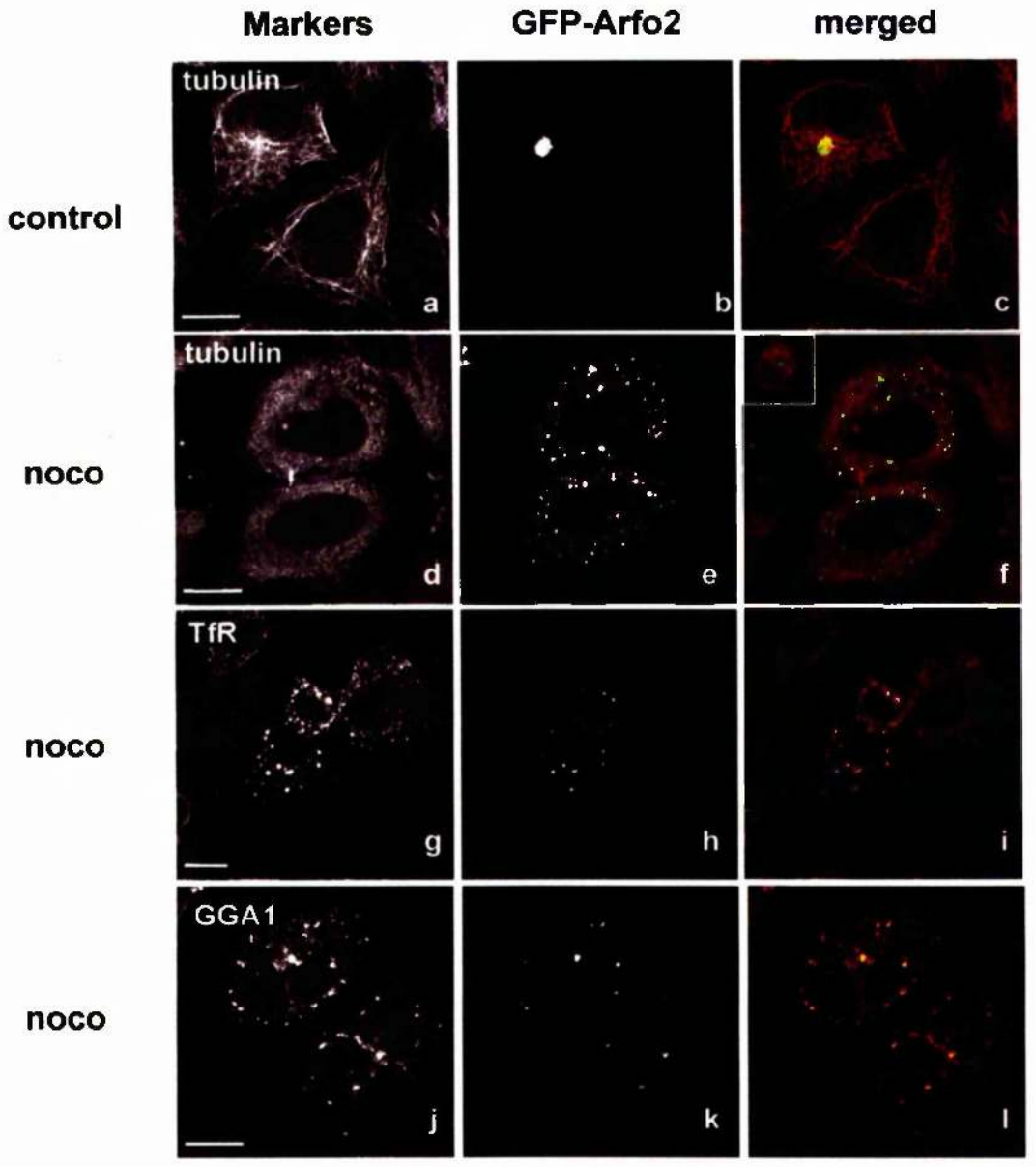

Fig. 5.3.3.3 The effect of microtubule disruption on GFP-Arfophilin-2 localisation.

HeLa cells on coverslips were transiently transfected with GFP-Arfophilin-2 (Arfo2). 18hrs post-transfection, the cells were incubated in serum free medium for 2 h and then with 50 ng/ml nocodazole (noco, **d-l**) or vehicle control (**a-c**) for 1 h. Cells were then fixed in ice-cold methanol and processed for immunofluorescence using anti-α tubulin (**a**,**d**, RED in **c**,**f**), αTfR (**g**, RED in **i**), or αGGA1 (**j**, RED in **l**) primary antibodies as indicated. The inset in **f** shows a typical GFP-arfophilin-2 expressing cell 1 hr following a washout of the drug. GFP fluorescence is in GREEN in the merged images. Scale bars, 10 μm.

5.3.4 Analysis of GFP-Nuf expression in HeLa cells

Given the fact that Arfophilin-2 is homologous to *Drosophila* nuclear fallout and that both proteins partly localise to the centrosome, I sought to determine whether they exhibited any functional similarities. Since the homology is in the carboxyl terminal where Arfs bind Arfophilin-2, one of the most obvious experiments was to investigate whether Nuf was itself an Arf-binding protein. To this end, a Nuf cDNA was obtained from W. Sullivan (Santa Cruz, CA, USA) and cDNAs of the *Drosophila* Class I, II and III Arfs were obtained from the Berkeley *Drosophila* Genome project (http://www.fruitfly.org/). These were then subcloned and tested for interactions in the yeast-two hybrid system in much the same way as described in chapter 3. Both full-length Nuf and the C-terminal 300 amino acids (the Arfophilin-homology domain) of Nuf fused to the GAL4-transactivation domain in pACT2 were tested against Q-L and T-N mutants of *Drosophila* and mammalian Arfs fused to the GAL4 DNA-binding domain in pGBT9. No interactions were detected with any combination suggesting that Nuf is not a direct Arf effector (data not shown).

In spite of these findings, it was decided to examine whether overexpression of Nuf in mammalian cells would lead to similar phenotypes as those observed for the Arfophilins and hence potentially shed some light on the requirement for Arfs with respect to these phenotypes. Therefore, Nuf was subcloned into a GFP vector as described in section 5.2.2 and transiently expressed in HeLa cells. The results were striking. As with the Arfophilins, GFP-Nuf localisation in the majority of cells was tightly around the γ-tubulin-positive centrosome (Fig. 5.3.4.1, panels a-c), and transferrin receptors and Rab11 were also concentrated in the same region (Fig. 5.3.4.1, panels d-i). In addition, endogenous Arfophilin-2 was itself enriched in the Nuf-positive peri-centriolar region (Fig. 5.3.4.1, panels j-l). However, GGA1 was not detected in the Nuf-positive compartment (not shown). It was also observed that a small proportion of GFP-Nuf-expressing cells (about 10%) exhibited a markedly different phenotype whereby GFP-Nuf was found packaged into a small 'bud' protruding from the cell surface (see Fig. 5.3.4.1, panels m-o). These buds also appeared to contain transferrin receptors (Fig. 5.3.4.1, panels m-o).

Transferrin pulse-chase experiments were also performed on cells expressing GFP-Nuf to see whether TfR recycling through the compartment was still functional, as it had been in GFP-Arfophilin-2-expressing cells. Fig. 5.3.4.2 shows the results of such an experiment where it can be seen that after a 30 min pulse, fluorescent transferrin accumulates in and around the Nuf-positive compartment (panels a-c). This fluorescence can subsequently be

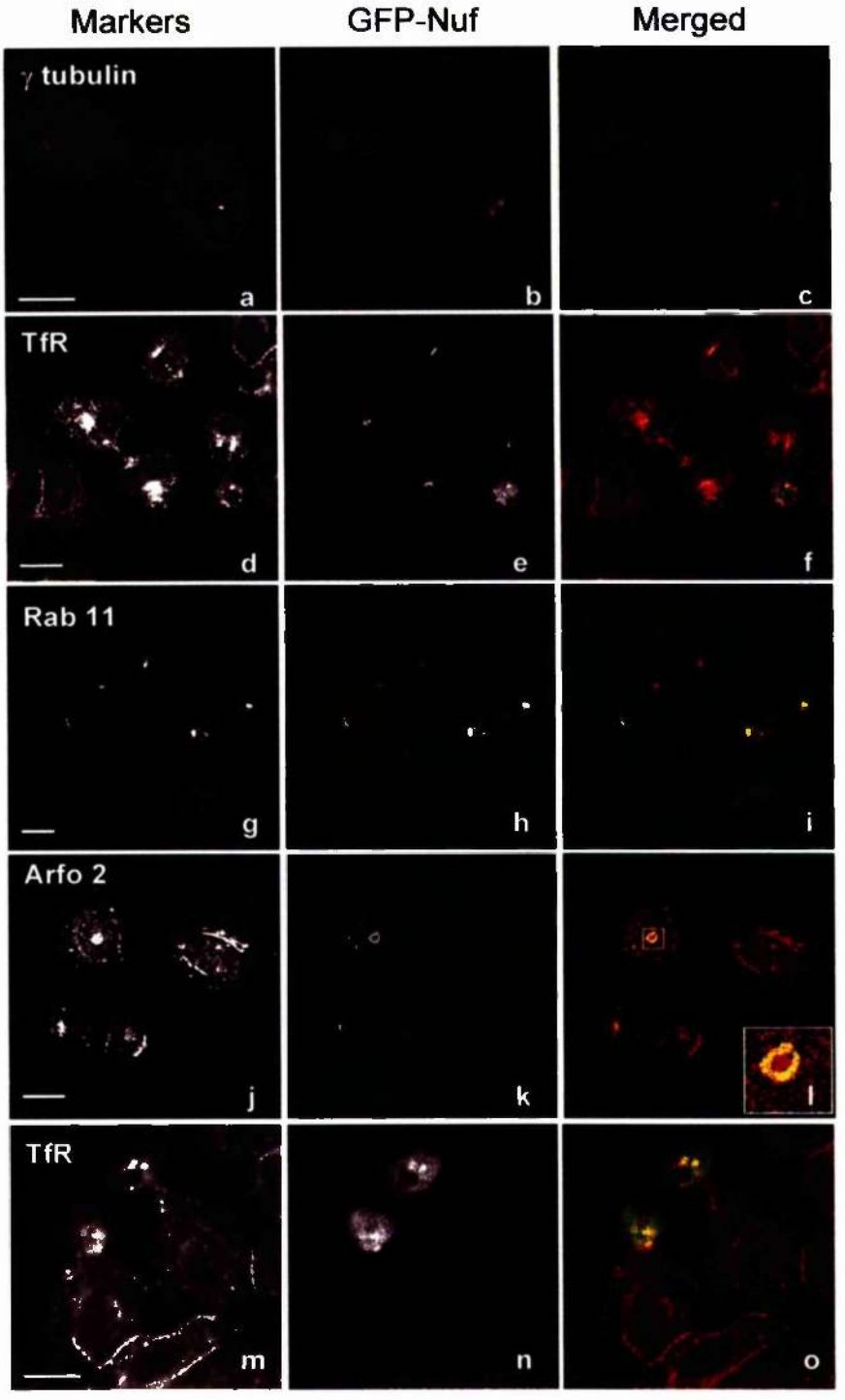

Fig. 5.3.4.1 **Localisation of GFP-Nuf in HeLa cells.**

Shown are confocal images of HeLa cells transiently expressing GFP-Nuf (centre panels and GREEN in right hand panels) counterstained for γ tubulin (**a**, RED in **c**), TfR (**d**,**m** RED in **f**,**o**), Rab11 (**g**, RED in **i**) and endogenous Arfophilin-2 (**j**, red in **l**). Merged images appear in the right-hand panels. Also shown are cells displaying GFP-Nuf-containing 'buds' that also contain TfRs (**m**-**o**). Note that low level expression of Nuf results in marked alterations in TfR and Rab11 distribution similar to that observed with Arfophilin-2 overexpression. Also note the colocalisation of Nuf with endogenous Arfophilin-2 encircling the Arfophilin-2 positive centrosome (inset in **l**). Scale bars, 10 μm.

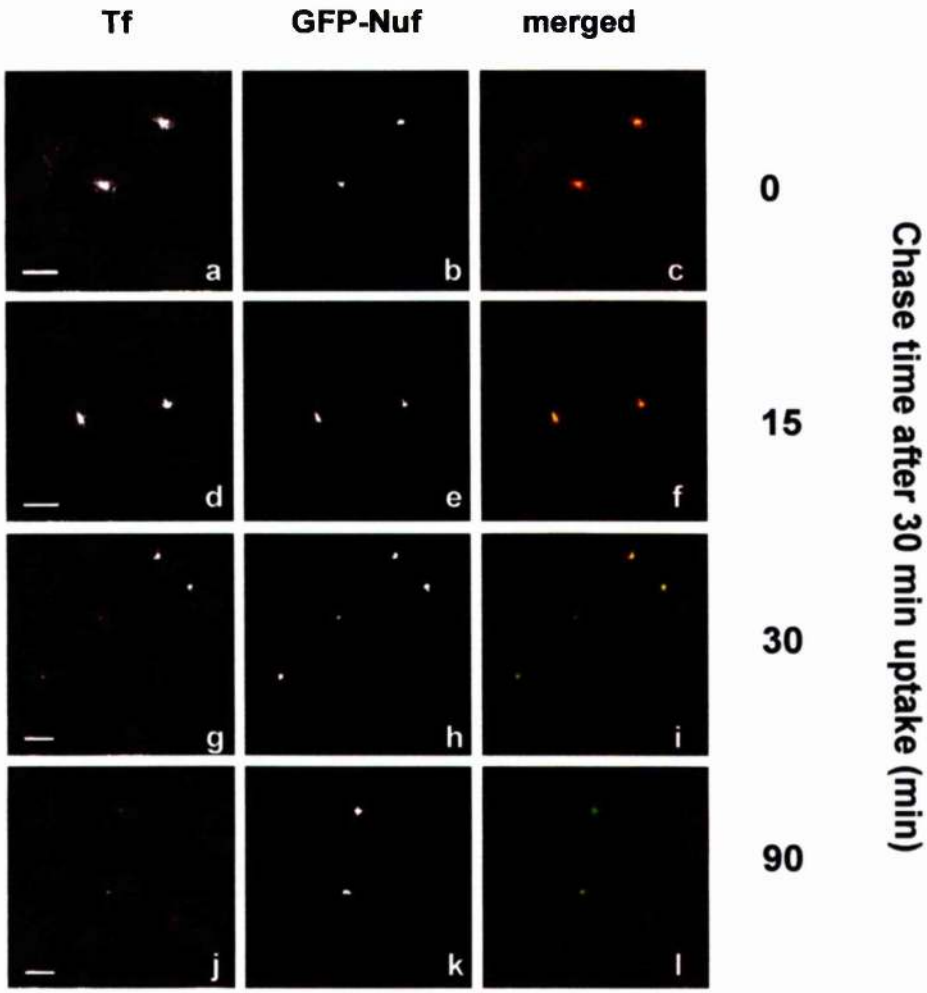

Fig. 5.3.4.2 **Effects of GFP-Nuf overexpression on fluorescent transferrin trafficking in HeLa cells.**

HeLa cells transiently expressing GFP-Nuf (centre panels and GREEN in right-hand panels) were serum starved for 1 hr then incubated for 30 minutes with 1 μg/ml Texas Red-transferrin (Tf). Cells were then washed and incubated in complete medium containing 100 μg/ml unlabelled transferrin for the indicated times (in min). Cells were then washed in ice-cold PBS, fixed in methanol and confocal images were taken. Transferrin fluorescence is shown in panels **a**,**d**,**g**,**j** and in RED in the merged images. Scale bars, 10 μm.

chased out over a similar time course to that observed with GFP-Arfophilin-2, with very little fluorescent transferrin remaining after 90 min (Fig. 5.3.4.2, panels j-l), again suggesting that there is no qualitative block on TfR recycling in these cells.

5.3.5 Analysis of untagged Arfophilin-2 expression in HeLa cells

Since GFP- and epitope-tags can interfere with the function of proteins, and since the Arfophilin-2-specific antibody was available, the constructs encoding untagged full-length Arfophilins-2A, -2B and -2C described in chapter 4 were also expressed in HeLa cells and visualised by indirect immunofluorescence. In particular, their localisations were monitored in relation to the markers of interest: transferrin receptors, Rab11 and GGA1. These are shown in Figs. 5.3.5.1A, 5.3.5.2, and 5.3.5.3. Untagged Arfophilin-2A lost most of its peri-centrosomal localisation, only marginally colocalised with the transferrin receptor (Fig. 5.3.5.1A, panels a-c) and did not appear to colocalise at all with Rab11 (panels d-f) or GGA1 (panels g-i). It seemed to be mainly scattered throughout the cytoplasm in small punctate vesicular structures with diffuse cytosolic staining also apparent (Fig. 5.3.5.1). By contrast, Arfophilins-2B and -2C (Figs. 5.3.5.2 and 5.3.5.3, respectively) retained their tight peri-centrosomal distributions, maintained strong colocalisation with the TfR (panels a-c) and showed less diffuse staining. Rab11 was only detected in the Arfophilin-2C-positive compartment (Fig. 5.3.5.3, panels d-f) and, to a lesser exten,t in the Arfophilin-2B compartment (Fig. 5.3.5.2, panels d-f). GGA1 did not appear coincident with either of these proteins (panels g-i), as it had been with the GFP chimeras. These results are summarised and compared to the GFP-Arfophilin-2 and the GFP-Nuf chimeras in Table 5.3.5.1.

Arfophilin-2A, which was shown in the last chapter to have the same electrophoretic mobility as the endogenous HeLa protein, was examined in more detail. Fig. 5.3.5.1B shows that its overexpression had little effect on the distributions of the βCOP (panels a-c), CI-MPR (panels d-f), or RME1 (panels g-i).

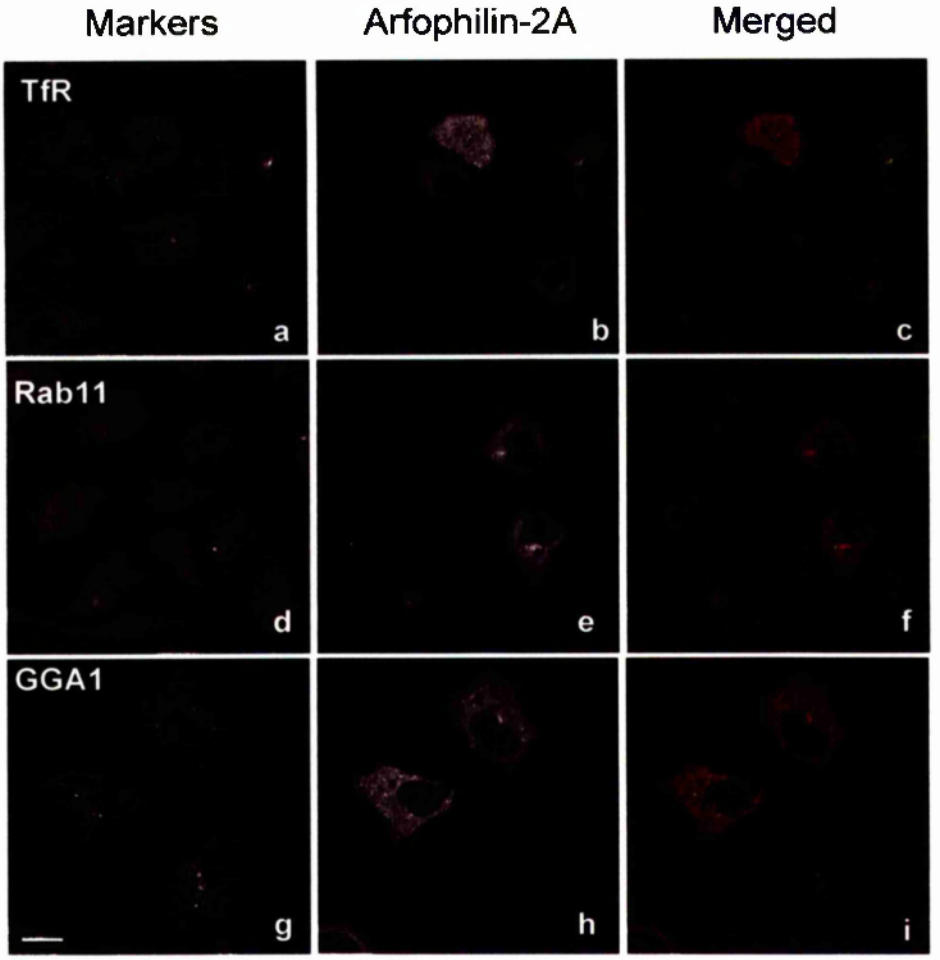

Fig. 5.3.5.1A **Localisation of untagged Arfophilin-2A in HeLa cells.**

HeLa cells transiently expressing Arfophilin-2A (shown in the centre panels and RED in the right-hand panels) were fixed in methanol 18 h after transfection and processed for immunofluorescence using the anti-Arfophilin-2 antibody (1:1000 dilution) in conjunction with primary antibodies against TfR (**a-c**), Rab11 (**d-f**), and GGA1 (**g-i**). Representative confocal images were taken and the marker proteins are shown in the left-hand panels and in GREEN in the merged images. Scale bar, 10 μm.

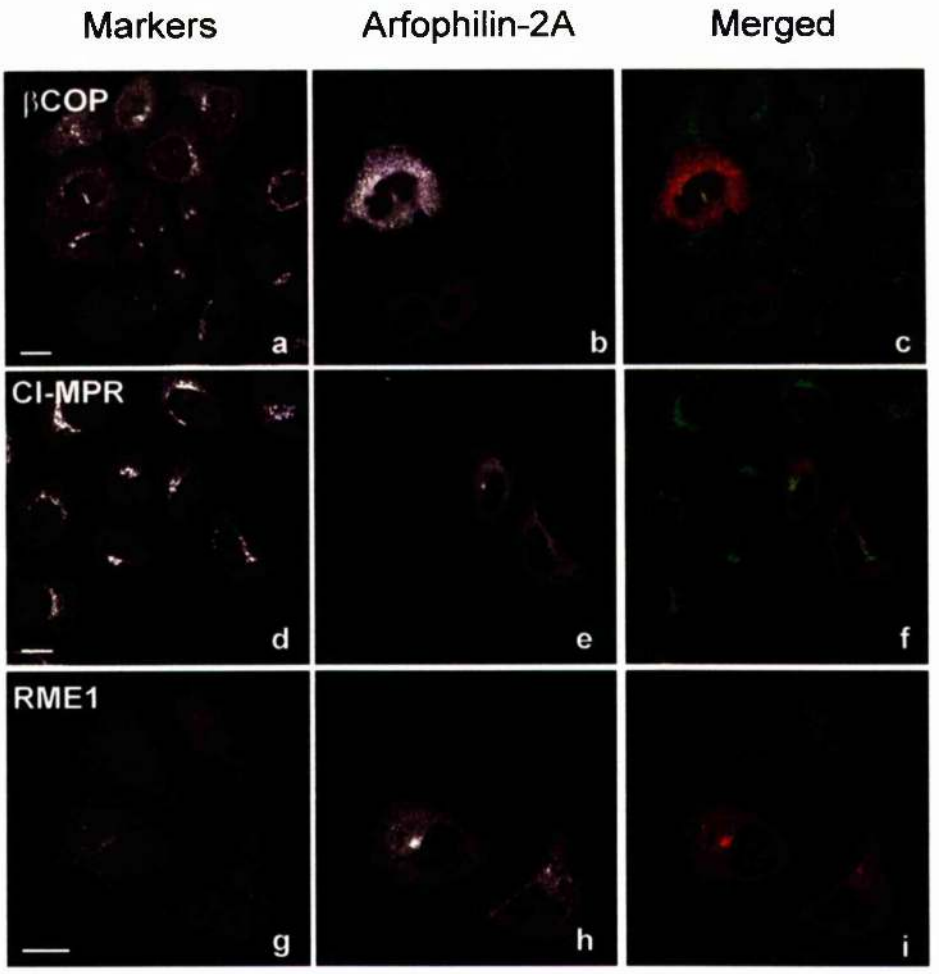

Fig. 5.3.5.1B **Localisation of untagged Arfophilin-2A in HeLa cells.**

HeLa cells transiently expressing Arfophilin-2A (shown in the centre panels and RED in the right-hand panels) were fixed in methanol 18 h after transfection and processed for immunofluorescence using the anti-Arfophilin-2 antibody (1:1000 dilution) in conjunction with primary antibodies against βCOP (**a-c**), CI-MPR (**d-f**), and RME1 (**g-i**). Representative confocal images were taken and the marker proteins are shown in the left-hand panels and in GREEN in the merged images. Scale bars, 10 μm.

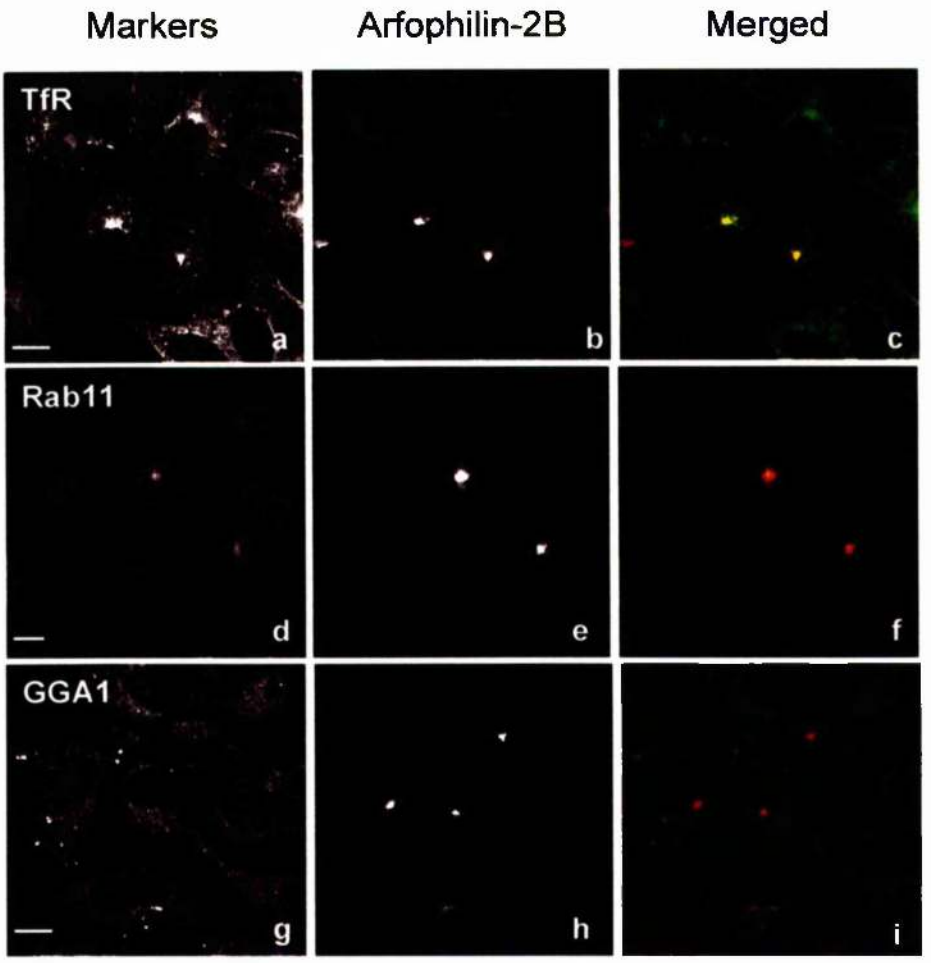

Fig. 5.3.5.2 **Localisation of untagged Arfophilin-2B in HeLa cells.**

HeLa cells transiently expressing Arfophilin-2B (shown in the centre panels and RED in the right-hand panels) were fixed in methanol 18 h after transfection and processed for immunofluorescence using the anti-Arfophilin-2 antibody (1:1000 dilution) in conjunction with primary antibodies against TfR (**a**-**c**), Rab11 (**d**-**f**), and GGA1 (**g**-**i**). Representative confocal images were taken and the marker proteins are shown in the left-hand panels and in GREEN in the merged images. Scale bars, 10 μm.

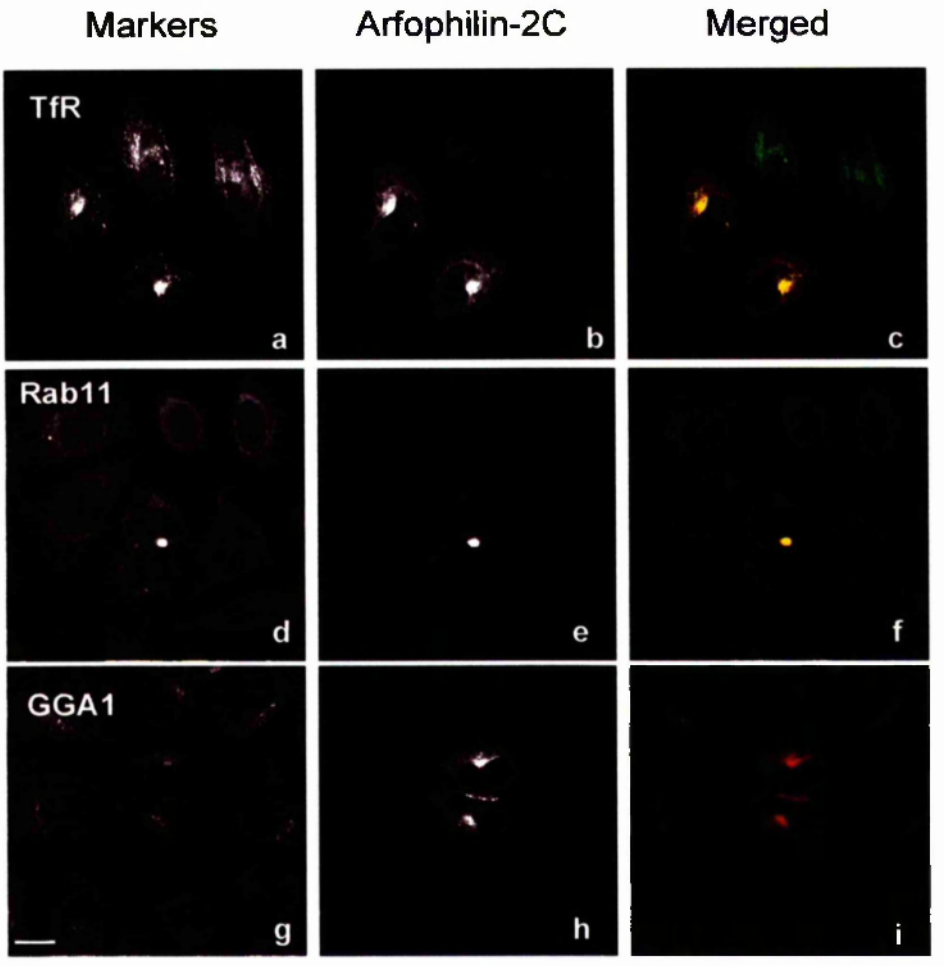

Fig. 5.3.5.3 **Localisation of untagged Arfophilin-2C in HeLa cells.**

HeLa cells transiently expressing Arfophilin-2C (shown in the centre panels and RED in the right-hand panels) were fixed in methanol 18 h after transfection and processed for immunofluorescence using the anti-Arfophilin-2 antibody (1:1000 dilution) in conjunction with primary antibodies against TfR (**a-c**), Rab11 (**d-f**), and GGA1 (**g-i**). Representative confocal images were taken and the marker proteins are shown in the left-hand panels and in GREEN in the merged images. Scale bar, 10 μm.

Construct	Pericentrosomal?	TfR colocalisation?	Rab11 colocalisation?	GGA1 colocalisation?
Arfo2A (I)	(✓)	(✓)	✗	✗
Arfo2B (J)	✓ ✓ ✓	✓ ✓ ✓	(✓)	✗
Arfo2C (K)	✓ ✓ ✓	✓ ✓ ✓	✓ ✓ ✓	(✓)
GFP-Arfo2 *	✓ ✓ ✓	✓ ✓ ✓	✓ ✓ ✓	✓ ✓ ✓
GFP-Nuf	✓ ✓ ✓	✓ ✓ ✓	✓ ✓ ✓	✗

Table 5.3.5.1 **Summary of phenotypes observed upon expression of different Arfophilin-2/Nuf constructs in HeLa cells.**

Untagged and tagged constructs are scored according to whether the resulting proteins exhibit pericentrosomal localisation and whether they colocalise with the transferrin receptor (TfR), Rab11 and GGA1. Three ticks represent strong colocalisation, one tick represents weak colocalisation, while a cross indicates the lack of discernible colocalisation. The constructs used are referred to by letter according to Fig. 5.2.1. *GFP-Arfo2 represents any of the Arfophilin-2 constructs containing the minimum Arf-binding domain (constructs B/C/E/F/G/H). GFP-Nuf represents full-length Nuf fused to the C-terminus of GFP.

5.3.6 The effect of over-expression of Arf mutants on Arfophilin-2 distribution

The Arfophilins were identified by virtue of their GTP-dependent interactions with Arf5. Therefore, I wished to examine the effects of over-expression of wild-type, constitutively active and dominant negative forms of Arf5 on Arfophilin-2 distribution. C-terminally epitope-tagged Arf5 constructs were, therefore, expressed in HeLa cells and the resulting proteins were monitored by immunofluorescence using antibodies to the epitope tags all according to the methods described in sections 2.2.2.4 and 2.2.3. Whereas wild-type Arf5-FLAG and activated Arf5Q71L-HA did not seem to affect endogenous Arfophilin-2 distribution to any great extent in these cells (Fig. 5.3.6, panels a-d), the expression of the dominant negative GTP-binding deficient Arf5T31N-HA mutant completely dispersed it into the cytoplasm even in relatively low-expressing cells (Fig. 5.3.6, panels e-f). The analogous Arf6 mutant, Arf6T27N-HA, was similarly analysed but it was not capable of disrupting Arfophilin-2 staining (Fig. 5.3.6, panel g-h).

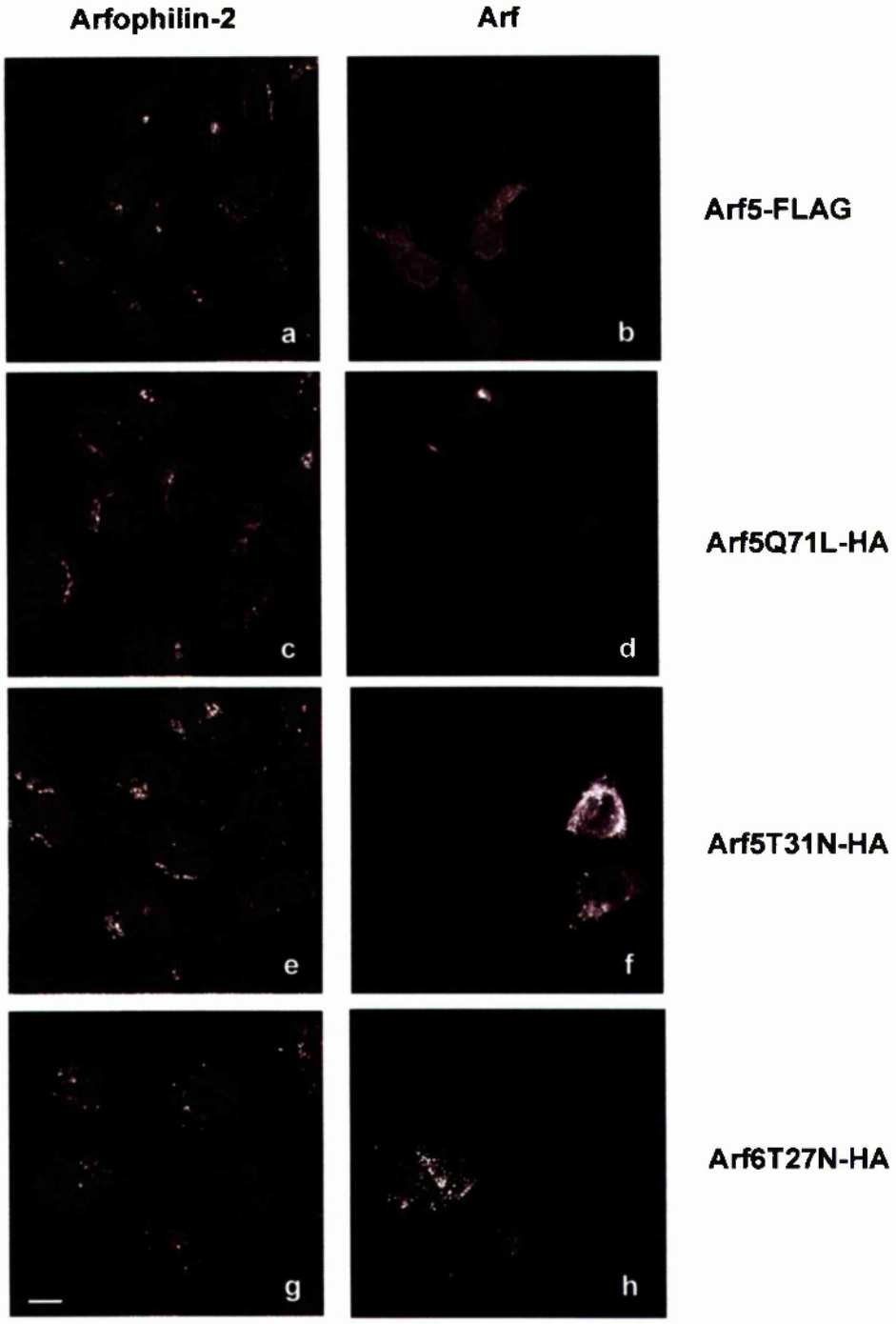

Fig. 5.3.6 **The effect of expression of Arf mutants on endogenous Arfophilin-2 distribution in HeLa cells**

HeLa cells on coverslips were transfected with mammalian expression vectors encoding Arf5-FLAG (**a-b**), Arf5Q71L-HA (**c-d**), Arf5T31N-HA (**e-f**) and Arf6T27N-HA (**g-h**) as indicated. After 18-20 h, the cells were fixed and processed for immunofluorescence using monoclonal anti-FLAG (Sigma) or anti-HA (Santa Cruz) antibodies (1:200 dilution, right-hand panels) and a polyclonal anti-Arfophilin-2 antibody (1:200, left hand panels), followed by Alexa^{488}-anti-mouse and Alexa^{594}-anti-sheep secondary antibodies. Shown are representative confocal images of cells expressing the Arf proteins. This experiment was performed twice with similar results. Scale bar, 10 μm.

5.3.7 The production of cell lines stably expressing a GFP-Arfophilin-2 chimera

It was decided to produce stable cell lines expressing GFP-Arfophilin-2 (C-terminal 330 amino acids) to facilitate future study. One particular application would be for electron microscopic analysis of the pericentrosomal TfR-positive compartment, as high resolution images of the structures may shed more light onto the function of Arfophilin-2. Other experiments in mind for stable cell lines included the analysis of the kinetics of radiolabelled ^{125}I-transferrin trafficking, and their use as a source of protein for biochemical Arf binding assays.

G418 resistant HEK 293 and CHO cell lines were produced as described in section 5.2.3, and clonal populations were then examined by confocal microscopy and immunoblotting, to check for GFP-Arfophilin-2 expression. As can be seen in the immunoblot in Fig 5.3.7.1 (panel B), several expressing lines were produced. Furthermore, immunofluorescence microscopy analysis of the HEK 293 clones revealed that the GFP-Arfophilin-2 protein was similarly concentrated in a TfR-positive (Fig 5.3.7.2, panels a-c), Rab11-positive (panels d-f) and GGA1-positive (panels g-i) pericentrosomal compartment. It was noted that these cells grew markedly slower that wild-type HEK 293 cells, with a doubling time roughly three to four times longer (data not shown). Endogenous Arfophilin-2 protein levels also seemed to be elevated in these cells given the increased intensity of the bands present in the immunoblot (see Fig. 5.3.7.1, panel B), when equal amounts of total protein were loaded (see the Ponceau-stained blot in panel A). This may have been a reflection of an adaptive mechanism trying to overcome a block induced by the overexpressed protein. The generation of stably expressing HeLa cells was also attempted, but while many G418-resistant clones were isolated, none exhibited any detectable GFP fluorescence (data not shown).

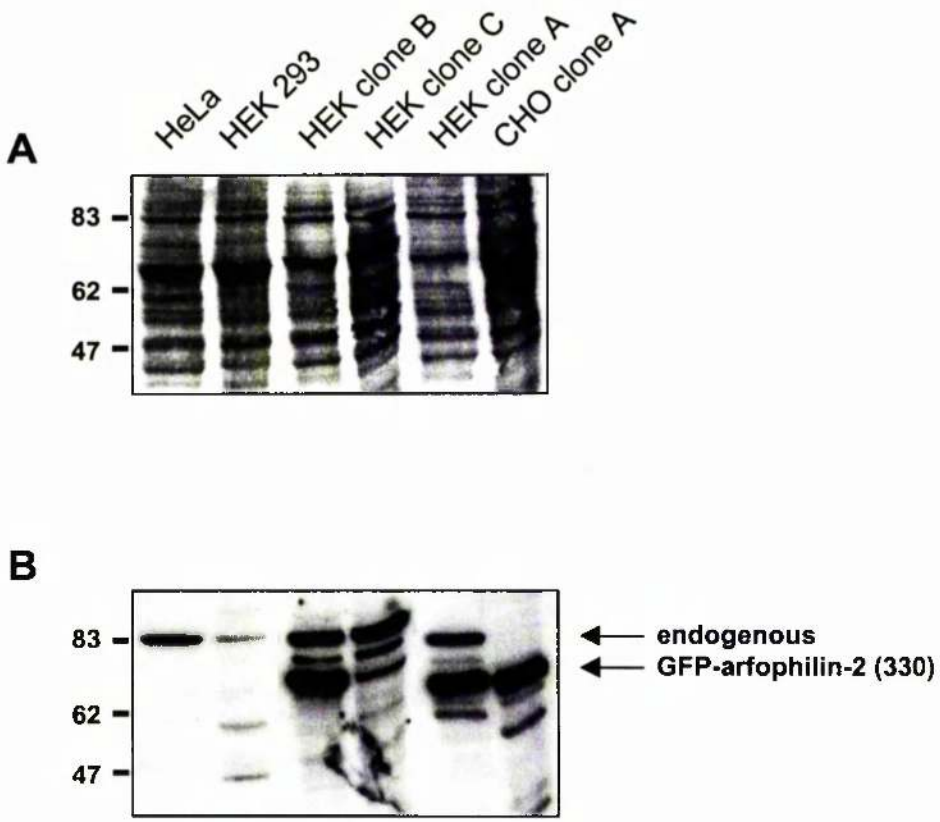

Fig. 5.3.7.1 **Analysis of GFP-Arfophilin-2 stable cell lines.**

HEK 293 and CHO cells were transfected with GFP-Arfophilin-2 (C-terminal 330 amino acids; construct C in Fig. 5.2.1) and clonal, G418-resistant cell lines were selected and cultured. Whole cell lysates were prepared from the different cells indicated and 20 μg protein per lane were separated on a 10% SDS-PAGE gel. The proteins were then transferred to nitrocellulose, stained with Ponceau-S (Panel A), and immunoblotted with anti-Arfophilin-2 antibodies (Panel B), all according to the methods in section 2.2.4. The positions of the endogenous and heterologously-expressed proteins are indicated on the right, and the sizes of molecular weight standards (in kDa) are given on the left. Wild-type HeLa and HEK 293 cells are present in the first two lanes for comparison. Note that all three HEK stable cell lines have markedly elevated endogenous Arfophilin-2 signals compared to the wild-type cells.

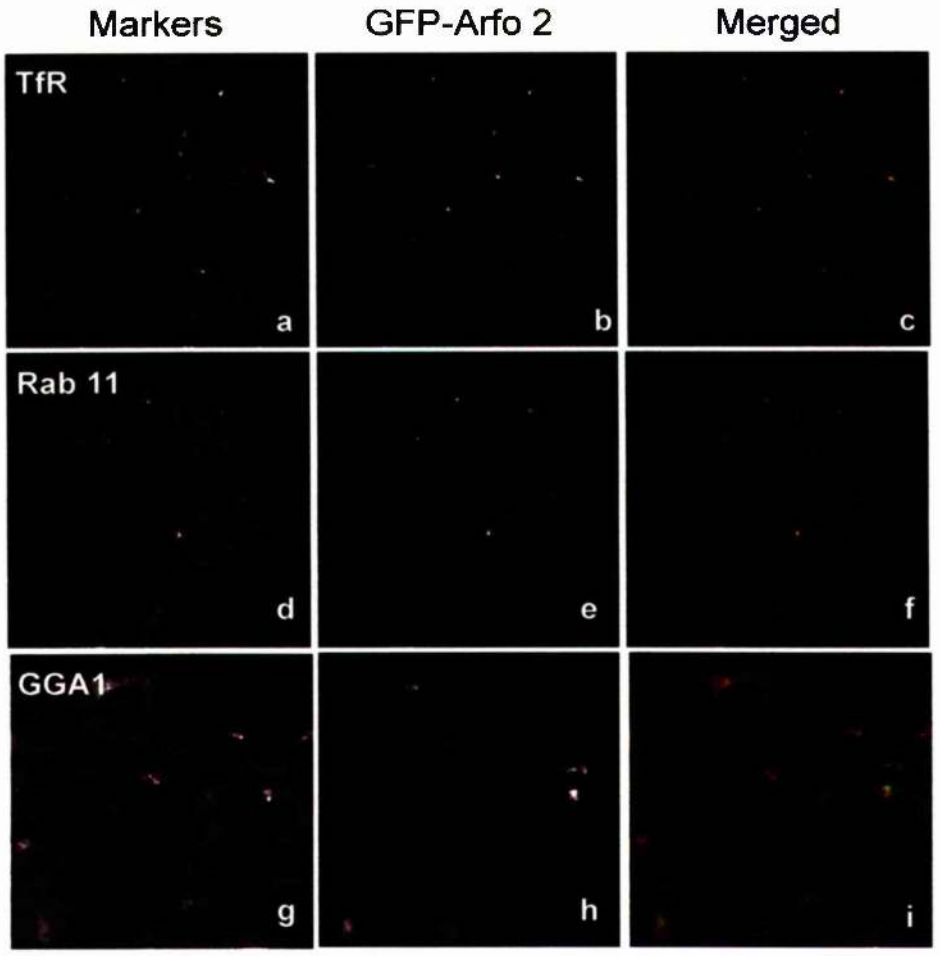

Fig. 5.3.7.2 **Confocal analysis of a HEK 293 cell line stably expressing GFP-Arfophilin-2.**

HEK 293 cells were transfected with GFP-Arfophilin-2 (C-terminal 330 amino acids; construct C in Fig. 5.2.1) and clonal, G418-resistant cell lines were selected. One such clone (clone A) was then cultured on glass coverslips, fixed in methanol and processed for immunofluorescence using primary antibodies against TfR (**a-c**), Rab11 (**d-f**), and GGA1 (**g-i**), and TRITC-conjugated secondary antibodies. Confocal images were taken and the marker proteins are shown in the left-hand panels and in RED in the merged images, while GFP fluorescence is shown in the centre panels and in green in the merged images.

5.4 Discussion

In this chapter, experiments have been described whereby the overexpression of various Arfophilin-2 constructs in HeLa cells results in very interesting phenotypes. The specific and drastic change in transferrin receptor distribution automatically implicates Arfophilin-2 in the regulation of the endosomal system since this receptor is the archetypal marker of this trafficking pathway (see section 1.1.2.1). Furthermore, the fact that Rab 11 was similarly affected strongly argues that Arfophilin-2 specifically affects the peri-centriolar recycling compartment (Ullrich et al., 1996) and (see sections 1.1.2.2 and 1.1.2.3). The specificity for this compartment is perhaps best demonstrated by the inability of Arfophilin-2 to alter the distributions of Rab 4 and EEA1, since these are found in the other subdomains of the endosomal system, although the former can be seen to partially overlap with Rab 11 (Sönnichsen et al., 2000).

The fact that fluorescent transferrin can still enter and leave the compartment relatively efficiently argues that the changes in TfR distribution are not due to a qualitative trafficking block. This is perhaps not particularly surprising given that nocodazole treatment does not interfere with transferrin receptor recycling (Jin and Snider, 1993), whereas the Arfophilin-2-mediated effects are sensitive to the drug. A TfR recycling block was however recently described upon overexpression of GFP-myosin Vb tail, which caused internalised transferrin to accumulate in a similar Rab 11-positive compartment around the centrosome, but in this case it could not be chased out even after 6 hours (Lapierre et al., 2001). While this is clearly not happening with Arfophilin-2 overexpression, subtle changes in the kinetics of entry/exit from the recycling endosomes may still be occurring and these could account for the observed effects. For instance, a slight decrease in the rate of exit or a slight increase in the rate of entry may produce the endosome morphology described here. Hopefully, future experiments monitoring ^{125}I-transferrin trafficking in the stable cell lines will uncover if this is the case.

A similar phenotype was also recently reported for overexpression of mammalian and worm RME1 (Grant et al., 2001; Lin et al., 2001), an EH domain-containing protein discovered in a *C. elegans* screen for mutants defective in receptor mediated endocytosis. Expression of a dominant negative RME1 point mutant in CHO cells lead to a slowing of transferrin receptor recycling and a slowing of the delivery of a TGN38 chimera to the TGN (Lin et al., 2001). In the case of Arfophilin-2, the effect seems to be on the distribution, but not necessarily the function, of the recycling endosomal compartment.

Exactly how Arfophilin-2 could regulate the distribution of this compartment is unclear. Potentially it could be involved in motor protein recruitment or the regulation of microtubule associated proteins.

The recycling endosomes exhibit heterogeneity, differences having been noted based on the analysis of cellubrevin versus transferrin receptor trafficking (Teter et al., 1998). They are also continually exchanging membrane with the plasma membrane, the late endocytic compartments and the TGN (Ghosh et al., 1998). It would therefore be very interesting to see whether GFP-Arfophilin-2 has a global effect on the recycling endosomes, or whether only a subset are affected, and if so, whether these are on a specific transport route to/from particular compartment.

The brefeldin A insensitivity of GFP-Arfophilin-2 localisation also supports the notion that it is the recycling endosomes that are being affected, since these organelles in particular are well documented as being remarkably resistant to the drug (Lippincott-Schwartz et al., 1991; Sönnichsen et al., 2000). It is conceivable that endogenous Arfophilin-2 traffics between a major BFA-sensitive pool in the TGN area and a BFA resistant recycling endosome pool and that it gets trapped in the latter upon expression of the various constructs described. This idea is supported by the observation that the endogenous Arfophilin-2 colocalises with GFP-Arfophilin-1 and GFP-Nuf in the pericentrosomal location. The addition of a GFP moiety or even the N-termini of putative Arfophilins-2B or -2C to Arfophilin-2A causes the clustered endosome morphology, whereas untagged Arfophilin-2A disperses throughout the cell and only marginally alters endosome morphology in some cells. This suggests that a free amino-terminus is probably required for Arfophilin-2 function, and can also be interpreted to imply that Arfophilin-2A is the endogenous isoform.

The nocodazole-sensitivity clearly demonstrates the microtubule-dependency of the compartment; also a well-documented characteristic of the recycling endosomes (Cole and Lippincott-Schwartz, 1995). The fact that it is reversible implies that minus-end-directed motor protein activity is still functional. It may be that plus-end directed motor recruitment or function is being inhibited upon GFP-Arfophilin-2/Nuf overexpression, and this would correlate nicely with the model proposed for Nuf function described in the introduction to this chapter (section 5.1.1). The TfR/Rab11 positive compartment induced by GFP-myosin Vb tail was also dispersed by nocodazole and the authors postulated that both actin-based and microtubule-based motor proteins were involved in trafficking through the compartment, and that they were interfering with a myosin/kinesin interaction (Lapierre et

al., 2001). It would be interesting to see where myosin V resides in cells overexpressing Arfophilin-2 and vice versa and to work out whether the two proteins function in parallel, or indeed in the same, pathways.

The change in GGA1 localisation is very interesting, not least because it too is an Arf-binding protein (Boman et al., 2000). The GGAs are less well described having only been discovered in the last year or two. Nevertheless, there is good evidence showing that they are clathrin-binding adaptors that also directly bind MPR cytoplasmic tails and are involved in their trafficking out of the TGN (Puertollano et al., 2001a; Puertollano et al., 2001b). The fact that MPRs themselves were unaffected by expression of any of the Arfophilin constructs implies that the GGA sequestration occurs at steps either before or after their involvement in MPR trafficking. It also strengthens the likelihood that Arfophilin-2 and the CI-MPR are not associated with one another despite the marked colocalisation of the endogenous proteins seen in chapter 5. A similar situation seems likely for sortilin, which was again unaffected by Arfophilin-2 expression despite a recent report that it interacts with the VHS domain of GGA2 (Nielsen et al., 2001).

The observation that Nuf overexpression results in largely the same phenotype is a particularly exciting finding. It is a strong indication that Nuf is functionally related to the Arfophilins and this has several important implications. Firstly it suggests a potential role for the Arfophilins in cell division and particularly cytokinesis, since Nuf exhibits cell-cycle-dependent behaviour and is required for the formation of cellularisation furrows in the *Drosophila* embryo. The findings also implicate the recycling endosomes in cytokinesis. This would be consistent with recent studies of cytokinesis in the early *Caenorhabditis elegans* embryo, where RNAi-induced suppression of Rab 11 was shown to lead to a very specific regression of the cleavage furrow at the final stage of abscission (Skop et al., 2001). There is a large body of evidence from diverse organisms that intracellularly-derived membrane delivery and syntaxin-mediated fusion is required for cytokinesis in addition to the well-characterised acto-myosin contractile mechanism (Sisson et al., 2000; Burgess et al., 1997; Conner and Wessel, 1999; Lauber et al., 1997; Jantsch-Plunger and Glotzer, 1999). It is conceivable that this membrane is delivered from/via the recycling endosomes in a Nuf/Arfophilin-regulated manner, from the centrosomal region to the cleavage site along the microtubule spindle. Since testis is a tissue undergoing a high degree of mitotic and meiotic cell division, such a role may help to explain the high level of expression observed in this tissue in the last chapter. It may also help to explain why HEK 293 cells stably expressing GFP-Arfophilin2 grow much slower than their wild-type counterparts.

Albeit indirectly, Arfs themselves have also been implicated in cell division since brefeldin A, which inhibits membrane trafficking and secretion by blocking Arf activation (Donaldson et al., 1992; Helms and Rothman, 1992; see section 1.3.2.3), also inhibits cellularisation in *Drosophila* (Sisson et al., 2000) and cytokinesis in the *Caenorhabditis elegans* embryo (Skop et al., 2001). Further circumstantial evidence is provided by the fact that Arfs also interact with the mitotic kinesin MKLP1 in a GTP-dependent manner (Boman et al., 1999), and that this motor protein is a microtubule bundling protein involved in cleavage furrow formation (Glotzer, 2001). It is found in the nucleus in interphase cells, at the spindle poles during metaphase and concentrates at the midbody and on the midzone microtubules during anaphase (Nislow et al., 1992; Sellitto and Kuriyama, 1988). Mutants of the *Drosophila* and *Caenorhabditis elegans* homologues of MKLP1, *pavarotti* and *Zen-4*, respectively, show cytokinetic defects (Adams et al., 1998; Powers et al., 1998; Raich et al., 1998). Collectively, these data could argue for a role for Arfs and Arfophilins in cytokinesis.

The fact that Arfophilins appear to be homologues of *nuclear fallout* and given that there are strong genetic interactions between *nuf* and *discontinuous actin hexagon* in *Drosophila*, prompts the investigation into a potential role for members of the related dystrobrevin family in Arfophilin-mediated events. Dystrophins and dystrobrevins form the core of large membrane- and actin-bound complexes in metazoans (reviewed in Roberts, 2001) Such an involvement might help explain the observation that some Arfophilin-2 immunoreactivity was detected at the plasma membrane. Attention should also be paid to the fact that Nuf is highly phosphorylated and exhibits cell-cycle-dependent behaviour (Rothwell et al., 1999; Rothwell et al., 1998). The Arfophilins are likely to be similarly regulated. Furthermore, their constitutive overexpression could lead to effects that normally only occur at precise points in the cell cycle, such as the accumulation of endosomes around the microtubule-organising centre (see section 1.2.3).

The differences in the distributions of TfRs/Rab11/GGA1 observed with different constructs suggest that the effects on each of these proteins are separable and, therefore, not induced by the same protein-protein interaction(s). Of the three proteins, the transferrin receptor was the commonest affected and GGA1 was the least affected. Perhaps different Arfophilins are involved in directing TfR-positive vesicles to different destinations. For example, one Arfophilin variant may sort it back to the TGN with GGA1, whereas another might sort it to the plasma membrane. It would be interesting to see whether the TfR-positive, Rab11-negative compartments induced by some constructs were positive for other Rab proteins such as Rab7, Rab9, Rab17, Rab18 and Rab20, all known to reside in sub-

compartments of the endosomal system (see Fig. 1.1.9). It would also be of interest to assess whether the absence of Rab11 results in defects in TfR trafficking, since this Rab has been implicated in its exit from recycling endosomes (Ren et al., 1998; Ullrich et al., 1996). However, this is probably not the case since the GFP-Nuf compartment did not contain Rab 11 and the TfRs seemed to traffic normally through it.

From the experiments performed to date, it is hard to draw many conclusions about the role of Arfs in Arfophilin function. The fact that similar effects were observed for GFP-Arfophilin-2 and GFP-Nuf overexpression, and given that Nuf does not seem to bind Arfs in the yeast two-hybrid system, suggests that Arf binding is secondary in the observed phenotype. On the other hand, expression of Arf5T31N in HeLa cells completely dispersed the endogenous Arfophilin-2 TGN staining implying that Arf5 regulates its membrane association. This is wholly consistent with the data presented by Shin et al. (1999), who showed that the C-terminal domain of Arfophilin-1 associates with intracellular CHO cell membranes in the presence of Arf5-GTPγS and dissociates in the presence of Arf5-GDPβS. The fact that the analogous Arf6 mutant did not disrupt the intracellular Arfophilin-2 localisation in this study argues that Arf6 does not regulate this Arfophilin-2 pool *in vivo*. Perhaps the Class II Arfs regulate Arfophilin recruitment/function at the TGN, while effects on the distribution of the recycling compartment are separate Arf-independent events. Then again, Arf6-GDP has been localised to the pericentriolar recycling endosomes by sensitive electron microscopy (D'Souza-Schorey et al., 1998), and it could potentially then interact with Arfophilins upon nucleotide exchange. Clearly a detailed analysis of the localisation of different Arfs and indeed the effects of different Arf mutations on endogenous/overexpressed Arfophilin-2 and the recycling endosomes in general is warranted. Isoform-specific Arf antibodies have been described (Cavenagh et al., 1996; West et al., 1997), and these would be highly useful reagents to help dissect the precise roles of the Arfs in these events.

The identification of further common and specific Arfophilin-1/Arfophilin-2/Nuf binding partners will be key in the elucidation of the precise cellular roles of this protein family. Yeast two-hybrid screening offers one potential and attractive method in this respect. Since similar phenotypes were observed upon overexpression of the different family members in HeLa cells, it would be predicted that they would all interact with common binding partners through their conserved C-terminal coiled-coil domains. Putative positives recovered from two-hybrid screens, could therefore be tested against all three proteins to classify them into common or specific interacting partners, the former being potentially more interesting in terms of explaining the phenotype observed in HeLa cells.

Furthermore, given that both Arfophilins are highly expressed in testis, this tissue is likely to express interacting partners at similarly high levels and therefore represents the best tissue to screen. Bait constructs encoding the C-terminal 330 amino acids of Arfophilin-1, Arfophilin-2 and Nuf have been constructed, shown not to allow trans-activation when cotransformed with an empty prey vector, and are awaiting use in such experiments.

Chapter 6

Conclusions and future directions

Arf proteins are important regulators of membrane trafficking and cytoskeletal remodelling in eukaryotic cells. It is not clear why mammalian cells possess three classes of these proteins consisting of six distinct isoforms. Most attention has been paid to the class I and III Arfs, while the class II members have been largely neglected. Recently, a class II/III Arf-interacting protein, Arfophilin, was identified but its function is unknown (Shin et al., 1999, 2001).

The work presented in this thesis has described the use of the yeast two-hybrid sytsem to identify two potential Arf effector protcins, HCR and Arfophilin-2 and the latter has been characterised in greater detail. Assuming that the Arfophilins are *bona fide* Arf effectors, this work together with that of the Exton laboratory, provides compelling evidence for the existence of specific class II Arf-regulated pathways. This in itself is a major step forward as many researchers in the field have assumed these Arfs to have merely redundant roles. Taking the situation one step further, the data presented here strongly suggest a role for the Arfophilins in regulating membrane dynamics in the *trans*-Golgi network (TGN) and/or endosomal recycling systems. This is based on the findings that endogenous Arfophilin-2 predominantly localises to a TGN compartment in HeLa cells and that expression of an N-terminally GFP-tagged or truncated mutant causes the Rab11 and transferrin receptor-positive endosomes to redistribute around the centrosome. Satisfyingly, previous studies in this laboratory using myristoylated synthetic Arf peptides suggested a role for Arf5 in regulating endosomal recycling in 3T3 L1 adipocytes (Millar et al., 1999). Hopefully, future studies will uncover the molecular basis of this regulation.

It will be important to dissect the precise roles of Arf5 and Arf6 in Arfophilin function. It has been suggested that these Arfs bind distinct sites on Arfophilin-1 (Shin et al., 2001), so it may be possible to generate mutants defective in one or both of these thus allowing the contributions of each Arf to be assessed individually. It may also be worthwhile disrupting the leucine zippers by site-directed mutagenesis and observing the effects on Arf binding and cellular phenotype.

It is particularly regrettable that a biochemical interaction between Arfophilin-2 and Arf5/Arf6 has not yet been demonstrated, and this is something that needs to be reproducibly shown despite the ~70% identity with Arfophilin-1 in the Arf-binding domain. It has been attempted unsuccessfully using several approaches including pulldown assays using bacterially produced GST-Arf proteins (mutants and wild-type, with and without GTPγS) and cell lysates overexpressing the Arfophilin-2 C-terminus. Coimmunoprecipitation of endogenous Arfophilin-2 from HeLa cells transfected with HA-

tagged Arf mutants has also failed to demonstrate binding. A direct interaction using purified His-tagged Arfophilin-2 and GST-Arfs has been problematic, primarily due to problems arising from the fact that Arfophilin-2 produced by *E. coli* often appeared as a ladder of (His-tag-positive) bands when resolved by SDS-PAGE. However, this appears to have been rectified by changing from a pQE (Qiagen) to a pET (Novagen) vector, although binding assays have not yet been attempted with this protein. It would probably be worthwhile repeating the exact method used by the Exton lab for Arfophilin-1 (Shin et al., 1999, 2001). By using Arfophilin-1 as a positive control, it should be possible to conclusively show whether Arfophilin-2 is a *bona fide* Arf binding partner. I believe that the interaction is genuine, but that the assay conditions tried so far have not been optimal. One problem may have arisen from too little protein being used to detect the interaction. Also, while an N-terminal fusion of the GAL4-binding domain with Arf in the yeast two-hybrid system supports an interaction, GST fused to the Arf N-terminus may not in pulldown experiments. In fact, it might be better if myristoylated untagged Arf proteins were used in binding experiments.

Other important challenges for future studies of Arfophilin function include the elucidation of additional Arfophilin-interacting proteins. In this respect, yeast-two hybrid screening and affinity chromatography could be fruitful approaches to take. Considering the high level of expression in testis, this would seem the logical tissue to screen. Given that highly homologous proteins are predicted from EST data in other species such as cattle, obtaining enough material for chromatography should not be problematic.

It will also be very interesting to uncover what the different roles are for the different Arfophilins. What functions do the distinct N-termini serve and where are these variants expressed? Similarly, why is the EE[H/Q]FEDYGEG motif conserved in both Arfophilin-1 and Arfophilin-2 and why is it spliced out in some variants? Why does the addition of the GFP moiety to the amino terminus of Arfophilin-2A result in a markedly different cellular phenotype? All of these questions need to be answered to obtain a more complete picture of the roles of these proteins.

The work presented here also uncovered similarities between the Arfophilins and *Drosophila* Nuclear Fallout. These include sequence homology and comparable phenotypes upon overexpression of GFP fusion proteins in HeLa cells. These data raise a whole new set of interesting questions since Nuclear Fallout is a cell-cycle regulated, highly phosphorylated protein required for cellularisation (Sullivan et al., 1993; Rothwell et al., 1998), a process akin to cytokinesis. The proposed model for the action of Nuf in

Drosophila involves it cycling between the cytosol and the centrosome, where it may regulate the association of vesicles with microtubules (see Fig. 5.1.1). This fits in nicely with the observed microtubule-dependent clustering of membranes around the centrosome described here upon GFP-Arfophilin expression. If the homology between the Arfophilins and Nuf can be extended to include the control of cytokinesis/cellularisation, and that Arfs were somehow involved in this regulation, this would be a major breakthrough in the field. As a first step, it should be relatively straightforward to monitor endogenous Arfophilins through the cell-cycle and see, for example, whether their expression, localisation and phosphorylation states are altered in different phases. Along the same lines, it would also be exciting to see whether the mammalian Arfophilins can rescue the lethal *Nuf* phenotype in *Drosophila*.

A role in cell division could explain the fact that high mRNA levels in testis were detected in a northern blot. Alternatively, this may reflect a role specific to this tissue. It would be very interesting to locate, by immunocytochemistry or *in situ* hybridisation, which cells are responsible for the high levels of expression as this could be very informative. During spermatogenesis, spermatids change from round to elongate cells in a process that involves them being translocated into apical invaginations of Sertoli cells (Beach and Vogl, 1999 and references therein). Furthermore, this translocation appears to involve microtubule-based motility (Beach and Vogl, 1999). Given the observed effects of GFP-Arfophilin-2 expression on the distribution of microtubule-associated membranes, it would be tempting to speculate that Arfophilin-2 might regulate spermatid translocation if it were found to be highly expressed in Sertoli cells.

To summarise, this thesis has uncovered and cloned a new class II/III Arf-binding protein and member of the Arfophilin family, Arfophilin-2. It has identified homologues in *Drosophila* and *C. elegans* and a high quality Arfophilin-2-specific antibody has been produced and characterised. Analysis of cultured cells has revealed that the endogenous protein is both membrane-associated and cytosolic, and is primarily localised in and around the TGN in interphase cells. Expression of GFP chimeras resulted in a dramatic and specific redistribution of the perinuclear recycling compartment to a tight pericentrosomal localisation. This phenomenon was dependent on the integrity of the microtubule cytoskeleton and did not result in gross changes in transferrin receptor recycling.

References

Achstetter,T., Franzusoff,A., Field,C., and Schekman,R. (1988). SEC7 encodes an unusual, high molecular weight protein required for membrane traffic from the yeast Golgi apparatus. J. Biol. Chem. *263*, 11711-11717.

Adams,R.R., Tavares,A.A., Salzberg,A., Bellen,H.J., and Glover,D.M. (1998). pavarotti encodes a kinesin-like protein required to organize the central spindle and contractile ring for cytokinesis. Genes Dev. *12*, 1483-1494.

Agatep,R., Kirkpatrick,R.D., Parchaliuk,D.L., Woods,R.A., and Gietz,R.D. (1998). Transformation of Saccharomyces cerevisiae by the lithium acetate/single carrier DNA/Polyethylene glycol (LiAc/ss-DNA/PEG) protocol. Technical Tips Online (http://tto. trends. com).

Ahle,S., Mann,A., Eichelsbacher,U., and Ungewickell,E. (1988). Structural relationships between clathrin assembly proteins from the Golgi and the plasma membrane. EMBO J. *7*, 919-929.

Al Awar,O., Radhakrishna,H., Powell,N.N., and Donaldson,J.G. (2000). Separation of membrane trafficking and actin remodeling functions of ARF6 with an effector domain mutant. Mol. Cell Biol. *20*, 5998-6007.

Allan,V.J. and Schroer,T.A. (1999). Membrane motors. Curr. Opin. Cell Biol. *11*, 476-482.

Altschul,S.F., Gish,W., Miller,W., Myers,E.W., and Lipman,D.J. (1990). Basic local alignment search tool. J. Mol. Biol. *215*, 403-410.

Altschuler,Y., Liu,S., Katz,L., Tang,K., Hardy,S., Brodsky,F., Apodaca,G., and Mostov,K. (1999). ADP-ribosylation factor 6 and endocytosis at the apical surface of Madin-Darby canine kidney cells. J. Cell Biol. *147*, 7-12.

Amor,J.C., Harrison,D.H., Kahn,R.A., and Ringe,D. (1994). Structure of the human ADP-ribosylation factor 1 complexed with GDP. Nature *372*, 704-708.

Aniento,F., Gu,F., Parton,R.G., and Gruenberg,J. (1996). An endosomal beta COP is involved in the pH-dependent formation of transport vesicles destined for late endosomes. J. Cell Biol. *133*, 29-41.

Antonny,B., Beraud-Dufour,S., Chardin,P., and Chabre,M. (1997). N-terminal hydrophobic residues of the G-protein ADP-ribosylation factor-1 insert into membrane phospholipids upon GDP to GTP exchange. Biochemistry *36*, 4675-4684.

Apodaca,G. (2001). Endocytic traffic in polarized epithelial cells: role of the actin and microtubule cytoskeleton. Traffic. *2*, 149-159.

Aridor,M. and Hannan,L.A. (2000). Traffic jam: a compendium of human diseases that affect intracellular transport processes. Traffic. *1*, 836-851.

Aspenstrom,P. (1997). A Cdc42 target protein with homology to the non-kinase domain of FER has a potential role in regulating the actin cytoskeleton. Curr. Biol. *7*, 479-487.

Aspenstrom,P., Lindberg,U., and Hall,A. (1996). Two GTPases, Cdc42 and Rac, bind directly to a protein implicated in the immunodeficiency disorder Wiskott-Aldrich syndrome. Curr. Biol. *6*, 70-75.

Asumalahti,K., Laitinen,T., Itkonen-Vatjus,R., Lokki,M.L., Suomela,S., Snellman,E., Saarialho-Kere,U., and Kere,J. (2000). A candidate gene for psoriasis near HLA-C, HCR (Pg8), is highly polymorphic with a disease-associated susceptibility allele. Hum. Mol. Genet. *9*, 1533-1542.

Austin,C., Hinners,I., and Tooze,S.A. (2000). Direct and GTP-dependent interaction of ADP-ribosylation factor 1 with clathrin adaptor protein AP-1 on immature secretory granules. J. Biol. Chem. *275*, 21862-21869.

Ayad,N., Hull,M., and Mellman,I. (1997). Mitotic phosphorylation of rab4 prevents binding to a specific receptor on endosome membranes. EMBO J. *16*, 4497-4507.

Bailly,E., McCaffrey,M., Touchot,N., Zahraoui,A., Goud,B., and Bornens,M. (1991). Phosphorylation of two small GTP-binding proteins of the Rab family by p34cdc2. Nature *350*, 715-718.

Bannykh,S.I., Rowe,T., and Balch,W.E. (1996). The organization of endoplasmic reticulum export complexes. J. Cell Biol. *135*, 19-35.

Barlowe,C. (2000). Traffic COPs of the early secretory pathway. Traffic. *1*, 371-377.

Barlowe,C., Orci,L., Yeung,T., Hosobuchi,M., Hamamoto,S., Salama,N., Rexach,M.F., Ravazzola,M., Amherdt,M., and Schekman,R. (1994). COPII: a membrane coat formed by Sec proteins that drive vesicle budding from the endoplasmic reticulum. Cell *77*, 895-907.

Barlowe,C. and Schekman,R. (1993). SEC12 encodes a guanine-nucleotide-exchange factor essential for transport vesicle budding from the ER. Nature *365*, 347-349.

Barr,F.A., Puype,M., Vandekerckhove,J., and Warren,G. (1997). GRASP65, a protein involved in the stacking of Golgi cisternae. Cell *91*, 253-262.

Barr,F.A. and Shorter,J. (2000). Membrane traffic: do cones mark sites of fission? Curr. Biol. *10*, R141-R144.

Barr,V.A., Phillips,S.A., Taylor,S.I., and Haft,C.R. (2000). Overexpression of a novel sorting nexin, SNX15, affects endosome morphology and protein trafficking. Traffic. *1*, 904-916.

Beach,S.F. and Vogl,A.W. (1999). Spermatid translocation in the rat seminiferous epithelium: coupling membrane trafficking machinery to a junction plaque. Biol. Reprod. *60*, 1036-1046.

Beck,K.A. and Keen,J.H. (1991). Interaction of phosphoinositide cycle intermediates with the plasma membrane-associated clathrin assembly protein AP-2. J. Biol. Chem. *266*, 4442-4447.

Benashski,S.E., Harrison,A., Patel-King,R.S., and King,S.M. (1997). Dimerization of the highly conserved light chain shared by dynein and myosin V. J. Biol. Chem. *272*, 20929-20935.

Bennett,E.M., Lin,S.X., Towler,M.C., Maxfield,F.R., and Brodsky,F.M. (2001). Clathrin hub expression affects early endosome distribution with minimal impact on receptor sorting and recycling. Mol. Biol. Cell *12*, 2790-2799.

Beraud-Dufour,S., Robineau,S., Chardin,P., Paris,S., Chabre,M., Cherfils,J., and Antonny,B. (1998). A glutamic finger in the guanine nucleotide exchange factor ARNO displaces Mg2+ and the beta-phosphate to destabilize GDP on ARF1. EMBO J. *17*, 3651-3659.

Berg,J.S., Powell,B.C., and Cheney,R.E. (2001). A millennial myosin census. Mol. Biol. Cell *12*, 780-794.

Bergeland,T., Widerberg,J., Bakke,O., and Nordeng,T.W. (2001). Mitotic partitioning of endosomes and lysosomes. Curr. Biol. *11*, 644-651.

Betz,S.F., Schnuchel,A., Wang,H., Olejniczak,E.T., Meadows,R.P., Lipsky,B.P., Harris,E.A., Staunton,D.E., and Fesik,S.W. (1998). Solution structure of the cytohesin-1 (B2-1) Sec7 domain and its interaction with the GTPase ADP ribosylation factor 1. Proc. Natl. Acad. Sci. U. S. A *95*, 7909-7914.

Bhamidipati,A., Lewis,S.A., and Cowan,N.J. (2000). ADP ribosylation factor-like protein 2 (Arl2) regulates the interaction of tubulin-folding cofactor D with native tubulin. J. Cell Biol. *149*, 1087-1096.

Bielli,A., Thornqvist,P.O., Hendrick,A.G., Finn,R., Fitzgerald,K., and McCaffrey,M.W. (2001). The small GTPase Rab4A interacts with the central region of cytoplasmic dynein light intermediate chain-1. Biochem. Biophys. Res. Commun. *281*, 1141-1153.

Black,M.W. and Pelham,H.R. (2000). A selective transport route from Golgi to late endosomes that requires the yeast GGA proteins. J. Cell Biol. *151*, 587-600.

Black,M.W. and Pelham,H.R. (2001). Membrane traffic: How do GGAs fit in with the adaptors? Curr. Biol. *11*, R460-R462.

Blomberg-Wirschell,M. and Doxsey,S.J. (1998). Rapid isolation of centrosomes. Methods Enzymol. *298*, 228-238.

Boll,W., Ohno,H., Songyang,Z., Rapoport,I., Cantley,L.C., Bonifacino,J.S., and Kirchhausen,T. (1996). Sequence requirements for the recognition of tyrosine-based endocytic signals by clathrin AP-2 complexes. EMBO J. *15*, 5789-5795.

Boman,A.L. and Kahn,R.A. (1995). Arf proteins: the membrane traffic police? Trends Biochem. Sci. *20*, 147-150.

Boman,A.L., Kuai,J., Zhu,X., Chen,J., Kuriyama,R., and Kahn,R.A. (1999). Arf proteins bind to mitotic kinesin-like protein 1 (MKLP1) in a GTP- dependent fashion. Cell Motil. Cytoskeleton *44*, 119-132.

Boman,A.L., Zhang,C., Zhu,X., and Kahn,R.A. (2000). A family of ADP-ribosylation factor effectors that can alter membrane transport through the trans-Golgi. Mol. Biol. Cell *11*, 1241-1255.

Bonifacino,J.S. and Dell'Angelica,E.C. (1999). Molecular bases for the recognition of tyrosine-based sorting signals. J. Cell Biol. *145*, 923-926.

Bose,A., Cherniack,A.D., Langille,S.E., Nicoloro,S.M., Buxton,J.M., Park,J.G., Chawla,A., and Czech,M.P. (2001). G(alpha)11 signaling through ARF6 regulates F-actin mobilization and GLUT4 glucose transporter translocation to the plasma membrane. Mol. Cell Biol. *21*, 5262-5275.

Bradford,M.M. (1976). A rapid and sensitive method for the quantitation of microgram quantities of protein utilizing the principle of protein-dye binding. Anal. Biochem. *72*, 248-254.

Brodsky,F.M., Chen,C.Y., Knuehl,C., Towler,M.C., and Wakeham,D.E. (2001). Biological basket weaving: formation and function of clathrin-coated vesicles. Annu. Rev. Cell Dev. Biol. *17*, 517-568.

Brondyk,W.H., McKiernan,C.J., Fortner,K.A., Stabila,P., Holz,R.W., and Macara,I.G. (1995). Interaction cloning of Rabin3, a novel protein that associates with the Ras-like GTPase Rab3A. Mol. Cell Biol. *15* , 1137-1143.

Brown,H.A., Gutowski,S., Moomaw,C.R., Slaughter,C., and Sternweis,P.C. (1993). ADP-ribosylation factor, a small GTP-dependent regulatory protein, stimulates phospholipase D activity. Cell *75*, 1137-1144.

Brown,M.T., Andrade,J., Radhakrishna,H., Donaldson,J.G., Cooper,J.A., and Randazzo,P.A. (1998). ASAP1, a phospholipid-dependent arf GTPase-activating protein that associates with and is phosphorylated by Src. Mol. Cell Biol. *18*, 7038-7051.

Bucci,C., Parton,R.G., Mather,I.H., Stunnenberg,H., Simons,K., Hoflack,B., and Zerial,M. (1992). The small GTPase rab5 functions as a regulatory factor in the early endocytic pathway. Cell *70*, 715-728.

Bucci,C., Thomsen,P., Nicoziani,P., McCarthy,J., and van Deurs,B. (2000). Rab7: a key to lysosome biogenesis. Mol. Biol. Cell *11*, 467-480.

Burgess,R.W., Deitcher,D.L., and Schwarz,T.L. (1997). The synaptic protein syntaxin1 is required for cellularization of Drosophila embryos. J. Cell Biol. *138*, 861-875.

Burkhardt,J.K., Echeverri,C.J., Nilsson,T., and Vallee,R.B. (1997). Overexpression of the dynamitin (p50) subunit of the dynactin complex disrupts dynein-dependent maintenance of membrane organelle distribution. J. Cell Biol. *139*, 469-484.

Busch,S.J. and Sassone-Corsi,P. (1990). Dimers, leucine zippers and DNA-binding domains. Trends Genet. *6*, 36-40.

Buss,F., Arden,S.D., Lindsay,M., Luzio,J.P., and Kendrick-Jones,J. (2001). Myosin VI isoform localized to clathrin-coated vesicles with a role in clathrin-mediated endocytosis. EMBO J. *20*, 3676-3684.

Callaghan,J., Nixon,S., Bucci,C., Toh,B.H., and Stenmark,H. (1999). Direct interaction of EEA1 with Rab5b. Eur. J. Biochem. *265*, 361-366.

Calvo,P.A., Frank,D.W., Bieler,B.M., Berson,J.F., and Marks,M.S. (1999). A cytoplasmic sequence in human tyrosinase defines a second class of di- leucine-based sorting signals for late endosomal and lysosomal delivery. J. Biol. Chem. *274*, 12780-12789.

Campbell, L. C. Green fluorescent protein as a tool to study GLUT4 trafficking. 1999. University of Glasgow. Thesis.

Cantalupo,G., Alifano,P., Roberti,V., Bruni,C.B., and Bucci,C. (2001). Rab-interacting lysosomal protein (RILP): the Rab7 effector required for transport to lysosomes. EMBO J. *20*, 683-693.

Carmena,M., Riparbelli,M.G., Minestrini,G., Tavares,A.M., Adams,R., Callaini,G., and Glover,D.M. (1998). Drosophila polo kinase is required for cytokinesis. J. Cell Biol. *143*, 659-671.

Carr,J.F. and Hinshaw,J.E. (1997). Dynamin assembles into spirals under physiological salt conditions upon the addition of GDP and gamma-phosphate analogues. J. Biol. Chem. *272*, 28030-28035.

Carroll,K.S., Hanna,J., Simon,I., Krise,J., Barbero,P., and Pfeffer,S.R. (2001). Role of Rab9 GTPase in facilitating receptor recruitment by TIP47. Science *292*, 1373-1376.

Cavenagh,M.M., Whitney,J.A., Carroll,K., Zhang,C., Boman,A.L., Rosenwald,A.G., Mellman,I., and Kahn,R.A. (1996). Intracellular distribution of Arf proteins in mammalian cells. Arf6 is uniquely localized to the plasma membrane. J. Biol. Chem. *271*, 21767-21774.

Cheatham,B., Vlahos,C.J., Cheatham,L., Wang,L., Blenis,J., and Kahn,C.R. (1994). Phosphatidylinositol 3-kinase activation is required for insulin stimulation of pp70 S6 kinase, DNA synthesis, and glucose transporter translocation. Mol. Cell Biol. *14*, 4902-4911.

Cheever,M.L., Sato,T.K., de Beer,T., Kutateladze,T.G., Emr,S.D., and Overduin,M. (2001). Phox domain interaction with PtdIns(3)P targets the Vam7 t-SNARE to vacuole membranes. Nat. Cell Biol. *3*, 613-618.

Chen,C.Y. and Graham,T.R. (1998). An arf1Delta synthetic lethal screen identifies a new clathrin heavy chain conditional allele that perturbs vacuolar protein transport in Saccharomyces cerevisiae. Genetics *150*, 577-589.

Chen,C.Y., Ingram,M.F., Rosal,P.H., and Graham,T.R. (1999). Role for Drs2p, a P-type ATPase and potential aminophospholipid translocase, in yeast late Golgi function. J. Cell Biol. *147*, 1223-1236.

Chen,H.J., Remmler,J., Delaney,J.C., Messner,D.J., and Lobel,P. (1993). Mutational analysis of the cation-independent mannose 6- phosphate/insulin-like growth factor II receptor. A consensus casein kinase II site followed by 2 leucines near the carboxyl terminus is important for intracellular targeting of lysosomal enzymes. J. Biol. Chem. *268*, 22338-22346.

Chen,H.J., Yuan,J., and Lobel,P. (1997). Systematic mutational analysis of the cation-independent mannose 6- phosphate/insulin-like growth factor II receptor cytoplasmic domain. An acidic cluster containing a key aspartate is important for function in lysosomal enzyme sorting. J. Biol. Chem. *272*, 7003-7012.

Cherfils,J., Menetrey,J., Mathieu,M., Le Bras,G., Robineau,S., Beraud-Dufour,S., Antonny,B., and Chardin,P. (1998). Structure of the Sec7 domain of the Arf exchange factor ARNO. Nature *392*, 101-105.

Christoforidis,S., McBride,H.M., Burgoyne,R.D., and Zerial,M. (1999a). The Rab5 effector EEA1 is a core component of endosome docking. Nature *397*, 621-625.

Christoforidis,S., Miaczynska,M., Ashman,K., Wilm,M., Zhao,L., Yip,S.C., Waterfield,M.D., Backer,J.M., and Zerial,M. (1999b). Phosphatidylinositol-3-OH kinases are Rab5 effectors. Nat. Cell Biol. *1*, 249-252.

Clague,M.J., Thorpe,C., and Jones,A.T. (1995). Phosphatidylinositol 3-kinase regulation of fluid phase endocytosis. FEBS Lett. *367*, 272-274.

Claing,A., Chen,W., Miller,W.E., Vitale,N., Moss,J., Premont,R.T., and Lefkowitz,R.J. (2001). Beta arrestin-mediated ARF6 activation and beta2-adrenergic receptor endocytosis. J. Biol. Chem.

Clark,J., Moore,L., Krasinskas,A., Way,J., Battey,J., Tamkun,J., and Kahn,R.A. (1993a). Selective amplification of additional members of the ADP-ribosylation factor (ARF) family: cloning of additional human and Drosophila ARF- like genes. Proc. Natl. Acad. Sci. U. S. A *90*, 8952-8956.

Clark,J., Moore,L., Krasinskas,A., Way,J., Battey,J., Tamkun,J., and Kahn,R.A. (1993b). Selective amplification of additional members of the ADP-ribosylation factor (ARF) family: cloning of additional human and Drosophila ARF- like genes. Proc. Natl. Acad. Sci. U. S. A *90*, 8952-8956.

Claude,A., Zhao,B.P., Kuziemsky,C.E., Dahan,S., Berger,S.J., Yan,J.P., Armold,A.D., Sullivan,E.M., and Melancon,P. (1999). GBF1: A novel Golgi-associated BFA-resistant guanine nucleotide exchange factor that displays specificity for ADP-ribosylation factor 5. J. Cell Biol. *146*, 71-84.

Clermont,Y., Rambourg,A., and Hermo,L. (1994). Connections between the various elements of the cis- and mid- compartments of the Golgi apparatus of early rat spermatids. Anat. Rec. *240*, 469-480.

Cockcroft,S., Thomas,G.M., Fensome,A., Geny,B., Cunningham,E., Gout,I., Hiles,I., Totty,N.F., Truong,O., and Hsuan,J.J. (1994). Phospholipase D: a downstream effector of ARF in granulocytes. Science *263*, 523-526.

Cole,N.B. and Lippincott-Schwartz,J. (1995). Organization of organelles and membrane traffic by microtubules. Curr. Opin. Cell Biol. *7*, 55-64.

Conner,S.D. and Wessel,G.M. (1999). Syntaxin is required for cell division. Mol. Biol. Cell *10*, 2735-2743.

Cormont,M., Mari,M., Galmiche,A., Hofman,P., and Marchand-Brustel,Y. (2001). A FYVE-finger-containing protein, Rabip4, is a Rab4 effector involved in early endosomal traffic. Proc. Natl. Acad. Sci. U. S. A *98*, 1637-1642.

Cosson,P. and Letourneur,F. (1994). Coatomer interaction with di-lysine endoplasmic reticulum retention motifs. Science *263*, 1629-1631.

Coy,D.L., Hancock,W.O., Wagenbach,M., and Howard,J. (1999). Kinesin's tail domain is an inhibitory regulator of the motor domain. Nat. Cell Biol. *1*, 288-292.

Cremona,O. and De Camilli,P. (2001). Phosphoinositides in membrane traffic at the synapse. J. Cell Sci. *114*, 1041-1052.

Cremona,O., Di Paolo,G., Wenk,M.R., Luthi,A., Kim,W.T., Takei,K., Daniell,L., Nemoto,Y., Shears,S.B., Flavell,R.A., McCormick,D.A., and De Camilli,P. (1999).

Essential role of phosphoinositide metabolism in synaptic vesicle recycling. Cell *99*, 179-188.

Cukierman,E., Huber,I., Rotman,M., and Cassel,D. (1995). The ARF1 GTPase-activating protein: zinc finger motif and Golgi complex localization. Science *270*, 1999-2002.

D'Souza-Schorey,C., Boshans,R.L., McDonough,M., Stahl,P.D., and van Aelst,L. (1997). A role for POR1, a Rac1-interacting protein, in ARF6-mediated cytoskeletal rearrangements. EMBO J. *16*, 5445-5454.

D'Souza-Schorey,C., Li,G., Colombo,M.I., and Stahl,P.D. (1995). A regulatory role for ARF6 in receptor-mediated endocytosis. Science *267*, 1175-1178.

D'Souza-Schorey,C. and Stahl,P.D. (1995). Myristoylation is required for the intracellular localization and endocytic function of ARF6. Exp. Cell Res. *221*, 153-159.

D'Souza-Schorey,C., van Donselaar,E., Hsu,V.W., Yang,C., Stahl,P.D., and Peters,P.J. (1998). ARF6 targets recycling vesicles to the plasma membrane: insights from an ultrastructural investigation. J. Cell Biol. *140*, 603-616.

Daro,E., Sheff,D., Gomez,M., Kreis,T., and Mellman,I. (1997). Inhibition of endosome function in CHO cells bearing a temperature- sensitive defect in the coatomer (COPI) component epsilon-COP. J. Cell Biol. *139*, 1747-1759.

Daro,E., van der,S.P., Galli,T., and Mellman,I. (1996). Rab4 and cellubrevin define different early endosome populations on the pathway of transferrin receptor recycling. Proc. Natl. Acad. Sci. U. S. A *93* , 9559-9564.

Dautry-Varsat,A. (1986). Receptor-mediated endocytosis: the intracellular journey of transferrin and its receptor. Biochimie *68*, 375-381.

De Matteis,M.A. and Morrow,J.S. (2000). Spectrin tethers and mesh in the biosynthetic pathway. J. Cell Sci. *113 (Pt 13)*, 2331-2343.

Deitz,S.B., Wu,C., Silve,S., Howell,K.E., Melancon,P., Kahn,R.A., and Franzusoff,A. (1996). Human ARF4 expression rescues sec7 mutant yeast cells. Mol. Cell Biol. *16*, 3275-3284.

Dell'Angelica,E.C., Klumperman,J., Stoorvogel,W., and Bonifacino,J.S. (1998). Association of the AP-3 adaptor complex with clathrin. Science *280*, 431-434.

Dell'Angelica,E.C., Mullins,C., and Bonifacino,J.S. (1999a). AP-4, a novel protein complex related to clathrin adaptors. J. Biol. Chem. *274*, 7278-7285.

Dell'Angelica,E.C., Ohno,H., Ooi,C.E., Rabinovich,E., Roche,K.W., and Bonifacino,J.S. (1997). AP-3: an adaptor-like protein complex with ubiquitous expression. EMBO J. *16*, 917-928.

Dell'Angelica,E.C. and Payne,G.S. (2001). Intracellular cycling of lysosomal enzyme receptors: cytoplasmic tails' tales. Cell *106*, 395-398.

Dell'Angelica,E.C., Puertollano,R., Mullins,C., Aguilar,R.C., Vargas,J.D., Hartnell,L.M., and Bonifacino,J.S. (2000). GGAs: a family of ADP ribosylation factor-binding proteins related to adaptors and associated with the Golgi complex. J. Cell Biol. *149*, 81-94.

Dell'Angelica,E.C., Shotelersuk,V., Aguilar,R.C., Gahl,W.A., and Bonifacino,J.S. (1999b). Altered trafficking of lysosomal proteins in Hermansky-Pudlak syndrome due to mutations in the beta 3A subunit of the AP-3 adaptor. Mol. Cell *3*, 11-21.

Dell,K.R., Turck,C.W., and Vale,R.D. (2000). Mitotic phosphorylation of the dynein light intermediate chain is mediated by cdc2 kinase. Traffic. *1*, 38-44.

Diaz,E. and Pfeffer,S.R. (1998). TIP47: a cargo selection device for mannose 6-phosphate receptor trafficking. Cell *93*, 433-443.

Diaz,E., Schimmoller,F., and Pfeffer,S.R. (1997). A novel Rab9 effector required for endosome-to-TGN transport. J. Cell Biol. *138*, 283-290.

Dirac-Svejstrup,A.B., Sumizawa,T., and Pfeffer,S.R. (1997). Identification of a GDI displacement factor that releases endosomal Rab GTPases from Rab-GDI. EMBO J. *16*, 465-472.

Divecha,N., Roefs,M., Halstead,J.R., D'Andrea,S., Fernandez-Borga,M., Oomen,L., Saqib,K.M., Wakelam,M.J., and D'Santos,C. (2000). Interaction of the type Ialpha PIPkinase with phospholipase D: a role for the local generation of phosphatidylinositol 4, 5-bisphosphate in the regulation of PLD2 activity. EMBO J. *19*, 5440-5449.

Don,R.H., Cox,P.T., Wainwright,B.J., Baker,K., and Mattick,J.S. (1991). 'Touchdown' PCR to circumvent spurious priming during gene amplification. Nucleic Acids Res. *19*, 4008.

Donaldson,J.G., Finazzi,D., and Klausner,R.D. (1992). Brefeldin A inhibits Golgi membrane-catalysed exchange of guanine nucleotide onto ARF protein. Nature *360*, 350-352.

Donaldson,J.G. and Jackson,C.L. (2000). Regulators and effectors of the ARF GTPases. Curr. Opin. Cell Biol. *12*, 475-482.

Drake,M.T., Zhu,Y., and Kornfeld,S. (2000). The assembly of AP-3 adaptor complex-containing clathrin-coated vesicles on synthetic liposomes. Mol. Biol. Cell *11*, 3723-3736.

Driessens,M.H., Hu,H., Nobes,C.D., Self,A., Jordens,I., Goodman,C.S., and Hall,A. (2001). Plexin-B semaphorin receptors interact directly with active Rac and regulate the actin cytoskeleton by activating Rho. Curr. Biol. *11*, 339-344.

Dulubova,I., Sugita,S., Hill,S., Hosaka,M., Fernandez,I., Sudhof,T.C., and Rizo,J. (1999). A conformational switch in syntaxin during exocytosis: role of munc18. EMBO J. *18*, 4372-4382.

Dunn,K.W. and Maxfield,F.R. (1992). Delivery of ligands from sorting endosomes to late endosomes occurs by maturation of sorting endosomes. J. Cell Biol. *117*, 301-310.

Dunn,K.W., McGraw,T.E., and Maxfield,F.R. (1989). Iterative fractionation of recycling receptors from lysosomally destined ligands in an early sorting endosome. J. Cell Biol. *109*, 3303-3314.

Ebneth,A., Godemann,R., Stamer,K., Illenberger,S., Trinczek,B., and Mandelkow,E. (1998). Overexpression of tau protein inhibits kinesin-dependent trafficking of vesicles, mitochondria, and endoplasmic reticulum: implications for Alzheimer's disease. J. Cell Biol. *143*, 777-794.

Echard,A., Jollivet,F., Martinez,O., Lacapere,J.J., Rousselet,A., Janoueix-Lerosey,I., and Goud,B. (1998). Interaction of a Golgi-associated kinesin-like protein with Rab6. Science *279*, 580-585.

Ellgaard,L. and Helenius,A. (2001). ER quality control: towards an understanding at the molecular level. Curr. Opin. Cell Biol. *13*, 431-437.

Ellson,C.D., Gobert-Gosse,S., Anderson,K.E., Davidson,K., Erdjument-Bromage,H., Tempst,P., Thuring,J.W., Cooper,M.A., Lim,Z.Y., Holmes,A.B., Gaffney,P.R., Coadwell,J., Chilvers,E.R., Hawkins,P.T., and Stephens,L.R. (2001). PtdIns(3)P regulates the neutrophil oxidase complex by binding to the PX domain of p40(phox). Nat. Cell Biol. *3*, 679-682.

Farnsworth,C.C., Seabra,M.C., Ericsson,L.H., Gelb,M.H., and Glomset,J.A. (1994). Rab geranylgeranyl transferase catalyzes the geranylgeranylation of adjacent cysteines in the small GTPases Rab1A, Rab3A, and Rab5A. Proc. Natl. Acad. Sci. U. S. A *91*, 11963-11967.

Fasshauer,D., Sutton,R.B., Brunger,A.T., and Jahn,R. (1998). Conserved structural features of the synaptic fusion complex: SNARE proteins reclassified as Q- and R-SNAREs. Proc. Natl. Acad. Sci. U. S. A *95* , 15781-15786.

Fields,S. and Song,O. (1989). A novel genetic system to detect protein-protein interactions. Nature *340*, 245-246.

Finger,F.P. and Novick,P. (1998). Spatial regulation of exocytosis: lessons from yeast. J. Cell Biol. *142*, 609-612.

Fingerhut,A., von Figura,K., and Honing,S. (2001). Binding of AP2 to sorting signals is modulated by AP2 phosphorylation. J. Biol. Chem. *276*, 5476-5482.

Franco,M., Boretto,J., Robineau,S., Monier,S., Goud,B., Chardin,P., and Chavrier,P. (1998). ARNO3, a Sec7-domain guanine nucleotide exchange factor for ADP ribosylation factor 1, is involved in the control of Golgi structure and function. Proc. Natl. Acad. Sci. U. S. A *95*, 9926-9931.

Franco,M., Peters,P.J., Boretto,J., van Donselaar,E., Neri,A., D'Souza-Schorey,C., and Chavrier,P. (1999). EFA6, a sec7 domain-containing exchange factor for ARF6, coordinates membrane recycling and actin cytoskeleton organization. EMBO J. *18*, 1480-1491.

Frohman,M.A. and Morris,A.J. (1996). Rho is only ARF the story. Phospholipid signalling. Curr. Biol. *6*, 945-947.

Fromont-Racine,M., Rain,J.C., and Legrain,P. (1997). Toward a functional analysis of the yeast genome through exhaustive two- hybrid screens. Nat. Genet. *16*, 277-282.

Fucini,R.V., Navarrete,A., Vadakkan,C., Lacomis,L., Erdjument-Bromage,H., Tempst,P., and Stamnes,M. (2000). Activated ADP-ribosylation factor assembles distinct pools of actin on golgi membranes. J. Biol. Chem. *275*, 18824-18829.

Fukami,K., Furuhashi,K., Inagaki,M., Endo,T., Hatano,S., and Takenawa,T. (1992). Requirement of phosphatidylinositol 4,5-bisphosphate for alpha-actinin function. Nature *359*, 150-152.

Galas,M.C., Helms,J.B., Vitale,N., Thiersc,D., Aunis,D., and Bader,M.F. (1997). Regulated exocytosis in chromaffin cells. A potential role for a secretory granule-associated ARF6 protein. J. Biol. Chem. *272*, 2788-2793.

Gaschet,J. and Hsu,V.W. (1999). Distribution of ARF6 between membrane and cytosol is regulated by its GTPase cycle. J. Biol. Chem. *274*, 20040-20045.

Gaynor,E.C., Chen,C.Y., Emr,S.D., and Graham,T.R. (1998). ARF is required for maintenance of yeast Golgi and endosome structure and function. Mol. Biol. Cell *9*, 653-670.

Geli,M.I. and Riezman,H. (1996). Role of type I myosins in receptor-mediated endocytosis in yeast. Science *272*, 533-535.

Gerald,N.J., Damer,C.K., O'Halloran,T.J., and De Lozanne,A. (2001). Cytokinesis failure in clathrin-minus cells is caused by cleavage furrow instability. Cell Motil. Cytoskeleton *48*, 213-223.

Ghosh,R.N., Mallet,W.G., Soe,T.T., McGraw,T.E., and Maxfield,F.R. (1998). An endocytosed TGN38 chimeric protein is delivered to the TGN after trafficking through the endocytic recycling compartment in CHO cells. J. Cell Biol. *142*, 923-936.

Glotzer,M. (2001). Animal cell cytokinesis. Annu. Rev. Cell Dev. Biol. *17*, 351-386.

Godi,A., Santone,I., Pertile,P., Devarajan,P., Stabach,P.R., Morrow,J.S., Di Tullio,G., Polishchuk,R., Petrucci,T.C., Luini,A., and De Matteis,M.A. (1998). ADP ribosylation factor regulates spectrin binding to the Golgi complex. Proc. Natl. Acad. Sci. U. S. A *95*, 8607-8612.

Goldberg,J. (1998). Structural basis for activation of ARF GTPase: mechanisms of guanine nucleotide exchange and GTP-myristoyl switching. Cell *95*, 237-248.

Goldberg,J. (1999). Structural and functional analysis of the ARF1-ARFGAP complex reveals a role for coatomer in GTP hydrolysis. Cell *96*, 893-902.

Gorvel,J.P., Chavrier,P., Zerial,M., and Gruenberg,J. (1991). rab5 controls early endosome fusion in vitro. Cell *64*, 915-925.

Gournier,H., Stenmark,H., Rybin,V., Lippe,R., and Zerial,M. (1998). Two distinct effectors of the small GTPase Rab5 cooperate in endocytic membrane fusion. EMBO J. *17*, 1930-1940.

Grant,B., Zhang,Y., Paupard,M.C., Lin,S.X., Hall,D.H., and Hirsh,D. (2001). Evidence that RME-1, a conserved C. elegans EH-domain protein, functions in endocytic recycling. Nat. Cell Biol. *3*, 573-579.

Greasley,S.E., Jhoti,H., Teahan,C., Solari,R., Fensome,A., Thomas,G.M., Cockcroft,S., and Bax,B. (1995). The structure of rat ADP-ribosylation factor-1 (ARF-1) complexed to GDP determined from two different crystal forms. Nat. Struct. Biol. *2*, 797-806.

Gress,T.M., Muller-Pillasch,F., Geng,M., Zimmerhackl,F., Zehetner,G., Friess,H., Buchler,M., Adler,G., and Lehrach,H. (1996). A pancreatic cancer-specific expression profile. Oncogene *13*, 1819-1830.

Griffiths,G. and Simons,K. (1986). The trans Golgi network: sorting at the exit site of the Golgi complex. Science *234*, 438-443.

Gruenberg,J. and Maxfield,F.R. (1995). Membrane transport in the endocytic pathway. Curr. Opin. Cell Biol. *7*, 552-563.

Gu,F. and Gruenberg,J. (1999). Biogenesis of transport intermediates in the endocytic pathway. FEBS Lett. *452*, 61-66.

Gu,F. and Gruenberg,J. (2000). ARF1 regulates pH-dependent COP functions in the early endocytic pathway. J. Biol. Chem. *275*, 8154-8160.

Guhaniyogi,J. and Brewer,G. (2001). Regulation of mRNA stability in mammalian cells. Gene *265*, 11-23.

Guo,Q., Vasile,E., and Krieger,M. (1994). Disruptions in Golgi structure and membrane traffic in a conditional lethal mammalian cell mutant are corrected by epsilon-COP. J. Cell Biol. *125*, 1213-1224.

Guo,W., Grant,A., and Novick,P. (1999a). Exo84p is an exocyst protein essential for secretion. J. Biol. Chem. *274*, 23558-23564.

Guo,W., Roth,D., Walch-Solimena,C., and Novick,P. (1999b). The exocyst is an effector for Sec4p, targeting secretory vesicles to sites of exocytosis. EMBO J. *18*, 1071-1080.

Hall,A. (1998). Rho GTPases and the actin cytoskeleton. Science *279*, 509-514.

Haruta,T., Morris,A.J., Rose,D.W., Nelson,J.G., Mueckler,M., and Olefsky,J.M. (1995). Insulin-stimulated GLUT4 translocation is mediated by a divergent intracellular signaling pathway. J. Biol. Chem. *270*, 27991-27994.

Hata,Y., Slaughter,C.A., and Sudhof,T.C. (1993). Synaptic vesicle fusion complex contains unc-18 homologue bound to syntaxin. Nature *366*, 347-351.

Hattula,K. and Peranen,J. (2000). FIP-2, a coiled-coil protein, links Huntingtin to Rab8 and modulates cellular morphogenesis. Curr. Biol. *10*, 1603-1606.

Helenius,A. and Aebi,M. (2001). Intracellular functions of N-linked glycans. Science *291*, 2364-2369.

Helms,J.B. and Rothman,J.E. (1992). Inhibition by brefeldin A of a Golgi membrane enzyme that catalyses exchange of guanine nucleotide bound to ARF. Nature *360*, 352-354.

Hicke,L. (2001). Protein regulation by monoubiquitin. Nat. Rev. Mol. Cell Biol. *2*, 195-201.

High,S. (1995). Protein translocation at the membrane of the endoplasmic reticulum. Prog. Biophys. Mol. Biol. *63*, 233-250.

Hinshaw,J.E. and Schmid,S.L. (1995). Dynamin self-assembles into rings suggesting a mechanism for coated vesicle budding. Nature *374*, 190-192.

Hirokawa,N. (1998). Kinesin and dynein superfamily proteins and the mechanism of organelle transport. Science *279*, 519-526.

Hirst,J., Bright,N.A., Rous,B., and Robinson,M.S. (1999). Characterization of a fourth adaptor-related protein complex. Mol. Biol. Cell *10*, 2787-2802.

Hirst,J., Lui,W.W., Bright,N.A., Totty,N., Seaman,M.N., and Robinson,M.S. (2000). A family of proteins with gamma-adaptin and VHS domains that facilitate trafficking between the trans-Golgi network and the vacuole/lysosome. J. Cell Biol. *149*, 67-80.

Hoffenberg,S., Liu,X., Nikolova,L., Hall,H.S., Dai,W., Baughn,R.E., Dickey,B.F., Barbieri,M.A., Aballay,A., Stahl,P.D., and Knoll,B.J. (2000). A novel membrane-anchored Rab5 interacting protein required for homotypic endosome fusion. J. Biol. Chem. *275*, 24661-24669.

Hofmann,M.W., Honing,S., Rodionov,D., Dobberstein,B., von Figura,K., and Bakke,O. (1999). The leucine-based sorting motifs in the cytoplasmic domain of the invariant chain are recognized by the clathrin adaptors AP1 and AP2 and their medium chains. J. Biol. Chem. *274*, 36153-36158.

Holleran,E.A., Tokito,M.K., Karki,S., and Holzbaur,E.L. (1996). Centractin (ARP1) associates with spectrin revealing a potential mechanism to link dynactin to intracellular organelles. J. Cell Biol. *135*, 1815-1829.

Honda,A., Nogami,M., Yokozeki,T., Yamazaki,M., Nakamura,H., Watanabe,H., Kawamoto,K., Nakayama,K., Morris,A.J., Frohman,M.A., and Kanaho,Y. (1999). Phosphatidylinositol 4-phosphate 5-kinase alpha is a downstream effector of the small G protein ARF6 in membrane ruffle formation. Cell *99*, 521-532.

Honing,S., Sandoval,I.V., and von Figura,K. (1998). A di-leucine-based motif in the cytoplasmic tail of LIMP-II and tyrosinase mediates selective binding of AP-3. EMBO J. *17*, 1304-1314.

Hopkins,C.R. (1983). Intracellular routing of transferrin and transferrin receptors in epidermoid carcinoma A431 cells. Cell *35*, 321-330.

Hopkins,C.R., Gibson,A., Shipman,M., Strickland,D.K., and Trowbridge,I.S. (1994). In migrating fibroblasts, recycling receptors are concentrated in narrow tubules in the pericentriolar area, and then routed to the plasma membrane of the leading lamella. J. Cell Biol. *125*, 1265-1274.

Horiuchi,H., Lippe,R., McBride,H.M., Rubino,M., Woodman,P., Stenmark,H., Rybin,V., Wilm,M., Ashman,K., Mann,M., and Zerial,M. (1997). A novel Rab5 GDP/GTP exchange factor complexed to Rabaptin-5 links nucleotide exchange to effector recruitment and function. Cell *90*, 1149-1159.

Hotta,K., Tanaka,K., Mino,A., Kohno,H., and Takai,Y. (1996). Interaction of the Rho family small G proteins with kinectin, an anchoring protein of kinesin motor. Biochem. Biophys. Res. Commun. *225*, 69-74.

Hoyt,M.A., Stearns,T., and Botstein,D. (1990). Chromosome instability mutants of Saccharomyces cerevisiae that are defective in microtubule-mediated processes. Mol. Cell Biol. *10*, 223-234.

Hsu,S.C., Ting,A.E., Hazuka,C.D., Davanger,S., Kenny,J.W., Kee,Y., and Scheller,R.H. (1996). The mammalian brain rsec6/8 complex. Neuron *17*, 1209-1219.

Huang,J.D., Brady,S.T., Richards,B.W., Stenolen,D., Resau,J.H., Copeland,N.G., and Jenkins,N.A. (1999). Direct interaction of microtubule- and actin-based transport motors. Nature *397*, 267-270.

Hunziker,W. and Peters,P.J. (1998). Rab17 localizes to recycling endosomes and regulates receptor-mediated transcytosis in epithelial cells. J. Biol. Chem. *273*, 15734-15741.

Ingley,E., Williams,J.H., Walker,C.E., Tsai,S., Colley,S., Sayer,M.S., Tilbrook,P.A., Sarna,M., Beaumont,J.G., and Klinken,S.P. (1999). A novel ADP-ribosylation like factor (ARL-6), interacts with the protein-conducting channel SEC61beta subunit. FEBS Lett. *459*, 69-74.

Ishihara,H., Shibasaki,Y., Kizuki,N., Katagiri,H., Yazaki,Y., Asano,T., and Oka,Y. (1996). Cloning of cDNAs encoding two isoforms of 68-kDa type I phosphatidylinositol-4-phosphate 5-kinase. J. Biol. Chem. *271*, 23611-23614.

Ishihara,H., Shibasaki,Y., Kizuki,N., Wada,T., Yazaki,Y., Asano,T., and Oka,Y. (1998). Type I phosphatidylinositol-4-phosphate 5-kinases. Cloning of the third isoform and deletion/substitution analysis of members of this novel lipid kinase family. J. Biol. Chem. *273*, 8741-8748.

Itin,C., Ulitzur,N., Muhlbauer,B., and Pfeffer,S.R. (1999). Mapmodulin, cytoplasmic dynein, and microtubules enhance the transport of mannose 6-phosphate receptors from endosomes to the trans-golgi network. Mol. Biol. Cell *10*, 2191-2197.

Jackson,C.L. and Casanova,J.E. (2000). Turning on ARF: the Sec7 family of guanine-nucleotide-exchange factors. Trends Cell Biol. *10*, 60-67.

Jackson,T.R., Kearns,B.G., and Theibert,A.B. (2000). Cytohesins and centaurins: mediators of PI 3-kinase-regulated Arf signaling. Trends Biochem. Sci. *25*, 489-495.

James,P., Halladay,J., and Craig,E.A. (1996). Genomic libraries and a host strain designed for highly efficient two- hybrid selection in yeast. Genetics *144*, 1425-1436.

Janmey,P.A. and Stossel,T.P. (1987). Modulation of gelsolin function by phosphatidylinositol 4,5- bisphosphate. Nature *325*, 362-364.

Jantsch-Plunger,V. and Glotzer,M. (1999). Depletion of syntaxins in the early Caenorhabditis elegans embryo reveals a role for membrane fusion events in cytokinesis. Curr. Biol. *9*, 738-745.

Jarousse,N. and Kelly,R.B. (2001). Endocytotic mechanisms in synapses. Curr. Opin. Cell Biol. *13*, 461-469.

Jeng,R. and Stearns,T. (1999). Gamma-tubulin complexes: size does matter. Trends Cell Biol. *9*, 339-342.

Jin,M. and Snider,M.D. (1993). Role of microtubules in transferrin receptor transport from the cell surface to endosomes and the Golgi complex. J. Biol. Chem. *268*, 18390-18397.

Johnson,A.O., Subtil,A., Petrush,R., Kobylarz,K., Keller,S.R., and McGraw,T.E. (1998). Identification of an insulin-responsive, slow endocytic recycling mechanism in Chinese hamster ovary cells. J. Biol. Chem. *273*, 17968-17977.

Jones,D.H., Morris,J.B., Morgan,C.P., Kondo,H., Irvine,R.F., and Cockcroft,S. (2000). Type I phosphatidylinositol 4-phosphate 5-kinase directly interacts with ADP-ribosylation factor 1 and is responsible for phosphatidylinositol 4,5-bisphosphate synthesis in the golgi compartment. J. Biol. Chem. *275*, 13962-13966.

Jones,S.M., Howell,K.E., Henley,J.R., Cao,H., and McNiven,M.A. (1998). Role of dynamin in the formation of transport vesicles from the trans- Golgi network. Science *279*, 573-577.

Kahn,R.A., Clark,J., Rulka,C., Stearns,T., Zhang,C.J., Randazzo,P.A., Terui,T., and Cavenagh,M. (1995). Mutational analysis of Saccharomyces cerevisiae ARF1. J. Biol. Chem. *270*, 143-150.

Kahn,R.A. and Gilman,A.G. (1984). Purification of a protein cofactor required for ADP-ribosylation of the stimulatory regulatory component of adenylate cyclase by cholera toxin. J. Biol. Chem. *259*, 6228-6234.

Kahn,R.A. and Gilman,A.G. (1986). The protein cofactor necessary for ADP-ribosylation of Gs by cholera toxin is itself a GTP binding protein. J. Biol. Chem. *261*, 7906-7911.

Kam,J.L., Miura,K., Jackson,T.R., Gruschus,J., Roller,P., Stauffer,S., Clark,J., Aneja,R., and Randazzo,P.A. (2000). Phosphoinositide-dependent activation of the ADP-ribosylation factor GTPase-activating protein ASAP1. Evidence for the pleckstrin homology domain functioning as an allosteric site. J. Biol. Chem. *275*, 9653-9663.

Kanai,F., Liu,H., Field,S.J., Akbary,H., Matsuo,T., Brown,G.E., Cantley,L.C., and Yaffe,M.B. (2001). The PX domains of p47phox and p40phox bind to lipid products of PI(3)K. Nat. Cell Biol. *3*, 675-678.

Kanoh,H., Williger,B.T., and Exton,J.H. (1997). Arfaptin 1, a putative cytosolic target protein of ADP-ribosylation factor, is recruited to Golgi membranes. J. Biol. Chem. *272*, 5421-5429.

Kaplan,K.B., Swedlow,J.R., Varmus,H.E., and Morgan,D.O. (1992). Association of p60c-src with endosomal membranes in mammalian fibroblasts. J. Cell Biol. *118*, 321-333.

Karki,S. and Holzbaur,E.L. (1995). Affinity chromatography demonstrates a direct binding between cytoplasmic dynein and the dynactin complex. J. Biol. Chem. *270*, 28806-28811.

Karki,S. and Holzbaur,E.L. (1999). Cytoplasmic dynein and dynactin in cell division and intracellular transport. Curr. Opin. Cell Biol. *11*, 45-53.

Katzmann,D.J., Babst,M., and Emr,S.D. (2001). Ubiquitin-dependent sorting into the multivesicular body pathway requires the function of a conserved endosomal protein sorting complex, ESCRT-I. Cell *106*, 145-155.

Kim,A.S., Kakalis,L.T., Abdul-Manan,N., Liu,G.A., and Rosen,M.K. (2000). Autoinhibition and activation mechanisms of the Wiskott-Aldrich syndrome protein. Nature *404*, 151-158.

Kirchhausen,T. (2000). Clathrin. Annu. Rev. Biochem. *69*, 699-727.

Kirchhausen,T., Bonifacino,J.S., and Riezman,H. (1997). Linking cargo to vesicle formation: receptor tail interactions with coat proteins. Curr. Opin. Cell Biol. *9*, 488-495.

Klarlund,J.K., Rameh,L.E., Cantley,L.C., Buxton,J.M., Holik,J.J., Sakelis,C., Patki,V., Corvera,S., and Czech,M.P. (1998). Regulation of GRP1-catalyzed ADP ribosylation factor guanine nucleotide exchange by phosphatidylinositol 3,4,5-trisphosphate. J. Biol. Chem. *273*, 1859-1862.

Klausner,R.D., Donaldson,J.G., and Lippincott-Schwartz,J. (1992). Brefeldin A: insights into the control of membrane traffic and organelle structure. J. Cell Biol. *116*, 1071-1080.

Kondo,A., Hashimoto,S., Yano,H., Nagayama,K., Mazaki,Y., and Sabe,H. (2000). A new paxillin-binding protein, PAG3/Papalpha/KIAA0400, bearing an ADP- ribosylation factor GTPase-activating protein activity, is involved in paxillin recruitment to focal adhesions and cell migration. Mol. Biol. Cell *11*, 1315-1327.

Kooy,J., Toh,B.H., Pettitt,J.M., Erlich,R., and Gleeson,P.A. (1992). Human autoantibodies as reagents to conserved Golgi components. Characterization of a peripheral, 230-kDa compartment-specific Golgi protein. J. Biol. Chem. *267*, 20255-20263.

Kosaka,T. and Ikeda,K. (1983a). Possible temperature-dependent blockage of synaptic vesicle recycling induced by a single gene mutation in Drosophila. J. Neurobiol. *14*, 207-225.

Kosaka,T. and Ikeda,K. (1983b). Reversible blockage of membrane retrieval and endocytosis in the garland cell of the temperature-sensitive mutant of Drosophila melanogaster, shibirets1. J. Cell Biol. *97*, 499-507.

Krijnse-Locker,J., Ericsson,M., Rottier,P.J., and Griffiths,G. (1994). Characterization of the budding compartment of mouse hepatitis virus: evidence that transport from the RER to the Golgi complex requires only one vesicular transport step. J. Cell Biol. *124*, 55-70.

Ktistakis,N.T., Brown,H.A., Waters,M.G., Sternweis,P.C., and Roth,M.G. (1996). Evidence that phospholipase D mediates ADP ribosylation factor- dependent formation of Golgi coated vesicles. J. Cell Biol. *134*, 295-306.

Kuai,J., Boman,A.L., Arnold,R.S., Zhu,X., and Kahn,R.A. (2000). Effects of activated ADP-ribosylation factors on Golgi morphology require neither activation of phospholipase D1 nor recruitment of coatomer. J. Biol. Chem. *275*, 4022-4032.

Kuehn,M.J., Herrmann,J.M., and Schekman,R. (1998). COPII-cargo interactions direct protein sorting into ER-derived transport vesicles. Nature *391*, 187-190.

Kuge,O., Dascher,C., Orci,L., Rowe,T., Amherdt,M., Plutner,H., Ravazzola,M., Tanigawa,G., Rothman,J.E., and Balch,W.E. (1994). Sar1 promotes vesicle budding from the endoplasmic reticulum but not Golgi compartments. J. Cell Biol. *125*, 51-65.

Kutateladze,T.G., Ogburn,K.D., Watson,W.T., de Beer,T., Emr,S.D., Burd,C.G., and Overduin,M. (1999). Phosphatidylinositol 3-phosphate recognition by the FYVE domain. Mol. Cell *3*, 805-811.

Ladinsky,M.S. and Howell,K.E. (1992). The trans-Golgi network can be dissected structurally and functionally from the cisternae of the Golgi complex by brefeldin A. Eur. J. Cell Biol. *59*, 92-105.

Langille,S.E., Patki,V., Klarlund,J.K., Buxton,J.M., Holik,J.J., Chawla,A., Corvera,S., and Czech,M.P. (1999). ADP-ribosylation factor 6 as a target of guanine nucleotide exchange factor GRP1. J. Biol. Chem. *274*, 27099-27104.

Lantz,V.A. and Miller,K.G. (1998). A class VI unconventional myosin is associated with a homologue of a microtubule-binding protein, cytoplasmic linker protein-170, in neurons and at the posterior pole of Drosophila embryos. J. Cell Biol. *140*, 897-910.

Lapierre,L.A., Kumar,R., Hales,C.M., Navarre,J., Bhartur,S.G., Burnette,J.O., Provance,D.W., Jr., Mercer,J.A., Bahler,M., and Goldenring,J.R. (2001). Myosin vb is associated with plasma membrane recycling systems. Mol. Biol. Cell *12*, 1843-1857.

Lauber,M.H., Waizenegger,I., Steinmann,T., Schwarz,H., Mayer,U., Hwang,I., Lukowitz,W., and Jurgens,G. (1997). The Arabidopsis KNOLLE protein is a cytokinesis-specific syntaxin. J. Cell Biol. *139*, 1485-1493.

Le Borgne,R. and Hoflack,B. (1997). Mannose 6-phosphate receptors regulate the formation of clathrin-coated vesicles in the TGN. J. Cell Biol. *137*, 335-345.

Le Borgne,R. and Hoflack,B. (1998). Protein transport from the secretory to the endocytic pathway in mammalian cells. Biochim. Biophys. Acta *1404*, 195-209.

Lee,A., Frank,D.W., Marks,M.S., and Lemmon,M.A. (1999). Dominant-negative inhibition of receptor-mediated endocytosis by a dynamin-1 mutant with a defective pleckstrin homology domain. Curr. Biol. *9*, 261-264.

Lee,F.J., Moss,J., and Vaughan,M. (1992). Human and Giardia ADP-ribosylation factors (ARFs) complement ARF function in Saccharomyces cerevisiae. J. Biol. Chem. *267*, 24441-24445.

Lee,F.J., Stevens,L.A., Hall,L.M., Murtagh,J.J., Jr., Kao,Y.L., Moss,J., and Vaughan,M. (1994a). Characterization of class II and class III ADP-ribosylation factor genes and proteins in Drosophila melanogaster. J. Biol. Chem. *269*, 21555-21560.

Lee,F.J., Stevens,L.A., Kao,Y.L., Moss,J., and Vaughan,M. (1994b). Characterization of a glucose-repressible ADP-ribosylation factor 3 (ARF3) from Saccharomyces cerevisiae. J. Biol. Chem. *269*, 20931-20937.

Lee,K.S., Yuan,Y.L., Kuriyama,R., and Erikson,R.L. (1995). Plk is an M-phase-specific protein kinase and interacts with a kinesin- like protein, CHO1/MKLP-1. Mol. Cell Biol. *15*, 7143-7151.

Lee,S.Y. and Pohajdak,B. (2000). N-terminal targeting of guanine nucleotide exchange factors (GEF) for ADP ribosylation factors (ARF) to the Golgi. J. Cell Sci. *113 (Pt 11)*, 1883-1889.

Lemmon,S.K. (2001). Clathrin uncoating: Auxilin comes to life. Curr. Biol. *11*, R49-R52.

Lewis,M.J. and Pelham,H.R. (1992). Ligand-induced redistribution of a human KDEL receptor from the Golgi complex to the endoplasmic reticulum. Cell *68*, 353-364.

Li,G., D'Souza-Schorey,C., Barbieri,M.A., Roberts,R.L., Klippel,A., Williams,L.T., and Stahl,P.D. (1995). Evidence for phosphatidylinositol 3-kinase as a regulator of endocytosis via activation of Rab5. Proc. Natl. Acad. Sci. U. S. A *92*, 10207-10211.

Lian,J.P., Stone,S., Jiang,Y., Lyons,P., and Ferro-Novick,S. (1994). Ypt1p implicated in v-SNARE activation. Nature *372*, 698-701.

Liang,J.O. and Kornfeld,S. (1997). Comparative activity of ADP-ribosylation factor family members in the early steps of coated vesicle formation on rat liver Golgi membranes. J. Biol. Chem. *272*, 4141-4148.

Lin,S.X., Grant,B., Hirsh,D., and Maxfield,F.R. (2001). Rme-1 regulates the distribution and function of the endocytic recycling compartment in mammalian cells. Nat. Cell Biol. *3*, 567-572.

Lingwood,C.A. (1993). Verotoxins and their glycolipid receptors. Adv. Lipid Res. *25*, 189-211.

Lippincott-Schwartz,J., Roberts,T.H., and Hirschberg,K. (2000). Secretory protein trafficking and organelle dynamics in living cells. Annu. Rev. Cell Dev. Biol. *16*, 557-589.

Lippincott-Schwartz,J., Snapp,E., and Kenworthy,A. (2001). Studying protein dynamics in living cells. Nat. Rev. Mol. Cell Biol. *2*, 444-456.

Lippincott-Schwartz,J., Yuan,L., Tipper,C., Amherdt,M., Orci,L., and Klausner,R.D. (1991). Brefeldin A's effects on endosomes, lysosomes, and the TGN suggest a general mechanism for regulating organelle structure and membrane traffic. Cell *67*, 601-616.

Lippincott-Schwartz,J., Yuan,L.C., Bonifacino,J.S., and Klausner,R.D. (1989). Rapid redistribution of Golgi proteins into the ER in cells treated with brefeldin A: evidence for membrane cycling from Golgi to ER. Cell *56*, 801-813.

Liscovitch,M., Czarny,M., Fiucci,G., and Tang,X. (2000). Phospholipase D: molecular and cell biology of a novel gene family. Biochem. J. *345 Pt 3*, 401-415.

Liu,S.H., Towler,M.C., Chen,E., Chen,C.Y., Song,W., Apodaca,G., and Brodsky,F.M. (2001). A novel clathrin homolog that co-distributes with cytoskeletal components functions in the trans-Golgi network. EMBO J. *20*, 272-284.

Lombardi,D., Soldati,T., Riederer,M.A., Goda,Y., Zerial,M., and Pfeffer,S.R. (1993). Rab9 functions in transport between late endosomes and the trans Golgi network. EMBO J. *12*, 677-682.

Lowe,M., Nakamura,N., and Warren,G. (1998a). Golgi division and membrane traffic. Trends Cell Biol. *8*, 40-44.

Lowe,M., Rabouille,C., Nakamura,N., Watson,R., Jackman,M., Jamsa,E., Rahman,D., Pappin,D.J., and Warren,G. (1998b). Cdc2 kinase directly phosphorylates the cis-Golgi matrix protein GM130 and is required for Golgi fragmentation in mitosis. Cell *94*, 783-793.

Lowe,S.L., Wong,S.H., and Hong,W. (1996). The mammalian ARF-like protein 1 (Arl1) is associated with the Golgi complex. J. Cell Sci. *109 (Pt 1)*, 209-220.

Lucocq,J.M. and Warren,G. (1987). Fragmentation and partitioning of the Golgi apparatus during mitosis in HeLa cells. EMBO J. *6*, 3239-3246.

Lupashin,V.V. and Waters,M.G. (1997). t-SNARE activation through transient interaction with a rab-like guanosine triphosphatase. Science *276*, 1255-1258.

Lutcke,A., Jansson,S., Parton,R.G., Chavrier,P., Valencia,A., Huber,L.A., Lehtonen,E., and Zerial,M. (1993). Rab17, a novel small GTPase, is specific for epithelial cells and is induced during cell polarization. J. Cell Biol. *121*, 553-564.

Luzio,J.P., Brake,B., Banting,G., Howell,K.E., Braghetta,P., and Stanley,K.K. (1990). Identification, sequencing and expression of an integral membrane protein of the trans-Golgi network (TGN38). Biochem. J. *270*, 97-102.

Luzio,J.P., Rous,B.A., Bright,N.A., Pryor,P.R., Mullock,B.M., and Piper,R.C. (2000). Lysosome-endosome fusion and lysosome biogenesis. J. Cell Sci. *113 (Pt 9)*, 1515-1524.

Ma,L., Cantley,L.C., Janmey,P.A., and Kirschner,M.W. (1998). Corequirement of specific phosphoinositides and small GTP-binding protein Cdc42 in inducing actin assembly in Xenopus egg extracts. J. Cell Biol. *140*, 1125-1136.

Macia,E., Chabre,M., and Franco,M. (2001). Specificities for the small G proteins ARF1 and ARF6 of the guanine nucleotide exchange factors ARNO and EFA6. J. Biol. Chem. *276*, 24925-24930.

Madaule,P., Furuyashiki,T., Reid,T., Ishizaki,T., Watanabe,G., Morii,N., and Narumiya,S. (1995). A novel partner for the GTP-bound forms of rho and rac. FEBS Lett. *377*, 243-248.

Mallard,F., Antony,C., Tenza,D., Salamero,J., Goud,B., and Johannes,L. (1998). Direct pathway from early/recycling endosomes to the Golgi apparatus revealed through the study of shiga toxin B-fragment transport. J. Cell Biol. *143*, 973-990.

Mallet,W.G. and Maxfield,F.R. (1999). Chimeric forms of furin and TGN38 are transported with the plasma membrane in the trans-Golgi network via distinct endosomal pathways. J. Cell Biol. *146*, 345-359.

Mammoto,A., Ohtsuka,T., Hotta,I., Sasaki,T., and Takai,Y. (1999). Rab11BP/Rabphilin-11, a downstream target of rab11 small G protein implicated in vesicle recycling. J. Biol. Chem. *274*, 25517-25524.

Mammoto,A., Sasaki,T., Kim,Y., and Takai,Y. (2000). Physical and functional interaction of rabphilin-11 with mammalian Sec13 protein. Implication in vesicle trafficking. J. Biol. Chem. *275*, 13167-13170.

Mandiyan,V., Andreev,J., Schlessinger,J., and Hubbard,S.R. (1999). Crystal structure of the ARF-GAP domain and ankyrin repeats of PYK2- associated protein beta. EMBO J. *18*, 6890-6898.

Marks,B., Stowell,M.H., Vallis,Y., Mills,I.G., Gibson,A., Hopkins,C.R., and McMahon,H.T. (2001). GTPase activity of dynamin and resulting conformation change are essential for endocytosis. Nature *410*, 231-235.

Marks,M.S. and Seabra,M.C. (2001). The melanosome: membrane dynamics in black and white. Nat. Rev. Mol. Cell Biol. *2*, 738-748.

Marsh,E.W., Leopold,P.L., Jones,N.L., and Maxfield,F.R. (1995). Oligomerized transferrin receptors are selectively retained by a lumenal sorting signal in a long-lived endocytic recycling compartment. J. Cell Biol. *129*, 1509-1522.

Martin,T.F. (2001). PI(4,5)P(2) regulation of surface membrane traffic. Curr. Opin. Cell Biol. *13*, 493-499.

Martys,J.L., Wjasow,C., Gangi,D.M., Kielian,M.C., McGraw,T.E., and Backer,J.M. (1996). Wortmannin-sensitive trafficking pathways in Chinese hamster ovary cells. Differential effects on endocytosis and lysosomal sorting. J. Biol. Chem. *271*, 10953-10962.

Matsuoka,K., Morimitsu,Y., Uchida,K., and Schekman,R. (1998a). Coat assembly directs v-SNARE concentration into synthetic COPII vesicles. Mol. Cell *2*, 703-708.

Matsuoka,K., Orci,L., Amherdt,M., Bednarek,S.Y., Hamamoto,S., Schekman,R., and Yeung,T. (1998b). COPII-coated vesicle formation reconstituted with purified coat proteins and chemically defined liposomes. Cell *93*, 263-275.

Mayer,A., Wickner,W., and Haas,A. (1996). Sec18p (NSF)-driven release of Sec17p (alpha-SNAP) can precede docking and fusion of yeast vacuoles. Cell *85*, 83-94.

Mayor,S., Presley,J.F., and Maxfield,F.R. (1993). Sorting of membrane components from endosomes and subsequent recycling to the cell surface occurs by a bulk flow process. J. Cell Biol. *121*, 1257-1269.

Mazaki,Y., Hashimoto,S., Okawa,K., Tsubouchi,A., Nakamura,K., Yagi,R., Yano,H., Kondo,A., Iwamatsu,A., Mizoguchi,A., and Sabe,H. (2001). An ADP-ribosylation factor GTPase-activating protein Git2- short/KIAA0148 is involved in subcellular localization of paxillin and actin cytoskeletal organization. Mol. Biol. Cell *12*, 645-662.

McLauchlan,H., Newell,J., Morrice,N., Osborne,A., West,M., and Smythe,E. (1998). A novel role for Rab5-GDI in ligand sequestration into clathrin-coated pits. Curr. Biol. *8*, 34-45.

McNiven,M.A., Cao,H., Pitts,K.R., and Yoon,Y. (2000). The dynamin family of mechanoenzymes: pinching in new places. Trends Biochem. Sci. *25*, 115-120.

Mellman,I. (1996). Endocytosis and molecular sorting. Annu. Rev. Cell Dev. Biol. *12*, 575-625.

Menetrey,J., Macia,E., Pasqualato,S., Franco,M., and Cherfils,J. (2000). Structure of Arf6-GDP suggests a basis for guanine nucleotide exchange factors specificity. Nat. Struct. Biol. *7*, 466-469.

Merrifield,C.J., Moss,S.E., Ballestrem,C., Imhof,B.A., Giese,G., Wunderlich,I., and Almers,W. (1999). Endocytic vesicles move at the tips of actin tails in cultured mast cells. Nat. Cell Biol. *1*, 72-74.

Miki,H., Miura,K., and Takenawa,T. (1996). N-WASP, a novel actin-depolymerizing protein, regulates the cortical cytoskeletal rearrangement in a PIP2-dependent manner downstream of tyrosine kinases. EMBO J. *15*, 5326-5335.

Millar,C.A., Powell,K.A., Hickson,G.R., Bader,M.F., and Gould,G.W. (1999). Evidence for a role for ADP-ribosylation factor 6 in insulin-stimulated glucose transporter-4 (GLUT4) trafficking in 3T3-L1 adipocytes. J. Biol. Chem. *274*, 17619-17625.

Miller,K.G. and Kiehart,D.P. (1995). Fly division. J. Cell Biol. *131*, 1-5.

Misumi,Y., Sohda,M., Yano,A., Fujiwara,T., and Ikehara,Y. (1997). Molecular characterization of GCP170, a 170-kDa protein associated with the cytoplasmic face of the Golgi membrane. J. Biol. Chem. *272*, 23851-23858.

Mitchison,T.J. and Kirschner,M.W. (1986). Isolation of mammalian centrosomes. Methods Enzymol. *134*, 261-268.

Monier,S., Chardin,P., Robineau,S., and Goud,B. (1998). Overexpression of the ARF1 exchange factor ARNO inhibits the early secretory pathway and causes the disassembly of the Golgi complex. J. Cell Sci. *111 (Pt 22)*, 3427-3436.

Morinaga,N., Adamik,R., Moss,J., and Vaughan,M. (1999). Brefeldin A inhibited activity of the sec7 domain of p200, a mammalian guanine nucleotide-exchange protein for ADP-ribosylation factors. J. Biol. Chem. *274*, 17417-17423.

Mossessova,E., Gulbis,J.M., and Goldberg,J. (1998). Structure of the guanine nucleotide exchange factor Sec7 domain of human arno and analysis of the interaction with ARF GTPase. Cell *92*, 415-423.

Mukherjee,S., Gurevich,V.V., Jones,J.C., Casanova,J.E., Frank,S.R., Maizels,E.T., Bader,M.F., Kahn,R.A., Palczewski,K., Aktories,K., and Hunzicker-Dunn,M. (2000). The ADP ribosylation factor nucleotide exchange factor ARNO promotes beta-arrestin release necessary for luteinizing hormone/choriogonadotropin receptor desensitization. Proc. Natl. Acad. Sci. U. S. A *97*, 5901-5906.

Mukherjee,S., Soe,T.T., and Maxfield,F.R. (1999). Endocytic sorting of lipid analogues differing solely in the chemistry of their hydrophobic tails. J. Cell Biol. *144*, 1271-1284.

Muniz,M., Morsomme,P., and Riezman,H. (2001). Protein sorting upon exit from the endoplasmic reticulum. Cell *104*, 313-320.

Munro,S. and Pelham,H.R. (1987). A C-terminal signal prevents secretion of luminal ER proteins. Cell *48*, 899-907.

Muresan,V., Stankewich,M.C., Steffen,W., Morrow,J.S., Holzbaur,E.L., and Schnapp,B.J. (2001). Dynactin-dependent, dynein-driven vesicle transport in the absence of membrane proteins: a role for spectrin and acidic phospholipids. Mol. Cell *7*, 173-183.

Murtagh,J.J., Jr., Lee,F.J., Deak,P., Hall,L.M., Monaco,L., Lee,C.M., Stevens,L.A., Moss,J., and Vaughan,M. (1993). Molecular characterization of a conserved, guanine nucleotide-dependent ADP-ribosylation factor in Drosophila melanogaster. Biochemistry *32*, 6011-6018.

Nakagawa,T., Setou,M., Seog,D., Ogasawara,K., Dohmae,N., Takio,K., and Hirokawa,N. (2000). A novel motor, KIF13A, transports mannose-6-phosphate receptor to plasma membrane through direct interaction with AP-1 complex. Cell *103*, 569-581.

Nakano,A., Brada,D., and Schekman,R. (1988). A membrane glycoprotein, Sec12p, required for protein transport from the endoplasmic reticulum to the Golgi apparatus in yeast. J. Cell Biol. *107*, 851-863.

Newman,C.M., Giannakouros,T., Hancock,J.F., Fawell,E.H., Armstrong,J., and Magee,A.I. (1992). Post-translational processing of Schizosaccharomyces pombe YPT proteins. J. Biol. Chem. *267*, 11329-11336.

Nicoziani,P., Vilhardt,F., Llorente,A., Hilout,L., Courtoy,P.J., Sandvig,K., and van Deurs,B. (2000). Role for dynamin in late endosome dynamics and trafficking of the cation-independent mannose 6-phosphate receptor. Mol. Biol. Cell *11*, 481-495.

Nielsen,E., Severin,F., Backer,J.M., Hyman,A.A., and Zerial,M. (1999). Rab5 regulates motility of early endosomes on microtubules. Nat. Cell Biol. *1*, 376-382.

Nielsen,M.S., Madsen,P., Christensen,E.I., Nykjaer,A., Gliemann,J., Kasper,D., Pohlmann,R., and Petersen,C.M. (2001). The sortilin cytoplasmic tail conveys Golgi-endosome transport and binds the VHS domain of the GGA2 sorting protein. EMBO J. *20*, 2180-2190.

Nigg,E.A. (1998). Polo-like kinases: positive regulators of cell division from start to finish. Curr. Opin. Cell Biol. *10*, 776-783.

Nislow,C., Lombillo,V.A., Kuriyama,R., and McIntosh,J.R. (1992). A plus-end-directed motor enzyme that moves antiparallel microtubules in vitro localizes to the interzone of mitotic spindles. Nature *359*, 543-547.

Niswonger,M.L. and O'Halloran,T.J. (1997). A novel role for clathrin in cytokinesis. Proc. Natl. Acad. Sci. U. S. A *94*, 8575-8578.

Norman,J.C., Joncs,D., Barry,S.T., Holt,M.R., Cockcroft,S., and Critchley,D.R. (1998). ARF1 mediates paxillin recruitment to focal adhesions and potentiates Rho-stimulated stress fiber formation in intact and permeabilized Swiss 3T3 fibroblasts. J. Cell Biol. *143*, 1981-1995.

Novick,P., Field,C., and Schekman,R. (1980). Identification of 23 complementation groups required for post- translational events in the yeast secretory pathway. Cell *21*, 205-215.

Nuoffer,C., Davidson,H.W., Matteson,J., Meinkoth,J., and Balch,W.E. (1994). A GDP-bound of rab1 inhibits protein export from the endoplasmic reticulum and transport between Golgi compartments. J. Cell Biol. *125*, 225-237.

O'Halloran,T.J. (2000). Membrane traffic and cytokinesis. Traffic. *1*, 921-926.

Ohno,H., Aguilar,R.C., Yeh,D., Taura,D., Saito,T., and Bonifacino,J.S. (1998). The medium subunits of adaptor complexes recognize distinct but overlapping sets of tyrosine-based sorting signals. J. Biol. Chem. *273*, 25915-25921.

Ohno,H., Fournier,M.C., Poy,G., and Bonifacino,J.S. (1996). Structural determinants of interaction of tyrosine-based sorting signals with the adaptor medium chains. J. Biol. Chem. *271*, 29009-29015.

Ohno,H., Stewart,J., Fournier,M.C., Bosshart,H., Rhee,I., Miyatake,S., Saito,T., Gallusser,A., Kirchhausen,T., and Bonifacino,J.S. (1995). Interaction of tyrosine-based sorting signals with clathrin-associated proteins. Science *269*, 1872-1875.

Olkkonen,V.M. and Ikonen,E. (2000). Genetic defects of intracellular-membrane transport. N. Engl. J. Med. *343*, 1095-1104.

Olusanya,O., Andrews,P.D., Swedlow,J.R., and Smythe,E. (2001). Phosphorylation of threonine 156 of the &mgr;2 subunit of the AP2 complex is essential for endocytosis in vitro and in vivo. Curr. Biol. *11*, 896-900.

Ooi,C.E., Dell'Angelica,E.C., and Bonifacino,J.S. (1998). ADP-Ribosylation factor 1 (ARF1) regulates recruitment of the AP-3 adaptor complex to membranes. J. Cell Biol. *142*, 391-402.

Orci,L., Palmer,D.J., Amherdt,M., and Rothman,J.E. (1993). Coated vesicle assembly in the Golgi requires only coatomer and ARF proteins from the cytosol. Nature *364*, 732-734.

Orzech,E., Livshits,L., Leyt,J., Okhrimenko,H., Reich,V., Cohen,S., Weiss,A., Melamed-Book,N., Lebendiker,M., Altschuler,Y., and Aroeti,B. (2001). Interactions between adaptor protein-1 of the clathrin coat and microtubules via type 1a microtubule-associated proteins. J. Biol. Chem. *276*, 31340-31348.

Ossig,R., Laufer,W., Schmitt,H.D., and Gallwitz,D. (1995). Functionality and specific membrane localization of transport GTPases carrying C-terminal membrane anchors of synaptobrevin-like proteins. EMBO J. *14*, 3645-3653.

Oude Weernink,P.A., Schulte,P., Guo,Y., Wetzel,J., Amano,M., Kaibuchi,K., Haverland,S., Voss,M., Schmidt,M., Mayr,G.W., and Jakobs,K.H. (2000). Stimulation of phosphatidylinositol-4-phosphate 5-kinase by Rho-kinase. J. Biol. Chem. *275*, 10168-10174.

Palade,G. (1975). Intracellular aspects of the process of protein synthesis. Science *189*, 347-358.

Palmer,D.J., Helms,J.B., Beckers,C.J., Orci,L., and Rothman,J.E. (1993). Binding of coatomer to Golgi membranes requires ADP-ribosylation factor. J. Biol. Chem. *268*, 12083-12089.

Parchaliuk,D.L., Kirkpatrick,R.D., Agatep,R., Simon,S.L., and Gietz,R.D. (1999). Yeast two-hybrid screening. Technical Tips Online (http://tto. trends. com).

Pasqualato,S., Menetrey,J., Franco,M., and Cherfils,J. (2001). The structural GDP/GTP cycle of human Arf6. EMBO Rep. *2*, 234-238.

Pelham,H.R. and Rothman,J.E. (2000). The debate about transport in the Golgi--two sides of the same coin? Cell *102*, 713-719.

Peters,P.J., Hsu,V.W., Ooi,C.E., Finazzi,D., Teal,S.B., Oorschot,V., Donaldson,J.G., and Klausner,R.D. (1995). Overexpression of wild-type and mutant ARF1 and ARF6: distinct perturbations of nonoverlapping membrane compartments. J. Cell Biol. *128*, 1003-1017.

Pevsner,J., Hsu,S.C., and Scheller,R.H. (1994). n-Sec1: a neural-specific syntaxin-binding protein. Proc. Natl. Acad. Sci. U. S. A *91*, 1445-1449.

Peyroche,A., Antonny,B., Robineau,S., Acker,J., Cherfils,J., and Jackson,C.L. (1999). Brefeldin A acts to stabilize an abortive ARF-GDP-Sec7 domain protein complex: involvement of specific residues of the Sec7 domain. Mol. Cell *3*, 275-285.

Peyroche,A., Courbeyrette,R., Rambourg,A., and Jackson,C.L. (2001). The ARF exchange factors Gea1p and Gea2p regulate Golgi structure and function in yeast. J. Cell Sci. *114*, 2241-2253.

Peyroche,A., Paris,S., and Jackson,C.L. (1996). Nucleotide exchange on ARF mediated by yeast Gea1 protein. Nature *384*, 479-481.

Pierre,P., Scheel,J., Rickard,J.E., and Kreis,T.E. (1992). CLIP-170 links endocytic vesicles to microtubules. Cell *70*, 887-900.

Pirone,D.M., Fukuhara,S., Gutkind,J.S., and Burbelo,P.D. (2000). SPECs, small binding proteins for Cdc42. J. Biol. Chem. *275* , 22650-22656.

Podos,S.D., Reddy,P., Ashkenas,J., and Krieger,M. (1994). LDLC encodes a brefeldin A-sensitive, peripheral Golgi protein required for normal Golgi function. J. Cell Biol. *127*, 679-691.

Ponka,P. and Lok,C.N. (1999). The transferrin receptor: role in health and disease. Int. J. Biochem. Cell Biol. *31*, 1111-1137.

Ponting,C.P. (1996). Novel domains in NADPH oxidase subunits, sorting nexins, and PtdIns 3- kinases: binding partners of SH3 domains? Protein Sci. *5*, 2353-2357.

Powers,J., Bossinger,O., Rose,D., Strome,S., and Saxton,W. (1998). A nematode kinesin required for cleavage furrow advancement. Curr. Biol. *8*, 1133-1136.

Prekeris,R., Foletti,D.L., and Scheller,R.H. (1999). Dynamics of tubulovesicular recycling endosomes in hippocampal neurons. J. Neurosci. *19*, 10324-10337.

Prekeris,R., Klumperman,J., Chen,Y.A., and Scheller,R.H. (1998). Syntaxin 13 mediates cycling of plasma membrane proteins via tubulovesicular recycling endosomes. J. Cell Biol. *143*, 957-971.

Prekeris,R., Klumperman,J., and Scheller,R.H. (2000). A Rab11/Rip11 protein complex regulates apical membrane trafficking via recycling endosomes. Mol. Cell *6*, 1437-1448.

Premont,R.T., Claing,A., Vitale,N., Freeman,J.L., Pitcher,J.A., Patton,W.A., Moss,J., Vaughan,M., and Lefkowitz,R.J. (1998). beta2-Adrenergic receptor regulation by GIT1, a G protein-coupled receptor kinase-associated ADP ribosylation factor GTPase-activating protein. Proc. Natl. Acad. Sci. U. S. A *95*, 14082-14087.

Puertollano,R., Aguilar,R.C., Gorshkova,I., Crouch,R.J., and Bonifacino,J.S. (2001a). Sorting of mannose 6-phosphate receptors mediated by the GGAs. Science *292*, 1712-1716.

Puertollano,R., Randazzo,P.A., Presley,J.F., Hartnell,L.M., and Bonifacino,J.S. (2001b). The GGAs promote ARF-dependent recruitment of clathrin to the TGN. Cell *105*, 93-102.

Pypaert,M., Mundy,D., Souter,E., Labbe,J.C., and Warren,G. (1991). Mitotic cytosol inhibits invagination of coated pits in broken mitotic cells. J. Cell Biol. *114*, 1159-1166.

Radhakrishna,H., Al Awar,O., Khachikian,Z., and Donaldson,J.G. (1999). ARF6 requirement for Rac ruffling suggests a role for membrane trafficking in cortical actin rearrangements. J. Cell Sci. *112 (Pt 6)* , 855-866.

Radhakrishna,H., Klausner,R.D., and Donaldson,J.G. (1996). Aluminum fluoride stimulates surface protrusions in cells overexpressing the ARF6 GTPase. J. Cell Biol. *134*, 935-947.

Raiborg,C., Bache,K.G., Mehlum,A., Stang,E., and Stenmark,H. (2001). Hrs recruits clathrin to early endosomes. EMBO J. *20*, 5008-5021.

Raich,W.B., Moran,A.N., Rothman,J.H., and Hardin,J. (1998). Cytokinesis and midzone microtubule organization in Caenorhabditis elegans require the kinesin-like protein ZEN-4. Mol. Biol. Cell *9*, 2037-2049.

Randazzo,P.A. (1997a). Functional interaction of ADP-ribosylation factor 1 with phosphatidylinositol 4,5-bisphosphate. J. Biol. Chem. *272*, 7688-7692.

Randazzo,P.A. (1997b). Resolution of two ADP-ribosylation factor 1 GTPase-activating proteins from rat liver. Biochem. J. *324 (Pt 2)*, 413-419.

Randazzo,P.A., Andrade,J., Miura,K., Brown,M.T., Long,Y.Q., Stauffer,S., Roller,P., and Cooper,J.A. (2000). The Arf GTPase-activating protein ASAP1 regulates the actin cytoskeleton. Proc. Natl. Acad. Sci. U. S. A *97*, 4011-4016.

Randazzo,P.A. and Kahn,R.A. (1994). GTP hydrolysis by ADP-ribosylation factor is dependent on both an ADP- ribosylation factor GTPase-activating protein and acid phospholipids. J. Biol. Chem. *269*, 10758-10763.

Randazzo,P.A., Terui,T., Sturch,S., Fales,H.M., Ferrige,A.G., and Kahn,R.A. (1995). The myristoylated amino terminus of ADP-ribosylation factor 1 is a phospholipid- and GTP-sensitive switch. J. Biol. Chem. *270*, 14809-14815.

Rapoport,I., Chen,Y.C., Cupers,P., Shoelson,S.E., and Kirchhausen,T. (1998). Dileucine-based sorting signals bind to the beta chain of AP-1 at a site distinct and regulated differently from the tyrosine-based motif- binding site. EMBO J. *17*, 2148-2155.

Rapoport,I., Miyazaki,M., Boll,W., Duckworth,B., Cantley,L.C., Shoelson,S., and Kirchhausen,T. (1997). Regulatory interactions in the recognition of endocytic sorting signals by AP-2 complexes. EMBO J. *16* , 2240-2250.

Raposo,G., Cordonnier,M.N., Tenza,D., Menichi,B., Durrbach,A., Louvard,D., and Coudrier,E. (1999). Association of myosin I alpha with endosomes and lysosomes in mammalian cells. Mol. Biol. Cell *10*, 1477-1494.

Rea,S. and James,D.E. (1997). Moving GLUT4: the biogenesis and trafficking of GLUT4 storage vesicles. Diabetes *46*, 1667-1677.

Reid,T., Furuyashiki,T., Ishizaki,T., Watanabe,G., Watanabe,N., Fujisawa,K., Morii,N., Madaule,P., and Narumiya,S. (1996). Rhotekin, a new putative target for Rho bearing homology to a serine/threonine kinase, PKN, and rhophilin in the rho-binding domain. J. Biol. Chem. *271*, 13556-13560.

Ren,M., Xu,G., Zeng,J., Lemos-Chiarandini,C., Adesnik,M., and Sabatini,D.D. (1998). Hydrolysis of GTP on rab11 is required for the direct delivery of transferrin from the pericentriolar recycling compartment to the cell surface but not from sorting endosomes. Proc. Natl. Acad. Sci. U. S. A *95*, 6187-6192.

Ren,M., Zeng,J., Lemos-Chiarandini,C., Rosenfeld,M., Adesnik,M., and Sabatini,D.D. (1996). In its active form, the GTP-binding protein rab8 interacts with a stress-activated protein kinase. Proc. Natl. Acad. Sci. U. S. A *93*, 5151-5155.

Riederer,M.A., Soldati,T., Shapiro,A.D., Lin,J., and Pfeffer,S.R. (1994). Lysosome biogenesis requires Rab9 function and receptor recycling from endosomes to the trans-Golgi network. J. Cell Biol. *125*, 573-582.

Riva,P., Corrado,L., Natacci,F., Castorina,P., Wu,B.L., Schneider,G.H., Clementi,M., Tenconi,R., Korf,B.R., and Larizza,L. (2000). NF1 microdeletion syndrome: refined FISH characterization of sporadic and familial deletions with locus-specific probes. Am. J. Hum. Genet. *66*, 100-109.

Roberts,R.G. (2001). Dystrophins and dystrobrevins. Genome Biol. *2*, REVIEWS3006.

Robertson,A.M. and Allan,V.J. (2000). Brefeldin A-dependent membrane tubule formation reconstituted in vitro is driven by a cell cycle-regulated microtubule motor. Mol. Biol. Cell *11*, 941-955.

Robineau,S., Chabre,M., and Antonny,B. (2000). Binding site of brefeldin A at the interface between the small G protein ADP-ribosylation factor 1 (ARF1) and the nucleotide-exchange factor Sec7 domain. Proc. Natl. Acad. Sci. U. S. A *97*, 9913-9918.

Robinson,M.S. and Bonifacino,J.S. (2001). Adaptor-related proteins. Curr. Opin. Cell Biol. *13*, 444-453.

Robinson,M.S. and Pearse,B.M. (1986). Immunofluorescent localization of 100K coated vesicle proteins. J. Cell Biol. *102*, 48-54.

Rodionov,D.G. and Bakke,O. (1998). Medium chains of adaptor complexes AP-1 and AP-2 recognize leucine- based sorting signals from the invariant chain. J. Biol. Chem. *273*, 6005-6008.

Rohatgi,R., Ma,L., Miki,H., Lopez,M., Kirchhausen,T., Takenawa,T., and Kirschner,M.W. (1999). The interaction between N-WASP and the Arp2/3 complex links Cdc42- dependent signals to actin assembly. Cell *97*, 221-231.

Rossanese,O.W. and Glick,B.S. (2001). Deconstructing golgi inheritance. Traffic. *2*, 589-596.

Roth,M.G. (1999). Inheriting the Golgi. Cell *99*, 559-562.

Rothman,J.E. and Wieland,F.T. (1996). Protein sorting by transport vesicles. Science *272*, 227-234.

Rothwell,W.F., Fogarty,P., Field,C.M., and Sullivan,W. (1998). Nuclear-fallout, a Drosophila protein that cycles from the cytoplasm to the centrosomes, regulates cortical microfilament organization. Development *125*, 1295-1303.

Rothwell,W.F. and Sullivan,W. (2000). The centrosome in early Drosophila embryogenesis. Curr. Top. Dev. Biol. *49*, 409-447.

Rothwell,W.F., Zhang,C.X., Zelano,C., Hsieh,T.S., and Sullivan,W. (1999). The Drosophila centrosomal protein Nuf is required for recruiting Dah, a membrane associated protein, to furrows in the early embryo. J. Cell Sci. *112 (Pt 17)*, 2885-2893.

Rouille,Y., Rohn,W., and Hoflack,B. (2000). Targeting of lysosomal proteins. Semin. Cell Dev. Biol. *11*, 165-171.

Rozelle,A.L., Machesky,L.M., Yamamoto,M., Driessens,M.H., Insall,R.H., Roth,M.G., Luby-Phelps,K., Marriott,G., Hall,A., and Yin,H.L. (2000). Phosphatidylinositol 4,5-bisphosphate induces actin-based movement of raft-enriched vesicles through WASP-Arp2/3. Curr. Biol. *10*, 311-320.

Rudge,S.A., Cavenagh,M.M., Kamath,R., Sciorra,V.A., Morris,A.J., Kahn,R.A., and Engebrecht,J. (1998). ADP-Ribosylation factors do not activate yeast phospholipase Ds but are required for sporulation. Mol. Biol. Cell *9*, 2025-2036.

Sakai,T., Yamashina,S., and Ohnishi,S. (1991). Microtubule-disrupting drugs blocked delivery of endocytosed transferrin to the cytocenter, but did not affect return of transferrin to plasma membrane. J. Biochem. (Tokyo) *109*, 528-533.

Santolini,E., Salcini,A.E., Kay,B.K., Yamabhai,M., and Di Fiore,P.P. (1999). The EH network. Exp. Cell Res. *253*, 186-209.

Santy,L.C., Frank,S.R., Hatfield,J.C., and Casanova,J.E. (1999). Regulation of ARNO nucleotide exchange by a PH domain electrostatic switch. Curr. Biol. *9*, 1173-1176.

Sasaki,T., Kikuchi,A., Araki,S., Hata,Y., Isomura,M., Kuroda,S., and Takai,Y. (1990). Purification and characterization from bovine brain cytosol of a protein that inhibits the dissociation of GDP from and the subsequent binding of GTP to smg p25A, a ras p21-like GTP-binding protein. J. Biol. Chem. *265*, 2333-2337.

Schafer,D.A., D'Souza-Schorey,C., and Cooper,J.A. (2000). Actin assembly at membranes controlled by ARF6. Traffic. *1*, 892-903.

Schafer,D.A., Gill,S.R., Cooper,J.A., Heuser,J.E., and Schroer,T.A. (1994). Ultrastructural analysis of the dynactin complex: an actin-related protein is a component of a filament that resembles F-actin. J. Cell Biol. *126*, 403-412.

Schejter,E.D. and Wieschaus,E. (1993). Functional elements of the cytoskeleton in the early Drosophila embryo. Annu. Rev. Cell Biol. *9*, 67-99.

Schekman,R. and Orci,L. (1996). Coat proteins and vesicle budding. Science *271*, 1526-1533.

Schmid,S.L., Fuchs,R., Male,P., and Mellman,I. (1988). Two distinct subpopulations of endosomes involved in membrane recycling and transport to lysosomes. Cell *52*, 73-83.

Schmidt,A., Wolde,M., Thiele,C., Fest,W., Kratzin,H., Podtelejnikov,A.V., Witke,W., Huttner,W.B., and Soling,H.D. (1999). Endophilin I mediates synaptic vesicle formation by transfer of arachidonate to lysophosphatidic acid. Nature *401*, 133-141.

Schu,P.V., Takegawa,K., Fry,M.J., Stack,J.H., Waterfield,M.D., and Emr,S.D. (1993). Phosphatidylinositol 3-kinase encoded by yeast VPS34 gene essential for protein sorting. Science *260*, 88-91.

Schurmann,A., Breiner,M., Becker,W., Huppertz,C., Kainulainen,H., Kentrup,H., and Joost,H.G. (1994). Cloning of two novel ADP-ribosylation factor-like proteins and characterization of their differential expression in 3T3-L1 cells. J. Biol. Chem. *269*, 15683-15688.

Sellitto,C. and Kuriyama,R. (1988). Distribution of a matrix component of the midbody during the cell cycle in Chinese hamster ovary cells. J. Cell Biol. *106*, 431-439.

Semenza,J.C., Hardwick,K.G., Dean,N., and Pelham,H.R. (1990). ERD2, a yeast gene required for the receptor-mediated retrieval of luminal ER proteins from the secretory pathway. Cell *61*, 1349-1357.

Sever,S., Damke,H., and Schmid,S.L. (2000). Garrotes, springs, ratchets, and whips: putting dynamin models to the test. Traffic. *1*, 385-392.

Sheff,D.R., Daro,E.A., Hull,M., and Mellman,I. (1999). The receptor recycling pathway contains two distinct populations of early endosomes with different sorting functions. J. Cell Biol. *145*, 123-139.

Shin,O.H., Couvillon,A.D., and Exton,J.H. (2001). Arfophilin is a common target of both class II and class III ADP- ribosylation factors. Biochemistry *40*, 10846-10852.

Shin,O.H. and Exton,J.H. (2001). Differential binding of arfaptin 2/POR1 to ADP-ribosylation factors and Rac1. Biochem. Biophys. Res. Commun. *285*, 1267-1273.

Shin,O.H., Ross,A.H., Mihai,I., and Exton,J.H. (1999). Identification of arfophilin, a target protein for GTP-bound class II ADP-ribosylation factors. J. Biol. Chem. *274*, 36609-36615.

Silletta,M.G., Di Girolamo,M., Fiucci,G., Weigert,R., Mironov,A., De Matteis,M.A., Luini,A., and Corda,D. (1997). Possible role of BARS-50, a substrate of brefeldin A-dependent mono-ADP- ribosylation, in intracellular transport. Adv. Exp. Med. Biol. *419*, 321-330.

Simon,J.P., Ivanov,I.E., Shopsin,B., Hersh,D., Adesnik,M., and Sabatini,D.D. (1996). The in vitro generation of post-Golgi vesicles carrying viral envelope glycoproteins requires an ARF-like GTP-binding protein and a protein kinase C associated with the Golgi apparatus. J. Biol. Chem. *271*, 16952-16961.

Simonsen,A., Lippe,R., Christoforidis,S., Gaullier,J.M., Brech,A., Callaghan,J., Toh,B.H., Murphy,C., Zerial,M., and Stenmark,H. (1998). EEA1 links PI(3)K function to Rab5 regulation of endosome fusion. Nature *394*, 494-498.

Simonsen,A., Wurmser,A.E., Emr,S.D., and Stenmark,H. (2001). The role of phosphoinositides in membrane transport. Curr. Opin. Cell Biol. *13*, 485-492.

Simpson,F., Bright,N.A., West,M.A., Newman,L.S., Darnell,R.B., and Robinson,M.S. (1996). A novel adaptor-related protein complex. J. Cell Biol. *133*, 749-760.

Simpson,F., Peden,A.A., Christopoulou,L., and Robinson,M.S. (1997). Characterization of the adaptor-related protein complex, AP-3. J. Cell Biol. *137*, 835-845.

Sisson,J.C., Field,C., Ventura,R., Royou,A., and Sullivan,W. (2000). Lava lamp, a novel peripheral golgi protein, is required for Drosophila melanogaster cellularization. J. Cell Biol. *151*, 905-918.

Skop,A.R., Bergmann,D., Mohler,W.A., and White,J.G. (2001). Completion of cytokinesis in C. elegans requires a brefeldin A- sensitive membrane accumulation at the cleavage furrow apex. Curr. Biol. *11*, 735-746.

Sollner,T., Whiteheart,S.W., Brunner,M., Erdjument-Bromage,H., Geromanos,S., Tempst,P., and Rothman,J.E. (1993). SNAP receptors implicated in vesicle targeting and fusion. Nature *362*, 318-324.

Sönnichsen,B., De Renzis,S., Nielsen,E., Rietdorf,J., and Zerial,M. (2000). Distinct membrane domains on endosomes in the recycling pathway visualized by multicolor imaging of Rab4, Rab5, and Rab11. J. Cell Biol. *149*, 901-914.

Spiro,D.J., Boll,W., Kirchhausen,T., and Wessling-Resnick,M. (1996). Wortmannin alters the transferrin receptor endocytic pathway in vivo and in vitro. Mol. Biol. Cell *7*, 355-367.

Springer,S. and Schekman,R. (1998). Nucleation of COPII vesicular coat complex by endoplasmic reticulum to Golgi vesicle SNAREs. Science *281*, 698-700.

Springer,S., Spang,A., and Schekman,R. (1999). A primer on vesicle budding. Cell *97*, 145-148.

Stamnes,M.A. and Rothman,J.E. (1993). The binding of AP-1 clathrin adaptor particles to Golgi membranes requires ADP-ribosylation factor, a small GTP-binding protein. Cell *73*, 999-1005.

Staudinger,J., Zhou,J., Burgess,R., Elledge,S.J., and Olson,E.N. (1995). PICK1: a perinuclear binding protein and substrate for protein kinase C isolated by the yeast two-hybrid system. J. Cell Biol. *128*, 263-271.

Stearns,T., Hoyt,M.A., and Botstein,D. (1990a). Yeast mutants sensitive to antimicrotubule drugs define three genes that affect microtubule function. Genetics *124*, 251-262.

Stearns,T., Kahn,R.A., Botstein,D., and Hoyt,M.A. (1990b). ADP ribosylation factor is an essential protein in Saccharomyces cerevisiae and is encoded by two genes. Mol. Cell Biol. *10*, 6690-6699.

Stearns,T., Willingham,M.C., Botstein,D., and Kahn,R.A. (1990c). ADP-ribosylation factor is functionally and physically associated with the Golgi complex. Proc. Natl. Acad. Sci. U. S. A *87*, 1238-1242.

Steiner,D.F., Docherty,K., and Carroll,R. (1984). Golgi/granule processing of peptide hormone and neuropeptide precursors: a minireview. J. Cell Biochem. *24*, 121-130.

Stenmark,H., Aasland,R., Toh,B.H., and D'Arrigo,A. (1996). Endosomal localization of the autoantigen EEA1 is mediated by a zinc- binding FYVE finger. J. Biol. Chem. *271*, 24048-24054.

Stenmark,H., Vitale,G., Ullrich,O., and Zerial,M. (1995). Rabaptin-5 is a direct effector of the small GTPase Rab5 in endocytic membrane fusion. Cell *83*, 423-432.

Stephens,D.J. and Banting,G. (2000). The use of yeast two-hybrid screens in studies of protein:protein interactions involved in trafficking. Traffic. *1*, 763-768.

Stephens,D.J., Lin-Marq,N., Pagano,A., Pepperkok,R., and Paccaud,J.P. (2000). COPI-coated ER-to-Golgi transport complexes segregate from COPII in close proximity to ER exit sites. J. Cell Sci. *113 (Pt 12)*, 2177-2185.

Stock,M.F., Guerrero,J., Cobb,B., Eggers,C.T., Huang,T.G., Li,X., and Hackney,D.D. (1999). Formation of the compact confomer of kinesin requires a COOH-terminal heavy chain domain and inhibits microtubule-stimulated ATPase activity. J. Biol. Chem. *274*, 14617-14623.

Stoorvogel,W., Oorschot,V., and Geuze,H.J. (1996). A novel class of clathrin-coated vesicles budding from endosomes. J. Cell Biol. *132*, 21-33.

Stow,J.L., Fath,K.R., and Burgess,D.R. (1998). Budding roles for myosin II on the Golgi. Trends Cell Biol. *8*, 138-141.

Subtil,A., Lampson,M.A., Keller,S.R., and McGraw,T.E. (2000). Characterization of the insulin-regulated endocytic recycling mechanism in 3T3-L1 adipocytes using a novel reporter molecule. J. Biol. Chem. *275*, 4787-4795.

Sullivan,W., Fogarty,P., and Theurkauf,W. (1993). Mutations affecting the cytoskeletal organization of syncytial Drosophila embryos. Development *118*, 1245-1254.

Sutton,R.B., Fasshauer,D., Jahn,R., and Brunger,A.T. (1998). Crystal structure of a SNARE complex involved in synaptic exocytosis at 2.4 A resolution. Nature *395*, 347-353.

Takai,Y., Sasaki,T., and Matozaki,T. (2001). Small GTP-binding proteins. Physiol Rev. *81*, 153-208.

Takatsu,H., Katoh,Y., Shiba,Y., and Nakayama,K. (2001). Golgi-localizing, gamma-adaptin ear homology domain, ADP-ribosylation factor-binding (GGA) proteins interact with acidic dileucine sequences within the cytoplasmic domains of sorting receptors through their Vps27p/Hrs/STAM (VHS) domains. J. Biol. Chem. *276*, 28541-28545.

Takeya,R., Takeshige,K., and Sumimoto,H. (2000). Interaction of the PDZ domain of human PICK1 with class I ADP- ribosylation factors. Biochem. Biophys. Res. Commun. *267*, 149-155.

Tamaki,H. and Yamashina,S. (1991). Changes in cell polarity during mitosis in rat parotid acinar cells. J. Histochem. Cytochem. *39*, 1077-1087.

Tamkun,J.W., Kahn,R.A., Kissinger,M., Brizuela,B.J., Rulka,C., Scott,M.P., and Kennison,J.A. (1991). The arflike gene encodes an essential GTP-binding protein in Drosophila. Proc. Natl. Acad. Sci. U. S. A *88*, 3120-3124.

Tanigawa,G., Orci,L., Amherdt,M., Ravazzola,M., Helms,J.B., and Rothman,J.E. (1993). Hydrolysis of bound GTP by ARF protein triggers uncoating of Golgi- derived COP-coated vesicles. J. Cell Biol. *123*, 1365-1371.

Tarricone,C., Xiao,B., Justin,N., Walker,P.A., Rittinger,K., Gamblin,S.J., and Smerdon,S.J. (2001). The structural basis of Arfaptin-mediated cross-talk between Rac and Arf signalling pathways. Nature *411* , 215-219.

Taunton,J. (2001). Actin filament nucleation by endosomes, lysosomes and secretory vesicles. Curr. Opin. Cell Biol. *13*, 85-91.

Taunton,J., Rowning,B.A., Coughlin,M.L., Wu,M., Moon,R.T., Mitchison,T.J., and Larabell,C.A. (2000). Actin-dependent propulsion of endosomes and lysosomes by recruitment of N-WASP. J. Cell Biol. *148*, 519-530.

Terbush,D.R., Maurice,T., Roth,D., and Novick,P. (1996). The Exocyst is a multiprotein complex required for exocytosis in Saccharomyces cerevisiae. EMBO J. *15*, 6483-6494.

Terui,T., Kahn,R.A., and Randazzo,P.A. (1994). Effects of acid phospholipids on nucleotide exchange properties of ADP- ribosylation factor 1. Evidence for specific interaction with phosphatidylinositol 4,5-bisphosphate. J. Biol. Chem. *269*, 28130-28135.

Teter,K., Chandy,G., Quinones,B., Percyra,K., Machen,T., and Moore,H.P. (1998). Cellubrevin-targeted fluorescence uncovers heterogeneity in the recycling endosomes. J. Biol. Chem. *273*, 19625-19633.

Thomas,L., Clarke,P.R., Pagano,M., and Gruenberg,J. (1992). Inhibition of membrane fusion in vitro via cyclin B but not cyclin A. J. Biol. Chem. *267*, 6183-6187.

Thyberg,J. and Moskalewski,S. (1985). Microtubules and the organization of the Golgi complex. Exp. Cell Res. *159*, 1-16.

Togawa,A., Morinaga,N., Ogasawara,M., Moss,J., and Vaughan,M. (1999). Purification and cloning of a brefeldin A-inhibited guanine nucleotide- exchange protein for ADP-ribosylation factors. J. Biol. Chem. *274*, 12308-12315.

Toker,A. (1998). The synthesis and cellular roles of phosphatidylinositol 4,5-bisphosphate. Curr. Opin. Cell Biol. *10*, 254-261.

Tolias,K.F., Cantley,L.C., and Carpenter,C.L. (1995). Rho family GTPases bind to phosphoinositide kinases. J. Biol. Chem. *270*, 17656-17659.

Tooze,J. and Hollinshead,M. (1992). Evidence that globular Golgi clusters in mitotic HeLa cells are clustered tubular endosomes. Eur. J. Cell Biol. *58*, 228-242.

Traub,L.M., Ostrom,J.A., and Kornfeld,S. (1993). Biochemical dissection of AP-1 recruitment onto Golgi membranes. J. Cell Biol. *123*, 561-573.

Trischler,M., Stoorvogel,W., and Ullrich,O. (1999). Biochemical analysis of distinct Rab5- and Rab11-positive endosomes along the transferrin pathway. J. Cell Sci. *112 (Pt 24)*, 4773-4783.

Tsai,S.C., Adamik,R., Hong,J.X., Moss,J., Vaughan,M., Kanoh,H., and Exton,J.H. (1998). Effects of arfaptin 1 on guanine nucleotide-dependent activation of phospholipase D and cholera toxin by ADP-ribosylation factor. J. Biol. Chem. *273*, 20697-20701.

Tuomikoski,T., Felix,M.A., Doree,M., and Gruenberg,J. (1989). Inhibition of endocytic vesicle fusion in vitro by the cell-cycle control protein kinase cdc2. Nature *342*, 942-945.

Turner,C.E., Brown,M.C., Perrotta,J.A., Riedy,M.C., Nikolopoulos,S.N., McDonald,A.R., Bagrodia,S., Thomas,S., and Leventhal,P.S. (1999). Paxillin LD4 motif binds PAK and PIX through a novel 95-kD ankyrin repeat, ARF-GAP protein: A role in cytoskeletal remodeling. J. Cell Biol. *145*, 851-863.

Turner,C.E., West,K.A., and Brown,M.C. (2001). Paxillin-ARF GAP signaling and the cytoskeleton. Curr. Opin. Cell Biol. *13*, 593-599.

Tuxworth,R.I. and Titus,M.A. (2000). Unconventional myosins: anchors in the membrane traffic relay. Traffic. *1*, 11-18.

Uetz,P., Giot,L., Cagney,G., Mansfield,T.A., Judson,R.S., Knight,J.R., Lockshon,D., Narayan,V., Srinivasan,M., Pochart,P., Qureshi-Emili,A., Li,Y., Godwin,B., Conover,D., Kalbfleisch,T., Vijayadamodar,G., Yang,M., Johnston,M., Fields,S., and Rothberg,J.M. (2000). A comprehensive analysis of protein-protein interactions in Saccharomyces cerevisiae. Nature *403*, 623-627.

Uetz,P. and Hughes,R.E. (2000). Systematic and large-scale two-hybrid screens. Curr. Opin. Microbiol. *3*, 303-308.

Ullrich,O., Reinsch,S., Urbe,S., Zerial,M., and Parton,R.G. (1996). Rab11 regulates recycling through the pericentriolar recycling endosome. J. Cell Biol. *135*, 913-924.

Ullrich,O., Stenmark,H., Alexandrov,K., Huber,L.A., Kaibuchi,K., Sasaki,T., Takai,Y., and Zerial,M. (1993). Rab GDP dissociation inhibitor as a general regulator for the membrane association of rab proteins. J. Biol. Chem. *268*, 18143-18150.

Urbe,S., Huber,L.A., Zerial,M., Tooze,S.A., and Parton,R.G. (1993). Rab11, a small GTPase associated with both constitutive and regulated secretory pathways in PC12 cells. FEBS Lett. *334*, 175-182.

Valetti,C., Wetzel,D.M., Schrader,M., Hasbani,M.J., Gill,S.R., Kreis,T.E., and Schroer,T.A. (1999). Role of dynactin in endocytic traffic: effects of dynamitin overexpression and colocalization with CLIP-170. Mol. Biol. Cell *10*, 4107-4120.

Vallis,Y., Wigge,P., Marks,B., Evans,P.R., and McMahon,H.T. (1999). Importance of the pleckstrin homology domain of dynamin in clathrin- mediated endocytosis. Curr. Biol. *9*, 257-260.

van Aelst,L., Joneson,T., and Bar-Sagi,D. (1996). Identification of a novel Rac1-interacting protein involved in membrane ruffling. EMBO J. *15*, 3778-3786.

van der Sluijs,P., Hull,M., Huber,L.A., Male,P., Goud,B., and Mellman,I. (1992a). Reversible phosphorylation--dephosphorylation determines the localization of rab4 during the cell cycle. EMBO J. *11*, 4379-4389.

van der Sluijs,P., Hull,M., Webster,P., Male,P., Goud,B., and Mellman,I. (1992b). The small GTP-binding protein rab4 controls an early sorting event on the endocytic pathway. Cell *70*, 729-740.

Van Valkenburgh,H., Shern,J.F., Sharer,J.D., Zhu,X., and Kahn,R.A. (2001). ADP-ribosylation factors (ARFs) and ARF-like 1 (ARL1) have both specific and shared effectors: characterizing ARL1-binding proteins. J. Biol. Chem. *276*, 22826-22837.

Varki,A. (1998). Factors controlling the glycosylation potential of the Golgi apparatus. Trends Cell Biol. *8*, 34-40.

Venkateswarlu,K. and Cullen,P.J. (2000). Signalling via ADP-ribosylation factor 6 lies downstream of phosphatidylinositide 3-kinase. Biochem. J. *345 Pt 3*, 719-724.

Venkateswarlu,K., Gunn-Moore,F., Oatey,P.B., Tavare,J.M., and Cullen,P.J. (1998a). Nerve growth factor- and epidermal growth factor-stimulated translocation of the ADP-ribosylation factor-exchange factor GRP1 to the plasma membrane of PC12 cells requires activation of phosphatidylinositol 3-kinase and the GRP1 pleckstrin homology domain. Biochem. J. *335 (Pt 1)*, 139-146.

Venkateswarlu,K., Gunn-Moore,F., Tavare,J.M., and Cullen,P.J. (1999). EGF-and NGF-stimulated translocation of cytohesin-1 to the plasma membrane of PC12 cells requires PI 3-kinase activation and a functional cytohesin-1 PH domain. J. Cell Sci. *112 (Pt 12)*, 1957-1965.

Venkateswarlu,K., Oatey,P.B., Tavare,J.M., and Cullen,P.J. (1998b). Insulin-dependent translocation of ARNO to the plasma membrane of adipocytes requires phosphatidylinositol 3-kinase. Curr. Biol. *8*, 463-466.

Vitale,N., Ferrans,V.J., Moss,J., and Vaughan,M. (2000a). Identification of lysosomal and Golgi localization signals in GAP and ARF domains of ARF domain protein 1. Mol. Cell Biol. *20*, 7342-7352.

Vitale,N., Moss,J., and Vaughan,M. (1996). ARD1, a 64-kDa bifunctional protein containing an 18-kDa GTP-binding ADP-ribosylation factor domain and a 46-kDa GTPase-activating domain. Proc. Natl. Acad. Sci. U. S. A *93*, 1941-1944.

Vitale,N., Patton,W.A., Moss,J., Vaughan,M., Lefkowitz,R.J., and Premont,R.T. (2000b). GIT proteins, A novel family of phosphatidylinositol 3,4, 5- trisphosphate-stimulated GTPase-activating proteins for ARF6. J. Biol. Chem. *275*, 13901-13906.

Vogel,F. and Motulsky,A.G. (1997). Human genetics: problems and approaches. (Berlin; Heidelberg; New York: Springer Verlag).

Vowels,J.J. and Payne,G.S. (1998). A dileucine-like sorting signal directs transport into an AP-3- dependent, clathrin-independent pathway to the yeast vacuole. EMBO J. *17*, 2482-2493.

Wan,L., Molloy,S.S., Thomas,L., Liu,G., Xiang,Y., Rybak,S.L., and Thomas,G. (1998). PACS-1 defines a novel gene family of cytosolic sorting proteins required for trans-Golgi network localization. Cell *94*, 205-216.

Warren,G., Davoust,J., and Cockcroft,A. (1984). Recycling of transferrin receptors in A431 cells is inhibited during mitosis. EMBO J. *3*, 2217-2225.

Watanabe,G., Saito,Y., Madaule,P., Ishizaki,T., Fujisawa,K., Morii,N., Mukai,H., Ono,Y., Kakizuka,A., and Narumiya,S. (1996). Protein kinase N (PKN) and PKN-related protein rhophilin as targets of small GTPase Rho. Science *271*, 645-648.

Waters,M.G. and Hughson,F.M. (2000). Membrane tethering and fusion in the secretory and endocytic pathways. Traffic. *1*, 588-597.

Weide,T., Bayer,M., Koster,M., Siebrasse,J.P., Peters,R., and Barnekow,A. (2001). The Golgi matrix protein GM130: a specific interacting partner of the small GTPase rab1b. EMBO Rep. *2*, 336-341.

Welch,M.D. (1999). The world according to Arp: regulation of actin nucleation by the Arp2/3 complex. Trends Cell Biol. *9*, 423-427.

Welch,M.D., Iwamatsu,A., and Mitchison,T.J. (1997). Actin polymerization is induced by Arp2/3 protein complex at the surface of Listeria monocytogenes. Nature *385*, 265-269.

Wells,A.L., Lin,A.W., Chen,L.Q., Safer,D., Cain,S.M., Hasson,T., Carragher,B.O., Milligan,R.A., and Sweeney,H.L. (1999). Myosin VI is an actin-based motor that moves backwards. Nature *401*, 505-508.

West,M.A., Bright,N.A., and Robinson,M.S. (1997). The role of ADP-ribosylation factor and phospholipase D in adaptor recruitment. J. Cell Biol. *138*, 1239-1254.

Whitney,J.A., Gomez,M., Sheff,D., Kreis,T.E., and Mellman,I. (1995). Cytoplasmic coat proteins involved in endosome function. Cell *83*, 703-713.

Williger,B.T., Ostermann,J., and Exton,J.H. (1999). Arfaptin 1, an ARF-binding protein, inhibits phospholipase D and endoplasmic reticulum/Golgi protein transport. FEBS Lett. *443*, 197-200.

Woehlke,G. and Schliwa,M. (2000). Walking on two heads: the many talents of kinesin. Nat. Rev. Mol. Cell Biol. *1*, 50-58.

Wood,S.A., Park,J.E., and Brown,W.J. (1991). Brefeldin A causes a microtubule-mediated fusion of the trans-Golgi network and early endosomes. Cell *67*, 591-600.

Woodman,P.G. (2000). Biogenesis of the sorting endosome: the role of Rab5. Traffic. *1*, 695-701.

Wu,W.J., Erickson,J.W., Lin,R., and Cerione,R.A. (2000). The gamma-subunit of the coatomer complex binds Cdc42 to mediate transformation. Nature *405*, 800-804.

Wu,X., Rao,K., Bowers,M.B., Copeland,N.G., Jenkins,N.A., and Hammer,J.A., III (2001). Rab27a enables myosin Va-dependent melanosome capture by recruiting the myosin to the organelle. J. Cell Sci. *114*, 1091-1100.

Xu,Y., Hortsman,H., Seet,L., Wong,S.H., and Hong,W. (2001). SNX3 regulates endosomal function through its PX-domain-mediated interaction with PtdIns(3)P. Nat. Cell Biol. *3*, 658-666.

Yamaji,R., Adamik,R., Takeda,K., Togawa,A., Pacheco-Rodriguez,G., Ferrans,V.J., Moss,J., and Vaughan,M. (2000). Identification and localization of two brefeldin A-inhibited guanine nucleotide-exchange proteins for ADP-ribosylation factors in a macromolecular complex. Proc. Natl. Acad. Sci. U. S. A *97*, 2567-2572.

Yamashiro,D.J. and Maxfield,F.R. (1984). Acidification of endocytic compartments and the intracellular pathways of ligands and receptors. J. Cell Biochem. *26*, 231-246.

Yamashiro,D.J., Tycko,B., Fluss,S.R., and Maxfield,F.R. (1984). Segregation of transferrin to a mildly acidic (pH 6.5) para-Golgi compartment in the recycling pathway. Cell *37*, 789-800.

Yang,B., Gonzalez,L., Jr., Prekeris,R., Steegmaier,M., Advani,R.J., and Scheller,R.H. (1999). SNARE interactions are not selective. Implications for membrane fusion specificity. J. Biol. Chem. *274*, 5649-5653.

Yang,B., Steegmaier,M., Gonzalez,L.C., Jr., and Scheller,R.H. (2000). nSec1 binds a closed conformation of syntaxin1A. J. Cell Biol. *148*, 247-252.

Yang,C.Z., Heimberg,H., D'Souza-Schorey,C., Mueckler,M.M., and Stahl,P.D. (1998). Subcellular distribution and differential expression of endogenous ADP- ribosylation factor 6 in mammalian cells. J. Biol. Chem. *273*, 4006-4011.

Yang,C.Z. and Mueckler,M. (1999). ADP-ribosylation factor 6 (ARF6) defines two insulin-regulated secretory pathways in adipocytes. J. Biol. Chem. *274*, 25297-25300.

Zacchi,P., Stenmark,H., Parton,R.G., Orioli,D., Lim,F., Giner,A., Mellman,I., Zerial,M., and Murphy,C. (1998). Rab17 regulates membrane trafficking through apical recycling endosomes in polarized epithelial cells. J. Cell Biol. *140*, 1039-1053.

Zeligs,J.D. and Wollman,S.H. (1979). Mitosis in rat thyroid epithelial cells in vivo. II. Centrioles and pericentriolar material. J. Ultrastruct. Res. *66*, 97-108.

Zeng,J., Ren,M., Gravotta,D., Lemos-Chiarandini,C., Lui,M., Erdjument-Bromage,H., Tempst,P., Xu,G., Shen,T.H., Morimoto,T., Adesnik,M., and Sabatini,D.D. (1999). Identification of a putative effector protein for rab11 that participates in transferrin recycling. Proc. Natl. Acad. Sci. U. S. A *96*, 2840-2845.

Zerial,M. and McBride,H.M. (2001). Rab proteins as mebrane organizers. Nat. Rev. Mol. Cell Biol. *2*, 107-117.

Zhang,C.J., Cavenagh,M.M., and Kahn,R.A. (1998a). A family of Arf effectors defined as suppressors of the loss of Arf function in the yeast Saccharomyces cerevisiae. J. Biol. Chem. *273*, 19792-19796.

Zhang,C.X., Rothwell,W.F., Sullivan,W., and Hsieh,T.S. (2000). Discontinuous actin hexagon, a protein essential for cortical furrow formation in Drosophila, is membrane associated and hyperphosphorylated. Mol. Biol. Cell *11*, 1011-1022.

Zhang,G.F., Patton,W.A., Lee,F.J., Liyanage,M., Han,J.S., Rhee,S.G., Moss,J., and Vaughan,M. (1995). Different ARF domains are required for the activation of cholera toxin and phospholipase D. J. Biol. Chem. *270*, 21-24.

Zhang,Q., Cox,D., Tseng,C.C., Donaldson,J.G., and Greenberg,S. (1998b). A requirement for ARF6 in Fcgamma receptor-mediated phagocytosis in macrophages. J. Biol. Chem. *273*, 19977-19981.

Zheng,J., Cahill,S.M., Lemmon,M.A., Fushman,D., Schlessinger,J., and Cowburn,D. (1996). Identification of the binding site for acidic phospholipids on the pH domain of dynamin: implications for stimulation of GTPase activity. J. Mol. Biol. *255*, 14-21.

Zhu,X., Boman,A.L., Kuai,J., Cieplak,W., and Kahn,R.A. (2000). Effectors increase the affinity of ADP-ribosylation factor for GTP to increase binding. J. Biol. Chem. *275*, 13465-13475.

Zhu,Y., Doray,B., Poussu,A., Lehto,V.P., and Kornfeld,S. (2001). Binding of GGA2 to the lysosomal enzyme sorting motif of the mannose 6- phosphate receptor. Science *292*, 1716-1718.

Zhu,Y., Drake,M.T., and Kornfeld,S. (1999). ADP-ribosylation factor 1 dependent clathrin-coat assembly on synthetic liposomes. Proc. Natl. Acad. Sci. U. S. A *96*, 5013-5018.

Appendix

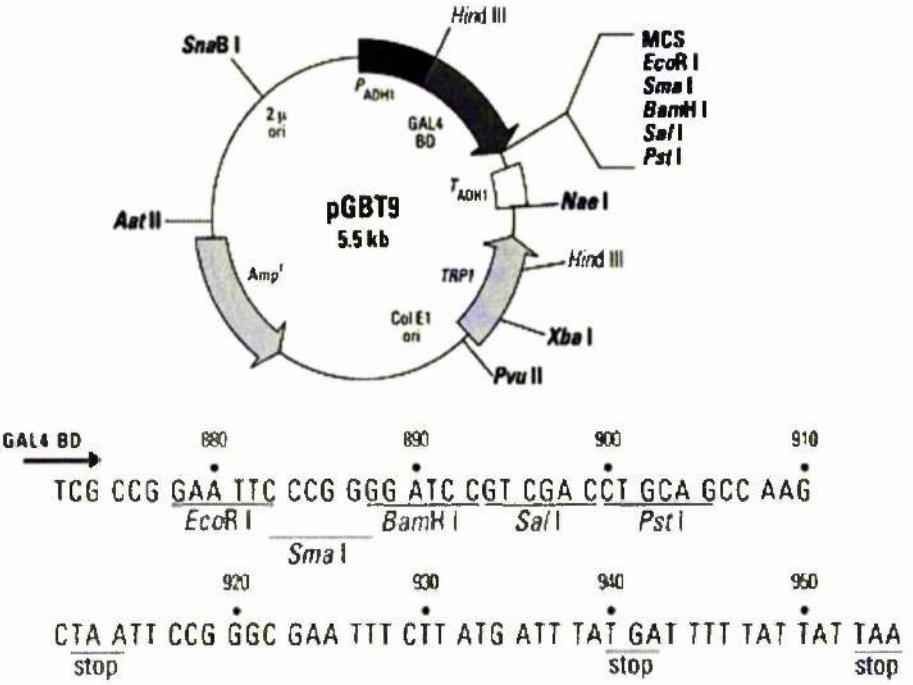

GBT9 generates a hybrid protein that contains the sequence of the GAL4 DNA-Binding domain (DNA-BD; a.a. 1-147). The fusion protein is expressed in yeast host cells from the constitutive ADH1 promoter; transcription is terminated at the ADH1 transcription signal. The hybrid protein is targeted to the yeast nucleus by nuclear localisation sequences that are an intrinsic part of the GAL4 DNA-BD. pGBT9 replicates autonomously in both E. coli and S. cerevisiae. It carries the bla gene (for ampicillin resistance in E. coli) and the TRP1 nutritional marker that allow yeast auxotrophs carrying pGBT9 to grow on limiting synthetic medium lacking Trp.

The Q71/67L and T27/31N mutants of Arf1, Arf2, Arf3, Arf4, Arf5 and Arf6 were cloned in frame into the BamHI and SalI sites. Arf5 and Arf6 cDNAs were cloned in using BglII and XhoI, so both BamHI/SalI restriction sites are abolished. Arf1, Arf2, Arf3 and Arf4 were cloned in using BamHI and XhoI, so the SalI restriction site is abolished.

N4Arf5 (BamHI and XhoI cut) and N5Arf4 (BglII and XhoI cut) constructs were also ligated into the BamHI and SalI sites of pGBT9.

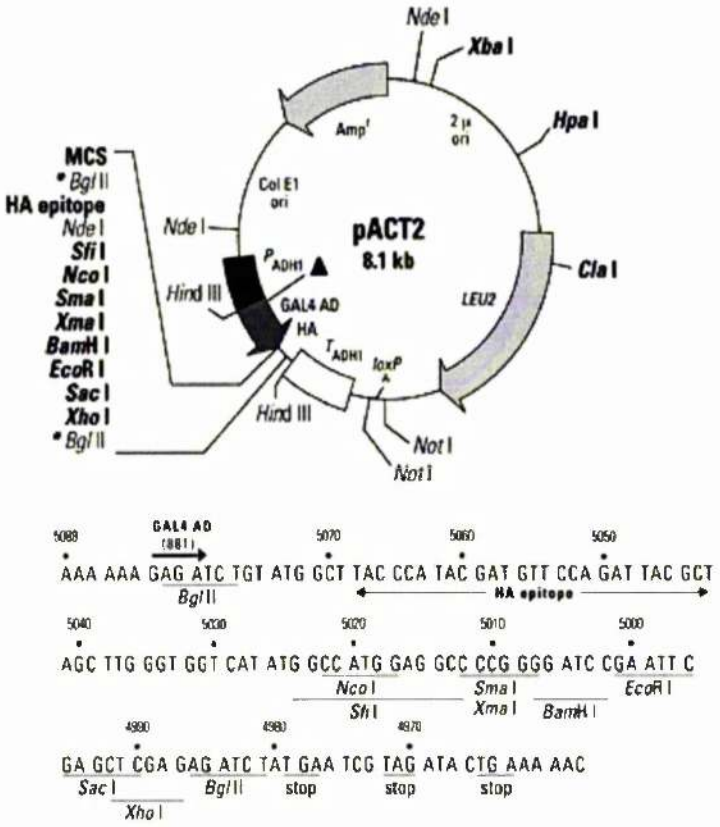

The hybrid protein is expressed at high levels in yeast host cells from the constitutive ADH1 promoter (P); transcription is terminated at the ADH1 transcription termination signal (T). The protein is targeted to the yeast nucleus by the nuclear localization sequence from SV40 T-antigen which has been cloned into the 5' end of the GAL4 AD sequence. pACT2 replicates autonomously in both *E. coli* and *S. cerevisiae*. It carries the bla gene, which confers ampicillin resistance in *E. coli* and the LEU2 nutritional gene that allows yeast auxotrophs to grow on limiting synthetic media.

The cDNAs of the putative Arf5 interacting proteins (T3, T4, T9, T12, T14 and T20) are located between the EcoR1 and Xho I sites of pACT2 (Clontech).

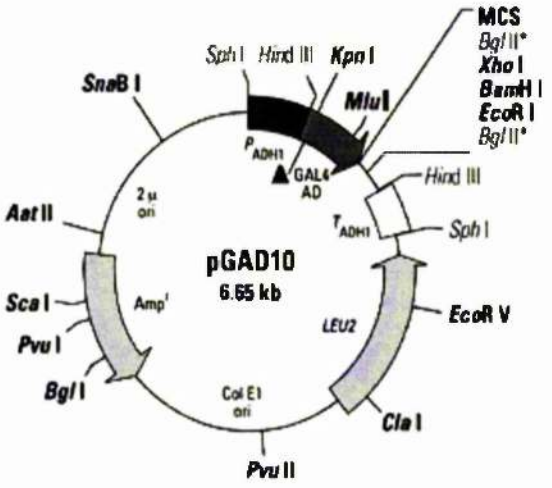

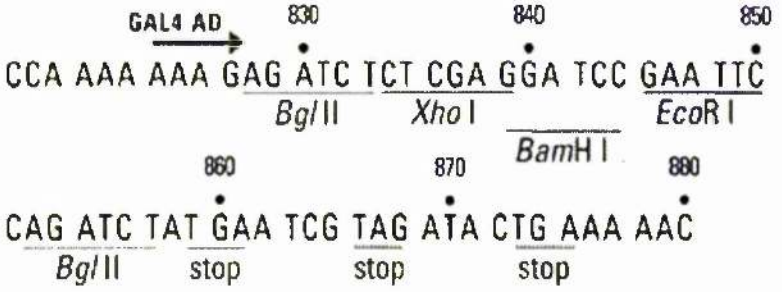

pGAD10 (Clontech) is similar to pACT2 but does not have a HA tag. The insert in plasmid B1 pGAD10 (600 bp of 3' ORF and 3'UTR of Arfophilin-1) is located between the EcoRI site and the 2nd BglII site.

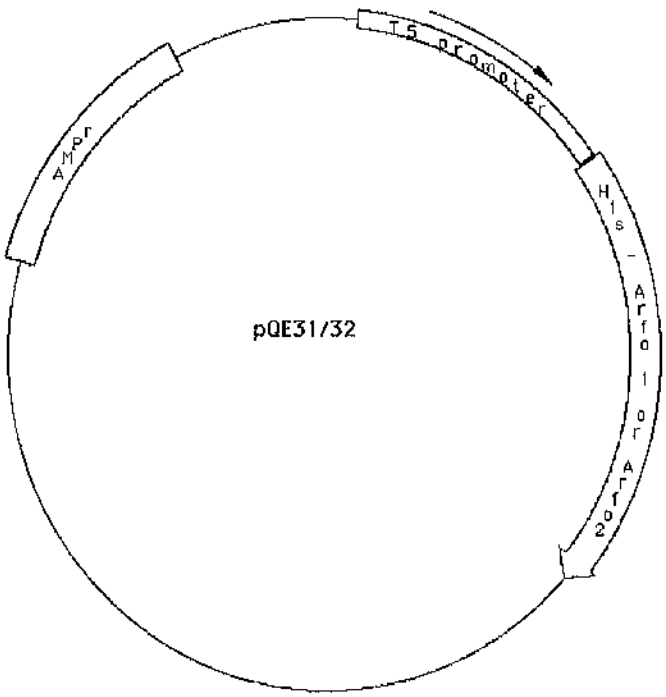

The 3' 990 bp of the Arfophilin-2 ORF (including 3'UTR directly cut using BglII from T20 pACT2) was subcloned into the BamHI site of pQE32 (Qiagen), in frame with the N-terminal RGS-His tag.

The 3' 600 bp of the Arfophilin-1 ORF together with the 3'UTR (the entire insert cut from B1 pGAD10 using BglII) was inserted into the BamHI site of pQE31 (Qiagen), in frame with the N-terminal RGS-IIis tag.

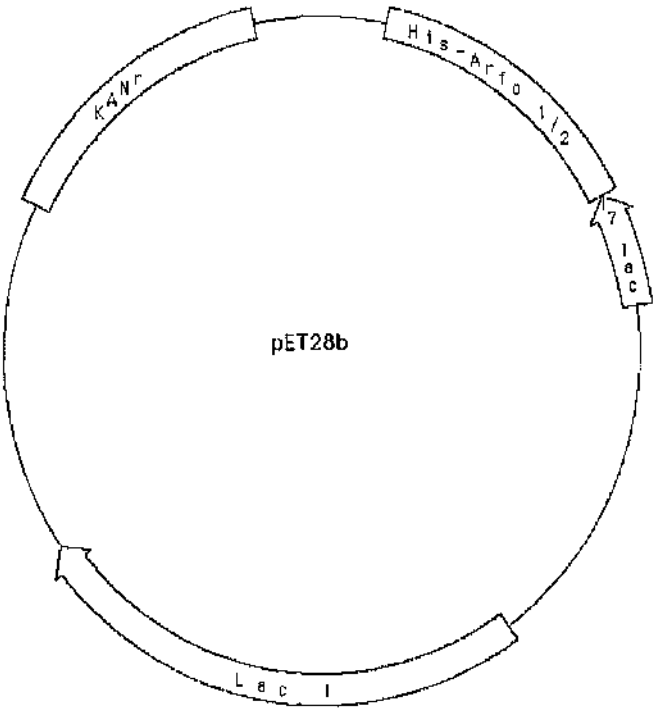

The 3' 990 bp of the Arfophilin-1 and Arfophilin-2 ORFs were subcloned into the BamH1 and SalI sites of pET28b (Novagen), in frame with the N-terminal hexahistidine tag.

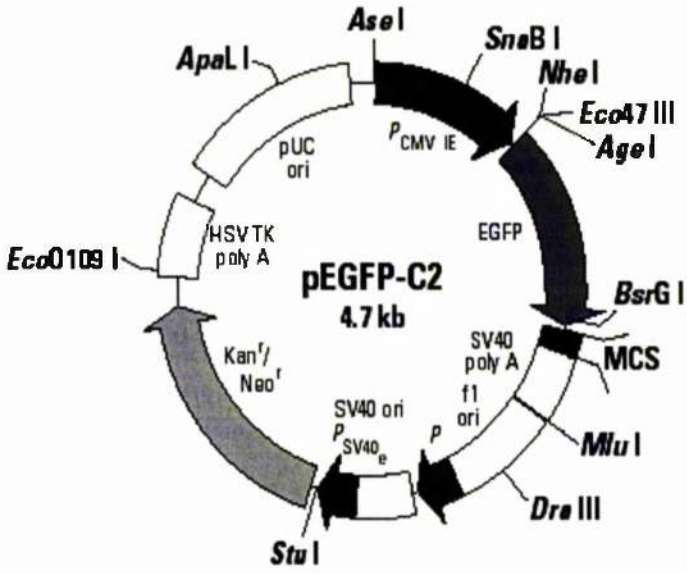

SV40 polyadenylation signals downstream of the EGFP gene direct proper processing of the 3' end of the EGFP mRNA. The vector backbone also contains an SV40 origin for replication in mammalian cells expressing the SV40 T-antigen. A neomycin-resistance cassette (neor), consisting of the SV40 early promoter, the neomycin/kanamycin resistance gene of Tn5, and polyadenylation signals from the Herpes simplex thymidine kinase gene, allows stably transfected eukaryotic cells to be selected using G418. A bacterial promoter upstream of this cassette (Pamp) expresses kanamycin resistance in E. coli. The pEGFP backbone also provides a pUC19 origin of replication for propagation in E. coli and an f1 origin for single-stranded DNA production.

The 3' 990 bp of the Arfophilin-2 ORF (including 3'UTR directly cut from T20 pACT2) was subcloned into the BglII site. Similarly a partially BglII digested Arfophilin-2 fragment containing the entire T20 pACT2 insert (including HA tag and 3'UTR) was also cloned into the BglII site of pEGFP-C2 (Clontech).

The full-length Arfophilin-2A ORF (digested with BamHI and SalI) was subcloned in frame into the Bgl II and SalI sites of this vector.

Full-length Arfophilin-2B and -2C ORFs were excised from pEGFP-N1 vectors using EcoR1 and SalI and were subcloned in frame into the same sites of pEGFP-C2.

The 3' 990 bp of the Arfophilin-1 ORF (digested with BamHI and SalI) was subcloned into the BglII and SalI sites of pEGFP-C2.

The full-length ORF of *Drosophila* nuclear fallout (Nuf; containing 5' BamHI and 3' Sal I sites) was also cloned into the BglII and SalI sites of pEGFP-C2.

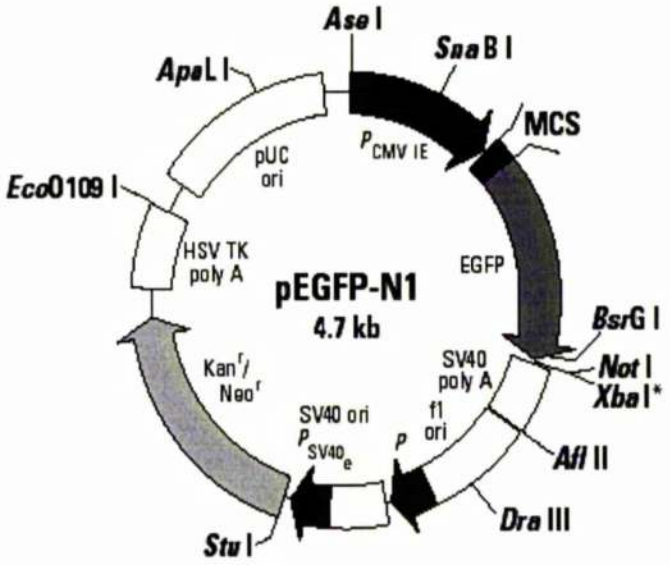

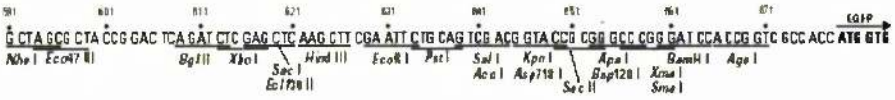

The pEGFP-N1 (Clontech) vector has the same features as pEGFP-C2 except that the multiple cloning site (MCS) precedes the EGFP sequence.

The full-length Arfophilin-2A ORF (digested with BamHI and SalI) was subcloned into the Bgl II and SalI sites of this vector (**note** that stop codon is present so no EGFP fusion is made).

Full-length Arfophilin-2B and -2C ORFs were assembled in this vector and are found between the EcoRI and Sal I sites (**note** that stop codons are present so no EGFP fusions are made).